The Organisation and Function of the Gut Microbiota in Cystic Fibrosis

R MARSH

PhD 2023

The Organisation and Function of the Gut Microbiota in Cystic Fibrosis

RYAN MARSH

A thesis submitted in partial fulfilment of the requirements of

Manchester Metropolitan University

for the degree of Doctor of Philosophy

Department of Life Sciences

Manchester Metropolitan University

2023

Declaration

The content discussed within this thesis has not been utilised to support the pursuit of any additional degree or qualification from this university or any other educational institution.

This thesis is being submitted in partial fulfilment of the requirements for the degree of PhD doctorate.

This thesis is the result of my own independent work/investigation, except where otherwise stated. Other sources are acknowledged by explicit references.

I hereby give consent for my thesis, if accepted, to be available for photocopying and for interlibrary loan, and for the title and summary to be made available to outside organisations.

Date: 22/08/2023

Abstract

People with cystic fibrosis (pwCF) suffer from a range of gastrointestinal manifestations of disease, which has increased in prevalence as respiratory outcomes improve and life expectancy raises. This translates to the occurrence of daily GI symptoms for many pwCF, which is a top research priority to alleviate. The gut microbiota is altered in CF and has been shown to associate with intestinal abnormalities, therefore offers a potential avenue of therapeutic intervention by its modulation. This thesis investigated relationships between the microbiota and associated functions, intestinal outcomes, and cystic fibrosis transmembrane regulator (CFTR) modulator usage.

Initially, relationships between altered intestinal function and physiology in CF were revealed with microbiota, by combining 16S rRNA gene sequencing data with magnetic resonance imaging (MRI) results and clinical metadata across pwCF and healthy controls. Significant differences in diversity and composition were observed between groups, which further associated with clinical factors and markers of intestinal function.

To understand how microbiota function might be compromised in CF, a sensitive method to profile and quantify faecal short-chain fatty acids (SCFAs) using gas chromatography-mass spectrometry (GC-MS) was validated. This was subsequently used to demonstrate that overall SCFA compositional differences persist between healthy controls pwCF receiving Tezacaftor/Ivacaftor CFTR modulator therapy, further extending to microbiota compositional differences, which were also not significantly altered by treatment.

Finally, microbiota composition and function were assessed across pwCF receiving more efficacious Elexacaftor/Tezacaftor/Ivacaftor (ETI) therapy. Subtle differences were observed following extended ETI administration, yet microbiota and SCFA

compositions remained significantly different from controls. Interestingly, there were no differences across the most abundant SCFAs, indicating possible functional redundancy in the CF microbiota.

Overall, the results obtained in this thesis advocate for further investigation of microbiota function through more sophisticated metagenomic and untargeted metabolomic approaches, to unravel the complex relationships between the microbiota, gastrointestinal (GI) manifestations, and patient symptoms in CF.

List of published Chapters

The following Chapters have been published:

Chapter 3: Intestinal function and transit relate to microbial dysbiosis in the CF gut:

This Chapter is published in the *Journal of Cystic Fibrosis* and is presented in submitted manuscript format:

Marsh R, Gavillet H, Hanson L, Ng C, Mitchell-Whyte M, Major G, Smyth AR, Rivett D, van der Gast C. 2022*. Intestinal function and transit associate with gut microbiota dysbiosis in cystic fibrosis*. J Cyst Fibros 21:506–513.

Chapter 5: Tezacaftor/Ivacaftor therapy has negligible effects on the cystic fibrosis gut microbiome:

This Chapter is published in the journal *Microbiology Spectrum* and is presented in submitted manuscript format:

Ryan M, Claudio DS, Liam H, Christabella N, Giles M, R. SA, Damian R, Christopher van der G. 2023. Tezacaftor/Ivacaftor therapy has negligible effects on the cystic fibrosis gut microbiome. Microbiol Spectr 0:e01175-23.

Acknowledgements

I would like to thank Professor Chris van der Gast for giving me the opportunity to undertake this PhD, and for his invaluable support and guidance. Aside from expanding my knowledge of the microbiota, I've amassed confidence for my own professional development in the world of academic research, for which I am eternally grateful. I'd also like to thank Dr. Damian Rivett for his support 'on the ground' and handling me with care during my rabbit-hole rants surrounding experimental methodology.

Thank you to my lab mates Helen, Lauren, and Michelle. We've shared a fair few laughs over the years and your emotional support is greatly appreciated. I will dearly miss our daily conundrums and games of hangman on the lab whiteboard.

A big thank you is necessary to all the people with cystic fibrosis who kindly donated the samples utilised in this thesis. On top of that, thank you to the clinical team at the Queens Medical Centre and Sir Peter Mansfield Imaging Centre, University of Nottingham, who collected the clinical metadata utilised in this thesis. You have taught me a thing or two about the CF gut, to say the least.

Thank you to my wife and family, who have sat and listened through endless rehearsals of thesis Chapters, microbiota talks, and academic presentations with great enthusiasm. I love you all and hope I can continue to make you proud.

List of Abbreviations

$\%FEV_1$ – Percentage Lung Capacity Expelled within 1 Second

AMP – Antimicrobial Peptide

ASV – Amplicon Sequence Variant

BMI – Body Mass Index

BSTFA – N,O-bis(trimethylsilyl)trifluoroacetamide

CF – Cystic Fibrosis

CFRD – Cystic Fibrosis-Related Diabetes

CFRLD – Cystic Fibrosis-Related Liver Disease

CFTR – Cystic Fibrosis Transmembrane Regulator

DE – Diethyl Ether

DGGE – Denaturing Gradient Gel Electrophoresis

DIOS – Distal Intestinal Obstruction Syndrome

ENaC – Epithelial Sodium Channel

ETI – Elexacaftor/Tezacaftor/Ivacaftor

FMT – Faecal Microbiota Transplant

GC-MS – Gas Chromatography-Mass Spectrometry

GI – Gastrointestinal

IBD – Inflammatory Bowel Disease

Ig – Immunoglobulin

IV – Intravenous

LC-MS – Liquid Chromatography-Mass Spectrometry

LGG – *Lactobacillus rhamnosus GG*

LOD – Limit of Detection

LOQ – Limit of Quantification

MI – Meconium Ileus

MRI – Magnetic Resonance Imaging

MS – Mass Spectrometry

NGS – Next Generation Sequencing

NMR – Nuclear Magnetic Resonance

OCTT – Oro-caecal Transit Time

OTU – Operational Taxonomic Unit

PCR – Polyermase Chain Reaction

PERT – Pancreatic Enzyme Replacement Therapy

PI – Pancreatic Insufficient

PMA – Propidium Monoazide

pp%FEV_1 – Predicted Percentage Lung Capacity Expelled within 1 Second

PPI – Proton Pump Inhibitor

PS – Pancreatic Sufficient

pwCF – People with Cystic Fibrosis

qPCR – Quantitative PCR

qRT-PCR – Quantitative Real-Time PCR

RSD – Relative Standard Deviation

RT – Retention Time

SBWC – Small Bowel Water Content

SCFA – Short-Chain Fatty Acid

SIBO – Small Intestinal Bacterial Overgrowth

SIM – Selected Ion Monitoring

Tez/Iva – Tezacaftor/Ivacaftor

TTGE – Temporal Temperature Gradient Electrophoresis

List of Tables

List of Figures

List of Supplementary Tables

List of Supplementary Figures

Chapter 1: Introduction

1.1 Cystic Fibrosis

1.1.1 Cystic Fibrosis – Genetics and worldwide statistics

Cystic fibrosis (CF) is the most common autosomal recessive genetic disorder that threatens to significantly reduce life expectancy, with over ten thousand active patients in the UK alone (Cystic Fibrosis Trust, 2020) and a significantly higher incidence in Caucasians. The underlying cellular mechanisms disrupted are attributable to mutations in the cystic fibrosis transmembrane regulator (CFTR) gene, which encodes a cAMP-regulated ATP-cassette binding protein aptly termed the CFTR protein. CFTR functions to transport chloride (Cl^-) and bicarbonate (HCO_3^-) ions at various epithelial sites throughout the body, whilst also inhibiting the reabsorption of sodium ions (Na^+) via the epithelial sodium channel (ENaC) (König et al., 2001). Mutations of the CFTR gene are typically divided into six classes, dependent on the resultant effect upon the CFTR protein. This includes a reduction in CFTR expression through introduced premature stop codons (Class I), post-translational processing issues such as misfolding (Class II), poor gating through open probability (Class III) or conductance issues (Class IV), changes to upstream transcriptional promotor regions leading to less protein expression overall (Class V), and finally increased destabilisation of the CFTR protein whilst present at the epithelial surface or during recycling processes involving endosomes (Class VI) (Veit et al., 2016; Deletang and Taulan-Cadars, 2022). As such, there are currently more than 2000 documented variants of the CFTR gene, with approximately 400 of these recognised as disease causing (Bareil and Bergougnoux, 2020; Allen et al., 2023). The majority of people with CF (pwCF) harbour at least one copy of the F508del mutation, a class II mutation that results in little to no functional CFTR protein and typically leads to more severe outcomes in disease.

1.1.2 Cystic Fibrosis – General pathophysiology of disease

As CFTR mRNA is primarily expressed at epithelial sites throughout the body, these are typically the locations at which manifestations of the disease present within pwCF. CFTR mRNA expression can be observed in nasal, tracheal, and bronchial epithelial cells (Trapnell et al., 1991), the gastrointestinal (GI) tract, where expression is higher in the tissues of the pancreas and within enterocytes of the small and large intestines (Strong et al., 1994), and finally within the reproductive tract (Chan et al., 2009). Disruption of CFTR function through mutations to the CFTR gene will ultimately lead to dehydration of the overlying mucosa, resulting in its increased viscosity and therefore decreased motility**.** This leads to a multitude of problems, including the well documented recurrent bacterial infections that persist in the airways of patients that often progresses into fatal respiratory disease, a hallmark characteristic of CF and the leading cause of mortality (O'Sullivan and Freedman, 2009; McBennett et al., 2022). Other common manifestations include reduced fertility; In males, congenital absence of the vas deferens is common (Cui et al., 2020), with impaired cervical sperm penetration present in females (Sueblinvong and Whittaker, 2007).

More local to the GI tract, pancreatic insufficiency (PI) is prevalent large proportion of sufferers (Akshintala et al., 2019) as failure of Cl^- and HCO_3^- secretion resultant of CFTR dysfunction leads to the zymogenic accumulation within blocked pancreatic ducts and acinar cells (Li and Somerset, 2014). Continued obstruction ultimately leads to epithelial damage, fibrosis, and inflammation. Genotype is often predictive of pancreatic outcomes, with those pwCF harbouring class I-III and VI mutations typically presenting with PI, and those with milder class IV-V mutations more often pancreatic sufficient (PS) (Wilschanski and Durie, 1998; Singh and Schwarzenberg, 2017). For those pwCF who do not develop pancreatic insufficiency, a small

proportion may develop pancreatitis as they exhibit the necessary balance of both pancreatic acinar loss with ductal obstructions mentioned previously (Ooi et al., 2011). Additionally, cystic fibrosis-related diabetes (CFRD) can arise due to compromised insulin secretion from the loss or impairment of pancreatic islets, which typically occurs later in life and again is more prominent in pwCF harbouring severe mutations (Granados et al., 2019). At the site of the liver, cystic fibrosis-related liver disease (CFRLD) can occur and is present in approximately a small minority of pwCF, yet is a leading cause of mortality (Paranjape and Mogayzel, 2018). Similar to the site of the pancreas, ductal cells at the site of the liver (cholangiocytes) that express CFTR are comprised, which comprises the classical theory of CFRLD pathophysiology. The secretion of bile that typically occurs is impaired, often leading to cholestasis and a progression into cirrhosis in surrounding tissues as a state of chronic inflammation is exhibited (Sherwood et al., 2022). Within the intestinal tract itself, a range of abnormalities present which are accompanied by array of patient symptoms, which will be discussed further in the subsequent subChapters.

1.1.3 Cystic Fibrosis – Manifestations of the intestinal tract and patient symptoms

Meconium Ileus

Perhaps the earliest GI manifestation presented in pwCF is meconium ileus (MI), which describes a viscous thick meconium (initial stool-like passage of the infant) that obstructs the junction between the small and large intestines prior to the ileo-caecal valve, labelled the terminal ileum. Meconium ileus can be simple or complex in nature; The latter typically describes the need for surgical intervention as previous efforts with fluid or gas fail to dislodge the meconium, or indicating surgical intervention is required as additional peritoneal or circulatory complications may

have arisen that would ultimately lead to a poor prognosis for the patient if left untreated (Waldhausen and Richards, 2018). Occurring in up to around 10-20% of newborns (Kelly and Buxbaum, 2015) and more common in those pwCF harbouring class I-III mutations (Sathe and Houwen, 2017), there is also evidence to suggest that alternate genes may modify outcomes of meconium ileus in CF. This includes alternate chloride channels such as SLC26A9, which is also expressed in the small intestine and demonstrates associations with meconium ileus prevalence in pwCF (Sun et al., 2012; Li et al., 2014), alongside augmentation of disease abnormalities in murine models (Liu et al., 2015). An overview of meconium ileus, alongside other manifestations of the intestinal tract, are provided in Figure 1.1.

Distal Intestinal Obstruction Syndrome (DIOS)

Although similar in symptoms to meconium ileus (MI), highlighted by the ileocecal blockage by sticky muco-faecal matter, DIOS is regarded as a separate condition later in life which is owed to differences in incidence (more common that DIOS do not suffer MI in infancy), additional symptoms, and a reduction in the influence of modifier genes (Houwen et al., 2010). Affecting about 20% of the adult CF population (Kelly and Buxbaum, 2015), DIOS itself can also persist as a complete or incomplete blockage, and is physiologically defined differently to constipation, which rather describes gradual muco-faecal build up throughout the whole colon (Green et al., 2018). DIOS exhibits a substantially large co-incidence with pancreatic insufficiency and more severe CFTR mutations, likely reflecting the enhanced disruption of muco-fecal motility in the intestine (Colombo et al., 2011).

Small Intestinal Bacterial Overgrowth (SIBO)

DIOS itself, and other motility disorders of the GI tract often facilitate small intestinal bacterial overgrowth (SIBO), as material consisting of food and bacteria remains in the upper GI tract, which can occur as gastric peristalsis, or down through towards the distal ileum prior to the ileocecal valve (Maneerattanaporn and Chey, 2007). SIBO presents itself in a significant proportion of CF patients throughout their lifetime as an enhanced bacterial CFU count often exceeding 10^5 CFU/ml (Lewindon et al., 1998; Lisowska et al., 2009; Franco et al., 2015), determined by culture of aspirate samples or inferred non-invasively by the use on glucose-ingested breath testing of either hydrogen or methane, although other substrates can be used to achieve various other diagnostic utilities (Ghoshal, 2011). While both techniques still have validity in use, they present significant limitations; glucose breath-testing has demonstrated insensitivities and specificity issues, whilst aspirate culture cannot account for microbes that are unculturable in a conventional laboratory setting, which includes a large proportion of the gut microbiota (Wang and Yang, 2013).

Intestinal malignancies and inflammation

Associations between CF and the increased incidence of GI cancers as compared to the general population are evident, particularly as life expectancy increases from improvements to the care and treatment of CF (Hough et al., 2020). This extends to both colorectal and small intestinal cancers (Yamada et al., 2018), perhaps unsurprising given the role of CFTR as a tumour suppressor in the GI tract of murine models (Than et al., 2016). Chronic, low-grade intestinal inflammation in the CF intestinal environment is now appreciated as a hallmark of CF GI abnormalities, with a multitude of studies demonstrating enhanced inflammation utilising faecal calprotectin (Rumman et al., 2014; Adriaanse et al., 2015; Garg et al., 2017) and

faecal M2-pyruvate kinase (Pang et al., 2015; Coffey et al., 2019), among other inflammatory markers (Smyth et al., 2000; Hendriks et al., 2001). Whilst the use of faecal calprotectin offers a non-invasive route of analysis, it is critical to exercise careful judgment in understanding study results, as a range of commercial kits have been utilised with variability also across cut-off values for ‘excessive’ inflammation (μg/g) (Tam et al., 2022).

Patient symptoms

Given the range of abnormalities at the site of the GI tract, it is unsurprising that the majority of pwCF suffer from intestinal symptoms daily, which remains a key issue to further understand within the CF community (Smith et al., 2020). Prevalent symptoms include abdominal pain (Baker et al., 2005; Jaudszus et al., 2022), flatulence (Borowitz et al., 2006; Anderson et al., 2022), bloating (Ramos et al., 2013; Subhi et al., 2014), constipation (Farjadian et al., 2013; Fraquelli et al., 2016), and a lack of appetite (Furnari et al., 2019). Given the high burden of GI abnormalities in CF, it remains to be elucidated on how these may associate with patient symptoms and how they can best be modulated to lessen the burden upon pwCF.

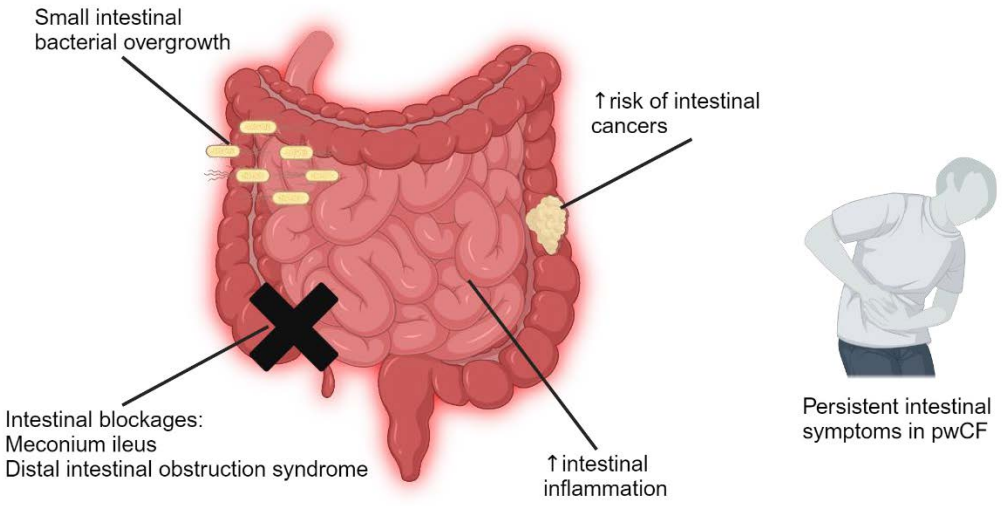

Figure 1.1 An overview of the intestinal abnormalities experienced by people with CF (pwCF) throughout life.

1.1.4 Management of disease

PwCF are administered a variety of drugs to manage the wide range of complications that can arise from disease. Antibiotics are used to treat the recurrent respiratory bacterial infections that deteriorate lung function and present as a hallmark of the disease. Examples include the use of the aminoglycoside tobramycin, which has been used extensively to treat lung infections with the highly predominant pathogen *Pseudomonas aeruginosa* (Ehsan and Clancy, 2015), or macrolide antibiotics that can target several certified CF pathogens, including *Staphylococcus aureus* and *Haemophilus influenzae* (Southern et al., 2012), by inhibiting bacterial protein synthesis via interactions with the 50S ribosomal subunit. Significant improvements in lung function have been described in the literature for patients administered treatments such as azithromycin (Southern et al., 2012), but secondary adverse effects of gastrointestinal complications also correlate with dosage (McCormack et al., 2007). Treatment also extends to periods of intravenous administration during ongoing pulmonary exacerbations (Bhatt, 2013). Other treatments to better respiratory health and improve symptoms include the common administration of bronchodilators, mucolytics, and hypertonic saline (Smith and Edwards, 2017).

Aside from antibiotic usage, lung function is evidently preserved in pwCF with better nutritional status (Steinkamp and Wiedemann, 2002), such that a diet higher in fat to meet enhanced energy demands has generally been implemented in CF following evidence of the aforementioned across different CF centres (Corey et al., 1988). For pancreatic insufficient pwCF, this dietary alteration is accompanied by the need to take pancreatic enzyme replacement therapy (PERT), to deliver essential lipase, amylase and protease to the intestinal tract, thus reducing typical maldigestion and malabsorption (Freswick et al., 2022). Proton pump inhibitors (PPIs) are another

treatment local to the GI tract that can aid PERT effectiveness by reducing gastric acidity, secondary to reducing heartburn and peptic ulcers that arise in pwCF (Ng and Moore, 2021).

The most recent era of CF treatment introduces the possibility to target the underlying defective mechanisms within the class range of CFTR mutations, as opposed to modulation of the mucus or targeting the bacterial infections that present within patients (Boyle and De Boeck, 2013). Termed ‘CFTR modulators’ these treatments usually encompass the mixed use of CFTR correctors and potentiators. The former act to reduce the degradation of the mutant CFTR protein by the host ERAD machinery and thus enhance trafficking and expression of the protein at the cell surface, whilst potentiators interact with defective protein already at the cell surface to increase activity (Gentzsch and Mall, 2018). As research has progressed, treatments have shifted from a state of monotherapy to combined treatment that allows for an increased repertoire of targetable mutations; the potentiator Ivacaftor was the first CFTR modulator approved for use, although only targeted individuals with the less severe G551D mutation (class III) (Van Goor et al., 2009). Further work demonstrated the ability of Lumacaftor to recoup the processing of CFTR in F508del patients to a level representative of a more mild CFTR function, which lead to its dual use alongside Ivacaftor to treat F508del homozygotes (Van Goor et al., 2011). The use of another corrector, Tezacaftor alongside Ivacaftor allows further widening of targetable patient genotypes, with the ability to enhance activity of the CFTR protein in F508del/G551D compound heterozygotes (Donaldson et al., 2018). The spectrum continues to widen further, with triple combination therapy of Elexacaftor/Tezacaftor/Ivacaftor showing promise in patients with F508del and another minimal function mutation (Taylor-Cousar et al., 2019).

1.2 The gut microbiome

With the wider human microbiome popularised at the start of the millennium (Lederberg and McCray, 2001), the term gut microbiome refers to the complex community of microorganisms that collectively inhabit the GI tract, including their collective genetic material and therefore functional potential. This includes the presence of bacteria, fungi, viruses, and protozoa, of which are increasingly recognised as important constituents in host health and disease. Amendments to the classical ratio of microbial to human cells in the body have been proposed in recent years with revised calculations substantially reducing previous estimates of 100-fold differences (Sender et al., 2016). Nonetheless, the human body still provides a habitat for approximately 10^{13} microbes, of which between 10^{2}-10^{8} cells/mL reside in the small intestine, with this figure rising up to 10^{11} cells/mL in the colon (Walter and Ley, 2011).

1.2.1 Gut microbiome from birth and throughout life

Whilst there is evidence to suggest that the gut microbiota may initially be established *in utero* (Jiménez et al., 2008; Walker et al., 2017), the mode of birth delivery for the new born is seemingly the first defining event of the gut microbiota blueprint, with changes evident between children born via caesarean section and those through a vaginal birth (Rutayisire et al., 2016). Infants born by caesarean typically contain a microbial community that resembles the maternal skin microbiota, including an enrichment of *Staphylococcus* and *Enterococcus*, whilst those born through the vaginal route contain relatively increased *Bifidobacterium* (Reyman et al., 2019; Coelho et al., 2021). Following this initial shaping event, the gut microbiota continues to be curated and remodelled throughout infancy, with a large role played by early life dietary habits. A prime example of this would be the introduction of

breastfeeding or formula feeding, which results in changes across microbiota structure early life (Ma et al., 2020; Niu et al., 2020), with the former generally considered preferable due to the expansion of immunogenically beneficial *Bifidobacteria* species as they preferentially ferment human milk oligosaccharides (Yao et al., 2021). Nonetheless, the microbiota of infants continues to expand over the first few years of life and increase in diversity (Derrien et al., 2019), with the phyla *Firmicutes* and *Bacteroidetes* generally dominating the composition after 3 years of life following the introduction of solid (more complex) foods for which they are better equip to utilise (Koenig et al., 2011). This maintains into adulthood where these phyla collectively account for 80-90% of the total relative abundance in the gut (Arumugam et al., 2011). Whilst diet remains an important determinant of gut microbiota composition in later life (Claesson et al., 2012), during later adulthood it is evident that bacterial diversity declines and particular taxa generally decrease in relative abundance. Examples include a reduction in the *Firmicutes*, including beneficial genera such as *Faecalibacterium* and *Eubacterium,* and beneficial *Actinobacteria* such as *Bifidobacterium* species (Jeffery et al., 2016; Salazar et al., 2017). Changes are hypothesised to commence following the natural changes to host physiology, including directly at the site of the gastrointestinal tract where changes to transit times and increased malabsorption are evident (Lovat, 1996), supplemented also by wider immunological changes to the host (Nagpal et al., 2018).

1.2.2 Changes in the microbiota across the intestinal tract

Although notably lower in abundance and species diversity compared to the colon, the small intestine exists as an important site for both host and microbe alike, with an array of possible interactions present. As the primary site of macromolecular digestion and subsequent nutrient acquisition, tight control of the small intestine and its contents are required to minimise microbial-related disease. Such control is often exerted through intestinal barrier function, as well as secretory methods including immunoglobulins (Ig's) and antimicrobial peptides (AMPs) (Muniz et al., 2012; Tezuka and Ohteki, 2019).

While a smaller abundance might indicate increased facilitation of determining functionality, characterisation of the small intestinal microbiota is hindered by various factors. Unlike the large intestine, whereby microbiota characterisation can be more reliably achieved by the sampling of faecal matter, the small intestinal microbiota requires more invasiveness. Understandably this can limit the ability to perform longitudinal cohort studies of the microbiota, due to issues with prolonged patient compliance, with the obtainment of samples usually during one-time surgical events, or samples obtained from autopsies (Hayashi et al., 2005; Tang et al., 2020). Even in a cross-sectional manner, determining the function of the small intestinal microbiota requires tight control of experimental methodology (Huse et al., 2014). The site of sampling must be consistent as the different species occupy both luminal and mucosal sub-environments, and are affected by overall conditional changes such as decreases in O_2 levels and increases in pH more distally, and also changes in host antimicrobial peptide (AMP) exposure (Judkins et al., 2020). On the whole, the small intestine is dominated by bacteria originating from two phyla: the *Firmicutes* and *Proteobacteria*, with predominant families consisting of *Lactobacillaceae* and *Enterobacteriaceae* although with the aforementioned

environmental changes family and genus compositions can be subject to change (Donaldson et al., 2015; Seekatz et al., 2019; Shin et al., 2019).

The reduced presence of host antimicrobial peptides and bile, in conjunction with a prolonged transit time and pH values closer to neutral allows for microbial biomass to rise up to figures of 10^{11} cells/mL, characterising the colon as a key site of microbial colonisation within the GI tract (Sender et al., 2016). While large species abundance and diversity renders this region more complex to divulge and interpret in the context of health and disease, the relative increased ease of sampling of faecal matter for metagenomic analyses has profoundly increased our knowledge. Due to the low oxygen levels present, the microbiota of the colon is distinct from other areas of the gastrointestinal tract and is highly dominated by obligate anaerobes, with the phyla *Firmicutes* and *Bacteroidetes* comprising >90% of the total abundance (Rinninella et al., 2019). While *Firmicutes* and *Bacteroidetes* often dominate, their ratio within each individual and the overall profile of the microbiota itself is usually determined by multiple factors, including mode of birth delivery, type of milk feeding, weaning, age, and general dietary habits. For example, comparisons between the typical western diet (characterised by higher protein intake) to that of rural communities in Africa or South America (characterised by diets richer in undigestible polysaccharides), reveal profound differences in both taxonomy and the functional gene profile of the communities (De Filippo et al., 2010; Yatsunenko et al., 2012). These long-term diet-induced profile changes seem to shape our “enterotypes” (Wu et al., 2011), which describes the clustering of certain bacterial groups that leads to defined cross-feeding pathways and other metabolic interactions that underly their functionality (Arumugam et al., 2011). It is therefore sensible to consider the underlying enterotype in the context of induced dysbiosis,

such different bacterial sensitivities to various classes of antibiotic (Iizumi et al., 2017) within CF.

1.2.3 Functions of the gut microbiota

Both innate and adaptive immune responses are also fine-tuned by the microbiota for optimal host outcomes (Renz et al., 2012). Early inhabitants of the GI tract play key roles in epithelial and mucosal homeostasis, alongside immune education. Molecular methods have demonstrated these roles for such inhabitants; qRT-PCR following *Bacteroides thetaiotaomicron* colonization of a germ-free mouse model demonstrates increases in the expression of genes relating to mucous layer production (*MUCLIN*) with decreases in the expression of genes relating to the suppression of the complement system (*DAF*), thereby promoting an environment that serves to reduce the likelihood of pathogenic invasion by maintaining mucosal integrity whilst eliciting no inflammatory responses in the process (Hooper et al., 2001). The development of gut-associated lymphoid tissue and the recruitment of plasma and activated T-cells to mucosal sites is also dependent on crosstalk between members of the microbiota and the host (Cerf-Bensussan and Gaboriau-Routhiau, 2010), with some resident taxa also inducing tolerogenic Treg cells that in turn helps sieve out potentially pathogenic members of the community (West et al., 2015). Thus, the resident microbiota itself can exert colonisation resistance upon taxa potentially detrimental to host health through these actions in tandem with their environmental nutrient acquisition and other aspects of metabolism (Khan et al., 2021), including the production of bacteriocins and the conjugation of bile acids that confer antimicrobial properties (Chai et al., 2023).

Throughout life, the gut microbiota continues to produce metabolites that modulate host health. Many bacterial genera from the *Firmicutes* and *Bacteroidetes* phyla

dedicate a significant proportion of their genome to encode proteins capable of degrading non-digestible polysaccharides that pass through the small intestine unscathed (Pokusaeva et al., 2011). In comparison to the human genome, which encodes less than 10 glycoside hydrolases (GH) and zero polysaccharide lyases (PL) directly dedicated to carbohydrate metabolism within digestion, the typical microbiome contained within a 'healthy' adult gut contains on average at least 50 GH and PL genes per genome (Kaoutari et al., 2013). This allows the microbiome to undertake the process of carbohydrate fermentation, in which short-chain fatty acids (SCFAs) are produced, including acetate, propionate, and butyrate. SCFAs are understood to increase protection against various diseases (including colorectal cancer and inflammatory bowel disease) due to their anti-inflammatory properties; Butyrate in particular is perhaps the most important due to the myriad of beneficial effects it has upon the host. This includes assisting in the maintenance of tight junctions at epithelial barriers (Peng et al., 2009), regulation of the inflammatory immune response (Vinolo et al., 2011; Arpaia et al., 2013), providing a source of energy for colonocytes (Donohoe et al., 2011), and also promoting satiety following meal consumption (Baxter et al., 2019).

1.2.4 Tools to investigate the gut microbiome

Techniques to study the microbiota have greatly advanced, allowing for a large expansion of our knowledge surrounding the microbiota. This is owed greatly to the shift from traditional culture-based methods into molecular analysis of the bacterial 16S rRNA gene, proposed by Woese and colleagues (Woese and Fox, 1977; Woese, 1987), which serves as a very suitable candidate. The 16S rRNA gene is ubiquitous across all bacterial species and is highly conserved, with a variety of targetable hypervariable regions. Although species-level identification is not always

attainable, the latter is relevant as different regions will confer better taxonomic resolution for certain bacterial families, which may be of interest when considering the taxa potentially implicated within a given research question (Bukin et al., 2019). As for the technology available to analyse the 16S rRNA gene, this has progressed from simple Sanger sequencing emergent of the late 1970s, with denaturing gradient gel electrophoresis (DGGE) introduced in the 1990's by Muyzer and colleagues, facilitating the investigation of multiple bacterial taxa from a given sample (Muyzer et al., 1993). Next, 454 pyrosequencing emerged and served as a huge break-through in obtaining thousands of reads per sample (Rothberg and Leamon, 2008). Today 16S rRNA gene analysis currently finds itself at a stage where very high-throughput reads are paired with increased accuracy utilising technologies such as Illumina's much improved sequencing-by-synthesis approach, providing a moderately low cost per sample with substantially increased read depth.

Aside from characterising the microbial community based on 16S rRNA sequences obtained from the site of sampling, it is possible to capture the genomic content and therefore the functional capacity of the wider microbial community. Aptly termed metagenomics, various technologies have arisen for this purpose. Illumina and PacBio employ systems utilising shotgun sequencing approaches prior to the reconstruction and alignment of contiguous sequences, whereas Oxford Nanopore utilises longer-read methods. All in all, these methods allow for the potential of novel biomarker discovery, understanding of community antimicrobial resistance profiles, and functional annotation of the wider metagenome, all likely to serve as key constituents when understanding the relationships between host and microbiota in states of health and disease.

To directly measure and profile biomarkers and metabolites of the microbiota, it is possible to survey the community metabolites through the application of

metabolomics. Again, various methodologies and technologies exist for this purpose, each with their own benefits and limitations. Therefore, the approach taken may be dependent on the research question involved and the metabolites or compounds of interest. Similar to the aforementioned DNA sequencing approaches, it is possible to profile and quantify known compounds (targeted metabolomics), or to survey the wider profile with an untargeted approach. Various methods for these exist, including the use of various chromatography techniques coupled with mass spectrometry (MS) to separate, and subsequently characterise metabolites of interest; gas-chromatography (GC-MS) is a suitable choice for the analysis of volatile compounds such as fatty acids, whereas liquid-chromatography (LC-MS) is preferable for investigating non-volatile polar compounds that might exist in complex mixtures, making it an ideal candidate for untargeted metabolomics also (Want, 2018). Nuclear magnetic resonance (NMR) spectroscopy is another technique, which takes advantage of atomic nuclei properties to infer compound structures and compositions within mixtures (Nagana Gowda and Raftery, 2021). Whilst it may not offer the same level of sensitivity needed for some low-abundant compounds (Emwas et al., 2019), NMR sample preparation is relatively straight forward and faster due to the absence of pre-separation techniques. Furthermore the absence of chemical modification or derivatisation renders samples re-usable if needed for further investigation (Emwas, 2015).

1.3 Gut microbiome differences across cystic fibrosis

1.3.1 The developing gut microbiome in cystic fibrosis

Immediately post-partum, there is evidence to suggest differences upon the composition of the intestinal microbiota in pwCF. Antosca and colleagues demonstrated a distinct microbiota composition in pwCF as compared to control infants over the first year of life, which included a reduction in *Bacteroides*, of which its members facilitate immunological tolerance development at the site of the intestinal epithelium (Antosca et al., 2019). Similarly, Hoffman and colleagues demonstrated dramatic differences across infants with and without CF, which included a significantly increased relative abundance of *E. coli* in the latter group (Hoffman et al., 2014). This was also confirmed by Kristensen and colleagues in pwCF 18 months and younger, even after controlling for confounding factors such as highly prevalent antibiotic usage (Kristensen et al., 2020). Further research confirmed previous findings, such that members of the *Bacteroidetes* decrease and *Proteobacteria* populations are increased in children with CF, correlating with supressed growth in the CF population over the first year of life (Hayden et al., 2020). The divergence between the healthy and pwCF intestinal microbiota is maintained throughout childhood, with reduced diversity sustained in the CF population with functional differences present also (Manor et al., 2016).

1.3.2 The cystic fibrosis gut microbiome in adolescents and adults

The interruption of intestinal microbiota development continues into adolescence, with evidence of particular families derived from the phyla *Firmicutes* unable to increase their abundance in pwCF as observed in healthy controls (Nielsen et al., 2016), including the *Ruminococcaceae* for which many members exert beneficial

effects upon the host through the production of short-chain fatty acids (Venegas et al., 2019). Similarly, Miragoli and colleagues used DGGE and quantitative PCR (qPCR) to demonstrate a depletion of key butyrate producers, namely *Faecalibacterium prausnitzii* and *Eubacterium rectale* in young adults with CF as compared to healthy controls of the same age (Miragoli et al., 2017). These results were somewhat replicated by Burke and colleagues, who performed a large single-centre study on the gut microbiota in adults with CF. Accompanying a decrease in *Faecalibacterium* and *Roseburia,* was an increase in *Enterococcus*, a genera well documented to demonstrate increased antibiotic resistance as compared to other commensals of the intestinal microbiota (Krista and G., 2017). What is clear from these studies is the need to further investigate changes to, and dysbiosis of, the intestinal microbiota in relation to other confounding lifestyle factors in CF. A general overview of the gut microbiota differences in pwCF, compared to healthy controls, can be seen in Figure 1.2.

1.3.3 Gut microbiome differences across different subsets of CF patients

PwCF are frequently administered antibiotics to treat the recurrent lung infections that persist as a hallmark of disease. Often described as a double-edged sword approach, the systemic effect of antibiotic usage seemingly can have knock-on detrimental effects upon the intestinal microbiota following their use to treat pulmonary issues in CF. Indeed, some impact of antibiotic usage is documented in the developing CF child, with evidence suggesting deleterious impacts upon microbiota diversity and composition. Recent antibiotic exposure has been shown to reduce alpha diversity of the microbiota and select for more potentially pathogenic *Enterococcus* species as prolonged use ensued (Kristensen et al., 2020; Loman et al., 2020). On the other hand, Vernocchi and colleagues demonstrated a milder

impact of antibiotic usage upon gut microbiota composition in children (Vernocchi et al., 2018), with a lack of impact even demonstrated for recent (>2 months) antibiotic usage within CF infants (Manor et al., 2016). The class and delivery mode of antibiotic is seemingly important, with discrepancies across the literature. Aerosol antibiotics present discrepancies, with evidence to suggest both an impacts (Li et al., 2017) and no effects (Flass et al., 2015; Vernocchi et al., 2018). The impact of IV antibiotics is unsurprisingly less conflicted, with extended administration related to further decreases in alpha diversity and the enhancement of dysbiosis as compared to heathy controls, with more pronounced shifts in larger community structures and associations with more detrimental patient outcomes (Burke et al., 2017; Enaud et al., 2019).

Given that mutation of the CFTR gene and subsequent disruption to CFTR activity is sufficient to induce microbial dysbiosis in a CF murine model (Meeker et al., 2020), it is sensible to investigate the effects of CFTR genotype upon microbiota dysbiosis as variation in residual function is evident across mutational classes. Changes are evident further down the phylogenetic tree, which includes increases in potentially harmful, and decreases in proposed beneficial genera in F508del homozygotes, as compared to heterozygotes and non-F508del carriers (Schippa et al., 2013; Dayama et al., 2020). Whilst Burke and colleagues also reported similar observations, including a significant increase in *Enterococcaceae* whilst *Ruminococcaceae* decreased, wider phylogenetic comparisons yielded no differences across pwCF harbouring severe (class I-III) and less severe (other class) genotypes (Burke et al., 2017). Interestingly, it has also been demonstrated that pwCF homozygous for F508del can contain significantly higher biodiversity and evenness compared to heterozygotes and non-carriers of this genotype (Schippa et al., 2013), however the method of analyses employed was highly limiting; Temporal temperature gradient

gel electrophoresis (TTGE) offers a much constrained examination of the microbial community as compared to sequencing-based approaches, and thus likely does not survey the true diversity and richness of a sample as reliably.

Given these results it may be the case that additional abnormalities relating to CFTR genotype are better served to predict the severity of dysbiosis in the intestinal tract. An example of this would be pancreatic insufficiency, of which around 85% of the CF population experience (Singh and Schwarzenberg, 2017). PERT therapy may not fully recover the detrimental effects of PI and subsequent malabsorption, due to poor compliance, dosage issues, reductions in effectiveness due to timing of administration, or muted effects from highly acidic intestinal environments (Freswick et al., 2022). As such, elements of malnutrition can often persist and a disturbed redox balance in the intestinal tract may arise, which has been linked with taxonomic changes to the gut microbiota outside CF (Million et al., 2016; Hankel et al., 2022). Indeed, changes have been documented with the pancreatic insufficient CF intestine as compared to PS, including decreases in *Ruminococcaceae* and *Coriobacteriaceae* (Burke et al., 2017). Other studies demonstrate reductions in diversity, both significantly (Coffey et al., 2019) and modestly over a gradient ranging from healthy controls to pancreatic sufficient, and finally insufficient pwCF (Vernocchi et al., 2017).

The absence of definitive understanding here further the highlights the need to comprehensively understand all CF-associated lifestyle factors in the context of microbial dysbiosis and potential functional consequences within the CF intestinal environment. One such CF-associated lifestyle factor may be the dietary habits of patients. Early life dietary habits, such as the breast-feeding or the switch to solid foods does not seemingly impact overall bacterial diversity (Madan et al., 2012; Loman et al., 2020). In adults, relationships between micronutrient intakes and gut

microbiota composition have been presented (Li et al., 2017), yet information surrounding wider macronutrient intake is scarce in human studies. This perhaps should be an area of research interest, given that a high-fat diet is often advised as a nutritional intervention in CF. Relationships between dietary fat intake (medium-chain triglycerides) and enhanced dysbiosis in CF murine models has been demonstrated (Debray et al., 2018), particularly with an enrichment of *E. coli*. Furthermore, Matamouros and colleagues have shown that *E. coli* strains obtained from donors with CF are very well-equipped to metabolise and use glycerol as a growth source in the CF intestinal environment (Matamouros et al., 2018).

1.3.4 The Gut-lung axis in cystic fibrosis

The 'gut-lung axis' describes the bidirectional communication between the respiratory and gastrointestinal sites in CF, which may describe direct translocation of the bacterial taxa between these sites (Al-Momani et al., 2016) or the metabolic, immune, and physiological alterations succeeding the actions of the microbiota at these sites. The relationships between intestinal microbiota and host respiratory outcomes remain to be fully elucidated as discrepancies are present in the literature. For example, in the developing infant with CF there is evidence of particular bacterial genera present at the site of the intestinal tract prior to their first detection within the respiratory microbiota (Madan et al., 2012). As for host respiratory outcomes relating to intestinal microbiota composition, Hoen and colleagues describe taxa shifts prior to initial pulmonary exacerbations and colonisation with *Pseudomonas aeruginosa* in children (Hoen et al., 2015), whilst Loman and colleagues did not find any association between bacterial taxa and exacerbation events or lung function as measured by percent predicted forced expiratory volume in one second (ppFEV$_1$%) (Loman et al., 2020). In a study encompassing both children and adolescents there

is evidence of some taxonomic shift, with members of the family *Ruminococcaceae* positively correlating with increased ppFEV$_1$%, despite no overall relationships between phyla or wider microbial diversity with lung function (Coffey et al., 2019). In adults with CF however, there is evidence of such relationships, with reduced diversity of the intestinal microbiota in pwCF with the severe decreases in lung function, and a higher relative abundance of the genus *Roseburia* in those with milder outcomes (Burke et al., 2017).

1.3.5 Relationships of the CF gut microbiome with manifestations of the lower GI tract

Further interest in the CF intestinal microbiota is attributable to its association with prevalent manifestations of the intestinal tract itself. Perhaps the most documented is that of microbial dysbiosis and intestinal inflammation, with numerous studies showing diverse relationships between the gut microbiota on intestinal inflammation. In children with CF, there are studies demonstrating variations in microbiota composition within pwCF exhibiting intestinal inflammation (Enaud et al., 2019), with significant reductions in particularly beneficial taxa as intestinal inflammation increases, including *Faecalibacterium prausnitzii* and *Lacticaseibacillus casei* (De Freitas et al., 2018; Enaud et al., 2019). Other studies demonstrate the expansion of potentially pathogenic commensals such as *E. coli* and other *Enterobacteriaceae* members (Hoffman et al., 2014; Ooi et al., 2018), with metagenomic analysis demonstrating enhanced butyrate catabolism in the CF intestine also (Manor et al., 2016). Whether this would further compound any detrimental effects of losing particularly beneficial taxa upon intestinal inflammation remains to be elucidated, as elements of functional redundancy have been demonstrated from the CF gut microbiota (Wang et al., 2019), with taxa capable of SCFA production also

increasing in abundance in those pwCF with increased inflammation (Coffey et al., 2019; Enaud et al., 2019).

Similarly, the relationship between antibiotic usage and intestinal inflammation in CF is unclear. Systemic antibiotic treatment has been shown to significantly reduce faecal calprotectin across pwCF (Schnapp et al., 2019), whilst other studies demonstrate increased faecal calprotectin as exposure to antibiotics increases (De Freitas et al., 2018; Enaud et al., 2019). Interpreting these findings is difficult due to the heterogeneous nature across these studies, which includes differences across participant age profiles, genotypes, antibiotic mode of delivery, and other patient characteristics such as intestinal symptoms.

In terms of intestinal physiology and function, again there is a paucity of knowledge surrounding the potential implications resultant of microbial dysbiosis. With respect to damage of the intestinal tract itself, Flass and colleagues have previously highlighted a potential role for the dysbiotic microbiota in pwCF. By combining capsule endoscopy scores with 16S rRNA gene sequencing data they demonstrated reduced macroscopic intestinal injury significantly associated with increased *Bacteroides*, with *Clostridium* species displaying the opposite trend (Flass et al., 2015). Intestinal function, such dysmotility is evidenced to be prolonged in the CF intestinal tract (Hedsund et al., 2012; Henen et al., 2021), yet there is no knowledge of the role played by, or associations with, the microbiota in pwCF. In murine models, the microbiota cross-talk with the enteric nervous system has been shown to modulate proper transit of material through the intestinal tract, with transit times increased in mice inoculated with conventional microbiota as compared to germ-free animals (Husebye et al., 1994). Further work demonstrated that particular species can have inhibitory effects also (Husebye et al., 2001). Perhaps unsurprisingly, CF murine models also suggest relationships between gut

microbiota and dysmotility in the intestinal tract. The majority of this work has been carried out by De Lisle and colleagues, who's work suggests that bacterial overgrowth and dysbiosis are key implications leading to smooth muscle dysfunction and subsequent intestinal dysmotility (De Lisle, 2007; De Lisle et al., 2010, 2012).

In conjunction with demonstrating intestinal lesions and morphological changes in the CF population, Flass and colleagues' findings also extend to the differences in microbiota composition across pwCF who also had CFRLD (Flass et al., 2015). In conjunction with their intestinal findings, this enables the consideration of a potential gut-liver axis in CF such that the microbiota and/or its metabolites can further compound CF-associated GI abnormalities, which is further supported in CFTR murine models (Fiorotto et al., 2011; Martin et al., 2012). A so-called 'gut-pancreas' axis is yet to be defined in CF, but may be plausible given the potential microbiota involvement in type-1 diabetes independent of CF (Zhou et al., 2020), and examples of typical gut commensals within the regulation of host glucose homeostasis (De Vadder et al., 2016). The CF intestinal tract is shown to suffer from compromised barrier function and increased permeability (Dalzell et al., 1990; Hallberg et al., 1997; De Lisle et al., 2011). As such, the translocation of potentially pathogenic taxa may arise from a 'leaky gut' in CF, which could also facilitate the progression of pancreatitis abnormalities as proposed elsewhere external to CF (Frost et al., 2020).

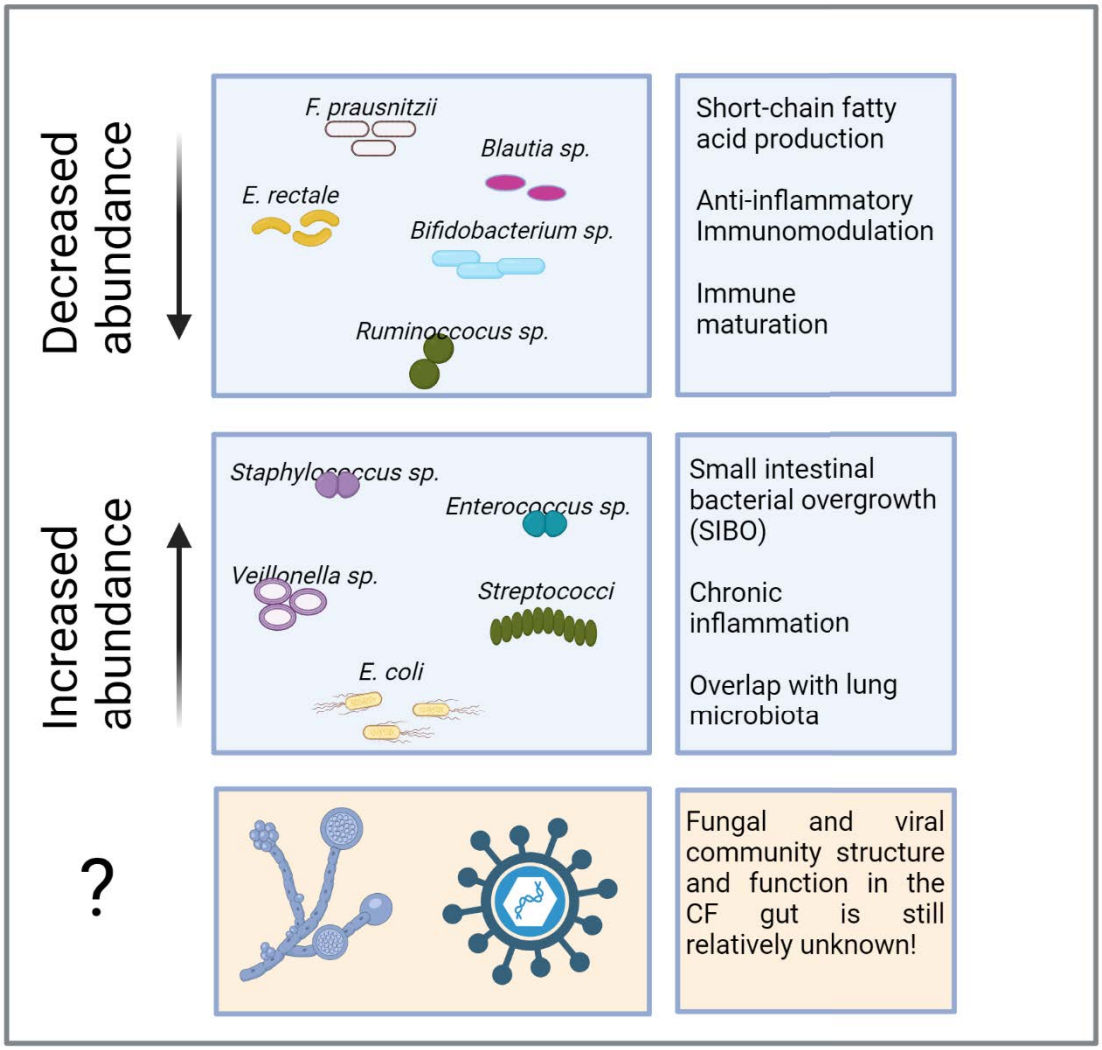

Figure 1.2 Common changes reported to the intestinal microbiota in pwCF, and the general relationships of such taxa and host function and intestinal abnormalities. The unknown impact of CF upon fungal and viral community structure is also highlighted.

1.4 Modulation of the CF gut microbiota

1.4.1 Effects of probiotics on CF intestinal health and microbiota

Given the speculation surrounding the microbiota and intestinal outcomes in CF, there have been multiple studies investigating whether probiotic administration can positively modulate microbiota dysbiosis in CF and subsequently improve patient outcomes such as abnormalities and symptoms. The probiotics administered across trials have varied, including the strains utilised and the method of administration. One of the most popular probiotics available is *Lactobacillus rhamnosus GG* (LGG), which exhibits numerous beneficial characteristics including strong mucosal adherence, production of antimicrobials, immunomodulatory pili, and anti-apoptotic protein secretion (Segers and Lebeer, 2014; Capurso, 2019). In pwCF, the earliest record of LGG use and intestinal outcome measurement was documented in children who received LGG in an oral rehydration solution, experiencing reduced episodes of abdominal pain as compared to placebo controls (Di Benedetto et al., 1998). This progressed into looking at relationships between LGG usage and clinical outcomes in a small case control series in children with CF, for which LGG administration significantly reduced faecal calprotectin and rectal nitric oxide (rNO) after the 4-week administration period (Bruzzese et al., 2004). Further insights were subsequently unravelled, incorporating microbiota analysis alongside the reporting of clinical outcomes following LGG administration in a randomly controlled trial setting (Bruzzese et al., 2014). LGG administration led to significantly increased counts of *Bacteroides* members as compared to placebo, coinciding with significant decreases in faecal calprotectin, with *Faecalibacterium prausnitzii* also increasing (non-significant) in the LGG group and *Eubacterium rectale* unchanged.

Similar to LGG, *Lactobacillus reuteri* has also been employed as a probiotic, with a wider age of participants encompassed in the respective studies. Similarly, initial insights revealed a beneficial impact upon patient symptoms, with intestinal comfort significantly increased in one study group following 6-months administration (del Campo et al., 2009). Again, subsequent work by this group expanded to demonstrate changes across the microbiota, with significant increases in *Firmicutes* and *Bacteroidetes*, and a substantial decrease in *Proteobacteria* accompanying significant decreases in faecal calprotectin levels across both children and adults with CF (Garriga et al., 2014). Di Nardo and colleagues on the other hand, failed to demonstrate such differences in faecal calprotectin when comparing shifts between *Lactobacillus reuteri* and placebo to their respective baselines across both children and adults (Di Nardo et al., 2014). In probiotic compositions containing a mixture of bacterial strains, the underlying narrative remains consistent. Improvements to patient symptoms (del Campo et al., 2009) and faecal calprotectin levels (Fallahi et al., 2013) have been shown across children and adolescents, including enhancements to intestinal epithelial integrity as improvements to permeability succeed probiotic usage (Van Biervliet et al., 2018). Despite this, the latter study did not unearth associations between probiotic usage, notable shifts in microbiota composition, and intestinal inflammation. The ambiguous and complex relationships between probiotic usage and clinical outcomes further extend to the gut-lung axis, whereby there is both evidence of no effect (del Campo et al., 2014), but also improvements to respiratory outcomes such as reductions in pulmonary exacerbations (Jafari et al., 2013) and improvements to lung function (Bruzzese et al., 2007).

1.4.2 Effects of CFTR modulator therapy on the CF gut and microbiota

As CFTR modulator therapy becomes the forefront of treatment for the vast majority of pwCF (Despotes and Donaldson, 2022), and demonstrates beneficial impacts upon the respiratory domain of disease (Gramegna et al., 2020), there is hope that this also extends to the site of the GI tract. This includes the restoration of CFTR function that may subsequently restore normal luminal and mucosal physiology, thereby also positively modulating the inhabiting microbial community and their functional output. This is perhaps plausible, given that the dysfunction of CFTR function alone is sufficient to drive microbial dysbiosis (Vernocchi et al., 2018; Meeker et al., 2020).

As research has progressed, treatments have shifted from a state of monotherapy, to combined treatments that allows for an increased repertoire of targetable mutations; the potentiator Ivacaftor was the first CFTR modulator developed that ultimately became available for pwCF harbouring the G551D mutation or other gating mutations (class III) (Van Goor et al., 2009). Despite its availability since 2012, very little is known about the effects of Ivacaftor upon the microbiota. In 2018, Ooi and colleagues investigated its use in a small cohort containing adults and children with at least one copy of G551D (Ooi et al., 2018). Whilst major phylogenetic changes did not occur following usage, there were more niche changes, such as increases in *Akkermansia*, a typical commensal bacteria of the intestinal mucosal layer (Belzer and de Vos, 2012) often associated with healthy controls when compared to diseased counterparts across other conditions such as inflammatory bowel disease (Png et al., 2010). Furthermore, Ivacaftor usage significantly decreased faecal calprotectin levels, which also correlated with decreased abundances of *Enterobacteriaceae*. Whilst larger-scale community changes were vacant, this preliminary data highlights the potential implications of

particular taxa in CF intestinal abnormalities. More recently, Ronan and colleagues investigated changes to the microbiota pre- and post-Ivacaftor usage in a cohort of G551D pwCF ranging from 3-12 months of usage, with no significant differences in community diversity metrics, compositional structure, or specific taxa across the sampling points (Ronan et al., 2022). Given that faecal calprotectin also failed to decrease across these patients, the study still lends support to the notion of microbiota involvement within intestinal inflammation.

Kristensen and colleagues also explored Ivacaftor usage and microbiota outcomes more recently, however in pwCF containing the S1251N mutation (Kristensen et al., 2021). Whilst the respiratory microbiota structure remained unchanged, at the site of the intestinal tract significant increases in microbial diversity and changes to microbiota composition ensued. More specifically this occurred 12 months post Ivacaftor treatment, implying time dependence of treatment and potential resilience of the CF microbiota.

The development of further modulators such as Lumacaftor enabled the recovery of CFTR processing in F508del homozygotes to a level representative of milder CFTR function, which led to its dual use alongside Ivacaftor to treat those with the F508del mutation (Van Goor et al., 2011). This has been studied in children and young adults, whereby the administration of Lumacaftor/Ivacaftor in F508del carriers failed to elicit changes in microbiota diversity or structure, yet subtle (non-significant) changes in bacterial phyla occurred (Pope et al., 2021). This includes increases in *Actinobacteria* and *Firmicutes*, whilst *Bacteroidetes* and *Proteobacteria* generally decreased. The use of another corrector, Tezacaftor alongside Ivacaftor allows further widening of targetable patient genotypes, such as the ability to enhance activity of the CFTR protein in F508del/G551D compound heterozygotes (Donaldson et al., 2018). Despite this, no information exists surrounding

Tezacaftor/Ivacaftor (Tez/Iva) usage and microbiota changes. Furthermore, the advancement of CFTR modulators has extended to the stage of triple-combination therapy (Ridley and Condren, 2020) in the form of Elexacaftor/Tezacaftor/Ivacaftor, which is administrable to the vast majority of pwCF and offers improved efficacy in the respiratory domain of disease for F508del carriers as compared to previous treatments (Middleton et al., 2019). As such, the CF community eagerly awaits information surrounding the impact of Elexacaftor/Tezacaftor/Ivacaftor (ETI) upon the intestinal microbiota and associated GI abnormalities and symptoms.

1.5 Summary and Aims

In summary, there is much interest surrounding the role of microbiota in CF intestinal health and disease, with interpretations across study results perhaps confounded by the wide array of clinical variables in the CF population. This includes (but not limited to), severity of *CFTR* mutation and subsequent CFTR protein dysfunction, pancreatic insufficiency, antibiotic usage, patient age, and dietary habits. The over-arching aim of this thesis is to expand on our current knowledge of the organisation and function of the gut microbiota in CF by further understanding such relationships between the microbiota with clinical outcomes, patient symptoms, and current treatments in CF (depicted in Figure 1.3).

More specifically, this includes:

1. Investigating the relationships between the CF gut microbiota, clinical outcomes alongside direct intestinal physiology and transit functional aspects, which has not yet (to the best of knowledge) been performed.
2. Elucidating the impact of more efficacious CFTR modulator therapies in the context of the CF gut microbiota, and how this also relates to the aforementioned clinical outcomes. This will directly address a current gap in the literature, as the effects of double and triple-combination therapies upon the microbiota are poorly understood.
3. Developing and integrating additional -omic approaches, such as targeted faecal metabolomics of short-chain fatty acids to understand functional aspects of the microbiota as compared to healthy controls, and upon usage of CFTR modulator therapy.

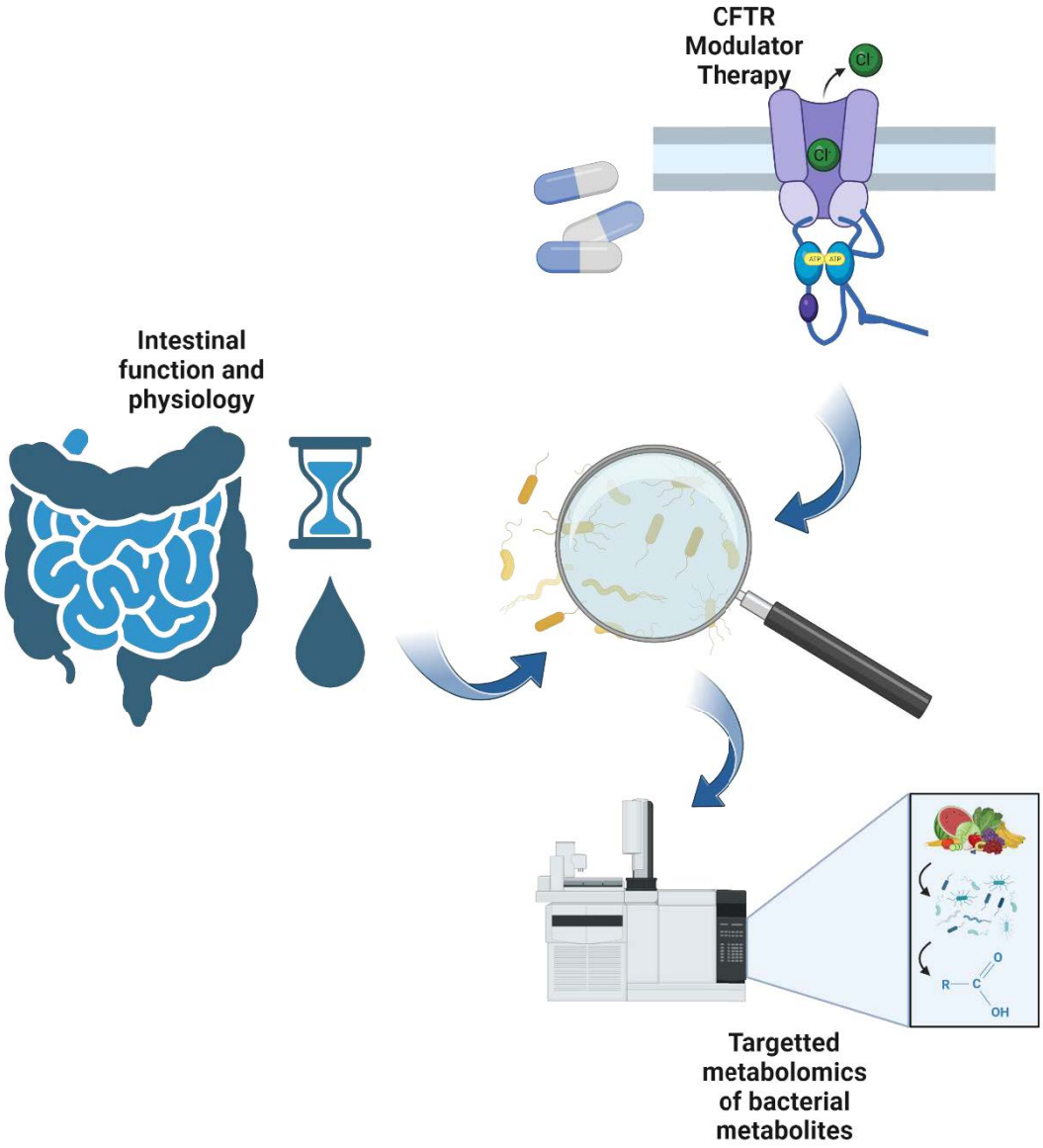

Figure 1.3 Illustration of the over-arching aims of this thesis. Relationships between the microbiota and clinical outcomes (including intestinal function) will be investigated, alongside impact of CFTR modulator therapies on the aforementioned. Targeted metabolomics will be used in tandem to better understand microbiota functionality.

Chapter 2: Materials and methods

2.1 Study characteristics and ethics

2.1.1 GIFT-CF1

Study Title: A Case-Control, Observational Study of the Postprandial Changes in Magnetic Resonance Imaging Parameters of Gastrointestinal Function in People with Cystic Fibrosis.

Relevant Thesis Chapter: Chapters 3 and 4

IRAS Project ID: 247028

REC Reference: 18/WM/0242

12 CF patients and age/gender matched controls were initially recruited, with stool samples ultimately collected for 10 CF patients (6 males;4 females, Mean age of CF patients, 19.3 ± 7.93 years, Median age, 19 years) and of 10 non-CF healthy controls (Mean age of controls, 21.4 ± 7.40 years, Median age, 20 years). Patients were under a period of clinical stability and abstained from taking laxatives and anti-diarrhoeal drugs during this visitation but were able to take routine pancreatic supplementation and perform standard physiotherapy procedures, with routine prophylactic antibiotic therapy recorded where applicable.

2.1.2 GIFT-CF2

Study Title: A Randomised Cross-Over Pilot Study of the Effects of Tezacaftor/Ivacaftor and Ivacaftor combination regimen on Gastrointestinal Function using Magnetic Resonance Imaging Parameters in People with Cystic Fibrosis.

Relevant Thesis Chapter: Chapter 5

IRAS Project ID: 254559

REC Reference: 19/WM/0130

14 pwCF, homozygous for F508del, were initially recruited from Nottingham University Hospitals NHS Trust, with 12 pwCF (mean age at baseline, 20.8 ± 7.80 years [± SD]) ultimately providing samples available for inclusion in the analyses. Individuals were enrolled into a double-blind, placebo-controlled randomised trial with Tezacaftor/Ivacaftor (Symkevi^{TM}) or placebo. Treatments were administered for 28 days with an intermediate 28-day washout period. At baseline, and between day 19 and 23 of each phase of treatment, participants attended clinic to provide faecal samples and have clinical assessments undertaken, including completion of the validated PAC-SYM and CFAbd-Score questionnaires to assess gut symptoms (Frank et al., 1999; Jaudszus et al., 2019). Additionally, faecal samples from 10 age-matched healthy controls from our previous study were available for microbiota and metabolomic comparison (Marsh et al., 2022). Participants were asked to fast overnight, and prior to, their visit refraining from the use of laxatives and anti-diarrhoeal drugs during time at clinic. Regular pancreatic enzyme replacement therapy and physiotherapy procedures were admitted.

2.1.3 GIFT-CF3

Study Title: Gut Imaging for Function & Transit in CF - GIFT-CF 3: Evaluation of Triple Combination Therapy.

Relevant Chapter: Chapter 6

IRAS Project ID: 281133

REC Reference: 20/PR/0508

24 pwCF harbouring the F508del mutation were originally recruited from Nottingham University Hospitals NHS Trust with 20 pwCF (mean age at baseline, 21.0 ± 8.6 years [± SD]) ultimately completing the study in some way adequate for subsequent analysis. Participants donated faecal samples at baseline and following the administration of Elexacaftor/Tezacaftor/Ivacaftor for 3, 6, or an extended (19.8 ± 2.0 months [mean ± SD]) period of months, to form an observational study observing the effects of triple combination modulator therapy upon the gut microbiota. Additional faecal samples and metadata for 10 age and sex-matched healthy controls from previous studies (Chapters 3 and 5) were available for microbiota and metabolomic comparison also. During visits to clinic participants provided faecal samples and completed magnetic resonance imaging (MRI) scans following the consumption of a standardised meal plan to detail their gut function as conducted previously (Chapters 3 and 5), alongside specifying gut symptoms. This included the validated PAC-SYM questionnaire (Frank et al., 1999). Participants were asked to fast overnight before attending clinic and withhold any medications impacting bowel habit, such as laxative treatment. Regular pancreatic enzyme replacement therapy, antibiotic regimes, and other CF-related medications were continued.

2.2 Sample processing and laboratory techniques

2.2.1 Initial storage, processing and washing of samples

All samples were stored at -80°C in house at the John Dalton Building. Approximately 150 mg of thawed stool was transferred to a 15 ml centrifuge tube containing 1.5 ml sterile PBS and vortexed thoroughly to mix. Following this, the mixture was centrifuged at 3200 x *g* for 5 minutes. The resultant pellet was resuspended in 500 µl PBS prior to PMA treatment. All sample types were thawed out before washing and subsequent DNA extraction, with less than 3 freeze/thaw cycles to reduce bias from altered community composition over time (Gorzelak et al., 2015).

2.2.2 Propidium monoazide (PMA) treatment

1 mg PMA (Biotium, CA, USA) was hydrated in 98 µl 20% dimethyl sulfoxide (DMSO) to give a working stock concentration of 20 mM. 1.25 µl of PMA (20 mM) was added to 500 µl resuspended cells from the pre-processed faecal samples in an opaque Eppendorf tube to give a final concentration of 50 µM. Following the addition of PMA, samples were mixed by vortexing for 10 seconds, followed by incubation for 15 minutes at room temperature (~20°C). This step was repeated again, before the transfer of samples to clear 1.5 ml Eppendorf tubes and placement within a LED lightbox. Treatment occurred for 15 minutes to allow PMA intercalation into DNA from compromised bacterial cells. Samples were then centrifuged at 10,000 x *g* for 5 minutes. The supernatant was discarded, and the cellular pellet was resuspended in 200 µl PBS.

2.2.3 DNA extraction methods

Following PMA treatment, cellular pellets resuspended in 200 µL PBS were loaded into the ZYMO Quick-DNA Fecal/Soil Microbe Miniprep Kit (Cambridge Bioscience, Cambridge, UK) as per the manufacturer's instructions, with the following amendments; ZR BashingBead Lysis Tubes were replaced with standard 1.5 mL Eppendorf tubes loaded with ZYMO Beads for mechanical homogenisation with the use of a RETSCH Mixer Mill MM 400 (Retsch, Haan, Germany). Samples were homogenised for 2 minutes at 17.5/s frequency.

Following the availability of a FastPrep-24™ 5G bead beating grinder and lysis system (MP Biomedicals, France), this replaced the RETSCH Mixer Mill MM 400 due its suitability for use with the ZYMO ZR BashingBead Lysis Tubes, and also for the processing of mock community standards, therefore reducing the time within the extraction workflow and increasing extraction validity. Cellular pellets resuspended in PBS were added to tubes according to the manufacturers' instructions and lysed at a speed of 6.0 m/s for 40 seconds.

2.2.4 2-step PCR strategy

2.2.4.1 Targeted amplicon sequencing – Bacterial 16S rRNA

Step 1 amplicon generation with primers based on the universal primer sequences 515F and 926R as described previously (Walters et al., 2016), was performed under the following conditions; Initial denaturation of 180 seconds at 98°C, followed by: 25 cycles of 30 seconds at 95°C, 30 seconds at 55°C and 30 seconds at 72°C. A final extension of 5 minutes at 72°C was also included to complete the reaction. Step 2, the addition of dual barcodes and Illumina adaptor sequences was performed under the following conditions: Initial denaturation of 30 seconds at 98°C, followed by: 10

cycles of 10 seconds at 98°C, 20 seconds at 62°C and 30 seconds at 72°C. A final extension of 2 minutes at 72°C was also included to complete this reaction. This resulted in the generation of a ~550 bp amplicon spanning the V4-V5 hypervariable regions of the 16S rRNA gene.

2.2.4.2 Targeted amplicon sequencing – Bacterial 16S rRNA gene with integrated phasing

Whilst the 2-step PCR approach mentioned previous was successful in generating adequate paired-end sequencing data for gut microbiota analysis, the 16s rRNA gene regions exhibit relatively low sequence diversity. Thus, base calling during the interpretation of emission spectra from the fluorescently labelled reversible terminator-bound dNTPs (A, C, G, and T) is hindered, as highly homogenous signals present across the entire flow cell prevent accurate cluster identification during the initial cycles of sequencing, alongside potentially reducing reads passing Illumina's chastity filter (%PF) (Kircher et al., 2009; Schirmer et al., 2015). Subsequently, this leads to poor fluorophore interpretation of subsequent reads, thereby reducing the number of reads passing the quality threshold, lowering the average quality scores (Q30), and in-turn decreasing in the yield of sequencing data. Whilst these issues can be partially alleviated with the addition of a control spike-in library such as PhiX, yet this can still significantly reduce sequencing yield dependent of the spike (%) necessary to provide adequate base diversity in the first few cycles of sequencing (Nelson et al., 2014).

Another approach to attain sufficient base diversity is the introduction of heterogenous 'N' spacers between the locus of interest (16S rRNA region) and the sequencing overhang adaptor that allows the addition of barcodes for subsequent demultiplexing and sample identification following sequencing (Wu et al., 2015;

Jensen et al., 2019). ‘N’ bases can be inserted upstream of the locus to create ‘phased’ primers, in which an artificial frameshift is introduced, thereby increasing the diversity of the initial bases read. Indeed, this approach has been successfully implemented across multiple of Illumina systems including The HiSeq and MiSeq platforms, with improved murine gut microbiome analysis attributed to the implementation of spacer regions resulting in enhanced nucleotide diversity (Jensen et al., 2019; Naik et al., 2020).

The use of heterogenous spacers was therefore implemented, with custom primers containing heterogenous ‘N’ spacers (N-NNNN) upstream of the 16S rRNA gene V4 and V5 regions. Following verification of amplification success, equal volumes of each 5 µM V4 forward (N-NNNN) and V5 reverse (N-NNNN) primer was pooled prior to the original 2-step PCR protocol.

To determine if the use of the heterogenous ‘N’ spaced primers was likely to elicit any amplification bias during the 1st step PCR, amplification of a mock community was performed, before the addition of barcodes and sequencing on the Illumina MiSeq platform. Downstream sequencing processing and statistical approaches (Chapter 2.3) were utilised. Analysis of the ZYMO Gut Microbiome Standard mock community, which contains a mixture of bacterial species native to the human gut across various phyla, demonstrated no significant differences in the community compositions measured (Table 2.1).

Table 2.1 Microbiota compositional analysis between original and phased V4-V5 16S primers

Sample	Bray-Curtis		Sørensen-Dice	
	ANOSIM	PERMANOVA	ANOSIM	PERMANOVA
ZymoBIOMICS® Gut Microbiome Standard	0.3348	0.3335	1	1

The ZymoBIOMICS® Gut Microbiome Standard was amplified in replicate with both the original, and phased V4-V5 primer set under the same PCR conditions and library preparation workflow. The mock community contains a defined composition of bacterial taxa, which were shared between individual sequencing samples. *p* values are given.

2.2.4.3 Clean-up of products from PCR

PCR clean-up was performed in two different ways. The initial method (Chapter 3) utilised the ZYMO DNA Clean & Concentrator-25 kit following the initial PCR reaction. Following Barcode attachment in the second PCR step, samples were cleaned and subsequently normalised using the SequalPrep™ Normalization Plate Kit (Thermo Fisher Scientific), pooled and diluted to the final library concentrations requited for use on the Illumina MiSeq system.

The later method utilised (Chapters 5 and 6) was with the use of solid-phase reversible immobilization (SPRI) beads to enable size selection of resultant products from the PCR reaction. Agencourt AMPureXP beads (Beckman Coulter, Brea, CA, USA) were used as per the manufacturer's instructions. For 16S rRNA gene amplicons, a 0.8x ratio of beads to PCR product was typically used to isolate amplicons > 300 bp, before subsequent washes with 70% ethanol and elution with 1X TE Buffer. For PCR reactions whereby alternate amplicons may have been produced, the desired final product (~550 bp) was obtained using a double-sided size selection approach. A 0.59x ratio of beads to PCR product was isolate fragments < 600 bp in the resulting supernatant. This was then taken forward, with additional beads added to a ratio of 0.8x, thereby eluting fragments ~300-550 bp in the final stage of the protocol.

2.2.5 Library quantification, normalisation, and pooling

Following DNA extraction and both PCR steps, DNA products were quantified using the Qubit dsDNA HS Assay Kit (high sensitivity, 0.2 to 100 ng) on the Qubit 3.0 fluorometer (Life Technologies) as per the manufacturer's protocol. For DNA samples, a volume of 2-10 µl was added to 190-198 µl of the prepared Qubit working solution to give a final volume of 200 µl. In some cases, particularly where off-target amplicons of different size were generated in the library preparation, a qPCR NGS Library quantification kit (Agilent Technologies, Santa Clara, CA) was utilised for increased accuracy of quantification.

Library normalisation was carried out either manually by dilution with distilled water to a defined concentration (nM), or with the SequalPrep Normalization Plate Kit (Invitrogen, Carlsbad, CA, USA) according to the manufacturer's instructions. Following quantitative normalisation (1-2 ng/µl per well for the SequalPrep Normalization Plate Kit), equal volumes were pooled to form the final library. The concentration of this final library was calculated with the Qubit 3.0 fluorometer as mentioned previous and the average library size was calculated using both agarose gel electrophoresis and with a DNA 1000 chip on the Aligent 2100 Bioanalyzer (Agilent Technologies, Santa Clara, CA). These values were then used to calculate the final library concentration in nM with the following equation:

$$\frac{(\text{concentration in ng/µl})}{(660\ \text{g/mol} \times \text{average library size})} \times 10^6 = \text{concentration in nM}$$

2.2.6 Library denaturation and dilution for use with the Illumina MiSeq

The final library concentration was then diluted to meet the specifications required within the Illumina MiSeq System Denature and Dilute Libraries Guide, typically 2-4 nM prior to dilution and denaturation to 6-20 pM.

PhiX Control v3 was used as a sequencing control, typically at a 10-20% spike in dependent on the anticipated diversity of the library, to determine the quality of cluster generation, error rates, and calibration throughout the sequencing experiment.

2.2.7 PCR and sequencing controls

PCR and DNA extraction negative controls were implemented, alongside the use of positive controls. This included DNA extracts from species commonly isolated from CF sputum such as *P. aeruginosa*, *S. aureus*, *S. maltophilia*, *B. cepacia* complex and a ZYMO Gut Microbiome Standard (Cambridge Bioscience, Cambridge, UK) mock community.

2.2.8 GC-MS

2.2.8.1 Chemicals and Standards

Analytical grade of hydrochloric acid (HCl), anhydrous diethyl ether (DE), anhydrous sodium sulphate (Na_2SO_4), and MS grade water were purchased from Fisher Scientific (Loughborough, UK). The ^{13}C-short chain fatty acids stool mixture, N, O-bis(trimethylsilyl)trifluoroacetamide) (BSTFA), and volatile free fatty acid mix were

purchased from Merck Life Science (Poole, UK). Helium CP grade was used as the carrier gas (99.999%, BOC Limited, UK).

2.2.8.2 Faecal sample processing, extraction and derivatisation

All faecal samples were stored at - 80°C prior to sample processing. Samples were ground and homogenised using liquid N_2. Approximately 50 mg of ground faecal sample was added to a ZYMO™ 2 mL screw cap microtube containing ultra-high density, chemically inert beads (Cambridge Bioscience, Cambridge, UK). 0.5 mL of MS grade water was added, including the internal standard (IS) mixture containing 30:10:10 µM of (sodium) acetate, propionate and butyrate respectively. Samples were then further lysed and aqueously homogenised utilising the FastPrep-24™ 5G system, with two cycles at a speed of 6.0 m/s for 40 seconds. Next, samples were mixed at 80 rpm for 30 minutes in a HulaMixer whilst incubated at 4°C.

After mixing, samples were centrifuged at 13,000 x *g* for 30 minutes at 4°C. The faecal water supernatant containing SCFAs was removed, before 150 µL was added to a Lo-Bind Eppendorf tube over ice containing 15 µl of 5 M HCl to protonate the sample. 3.15 µl internal standard was also added, alongside 150 µl DE. Samples were then vortexed for 10 seconds before mixing for 15 minutes utilising the HulaMixer as previously described. Samples were then centrifuged at 10,000 x *g* for 5 minutes at 4°C. The DE layer containing volatile fatty acids was then accurately transferred to a Lo-Bind Eppendorf tube pre-loaded with 25 mg Na_2SO_4 to remove residual water. The remaining layer was then re-extracted with another 150 µL DE as before. The two extraction tubes were then centrifuged at 10,000 x *g* for 1 minute to ensure sedimentation of Na_2SO_4 prior to combination by equal volume. 40 µl of the pooled sample was transferred then an amber GC vial with a fused insert, 2 µl BSTFA was added, vortexed for 5 seconds, and then capped tightly and incubated

at 37°C with constant shaking for 3 hours. Following derivatisation, all samples were immediately quenched on ice before GC-MS analysis.

MS grade water was used as a blank sample to correct the background. Independent blank samples were processed with the same method as faecal samples and acquired along the acquisition. The corrected peak areas of SCFAs were calculated by those peak areas of samples minus that of the average blank sample detected under the same conditions and along the same acquisition.

2.2.8.3 GC-MS parameters

GC-MS analysis was carried out using an Agilent 7890B/5977 Single Quadrupole Mass Selective Detector (MSD) (Agilent Technologies) equipped with a non-polar HP-5ms Ultra Inert capillary column (30 m × 0.25 mm × 0.25 µm, Agilent Technologies). Helium was used as the carrier gas at a flow rate of 1 mL/min, and methanol and hexane were utilised for pre- and post-wash. Agilent 7693 Autosampler was used to inject 1.0 µL of the derivatised sample at a split ratio of 20:1 at 265°C, with a solvent delay of 2 minutes 30 seconds. The initial oven temperature was held at 40°C for 2 minutes, followed by a 10°C/min temperature ramped to 140°C, increased to 300°C at the rate of 40°C/min and kept at this temperature for 6 minutes. Electron impact (EI) mode ionisation was utilised at 70 eV, with the instrumental parameters set at 230, 150 and 300°C for source, quadrupole and interface temperatures, respectively.

SCFA identification was achieved by combining pure reference mix standards and the NIST 2005 MS library (Standard Reference Data Program, National Institute of Standards and Technology, Gaithersburg, MD. Standard Reference Database IA., n.d.). Selected ion monitoring (SIM) mode was used for quantification; all

confirmation and target ions lists are summarised in Table 4.1. Agilent MassHunter workstation version B.07.00 programs were used to perform post-run analyses.

2.2.8.4 Method Validation

The GC-MS method validation was carried out by establishing specificity, linearity and range, precision, accuracy, recovery, limit of detection (LOD) and limit of quantification (LOQ). Before acquisitions, system suitability test (SST) was conducted to assess the GC-MS system for no interferences present, sensitivity and repeatability using 5 µM of extracted and derivatised reference standard mix. Percentage relative standard deviation (%RSD) of the peak areas and retention times (RT), signal to noise of all five injections were calculated.

2.2.8.5 Specificity

The specificity of the method was studied by overlay of chromatograms obtained from blanks, reference mix standards, spiked and un-spiked, and degradation samples tested for interferences and resolution, using the follow formula:

$$Resolution = \frac{(t_2 - t_1)}{0.5\ x\ (W_1 + W_2)}$$

where t_1 and t_2 represent the retention times of peaks 1 and 2, and $W_{1/2}$ and $W_{2/2}$ represent the widths at half height of the peaks.

2.2.8.6 Linearity and range

Linearity was determined by constructing individual SCFA calibration curves over the concentration range, 5 and 2500 µM, using a reference standard mix of volatile

fatty acids. A single stock mix standard of 2860 µM after extraction and derivatisation was prepared and diluted into 5, 50, 500, 1000, 2000 and 2500 µM with 30:10:10 µM of ^{13}C-sodium acetate, propionate, and butyrate respectively. The range was determined based on acceptable linearity, precision, and accuracy. The calibration curves were established by plotting the average corrected peak areas of SCFA standards (triplicates) by those peak areas minus that of the average blank sample detected to remove background under the same conditions and along the same acquisition. The linear regression equation and correlation coefficient were calculated using XLSTAT v2021.1.1 (Addinsoft, Paris, France).

2.2.8.7. Precision - Repeatability

Precision and accuracy of the method were determined by an intra-day and inter-day analysis across a range of concentration of the calibration standards. Nine individual fatty acid standards covering the specific range were prepared and injected in triplicate according. The resulting peak area was used to calculate the %RSD and thus precision along the range concentration. Moreover, %RSD of the obtained retention times for each analyte for 6 injections was calculated to predict the retention time repeatability of the method.

2.2.8.8 Recovery assay - Accuracy

For extraction recovery, the above extraction and derivatisation procedure was implemented across the linearity range of the method, and three independent faecal human samples were prepared where pre- and post-spike across a wide level of concentrations (5, 500 and 1000 µM) of the standard free mixture of fatty acids were prepared. The post-spike was reconstituted the same way as the pre-spike to make

a direct comparison. All fatty acids extract peak areas from pre-, and post-spike and samples were used to calculate the percentage recovery using the following formula:

$$\%\ Recovery\ =\ \frac{(Peak\ area\ of\ pre-spike)}{(Average\ peak\ area\ of\ n\ pos-spike,\ where\ n\geq 3)}\ x\ 100$$

2.2.8.9. Limit of detection (LOD) and limit of quantification (LOQ)

Limit of detection (LOD) and limit of quantification (LOQ) are two important performance characteristics in method validation for sensitivity and quantification. LOD and LOQ were calculated based on the standard deviation of the response (Sy) of the curve and the slope of the calibration curve (S) at levels approximating the LOD according to the formula: LOD = 3.3 x (Sy/S), and the LOQ according to the formula: LOQ = 10 x (Sy/S). The standard deviation of the response was determined based on the standard deviation of y-intercepts of regression lines.

2.2.8.10 Matrix effects

To determine the presence of any matrix effects within faecal samples, the following equation was used across samples spiked with 5, 500 and 1000 µM of the reference fatty acid mixture:

$$Matrix\ Effect\ =\ \frac{\left[1-\left((Peak\ Area\ of\ SPS)\ -(Peak\ Area\ of\ SWS)\right)\right]}{(Average\ Peak\ Area\ of\ n\ neat,\ n\geq 3)}\ x\ 100$$

where SPS and SWS represent the samples pre-spiked and sample without spiked respectively. The corrected peak areas of pre-spiked samples were calculated by those peak areas of pre-spiked samples minus that of the average blanks and samples prepared and acquired under the same conditions. This procedure will clean the background and provide the correct peak area for the reference standards added to compare with independent standard samples.

2.2.8.11 Stability

After collection, all human faecal samples were stored at -80°C. Ground and homogenised faecal samples were stored at - 80°C and analysed on different days. Extract and derivatised samples were quenched on ice immediately after derivatisation, before loading onto the GC-MS prior to injection, which occurred at room temperature. Samples were stored at - 20°C degrees for inter-day analyses.

Following normalisation with the internal standard, the relative signal of each acid was used as to determine the profile. For absolute quantification, the addition of a calibration curve containing the normalised volatile fatty acid reference mix was implemented. After identifying the concentration of the sample using the calibration curve in μM, the dilution factors of the extraction (1:4) and derivatisation process (1:1.05) were applied to give the theoretical initial concentration of the sample. Next, the number of the moles of each acid in the starting sample was calculated by scaling to the original starting volume of the sample for homogenisation. Finally, number of moles was scaled up alongside the weight of the sample (weighed as closely to 50 mg as possible), to 1 kg, giving a final concentration of the acids as mmol/kg.

2.2.8.12 Profiling and quantification of short to medium-chain fatty acids

The integrated peak area was initially normalised, using the added internal standard consisting of ^{13}C-acetate, propionate, and butyrate. Following investigation of the fragmentation patterns of acetic, propionic, and butyric acid from the reference mix, based on the total ion count (TIC) scan (Figure S4.1), it was determined that only ^{13}C-butyric acid was suitable for subsequent normalisation and quantification. This was due to an overlap in fragmented ions produced by the ^{13}C and standard C isotopes of acetic (119 m/z) and propionic acid (134 m/z). Butyric acid did not produce the fragment of 149 m/z observed in the ^{13}C standard, therefore was designated as the target ion for quantification of the ^{13}C internal standard.

Following normalisation with the internal standard, the relative signal of each acid was used as to determine the profile. For absolute quantification, the addition of a calibration curve containing the normalised volatile fatty acid reference mix was implemented. After identifying the concentration of the sample using the calibration curve in µM, the dilution factors of the extraction (1:4) and derivatisation process (1:1.05) were applied to give the theoretical initial concentration of the sample. Next, the number of the moles of each acid in the starting sample was calculated by scaling to the original starting volume of the sample for homogenisation. Finally, number of moles was scaled up alongside the weight of the sample (weighed as closely to 50 mg as possible), to 1 kg, giving a final concentration of the acids as mmol/kg.

2.3 Bioinformatics and statistical approaches

2.3.1 FASTQ sequence processing

Following demultiplexing of sequences directly from the Illumina MiSeq platform, samples with the inclusion of heterogenous 'N' spacers were initially passed through Cutadapt v3.5 on Ubuntu 20.04 (Martin, 2011). The command "--action=retain" was used to identify the locus of the 16S rRNA gene for each forward (V4;515F) and reverse (V5;926R) read, trimming everything upstream including the 'N' spacers and Illumina overhang adaptors. "--max-n 0" was used to discard any reads with ambiguous 'N' nucleotides following sequencing. "-m 1" was implemented that all sequences passing through the pipeline exceeded 1 bp, as to minimise any downstream issues in the bioinformatics pipeline. Any untrimmed reads were discarded with "--discard-untrimmed". The error rate of the locus to be identified was set to 20%, using the command "-e 0.2".

Any reads passing through the Cutadapt pipeline, or FASTQ files directly attained following demultiplexing from the Illumina MiSeq (no heterogenous 'N' spacers) were subsequently processed in R (Version 4.0.1) using the package DADA2 (Callahan et al., 2016). DADA2 was used to remove primer sequences, before validation of forward and reverse read quality. Following read trimming, sequence variants were inferred and denoised paired reads were merged, with the removal of chimeras also. Finally, taxonomy was assigned utilising Naïve Bayesian Classifier Implementation, with the use of the Genome Taxonomy Database (GTDB) reference sequences (Parks et al., 2018), or the dedicated human intestinal 16S rRNA gene reference database (Ritari et al., 2015).

Any amplicon sequence variants (ASVs) were deemed unidentifiable following this procedure were BLAST searched (https://blast.ncbi.nlm.nih.gov/Blast.cgi) and labelled based on query coverage where appropriate. Taxa lacking ≥2 reads for a

single sample were discarded and removed from subsequent statistical analyses. Following ASV identification, ASVs from the same bacterial species were collapsed to form a single operational taxonomic unit (OTU) for a given taxon. The R package decontam was used to remove any potential source of contamination across samples (Davis et al., 2018), utilising the prevalence-based contamination identification approach with a threshold classification of $P = 0.1$.

2.3.2 Distribution abundance relationships

Regression analysis, including calculated coefficients of determination (r^2), degrees of freedom (df), *F*-statistic and significance values (*P*) were utilised for microbial partitioning into common core and rarer satellite groups based on significant distribution abundance relationships, and were calculated using XLSTAT v2021.1.1 (Addinsoft, Paris, France). This methodology originates from previous usage to demonstrate ecological patterns of species persistence and abundance over time in a single habitat in a temporal fashion (Magurran and Henderson, 2003; Magurran, 2007; van der Gast et al., 2011). Core taxa were identified as those that fall up in the upper quartile of distribution across a given group, whilst satellite taxa were those below this measure.

2.3.3 Alpha diversity measurement

To determine the diversity of the microbiota within each sample, the Fisher's alpha index was calculated from the finalised OTU tables of samples within their respective studies using PAST (Hammer et al., 2001). Incorporating both richness and evenness throughout a sample, this particular method was also used as it is less affected by differences across sequencing depth that can often occur whilst

sequencing many samples during a single experiment on the Illumina MiSeq platform (Fisher et al., 1943; Beck and Schwanghart, 2010).

2.3.4 Beta diversity measurement

To determine compositional differences between groups of interest, the Bray-Curtis index was utilised, to measure the bacterial compositional dissimilarity between the groups tested (Bray and Curtis, 1957), again using PAST. These dissimilarity values were subsequently used for analysis of similarity (ANOSIM) or permutational multivariate analysis of variance (PERMANOVA) calculation with Bonferroni correction in PAST. When comparing the sequencing results obtained between original and phased primers of the 16S rRNA gene upon the Gut Microbiome Standard, use of the Sørensen-Dice was also included. As this measures similarity based on presence/absence of taxa (Dice, 1945), it demonstrated that all members of the mock community, regardless of relative abundance were able to identified across both primer strategies. To graphically visualise any compositional differences, Principal Coordinate Analysis (PCoA) was used represent differences across sample microbiota composition based on their Bray-Curtis dissimilarity and was performed using PAST. Principal component analysis (PCA) was used to visualise relationships and patterns between individual samples relevant to their SCFA composition and was also performed in PAST.

2.3.5 Compositional analysis of bacterial taxa and SCFAs

To determine which bacterial taxa or SCFAs were driving dissimilarity between two tested groups, a similarity of percentages (SIMPER) analysis was conducted, based on the Bray-Curtis dissimilarity between groups. The variables (taxa/SCFA) were then ordered based on their relative contribution to the overall dissimilarity between two groups, with cumulative contribution calculated across the various taxa or SCFAs (Clarke, 1993).

2.3.6 Multivariate statistical approaches

To determine the relationships between the whole microbiota, and the partitioned core and satellite taxa with clinical metadata and measurements of gut function, redundancy analysis (RDA) was performed using CANOCO v5 (ter Braak and Smilauer, 2012). An interactive forward selection model was utilised, selecting variables sequentially based on their significance in explaining the variation across microbial composition. Variables were transformed (*Z* scores) where applicable. Following the determination of clinical variables significantly explanatory for microbiome composition, RDA biplots with these variables were plotted in PAST v3.21. Statistical significance for all tests was deemed at the $p \leq 0.05$ level.

2.3.7 Comparison of clinical outcomes and diversity metrics between groups

All analysis was performed using XLSTAT. Clinical data between participants and/or groups was initially tested for normality, using the Shapiro-Wilk test. Student's t-tests (including paired where necessary) were used for parametric data, whereas the Kruskal-Wallis was used for non-parametric tests, which included comparisons

of bacterial alpha diversity and SCFA abundance between groups. Statistical significance for all tests was deemed at the $p \leq 0.05$ level.

2.4 Clinical data

All clinical metadata, including participant characteristics, symptoms, markers of intestinal function, and faecal calprotectin were carried out at Queens Medical Centre and Sir Peter Mansfield Imaging Centre, University of Nottingham.

Chapter 3: Intestinal function and transit relate to microbial dysbiosis in the CF gut

This Chapter is published in the *Journal of Cystic Fibrosis* and is presented in submitted manuscript format (except methodology):

Marsh R, Gavillet H, Hanson L, Ng C, Mitchell-Whyte M, Major G, Smyth AR, Rivett D, van der Gast C. 2022. *Intestinal function and transit associate with gut microbiota dysbiosis in cystic fibrosis*. J Cyst Fibros 21:506–513.

Intestinal function and transit associate with gut microbiota dysbiosis in cystic fibrosis

Ryan Marsh [a], Helen Gavillet [a], Liam Hanson [a,b], Christabella Ng [c,d], Mandisa Mitchell-Whyte [e], Giles Major [c], Alan R Smyth [c,d], Damian Rivett [b], Christopher van der Gast [a,f] *

[a] Department of Life Sciences, Manchester Metropolitan University, UK

[b] Department of Natural Sciences, Manchester Metropolitan University, UK

[c] School of Medicine, University of Nottingham, UK

[d] NIHR Nottingham Biomedical Research Centre, Nottingham University Hospitals NHS Trust and University of Nottingham, Nottingham, UK

[e] Wolfson CF Unit, Nottingham University Hospitals NHS Trust, Nottingham, UK

[f] Department of Respiratory Medicine, Northern Care Alliance NHS Foundation Trust, Salford, UK

*Correspondence to Professor Chris van der Gast, Department of Life Sciences, Faculty of Science and Engineering, John Dalton Building, Chester Street, Manchester, M1 5GD, UK; C.vanderGast@mmu.ac.uk

Highlights

- Faecal microbiota significantly differs between pwCF and controls.
- Known SCFA producers contributed to microbiota dissimilarity between groups.
- Pulmonary antibiotic treatment heavily impacted gut microbiota.
- Intestinal physiology and transit impacted satellite microbiota composition.

Abstract

Background: Most people with cystic fibrosis (pwCF) suffer from gastrointestinal symptoms and are at risk of gut complications. Gut microbiota dysbiosis is apparent within the CF population across all age groups, with evidence linking dysbiosis to intestinal inflammation and other markers of health. This pilot study aimed to investigate the potential relationships between the gut microbiota and gastrointestinal physiology, transit, and health.

Study Design: Faecal samples from 10 pwCF and matched controls were subject to 16S rRNA sequencing. Results were combined with clinical metadata and MRI metrics of gut function to investigate relationships.

Results: pwCF had significantly reduced microbiota diversity compared to controls. Microbiota compositions were significantly different, suggesting remodelling of core and rarer satellite taxa in CF. Dissimilarity between groups was driven by a variety of taxa, including *Escherichia coli*, *Bacteroides spp., Clostridium spp.,* and *Faecalibacterium prausnitzii*. The core taxa were explained primarily by CF disease, whilst the satellite taxa were associated with pulmonary antibiotic usage, CF disease, and gut function metrics. Species-specific ordination biplots revealed relationships between taxa and the clinical or MRI-based variables observed.

Conclusions: Alterations in gut function and transit resultant of CF disease are associated with the gut microbiota composition, notably the satellite taxa. Delayed transit in the small intestine might allow for the expansion of satellite taxa resulting in potential downstream consequences for core community function in the colon.

3.1 Introduction

Cystic fibrosis (CF) associated respiratory infections are the major cause of disease morbidity and mortality. However, a number of gastrointestinal (GI) problems may also arise, limiting the quality of life, including meconium ileus at birth, distal intestinal obstruction syndrome, small intestinal bacterial overgrowth (SIBO), increased risk of malignancy, and intestinal inflammation (De Lisle and Borowitz, 2013; Ooi and Durie, 2016). It is therefore unsurprising that people with CF experience persistent GI symptoms (Tabori et al., 2017; Hayee et al., 2019) with "how can we relieve gastrointestinal symptoms in people with CF?" a top priority question for research (Smith et al., 2020).

Microbial dysbiosis at the site of the GI tract in CF patients has been described, with changes evident from birth through to adulthood (Nielsen et al., 2016; Burke et al., 2017; Antosca et al., 2019; Kristensen et al., 2020; Loman et al., 2020). Moreover, the extent of this divergence from healthy microbiota, initially due to loss of cystic fibrosis transmembrane conductance regulator (CFTR) function (Vernocchi et al., 2018), is further compounded by routine treatment with broad spectrum antibiotics (Kristensen et al., 2020). The reshaping of the gut microbiota may have functional consequences that could further impact on patients. These include the reduction of taxa associated with the production of short-chain fatty acids (SCFAs) which play key roles in modulating local inflammatory responses and promoting gut epithelial barrier integrity (Donohoe et al., 2011; Arpaia et al., 2013; Chang et al., 2014). Furthermore, studies of microbiota dysbiosis in CF have demonstrated its relationship with intestinal inflammation, intestinal lesions, and increased gene expression relating to intestinal cancers (Flass et al., 2015; De Freitas et al., 2018; Coffey et al., 2019; Dayama et al., 2020). Whilst many of these clinical parameters have ties to gut microbiota changes, they remain understudied exclusively past

childhood despite advances in less invasive approaches to investigate CF gut physiology and function (Malagelada et al., 2020). Our group has recently published on the use of magnetic resonance imaging (MRI) to assess gut transit time, along with other parameters, in adolescents and adults (Ng et al., 2021).

In this pilot study, we linked those MRI physiology metrics and clinical metadata directly to high-throughput amplicon sequencing data identifying constituent members of the gut microbiota, to explore the relationships between microbial dysbiosis, intestinal function and clinical state.

3.2 Materials and methods

3.2.1 Study participants and design

Twelve people with CF, homozygous for F508del along with 12 healthy controls, matched by age and gender, were recruited from Nottingham University Hospitals NHS Trust. Participants were asked to provide stool samples when attending for MRI scanning, with the study design and MRI protocols described previously (Ng et al., 2021). A patient clinical features were also recorded upon visitation (Table 3.1), including a three-day food diary preceding sample collection (Table S3.1). Further descriptive statistics of the study population can be found in the Supplementary Materials, including MRI metrics (Table S3.2), and summary statistics on diet (Tables S3.3-S3.6). Faecal samples were only obtained from ten individuals in each group. Written informed consent, or parental consent and assent for paediatric participants, was obtained from all participants. Study approval was obtained from the West Midlands Coventry and Warwickshire Research Ethics Committee (18/WM/0242). All stool samples obtained were immediately stored at -80°C prior to DNA extraction to reduce changes before downstream community analysis (Gorzelak et al., 2015).

3.2.2 Targeted amplicon sequencing

DNA from dead or damaged cells, as well as extracellular DNA was excluded from analysis via cross-linking with propidium monoazide (PMA) prior to DNA extraction (Chapter 2.2.2), as previously described (Rogers et al., 2013). Next, cellular pellets resuspended in PBS were loaded into the ZYMO Quick-DNA Fecal/Soil Microbe Miniprep Kit (Cambridge Bioscience, Cambridge, UK) as per manufacturer's instructions, with amendments as described in Chapter 2.2.3. Following DNA extraction, approximately 20 ng of template DNA was then amplified using the 16S

rRNA approach highlighted in Chapter 2.2.4.1. Primers and PCR conditions can be found in the Supplementary Materials. Pooled barcoded amplicon libraries were sequenced on the Illumina MiSeq platform (V3 Chemistry).

3.2.3 Sequence processing and analysis

Sequence processing and data analysis were initially carried out in R (Version 4.0.1), utilising the package DADA2 (Callahan et al., 2016) as described in Chapter 2.3.1. Raw sequence data reported in this study has been deposited in the European Nucleotide Archive under the study accession number PRJEB44071.

3.2.4 Faecal Calprotectin

Stool was extracted for downstream assays using the ScheBo® Master Quick-Prep (ScheBo Biotech, Giessen, Germany), according to the manufacturer instructions. Faecal calprotectin was analysed using the Bühlmann fCAL ELISA (Bühlmann Laboratories Aktiengesellschaft, Schonenbuch, Switzerland), according to the manufacturer's protocol.

3.2.5 Statistical Analysis

Regression analysis, including calculated coefficients of determination (r^2), degrees of freedom (df), *F*-statistic and significance values (*P*) were calculated as described in Chapter 2.3.2. Fisher's alpha index of diversity and the Bray-Curtis index of similarity were calculated using PAST v3.21 (Hammer et al., 2001), as described in Chapters 2.3.3 and 2.3.4 respectively. Significant differences in microbiota diversity were determined using Kruskal-Wallis performed using XLSTAT. Analysis of similarities (ANOSIM) with Bonferroni correction was used to test for significance in microbiota composition and was performed in PAST, including SIMPER analysis to

determine which taxa contributed most to compositional differences between groups (Chapter 2.3.4).

Multivariate approaches, including Redundancy analysis (RDA) and subsequent biplots, were performed in CANOCO v5 (ter Braak and Smilauer, 2012) as described in Chapter 2.3.6. Statistical significance for all tests was deemed at the $p \leq 0.05$ level. Supplementary information, including metadata, are available at figshare.com; https://doi.org/10.6084/m9.figshare.15073797.v1, https://doi.org/10.6084/m9.figshare.15073899.v1.

Table 3.1 Clincial characteristics of study participants.

Study I.D	Sex	Age (Years)	Group	Pancreatic Status	Calprotectin (µg/g)	FEV1%	BMI	Antibiotic Usage				
								P	A	M	β	S
365	M	12	CF	PI	4.22	87	16.18	-	-	-	+	-
431	M	12	HC	PS	2.44	-	17.95	-	-	-	-	-
128	M	13	CF	PI	27.59	97	17.72	+	-	-	-	-
296*	M	13	HC	PS	-	-	23.44	-	-	-	-	-
643	M	13	CF	PI	9.77	90	21.83	-	-	+	-	-
159	M	13	HC	PS	2.72	-	23.49	-	-	-	-	-
297	M	15	CF	PI	27.61	126	20.83	-	-	-	-	-
947*	M	15	HC	PS	-	-	20.94	-	-	-	-	-
617	F	15	CF	PI	21.15	72	18.42	-	-	+	+	+
964	F	15	HC	PS	12.71	-	19.15	-	-	-	-	-
167	M	19	CF	PI	7.37	99	20.63	-	-	-	-	-
673	M	19	HC	PS	0.94	-	20.34	-	-	-	-	-
279	F	19	CF	PI	27.32	66	20.87	-	-	+	-	-
205	F	19	HC	PS	3.84	-	31.91	-	-	-	-	-
596	F	21	CF	PI	14.05	61	21.91	-	-	+	-	-
152	F	21	HC	PS	4.22	-	21.26	-	-	-	-	-
610*	M	23	CF	PI	-	66	18.64	-	+	+	-	-
548	M	24	HC	PS	3.56	-	24.49	-	-	-	-	-
619*	F	27	CF	PI	-	60	19.27	-	-	-	-	-
501	F	27	HC	PS	7.19	-	28.66	-	-	-	-	-
259	M	30	CF	PI	28.30	61	20.21	-	-	+	+	-
986	M	29	HC	PS	4.96	-	22.64	-	-	-	-	-
681	F	36	CF	PI	11.79	88	21.71	+	-	+	-	-
749	F	35	HC	PS	3.00	-	19.57	-	-	-	-	-

Subjects marked with an asterisk* indicate those who failed to produce a stool sample for subsequent metagenomic and metabolomic analysis and thus were excluded from downstream analyses. All participants with CF had the gene mutation F508del/F508del, with pancreatic insufficiency but no CF-related diabetes. For antibiotic usage, '+' indicates routine administration of the given antibiotic class prior to sampling. Abbreviations: FEV1 – Percent predicted forced expiratory volume in 1 second, BMI – Body mass index, P – Polymyxin, A – Aminoglycoside, M – Macrolide, β – β-lactam, S – Sulfonamide. Asterisks denote participants who did not provide any stool samples upon visitation, and thus were excluded from downstream microbiota analysis.

3.3 Results

To investigate the contributions of common and rare bacterial taxa in the gut microbiota of individuals within and between study cohorts (Hedin et al., 2016; Cuthbertson et al., 2020), taxa were partitioned into either common and abundant core taxa or rarer and infrequent satellite taxa, based upon their prevalence and relative abundance across samples within each cohort (Fig. 3.1). Within the healthy control group, 30 taxa were core constituting 60.5% of the total abundance, with the remainder accounted for by 386 satellite taxa. In the CF group, 22 core taxa represented 34.7% of the abundance, with 323 satellite taxa constituting the remainder. Core taxa are listed in Table S3.7. The whole, core, and satellite microbiota demonstrated similar patterns in diversity, whereby there was significantly reduced diversity in the CF group (Fig. 3.2A, Table S3.8).

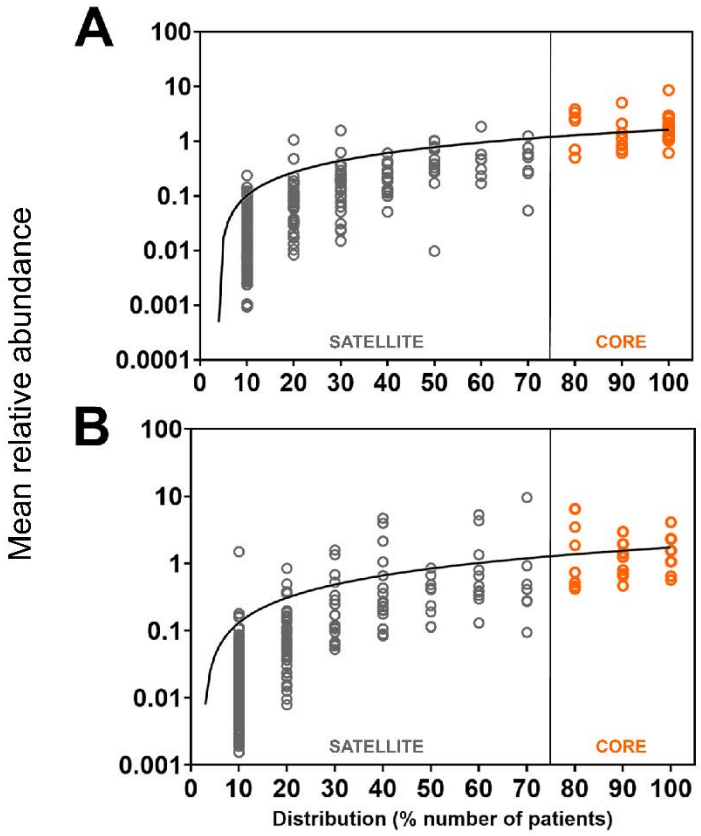

Figure 3.1 Distribution and abundance of bacterial taxa across different sample groups. (A) Healthy control. (B) Cystic fibrosis. Given is the percentage number of patient stool samples each bacterial taxon was observed to be distributed across, plotted against the mean percentage abundance across those samples. Core taxa are defined as those that fall within the upper quartile of distribution (orange circles), and satellite taxa (grey circles) defined as those that do not, separated by the vertical line at 75% distribution and labelled respectively. Distribution-abundance relationship regression statistics: (a) r^2 = 0.50, $F_{1,414}$ = 407.3, P < 0.0001; (b) r^2 = 0.29, $F_{1,343}$ = 137.3, P < 0.0001. Core taxa are listed in Table S3.7.

Within-group core microbiota similarity was higher within the healthy control group, with a mean similarity (± SD) of 0.60 ± 0.08 compared to 0.40 ± 0.11 for the CF group (Fig. 3.2B). As expected, satellite taxa similarity within groups was much lower than for the core but was also significantly reduced in CF compared to controls, at 0.35 ± 0.08 and 0.21 ± 0.09 for the healthy control and CF group respectively. ANOSIM testing determined the whole microbiota, core, and satellite taxa of the CF group were significantly different in composition compared to healthy controls (Fig. 3.2B, Table S3.9). SIMPER analysis was implemented to reveal which taxa were responsible for driving this dissimilarity (Table 3.2). Of the taxa contributing to > 50% of the differences between healthy control and CF groups, those within the genus *Bacteroides* were represented most. *Escherichia coli* contributed most towards the differences between groups, despite satellite status, followed by *Bacteroides* sp. (OTU 3), *Clostridium* sp. (OTU 5), *Faecalibacterium prausnitzii*, and *Bacteroides fragilis*.

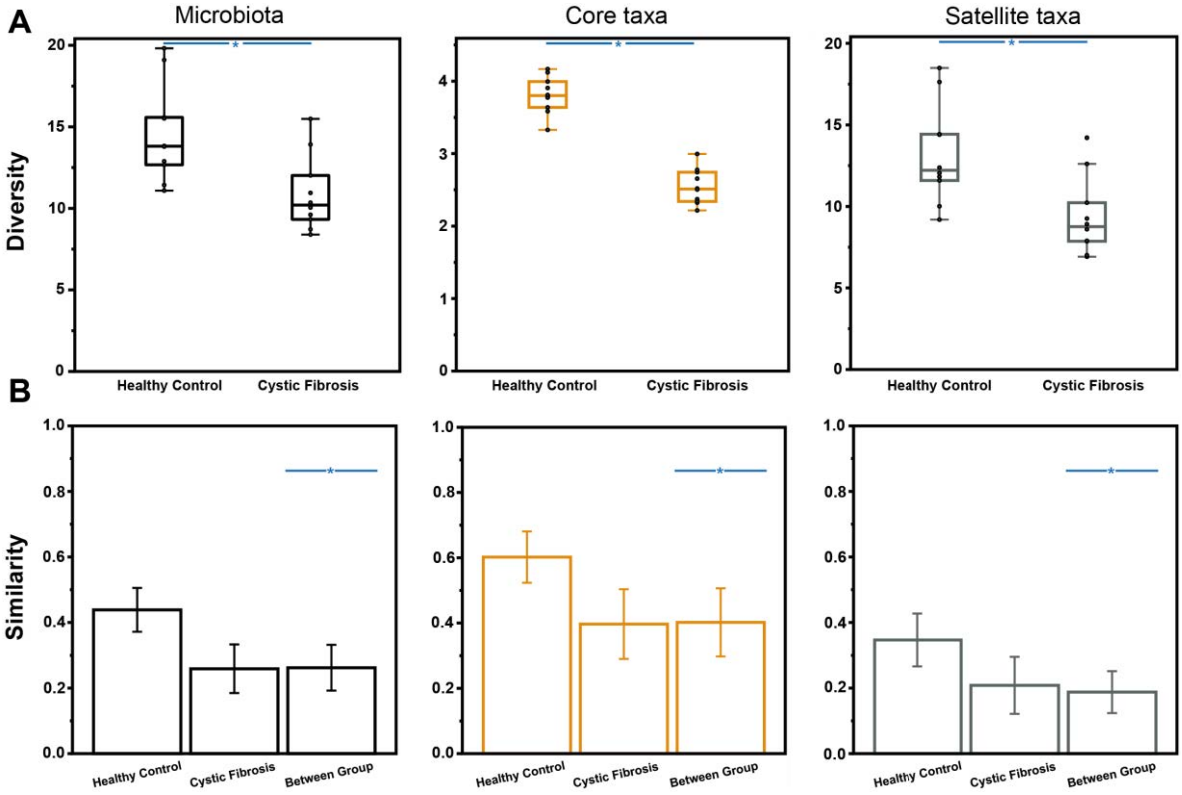

Figure 3.2 Microbiome diversity and similarity compared across healthy controls and cystic fibrosis samples. Whole microbiota (black plots) and partitioned data into core (orange plots) and satellite taxa (grey plots) are given. (**A**) Differences in Fisher's alpha index of diversity between healthy controls and cystic fibrosis samples. Black circles indicate individual patient data. Error bars represent 1.5 times inter-quartile range (IQR). Asterisks between groups denote a significant difference in diversity following use of Kruskal-Wallis tests ($P < 0.001$). Summary statistics are provided in Table S3.8. (**B**) Microbiome variation measured within and between sampling groups, utilising the Bray-Curtis index of similarity. Error bars represent standard deviation of the mean. Asterisks indicate significant differences between sampling groups following the use of one-way ANOSIM testing ($P < 0.001$). Summary statistics are provided in Table S3.9.

Table 3.2 Similarity of percentage (SIMPER) analysis of microbiota dissimilarity (Bray-Curtis) between Healthy Control (HC) and Cystic Fibrosis (CF) stool samples.

Taxa	%Relative abundance		Av. Dissimilarity	% Contribution	Cumulative %
	Mean HC	Mean CF			
Escherichia coli	1.84	9.54	4.72	6.39	6.39
Bacteroides 3	3.84	4.69	3.36	4.55	10.94
Clostridium 5	0.77	6.44	3.09	4.18	15.13
Faecalibacterium prausnitzii	8.56	2.95	2.99	4.05	19.18
Bacteroides fragilis	1.02	5.29	2.75	3.73	22.90
Bacteroides dorei	3.32	4.31	2.52	3.42	26.32
Eubacterium rectale	5.03	1.35	2.18	2.95	29.27
Romboutsia timonensis	1.24	3.95	2.15	2.91	32.18
Bacteroides uniformis	2.72	4.09	1.62	2.20	34.38
Dialister invisus	1.00	3.45	1.61	2.19	36.57
Bacteroides vulgatus	2.37	2.14	1.56	2.11	38.68
Ruminococcus bromii	2.69	0.42	1.24	1.68	40.36
Alistipes putredinis	2.08	0.06	1.02	1.38	41.74
Bacteroides coprocola	1.56	0.92	1.01	1.37	43.11
Fusicatenibacter saccharivorans	2.62	0.8	1.00	1.36	44.47
Streptococcus 18	0.26	1.95	0.88	1.19	45.66
Blautia luti	2.93	2.31	0.86	1.16	46.82
Oscillibacter ruminantium	1.90	0.27	0.84	1.14	47.96
Clostridium perfringens	0.00	1.58	0.79	1.07	49.03
Parabacteroides distasonis	1.38	1.85	0.77	1.05	50.08

Taxa identified as core are highlighted in orange, whereas satellite taxa are highlighted in grey. Mean relative abundance (%) is also provided for each group. Percentage contribution is the mean contribution divided by the mean dissimilarity across samples (73.79%). Cumulative percent does not equal 100% as the list is not exhaustive. Given the sequencing length of 16S gene regions, taxon identification should be considered putative.

Table 3.3 Redundancy analysis to explain percent variation in whole microbiota, core taxa and satellite taxa between all subjects from significant clinical variables measured.
Var. Exp (%) represents the percentage of the microbiota variation explained by a given parameter within the redundancy analysis model. *P* (adj) is the adjusted significance value following false discovery rate correction. Antibiotics is the presence/absence of recurrent antibiotic regimes for a given patient. BMI – Body mass index, Colon Fasting Vol – Colon volume at baseline corrected for body surface area, OCTT – Oro-caecal transit time, Antibiotics, SBWC – Small bowel water content corrected for body surface area.

	Microbiota			**Core taxa**			**Satellite taxa**		
	Var. Exp (%)	pseudo-*F*	*P* (adj)	Var. Exp (%)	pseudo-*F*	*P* (adj)	Var. Exp (%)	pseudo-*F*	*P* (adj)
Antibiotics	21.5	5.4	0.002				27.1	7.3	0.002
BMI				7.0	2.0	0.042			
Calprotectin							5.9	1.8	0.050
CF Disease	10.9	2.2	0.002	28.9	7.3	0.002	10.3	2.1	0.006
Colon Fasting Vol.	7.5	2.0	0.016						
OCTT	7.4	2.1	0.012				6.7	1.9	0.046
SBWC	5.6	1.7	0.048				7.2	2.4	0.048
Sex				7.9	2.1	0.010			
Total	**52.9**			**43.8**			**57.2**		

Redundancy analysis (RDA) was used to relate variability in microbiota composition to associated MRI metrics and clinical factors (Table 3.3). Pulmonary antibiotics and CF disease significantly explained the most variance across the whole and satellite microbiota. Measurements of intestinal transit and function contributed to the whole microbiota variance, albeit to a lesser extent, with variation in OCTT and SWBC also contributing to satellite taxa variance alongside faecal calprotectin levels. In the core taxa analysis, the presence of CF disease was the dominant factor in significantly explaining the compositional variability, followed by sex and body mass index (BMI).

A species redundancy analysis biplot (RDA) was constructed to investigate how significant clinical variables from the whole microbiota direct ordination approach explained the relative abundance of taxa from the SIMPER analysis (Fig. 3.3). Certain taxa grouped away from many of the significant clinical variables shown in a similar manner. This effect was most pronounced for *F. prausnitzii, Eubacterium rectale* and *Ruminoccocus bromii*. A combination of clinical factors, including CF disease, increased fasting colonic volume, increased SBWC and prolonged OCTT, explained the variance observed in relative *E. coli* abundance, whilst a more modest effect was observed towards *Streptococcus* sp. (OTU 18), *Dialister invisus*, *Clostridium perfringens* and *Romboutsia timonensis*. Species of *Bacteroides*, which was the most common genus within the top-contributing SIMPER analysis, were explained by the clinical variables to high variability.

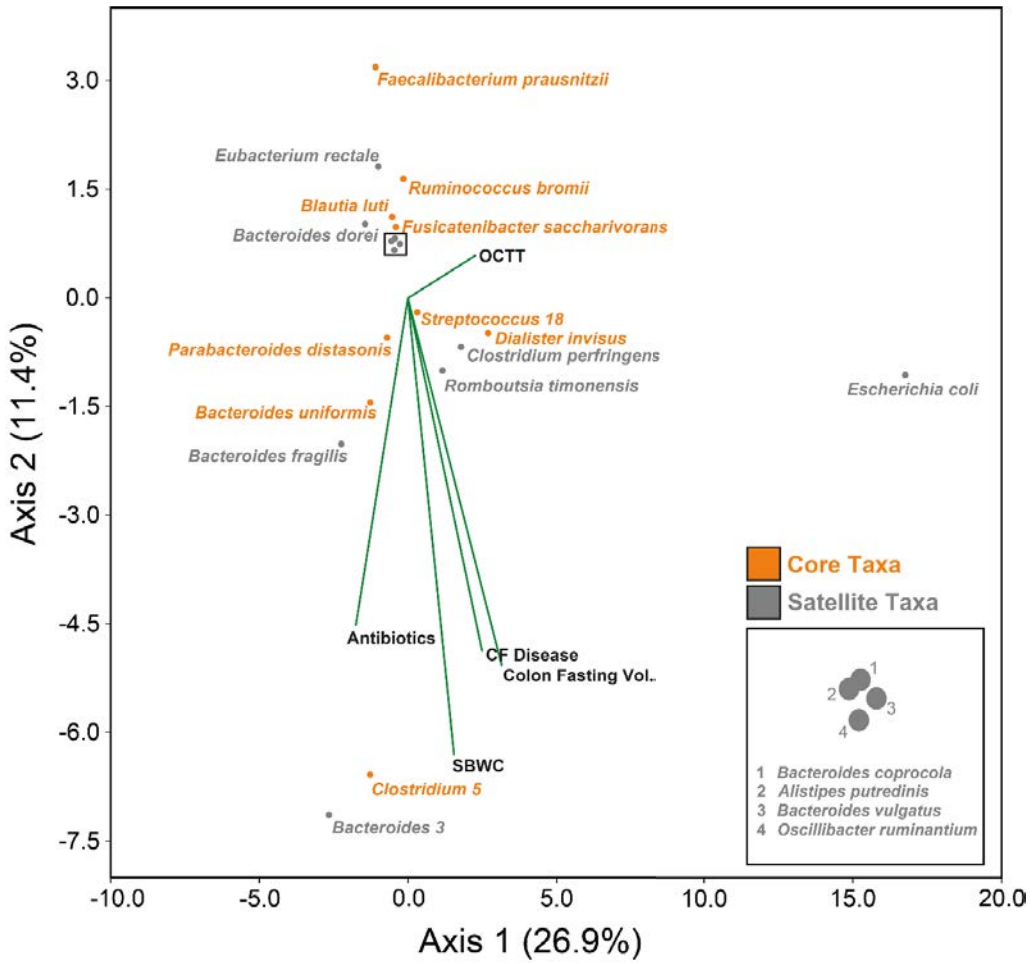

Figure. 3.3 Redundancy analysis species biplots for whole microbiota. The 20 taxa contributing most to the dissimilarity (cumulatively > 50%) between healthy and cystic fibrosis groups from the SIMPER analysis (Table 3.2) are shown independently of the total number of ASVs identified (345). Orange circles represent core taxa within the CF group, whilst grey circles denote satellite taxa. Biplot lines depict clinical variables that significantly account for the total variation in taxa relative abundance within the whole microbiota analysis at the $p \leq 0.05$ level as seen in Table 3.3, with species plots indicating the strength of explanation provided by the given clinical variables. 'OCTT' – Oro-caecal transit time, Antibiotics, 'SBWC' – Small bowel water content corrected for body surface area, Colon Fasting Volume corrected for body surface area, CF disease. For example, biplot lines depicting the MRI metrics represent how changes in the metric influences the relative abundance of each of the taxa shown. Those taxa shown in the same direction of the metric label are considered to have a higher value than those taxa that are not. The percentage of microbiome variation explained by each axis is given in parentheses.

3.4 Discussion

In this pilot study, we investigated the relationships between clinical factors, MRI markers of GI function and the composition of faecal bacterial microbiota. Demonstrated previously for CF lung and Crohn's gut microbiota (Hedin et al., 2016; Cuthbertson et al., 2020), we have shown here that it is possible to partition the CF gut microbiota into core and satellite taxa to investigate potential community functions and relationships, with the notion that the core constituents contribute to the majority of functionality exhibited by the community (Rogers et al., 2013; Cuthbertson et al., 2020). As to be expected, the core taxa made up most of the abundance within the healthy control group. Whilst many taxa were also commonly represented in the CF group, the latter was dominated in abundance by the satellite taxa. Our findings of reduced diversity across the whole, core, and satellite microbiota are in agreement with previous findings described within the CF gut (Burke et al., 2017; Kristensen et al., 2020; Loman et al., 2020). Along with reduced within group similarity in CF compared to healthy controls across all microbiota partitions, this suggests a perturbed community harbouring greater instability, less subsequent resilience, and inherent challenges to the colonisation and establishment of normal commensals. CF associated factors such as varied antibiotic usage will contribute to this reduced similarity, further augmented by the wide age range of pwCF within this study and variation across lifestyle factors. The combination of the aforementioned may elicit stochastic community disruption and increased inter-individual variation as observed across other mammalian microbiomes (Zaneveld et al., 2017).

At the surface, a reduction in the number of taxa labelled as core within the CF group hinted at perturbation and restructuring, further evidenced by the occurrence of taxa exclusively core to this group. This included species of *Streptococcus*,

Pseudomonas, *Veillonella*, and *Enterococcus*, all of which were significantly more abundant in the CF group (Table S3.7), and of which are implicated in both CF lung and gut microbiomes (Madan et al., 2012; Burke et al., 2017; Vernocchi et al., 2018; Coffey et al., 2019; Enaud et al., 2019; Cuthbertson et al., 2020). The concept of the "gut-lung axis" in CF arises from the direct translocation of the respiratory microbiota from sputum swallowing to the gut (Al-Momani et al., 2016), but also the emergence of species in the gut prior to the respiratory environment (Madan et al., 2012). This apparent bidirectionality is further supported by the administration of oral probiotics to decrease pulmonary exacerbations in CF (Anderson et al., 2017). Aside from sputum swallowing, the increase in *Streptococcus* and *Veillonella* here could reflect an increased availability of simple carbohydrates from the observed dysmotility of the gut (Ng et al., 2021). *Streptococci* are well equipped with numerous genes for rapid carbohydrate degradation in an environment usually fluctuating in substrate availability, with fermentation-derived lactic acid supporting the expansion of *Veillonella* species in the small intestine (Kastl et al., 2020).

E. coli contributed most to the dissimilarity between healthy and CF groups despite maintaining satellite status throughout both the healthy and CF groups, seemingly resultant of the wide age range of our study participants, of which the higher relative abundances were observed in the younger adolescent patients (Table 3.2). In childhood studies, a significantly higher relative abundance of *Proteobacteria* is often reported in relation to dysbiosis, with *E. coli* abundance associating with poor growth outcomes and intestinal inflammation (Hoffman et al., 2014; Manor et al., 2016; Hayden et al., 2020). Other notable taxa contributing to the dissimilarity observed between groups encompassed a variety of key species associated with SCFA production in the colon. This included *F. prausnitizii* and *E. rectale,* both of which were significantly decreased in abundance within the CF group, but also *R.*

bromii and *B. luti*. These taxa have all been previously reported to decrease in the CF gut (Duytschaever et al., 2013; Burke et al., 2017; Enaud et al., 2019) alongside other inflammatory conditions (Li et al., 2016). There were also notable contributions to the dissimilarity between groups by *Clostridium* sp. (OTU 5) (significant difference in relative abundance) and *D. invisu*s (not significant). *Clostridium* OTU 5 aligned exclusively with cluster I members at the 97% threshold, of whom demonstrate the capacity to generate lactate, acetate, propionate, and butyrate via carbohydrate fermentation (Rainey et al., 2009), whilst *D. invisu*s is an intermediary fermenter capable of both acetate and propionate production. This may lend support to the theory that alternate species can retain some functional redundancy in the presence of perturbation to the local community in the CF gut (Wang et al., 2019).

Variance across the whole microbiota and satellite taxa was significantly explained by the use of antibiotics (Table 3.3), of which most pwCF are administered on a routine basis to supress lung infection (Elborn, 2016). The occurrence of both OCTT and SBWC accounting for significant explanation in both the whole microbiota and satellite, but not core taxa analysis, underpins the strong impact of gut physiology and transit on the microbiota in CF. Faecal calprotectin also explained the variance across the satellite taxa, and has been associated with increased abundances of *Escherichia*, *Streptococcus*, *Staphylococcus* and *Veillonella*, of which contained satellite species significantly increased in our CF group (Enaud et al., 2019; Meeker et al., 2020). *Acidaminococcus sp.* have also associated with increased faecal calprotectin levels (Coffey et al., 2019), with *Acidaminococcus intestinii* another constituent of the CF satellite microbiota that was not present in healthy controls (data not shown). The core taxa was only largely explained by the presence of CF disease itself, perhaps relating to the direct disruption of CFTR function which alone can influence changes in the microbiome (Meeker et al., 2020).

Perhaps unsurprisingly, the species ordination biplots of the taxa from SIMPER analysis demonstrated clustering of the key SCFA producers mentioned previously away from the significant disease-associated clinical factors, with antibiotic usage and transit metrics previously shown to reduce the abundance of such taxa (Roager et al., 2016; De Freitas et al., 2018). Similarly affected were taxa from genera that are associated with better outcomes in other similarly pro-inflammatory intestinal environments, such as Crohn's disease or ulcerative colitis , including *Oscillibacter and Fusicanterbacter* (Takeshita et al., 2016; Vermeire et al., 2016).

C. perfringens has been associated with disease exacerbation in ulcerative colitis (Li et al., 2016), SIBO in the CF mouse small intestine (Norkina et al., 2004) and increased deconjugation of bile salts leading to further fat malabsorption by the host (De Lisle, 2007). Here it was completely absent from our healthy control group, whilst in the CF group was found to associate with a variety of CF-induced clinical factors as well as OCTT. Also strongly associating with OCTT and impacted substantially more, was *E. coli*. Increased bacterial load relates to slower transit within the CF mouse small intestine (De Lisle, 2007). Concurrently with the observed increase in SWBC reported prior (Ng et al., 2021), this in theory allows for the expansion of such facultative anaerobes in the small intestine that could potentially affect downstream community dynamics and functional profiles in the colon, given that PMA treatment was utilised to select for viable living taxa from faecal sampling.

Although dietary profiles were similar between groups (Tables S3.3-3.6) and did not contribute to significant variation in the microbiota, increased fat intake to meet energy requirements is a staple of the CF diet (Collins, 2018). The infant gut metagenome demonstrates enrichment of fatty acid degradation genes (Manor et al., 2016) whilst CF-derived *E. coli* strains exhibit improved utilisation of exogenous

glycerol as a growth source (Matamouros et al., 2018). Finally, the genus *Bacteroides*, which has been reported to both increase and decrease within CF disease across different age groups (Burke et al., 2017; De Freitas et al., 2018; Vernocchi et al., 2018), displayed high variability within the species ordination biplot (Fig. 3.3), perhaps resultant of the varying antimicrobial susceptibility within the genus (Nagy et al., 2011).

We acknowledge the small sample size of this pilot study limits the power of specific analyses, with the absence of within-group direct ordination approaches which would have allowed for investigation of CF group antibiotic usage and extra clinical factors such as lung function. However, the principal strength of this study is the valuable insight into the relationships between microbiota composition and intestinal physiology and function in CF. Future studies should encompass larger cohorts in a longitudinal fashion with the combination of both lung and faecal microbiota data to elucidate such relationships better, including the impact of pulmonary antibiotic usage on the gut microbiota, and the aptly termed gut-lung axis. Evaluation of associations between the microbiota, physiology and the immune response would also improve our understanding of the mechanisms contributing to GI health in CF. Given their possible beneficial effect on intestinal inflammation (Tetard et al., 2020), the impact of CFTR modulator therapy will provide further insights.

3.5 Conclusion

This cross-sectional pilot study has identified relationships between markers of clinical status, gastrointestinal function and bacterial dysbiosis in the CF population. By partitioning the community into core and satellite taxa, we were able to reveal the relative contributions of CF-associated lifestyle factors and elements of intestinal function to these subcommunity compositions, and how specific taxa were affected

by these clinical factors. Further, as the first study to combine high-throughput gene amplicon sequencing with non-invasive MRI to assess underlying gut pathologies, we demonstrate the potential for future collaborations between gastroenterology and microbiology with larger cohort recruitment to investigate these relationships between gut function and the microbiome further.

3.6 Author Contributions

CvdG, AS, GM, and RJM conceived the study. RJM, HG, LH, and MMW performed sample processing and analysis. RJM, DR, and CvdG performed the data and statistical analysis. CN, GM, and AS were responsible for sample collection, clinical care records and documentation. RJM, CN, GM and CvdG verified the underlying data. RJM, DR, and CvdG were responsible for the creation of the original draft of the manuscript. RJM, CN, GM, DR, AS, and CvdG contributed to the development of the final manuscript. CvdG is the guarantor of this work. All authors read and approved the final manuscript.

3.7 Funding

A CF Trust Venture and Innovation Award (VIA 77) awarded to CvdG funded this work. Funding for the Gut Imaging for Function and Transit in CF (GIFT-CF) study was received from the Cystic Fibrosis Trust (VIA 061), Cystic Fibrosis Foundation (Clinical Pilot and Feasibility Award SMYTH18A0-I), and National Institute for Health Research Biomedical Research Centre, Nottingham.

3.8 Declaration of Competing Interest

RJM, HG, LH, DM, and CvdG declare support from the CF Trust. CN and GM report grants and speaker honorarium from Vertex, outside the submitted work. ARS reports grants from Vertex, as well as speaker honoraria and expenses from Teva and Novartis and personal fees from Vertex, outside the submitted work. In addition, ARS has a patent issued “Alkyl quinolones as biomarkers of *Pseudomonas aeruginosa* infection and uses thereof”.

3.9 Acknowledgements

We would like to thank Neele Dellschaft, Caroline Hoad, Luca Marciani, and Penny Gowland of the Sir Peter Mansfield Imaging Centre, University of Nottingham, who acquired the original MRI data (Ng et al., 2021).

3.10 Supplementary methods

3.10.1 Study participants and design

Although 12 patients and controls were initially recruited, stool samples ultimately collected for 10 CF patients (6 males;4 females, Mean age of CF patients, 19.3 ± 7.93 years, Median age, 19 years) and of 10 non-CF healthy controls (Mean age of controls, 21.4 ± 7.40 years, Median age, 20 years). Patients were under a period of clinical stability and abstained from taking laxatives and anti-diarrhoeals during this visitation but were able to take routine pancreatic supplementation and perform standard physiotherapy procedures, with routine prophylactic antibiotic therapy recorded where applicable for patients.

3.10.2 PMA treatment prior to DNA extraction

1 mg PMA (Biotium, CA, USA) was hydrated in 98 µl 20% dimethyl sulfoxide (DMSO) to give a working stock concentration of 20 mM. 300 mg of stool thawed out from -80°C was homogenised in 3 ml PBS, and centrifuged at 3200 g, for 5 minutes. The pellet was then resuspended in 1 ml prior to splitting into 500 µl fractions for subsequent PMA treatment. PMA 1.25 µl of PMA (20 mM) was added to give a final concentration of 50 µM. Following the addition of PMA to samples in opaque Eppendorf tubes, PMA was mixed by vortexing for 10 seconds, followed by incubation for 15 minutes at room temperature (~20°C). This step was repeated before the transfer of samples to clear 1.5 mL Eppendorf tubes and placement within a LED lightbox. Treatment occurred for 15 minutes to allow PMA intercalation into DNA from compromised bacterial cells. Samples were then centrifuged at 10,000 x *g* for 5 minutes. The supernatant was discarded, and the cellular pellet was resuspended in 200 µl PBS.

3.10.3 Targeted amplicon sequencing – Bacterial 16S rRNA gene

Step 1 amplicon generation with primers based on the universal primer sequences 515F and 926R as described by Walters et al. (Walters et al., 2016), was performed under the following conditions; Initial denaturation of 180 seconds at 98°C, followed by: 25 cycles of 30 seconds at 95°C, 30 seconds at 55°C and 30 seconds at 72°C. A final extension of 5 minutes at 72°C was also included to complete the reaction. Step 2, the addition of dual barcodes and Illumina adaptor sequences was performed under the following conditions: Initial denaturation of 30 seconds at 98°C, followed by: 10 cycles of 10 seconds at 98°C, 20 seconds at 62°C and 30 seconds at 72°C. A final extension of 2 minutes at 72°C was also included to complete this reaction. This resulted in the generation of an ~550 bp amplicon spanning the V4-V5 hypervariable regions of the 16S rRNA gene.

3.10.4 Sequencing Controls and Library Pooling

PCR and DNA extraction negative controls were implemented, alongside the use of mock community positive controls, which included a Gut Microbiome Standard (ZYMO RESEARCH™). Following Barcode attachment in the second PCR step, samples were normalised using the SequalPrep™ Normalization Plate Kit (Thermo Fisher Scientific), pooled and diluted to the final library concentrations requited for use on the Illumina MiSeq system.

3.10.5 Sequence processing and analysis

DADA2 was used to demultiplex and remove primer sequences, validate the quality profiles of forward and reverse reads and subsequently trim, infer sequence variants, merge denoised paired-reads, remove chimeras, and finally assign taxonomy via Naive Bayesian Classifier implementation (Callahan et al., 2016). This included the use of the Genome Taxonomy Database (GTDB) reference sequences

(Parks et al., 2018). Unidentifiable ASVs were run through a BLAST (https://blast.ncbi.nlm.nih.gov/Blast.cgi) and matched appropriately based on query coverage where possible. Taxa with 2 ≥ reads for a single sample were removed and excluded from subsequent statistical analysis. ASVs from the same bacterial taxon were collapsed to form a single OTU for a given taxon.

3.11 Supplemntary Results

Table S3.1 Dietary information obtained from study participants

Study I.D.	Group	Mean % Kcal Protein	Mean % Kcal CHO	Mean % Kcal Fat	Mean % Fibre (g)
152	HC	18.33	45.61	36.04	6.80
159	HC	18.16	46.96	32.91	4.46
205	HC	21.55	40.66	37.74	2.70
431	HC	8.46	63.62	27.98	3.38
501	HC	19.41	65.76	14.90	3.07
548	HC	16.55	43.20	34.01	6.28
673	HC	12.29	54.99	32.49	10.44
749	HC	14.70	42.82	36.14	6.79
964	HC	15.97	46.63	37.34	3.94
986	HC	15.88	43.83	40.25	4.88
128	CF	10.24	55.38	34.36	3.33
167	CF	17.38	44.21	38.59	5.07
259	CF	15.54	61.47	27.90	4.62
279	CF	11.97	47.36	40.41	2.11
297	CF	16.53	54.80	28.71	4.39
365	CF	17.19	49.28	33.51	4.21
596	CF	18.24	46.75	31.41	4.98
617	CF	12.15	51.63	32.89	4.07
643	CF	16.82	50.51	32.75	3.86
681	CF	15.46	50.70	33.74	3.47

Macronutrient intake 3 days prior to faecal sampling was recorded from participants through a food diary. The mean daily proportion of calories obtained from each macronutrient (Protein, CHO - Carbohydrates, Fat) was calculated. Mean relative weight of fibre intake was also calculated.

Table S3.2 Magnetic resonance imaging (MRI) metrics utilised for the direct ordination approach.

Study I.D.	Group (HC/CF)	OCTT (mins)	Corrected SBWC (mL/m^2)	Corrected Fasting Colon Volume (mL/m^2)
152	HC	180	61.51	755.63
159	HC	150	18.40	772.06
205	HC	360	40.35	708.42
431	HC	150	72.69	948.15
501	HC	360	47.56	393.86
548	HC	300	57.04	665.40
673	HC	360	24.16	985.48
749	HC	240	10.79	233.35
964	HC	180	26.19	649.25
986	HC	180	89.90	817.08
128	CF	150	55.44	435.61
167	CF	390	133.05	1389.02
259	CF	360	19.37	1048.02
279	CF	360	105.60	564.99
297	CF	180	273.09	845.09
365	CF	390	205.19	581.98
596	CF	120	83.36	646.69
617	CF	300	229.21	869.81
643	CF	390	82.92	719.90
681	CF	300	376.24	1667.85

HC - Healthy control, CF - Cystic fibrosis, OCTT – Oro-caecal transit time, SBWC – Small bowel water content corrected for body surface area, Colon Fasting Volume corrected for body surface area.

Table S3.3 Summary statistics: Mean % Kcal Protein.

Variable	Observations	Obs. with missing data	Obs. without missing data	Minimum	Maximum	Mean	Std. deviation
CF	10	0	10	10.244	18.236	15.153	2.725
HC	10	0	10	8.464	21.552	16.131	3.726

Kruskal-Wallis test / Two-tailed test:

K (Observed value)	0.691
K (Critical value)	3.841
DF	1
P-value (one-tailed)	0.406
alpha	0.050

An approximation has been used to compute the *P*-value.

Table S3.4 Summary statistics: Mean % Kcal CHO.

Variable	Observations	Obs. with missing data	Obs. without missing data	Minimum	Maximum	Mean	Std. deviation
CF	10	0	10	44.211	61.475	51.211	4.989
HC	10	0	10	40.664	65.757	49.409	8.932

Kruskal-Wallis test / Two-tailed test:

K (Observed value)	1.851
K (Critical value)	3.841
DF	1
P-value (one-tailed)	0.174
alpha	0.050

An approximation has been used to compute the *P*-value.

Table S3.5 Summary statistics: Mean % Kcal Fat.

Variable	Observations	Obs. with missing data	Obs. without missing data	Minimum	Maximum	Mean	Std. deviation
CF	10	0	10	27.896	40.415	33.427	3.860
HC	10	0	10	14.902	40.254	32.981	7.203

Kruskal-Wallis test / Two-tailed test:

K (Observed value)	0.280
K (Critical value)	3.841
DF	1
P-value (one-tailed)	0.597
alpha	0.050

An approximation has been used to compute the *P*-value.

Table S3.6 Summary statistics: Mean % Fibre (g).

Variable	Observations	Obs. with missing data	Obs. without missing data	Minimum	Maximum	Mean	Std. deviation
CF	10	0	10	2.106	5.070	4.010	0.883
HC	10	0	10	2.703	10.438	5.274	2.356

Kruskal-Wallis test / Two-tailed test:

K (Observed value)	0.966
K (Critical value)	3.841
DF	1
p-value (one-tailed)	0.326
alpha	0.050

An approximation has been used to compute the *P*-value.

Table S3.7 Core taxa within each group throughout the study.

	Healthy Control		Cystic Fibrosis		
Taxa	Prevalence	Abundance	Prevalence	Abundance	Sig. Difference
Faecalibacterium prausnitzii	100	8.56	90	2.95	***
Bacteroides 3	80	3.84	40	4.69	
Bacteroides dorei	80	3.32	60	4.31	
Clostridium 5	50	0.77	80	6.44	*
Bacteroides uniformis	100	2.72	100	4.09	
Eubacterium rectale	90	5.03	60	1.35	*
Blautia luti	100	2.93	100	2.31	
Dialister invisus	50	1	80	3.45	
Bacteroides vulgatus	80	2.37	40	2.14	
Anaerostipes hadrus	100	1.76	90	1.24	*
Eubacterium hallii	100	2.18	100	1.55	
Fusicatenibacter saccharivorans	100	2.62	90	0.8	**
Parabacteroides distasonis	90	1.38	80	1.85	
Dorea longicatena	100	1.3	90	1.44	
Streptococcus 18	70	0.26	90	1.95	**
Ruminococcus bromii	80	2.69	80	0.42	
Blautia faecis	100	1.7	90	0.65	**
Alistipes putredinis	90	2.08	30	0.06	***
Blautia wexlerae	100	1.14	100	0.65	
Blautia massiliensis	100	1.04	60	0.8	
Blautia obeum	100	1.57	100	0.56	*
Erysipelatoclostridium saccharogumia	100	1.58	60	0.39	**
Alistipes onderdonkii	100	1.03	90	0.7	
Oscillibacter ruminantium	100	1.9	70	0.27	**
Ruminococcus faecis	100	1.18	60	0.65	
Enterococcus faecalis	10	0.24	90	1.41	**
Coprobacter secundus	100	1.69	40	0.28	**
Subdoligranulum variabile	90	1.11	60	0.46	*
Odoribacter splanchnicus	90	0.85	70	0.49	
Pseudomonas fluorescens	30	0.02	100	1.06	***
Veillonella dispar	20	0.03	80	0.74	**
Butyricicoccus faecihominis	70	0.51	90	0.47	
Anaerotignum lactatifermentans	50	0.17	80	0.52	
Oscillibacter valericigenes	90	0.7	40	0.2	*
Bifidobacterium adolescentis	80	0.7	10	0.16	*
Coprococcus comes	30	0.26	80	0.45	
Alistipes obesi	100	0.61	70	0.09	**
Monoglobus pectinilyticus	90	0.61	50	0.12	**
Alistipes ihumii	80	0.5	10	0.02	**

Given is prevalence, the percent number of samples a given core taxon was detected in, and average relative abundance across those samples. Taxon names are derived from condensed ASVs of the same species. ASV numbers have been used to differentiate between taxa within the same genus that could not be identified at the species level. Core taxa are highlighted orange, whereas satellite taxa are grey. Given the length of the ribosomal sequences analysed, species identities should be considered putative. *** - $p < 0.001$, ** - $p < 0.01$, * - $p < 0.05$.

Table S3.8 Bacterial Kruskal-Wallis tests of alpha diversity.

Microbiota		**Core taxa**		**Satellite taxa**	
H:	7.406	H:	14.29	H:	7
Hc (tie corrected):	7.406	Hc (tie corrected):	14.29	Hc (tie corrected):	7
p (same):	**0.006502**	*p* (same):	**0.000157**	*p* (same):	**0.008151**

Table S3.9 Bacterial ANOSIM summary statistics utilising Bray-Curtis index.

Microbiota		**Core taxa**		**Satellite taxa**	
R value:	0.4729	R value:	0.9022	R value:	0.5609
p (same):	**0.0001**	*p* (same):	**0.0001**	*p* (same):	**0.0001**
Bonferroni-corrected p value:	0.0001	Bonferroni-corrected p value:	0.0001	Bonferroni-corrected p value:	0.0001
permutation *N*:	9999	permutation *N*:	9999	permutation *N*:	9999

Chapter 4: A qualitative and quantitative validated method for short-chain fatty acids analysis from human faecal samples by gas chromatography-mass spectrometry.

This Chapter is written in manuscript format ready for submission to *Journal of Microbiological Methods.*

Ryan Marsh[1], Claudio H Dos Santos[2,3], Damian Rivett[3], Christopher van der Gast[4,5]

[1] *Department of Life Sciences, Manchester Metropolitan University, Manchester, United Kingdom.*

[2] *Core Analytical Facility, Manchester Metropolitan University, Manchester, United Kingdom.*

[3] *Department of Natural Sciences, Manchester Metropolitan University, Manchester, United Kingdom.*

[4] *Department of Applied Sciences, Northumbria University, Newcastle, UK.*

[5] *Department of Respiratory Medicine, Northern Care Alliance NHS Foundation Trust, Salford, United Kingdom.*

Keywords

Gas chromatography-mass spectrometry, chemical derivatisation, short chain fatty acids, human faecal samples

Highlights

- A wide range of faecal short chain fatty acids were captured by the sample extraction and derivatisation.
- Short chain fatty acids were successfully profiled and quantified using GC-MS.
- Analysis showed the GC-MS method was robust and highly sensitive.
- Two additional short-chain fatty acids were putatively identified.

Abstract

The gut microbiota plays a key role in the maintenance of normal physiology and immune homeostasis at the site of the intestine. This is largely due to the production of short-chain fatty acids (SCFAs) from the fermentation of non-digestible carbohydrates and resistant starch by select bacteria in the colon. Such taxa are routinely implicated in states of dysbiosis within the intestinal microbiota, frequently observed in chronic diseases such as cystic fibrosis. Profiling and quantification of such metabolites, in tandem with bacterial abundance data is desirable for an enhanced understanding of the functional consequences of dysbiosis in disease. Simple, highly sensitive methods are therefore necessary for thorough integrative analyses.

This work presents a targeted method for highly sensitive gas chromatography-mass spectrometry (GC-MS) profiling and quantification of SCFAs, in human faecal samples. SCFAs were acidified and extracted from water with anhydrous ether, followed by dehydration and derivatization at 37°C for three hours. Analytes were acquired in selected ion monitoring (SIM) mode and quantified using internal standards and external calibration curves.

SCFAs presented excellent linearity (R^2 > 0.99), alongside low limit of detections (LOD) (0.055 to 0.142 µM) and quantification (0.185 to 0.473 µM). Following a process of sample reconstitution, matrix effects were close to zero percent, enabling the use of a water surrogate for calibration and quantification across the range of linearity observed. Good recovery rates (77.49 - 93.03%) and reproducibility (%RSD < 5%) were calculated during the validation procedure. Acetic, propionic, isobutyric, butyric, isovaleric, valeric, 4-methylvaleric, hexanoic and heptanoic acid were identified and quantified accurately from donor faecal samples. Additionally, two

additional metabolites were identified in human faecal samples using the National Institute of Standards and Technology (NIST) library.

In conclusion, a robust, fast, and sensitive GC-MS method for fatty acid profiling and quantification was developed. This included testing of both healthy and cystic fibrosis faecal samples, demonstrating the applicability of the method across biological samples potentially altered from disease.

4.1 Introduction

Short-chain fatty acids (SCFAs) are carboxylic acids consisting of a chain of 2-6 carbon atoms produced by the gut microbiota mainly through the fermentation of non-digestible carbohydrates and resistant starch (Venegas et al., 2019), SCFAs are associated with various pathologies, including those endocrinal, neurologic, hepatic, cardiovascular, and cancerous by nature (Marks et al., 2001; Z. Gao et al., 2009; de la Cuesta-Zuluaga et al., 2019; Silva et al., 2020; Mirzaei et al., 2021). Following their translocation by passive diffusion, dedicated transporters, and the activation of signalling cascades such as via G-protein coupled receptor (GPCR) activation, SCFA effects are therefore observed systemically (Venegas et al., 2019). Local to the intestinal tract, SCFAs harbour important roles in modulating the local inflammatory response and promoting gut epithelial barrier integrity (Donohoe et al., 2011). Bacteria equipped with genes for the synthesis of SCFAs have been implicated in various intestinal pathologies, including forms of inflammatory bowel disease (IBD) such as Crohn's disease and ulcerative colitis, alongside cystic fibrosis (CF) (Joossens et al., 2011; Takeshita et al., 2016; Marsh et al., 2022). SCFAs such as butyrate exhibit anti-tumorigenic properties and may play key roles in controlling intestinal malignancies (Arpaia et al., 2013; Chang et al., 2014). The vast majority of SCFA are absorbed, leaving approximately 5% excreted in faeces (Ruppin et al., 1980; Rechkemmer et al., 1988). However, relationships between faecal levels and absorption have been demonstrated, particularly for acetic acid (Vogt, 2003). Furthermore, faecal levels of SCFAs seemingly relate to gut symptoms (Müller et al., 2021) and disease characteristics in IBD (Treem et al., 1994; Huda-Faujan et al., 2010). This warrants the development of convenient, accurate and reliable analytical techniques to quantify and profile SCFAs from faecal samples to

better elucidate the functional consequences of gut microbiota dysbiosis in the context of intestinal disease.

The analysis of SCFAs has previously been achieved utilising various analytical techniques, including gas chromatography (GC) and liquid chromatography (LC) coupled with various kinds of detectors, such as ultraviolet (UV), flame ionization detector (FID), and mass spectrometry (MS) (De Baere et al., 2013; Hoving et al., 2018; Song et al., 2019; Scortichini et al., 2020). Unfortunately, due to their poor chromatographic and ionisation properties, SCFAs are challenging targets for liquid chromatography-mass spectrometry (LC-MS) (Saha et al., 2021; Bihan et al., 2022). Quantifying SCFAs without chemical derivatisation requires harsh experimental conditions in LC-MS, such as an aqueous mobile phase containing hydrochloric acid (van Eijk et al., 2009). Additionally, it is challenging to detect SCFAs by LC-MS due to their masses in the lower mass range and overlapping numerous interfering peaks from solvents and additives present (van Eijk et al., 2009). The inclusion of several chemical derivatisation methods, including derivatisation by 3-nitrophenylhydrazines and aniline, have been implemented during quantification of SCFAs while using LC-MS to overcome these problems (Chan et al., 2017; Liebisch et al., 2019). Both reagent agents produce high yields and are compatible with LC solvents.

GC-MS has emerged as a desirable method for quantifying fatty acids (Primec et al., 2017). This analytical technique requires suitable volatile compounds, and fatty acids are commonly derivatised into their methyl ester or trimethylsilyl ester derivatives. However, many derivatisation agents are moisture-sensitive and thus unsuitable for the aqueous matrices containing SCFAs, where the derivatisation agent must be chosen carefully (X. Gao et al., 2009; Zheng et al., 2013; Den Besten et al., 2014). Water-free conditions have been achieved for SCFA analysis, including

sample extract dehydration with anhydrous sodium sulphate (Na_2SO_4), but this has mainly been limited to studies in rodent-derived tissues (Zhang et al., 2019; Wang et al., 2020). Recent derivatisation-free approaches using solid-phase extraction (SPE) (Di Cagno et al., 2011; Ahmed et al., 2013) or directly analysing acidified water/extracts using HCl (Zhao et al., 2006; Zhang et al., 2013) or phosphoric acid (Achour et al., 2007; Majid et al., 2011) have been implemented previously. However, these methods might render low recoveries and sensitivity and bear the risk of impurities and GC column contaminations (García-Villalba et al., 2012).

The present study aimed to develop and validate a robust, sensitive, and accurate GC-MS-based profiling and quantification of SCFAs from human faecal samples. This analytical method included three steps: (1) extraction of the fatty acids from the sample matrix, where convenient sample clean-up involving a liquid-liquid extraction was performed, (2) derivatisation of the extracted fatty acids with N, O-bis(trimethylsilyl) trifluoroacetamide (BSTFA) for 3 hours at 37°C, and (3) GC–MS analysis. The extraction and derivatisation reaction conditions, storage and injection conditions were optimised and validated for human faecal samples. Validation parameters such as selectivity and specificity, precision, accuracy, linearity, range, stability, limit of detection (LOD) and limit of quantitation (LOQ) were evaluated. Finally, the validated method was used to profile and quantify fatty acid metabolites from a donor faecal sample.

4.2 Materials and methods

4.2.1 Chemicals and Standards

Analytical grade of hydrochloric acid (HCl), anhydrous diethyl ether (DE), anhydrous sodium sulphate (Na_2SO_4), and MS grade water were purchased from Fisher Scientific (Loughborough, UK). The ^{13}C-short chain fatty acids stool mixture, N, O-bis(trimethylsilyl)trifluoroacetamide) (BSTFA), and volatile free acid mix were purchased from Merck Life Science (Poole, UK). Helium CP grade was used as the carrier gas (99.999%, BOC Limited, UK).

4.2.2 Faecal sample collection

Healthy control and CF faecal samples were available from a previously approved study, whereby approval was obtained from the West Midlands Coventry and Warwickshire NHS Research Ethics Committee (18/WM/0242). All samples were provided during visits to the Nottingham University Hospitals NHS Trust.

4.2.3 Faecal sample processing, extraction, and derivatisation

All faecal samples were stored at - 80°C prior to sample processing. Samples were ground and homogenised using liquid N_2. Approximately 50 mg of ground faecal sample was added to a ZYMO™ 2 mL screw cap microtube containing ultra-high density, chemically inert beads (Cambridge Bioscience, Cambridge, UK). 0.5 mL of MS grade water was added, Samples were then further lysed and aqueously homogenised utilising the FastPrep-24™ 5G system, with two cycles at a speed of 6.0 m/s for 40 seconds. Next, samples were mixed at 80 rpm for 30 minutes using the RM-2L Intelli Mixer (ELMI, location) whilst incubated at 4°C.

After mixing, samples were centrifuged at 13,000 x *g* for 30 minutes at 4°C. The faecal water supernatant containing SCFAs was removed, before 150 µL was added to a Lo-Bind Eppendorf tube over ice containing 15 µl of 5 M HCl to protonate the sample. 150 µl DE solvent was added, alongside 3.15 µl internal standard. The internal standard was added to produce a theoretical final concentration of 30:10:10 µM (sodium) acetate, propionate and butyrate respectively in the sample following extraction and derivatisation. Samples were then vortexed for 10 seconds before mixing for 15 minutes utilising the RM-2L Intelli Mixer as previously described. Samples were then centrifuged at 10,000 x *g* for 5 minutes at 4°C. The DE layer containing volatile fatty acids was then accurately transferred to a Lo-Bind Eppendorf tube pre-loaded with 25 mg Na_2SO_4 to remove residual water. The remaining layer was then re-extracted with another 150 µL DE as before (no additional internal standard added). The two extraction tubes were then centrifuged at 280 x *g* for 1 minute to ensure sedimentation of Na_2SO_4 prior to combination by equal volume. 40 µl of the pooled sample was transferred then an amber GC vial with a fused insert, 2 µl was BSTFA added, vortexed for 5 seconds, and then capped tightly and incubated at 37°C with constant shaking for 3 hours. Following derivatisation, all samples were immediately quenched on ice then stored at -20°C before GC-MS analysis.

MS grade water was used as a blank sample control and to correct the background from use of the solvent and derivatisation agent. Independent blank samples were processed with the same method as faecal samples and acquired along the acquisition. The corrected peak areas of metabolites were calculated by taking the normalised spectra (using integrals of targets and internal standards) and subtracting normalised blank water samples detected under the same conditions and along the same acquisition.

4.2.4 GC-MS parameters

GC-MS analysis was carried out using an Agilent 7890B/5977 Single Quadrupole Mass Selective Detector (MSD) (Agilent Technologies) equipped with a non-polar HP-5ms Ultra Inert capillary column (30 m × 0.25 mm × 0.25 µm, Agilent Technologies). Carrier gas, wash steps, autosampler settings, oven temperatures, and ionisation properties were implemented as outlined in Chapter 2.2.8.3. SCFA identification, quantification, and downstream processing was achieved as described in Chapter 2.2.8.3.

4.2.5 Method Validation

The GC-MS method validation was carried out by establishing specificity, linearity and range, precision, accuracy, recovery, LOD and LOQ. These methods are described across Chapters 2.2.8.5 to 2.2.8.9. Before acquisitions, a system suitability test (SST) was conducted to assess the GC-MS system for no interferences present, sensitivity and repeatability using 5 µM of extracted and derivatised reference standard mix. Percentage relative standard deviation (%RSD) of the peak areas and retention times (RT), signal to noise of all five injections were calculated.

4.2.5.1 Matrix effects

Matrix effects within faecal samples were investigating using the approach detailed in Chapter 2.2.8.10, across samples spiked with 5, 500 and 1000 µM of the reference fatty acid mixture.

4.2.5.2 Stability

Sample storage and subsequent stability testing techniques of the processed samples was carried out as described in Chapter 2.2.8.11.

4.2.5.3 Profiling and quantification of short to medium-chain fatty acids

Profiling of fatty acid composition and absolute quantification of metabolites was performed in accordance to Chapter 2.2.8.12, whereby the ^{13}C butyric acid standard was the designated as a suitable component of the standard reference mix for this purpose, based on the fragmentation pattern and subsequent ions produced.

4.3 Results and discussion

4.3.1 Extraction and derivatisation method

Initially we sought to determine how the extraction method could be optimised, specifically involving the mixing time of DE solvent with protonated water containing the SCFA reference mix. Extraction with DE was selected based on previous results indicating the increased yield of shorter SCFAs (C2-C4) from murine faecal samples (Zhang et al., 2019). Other methods in the literature have also implemented anhydrous Na_2SO_4 addition before sample derivatisation (Polyakova et al., 2013; De Paola et al., 2017), but information concerning the amount to be added for optimal sample dehydration is limited. Increasing sample mixing time compared to alternate approaches (Zhang et al., 2019) during the extraction procedure, to 15 mins per extraction round, and using 25 mg Na_2SO_4 per 150 µl of extracted SCFA supernatant was opted for, to enable the highest possible recovery rates.

BSTFA has previously been used for the derivatisation of faecal-derived SCFAs with great success (Wu et al., 2009; He et al., 2019), and so was chosen as a suitable agent for the human faecal samples obtained. 37°C was selected as a suitable temperature for the derivatisation procedure given the practicality of derivatising samples over a shorter timeframe and allowing for consistency of time control (compared to overnight methods), all without substantially increasing the temperature and thus reducing potential volatility issues with the solvent and metabolites inside the GC vial, which has also been described previously (Zhang et al., 2019). To ensure sufficient derivatisation time at 37°C for the reformed extraction method, extracted SCFA reference samples were derivatisation at 37°C for 3 hours, which was sufficient to ensure complete derivatisation of the target sample. Grinding of samples in liquid nitrogen and subsequent storage at -80°C was commonly performed and did not impact yields obtained. Additionally, extracted acids were able to be stored at -20°C prior to derivatisation and GC-MS analysis.

4.3.2 Method validation

Table 4.1 depicts parameters obtained for each SCFA tested, including the confirmation and quantification ions (m/z). Selected ion monitoring (SIM) provided greater sensitivity and separation of the SCFA peaks within the spectra, aiding the analysis of SCFAs. All SCFAs demonstrated high correlation coefficients ($R^2 \geq 0.993$), with the limit of linearity ranging between SCFAs. Acetic acid had a limit of linearity of 2000 µM, with propionic acid 2500 µM. All other SCFAs had a limit of linearity of 1000 µM. The limit of detection (LOD) and limit of quantification (LOQ) were calculated using signal to noise ratios of 3:1 and 10:1 respectively. LOD Values ranged from 0.055 to 0.142 µM, demonstrating the enhanced sensitivity as compared to derivatisation-free GC-MS approaches (Bianchi et al., 2011; García-

Villalba et al., 2012) and even those utilising other agents such as pentafluorobenzyl bromide (PFBBr) (Hoving et al., 2018). Likewise, the LOQ, which ranged from 0.185 to 0.473 μM, demonstrated the high sensitivity of the derivatisation-based method, with similarity to values obtained across murine faecal SCFA analysis (Zhang et al., 2019).

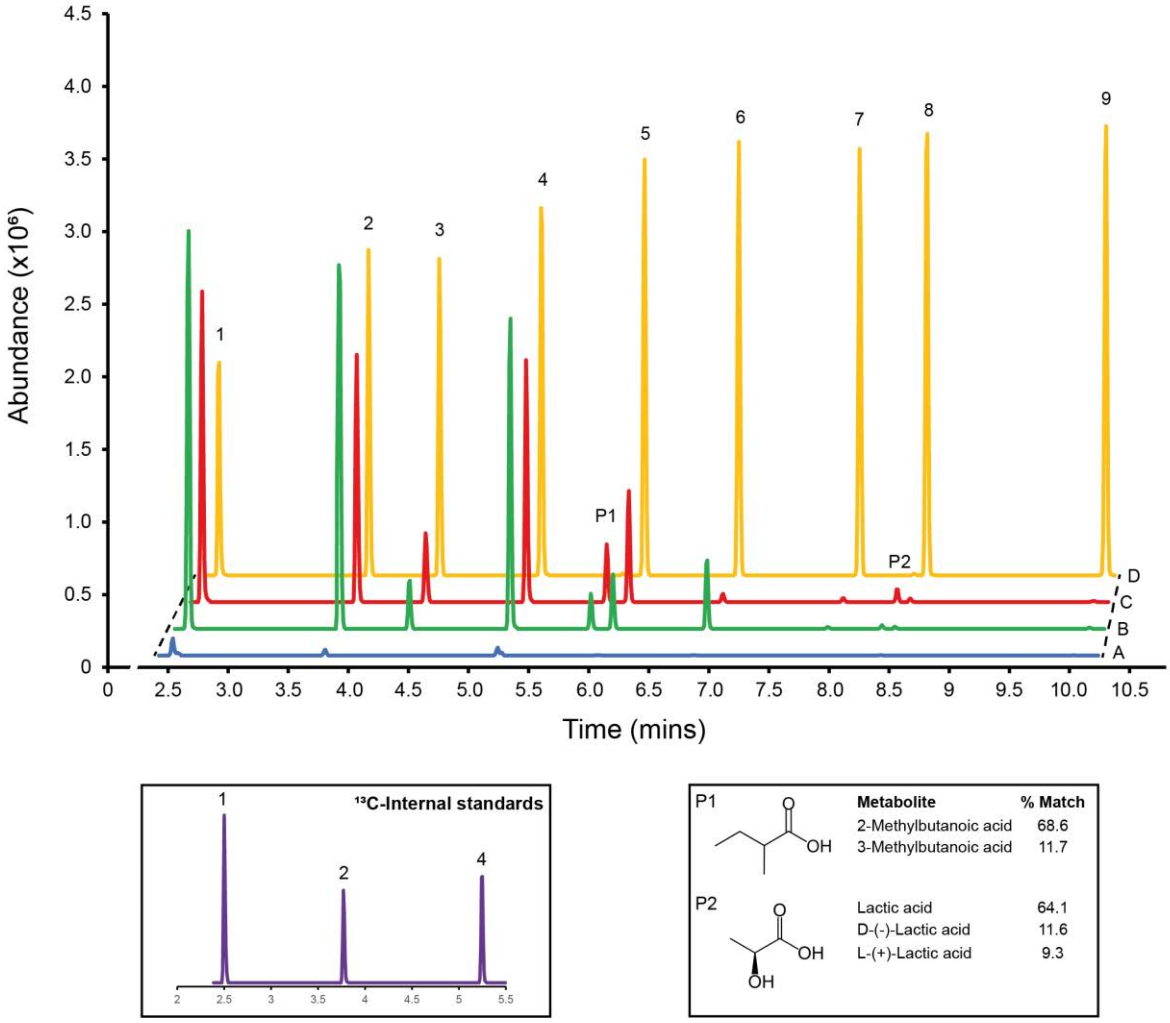

Figure 4.1 Representative total ion count (TIC) chromatograms from various elements of the method development. A representative selective ion monitoring (SIM) chromatogram of the ^{13}C-SCFA internal standard is also demonstrated underneath. (A) TIC of a water blank sample. (B) TIC of a healthy control human sample. (C) TIC from a cystic fibrosis patient harbouring intestinal inflammation. (D) TIC from 0.5 mM volatile fatty acid reference mixture. Peak identification is as follows: 1 – acetic acid, 2- propionic acid, 3 – isobutyric acid, 4 – butyric acid, 5 – isovaleric acid, 6 – valeric acid, 7 - 4-methylvaleric acid, 8 – hexanoic acid, 9 – heptanoic acid. Provisional peak identification based on NIST library: P1 – 2-methylbutanoic acid, P2 – Lactic acid.

Table 4.1 Analytical parameters for SCFA analysis with GC-MS

SCFA	t_R (min)	Target ion (m/z)	Confirmation ion (m/z)	R^2	Linearity limit (µM)	LOD (µM)	LOQ (µM)	Res
Acetic acid	2.52	117	75	0.9936	2000	0.142	0.473	17.06
Propionic acid	3.81	131	75	0.9928	2500	0.091	0.304	8.21
Isobutyric acid	4.39	145	117	0.9972	1000	0.080	0.266	11.16
Butyric acid	5.22	145	117	0.9972	1000	0.067	0.222	11.31
Isovaleric acid	6.07	159	117	0.997	1000	0.071	0.237	12.65
Valeric acid	6.85	159	117	0.9974	1000	0.071	0.238	20.70
4-methylvaleric acid	7.86	173	117	0.9970	1000	0.056	0.188	12.61
Hexanoic acid	8.41	173	117	0.9979	1000	0.056	0.187	38.58
Heptanoic acid	9.90	187	117	0.9971	1000	0.055	0.185	NA
^{13}C-acetic acid§	2.52	119	77	NC	NC	NC	NC	NC
^{13}C-propionic acid§	3.81	134	77	NC	NC	NC	NC	NC
^{13}C-butyric acid	5.22	149	119	NC	NC	NC	NC	NC
***2-methylbutanoic acid**	5.87	145	117	NC	NC	NC	NC	NC
***Lactic acid**	8.35	173	117	NC	NC	NC	NC	NC

t_R: Retention time for given SCFA; LOD: Limit of detection; LOQ: Limit of quantification; Res: Resolution between target and subsequent peak of interest; NC: Not calculated. *Should be considered putative based on NIST library search.
§Internal standards not used for downstream profiling and quantification.

4.3.3 Recovery and reproducibility

Recoveries within the range of 5 to 1000 µM tested, ranged from 78.80 ± 5.57% to 93.03 ± 2.81% (mean ± SD) across all the metabolites tested (Table 4.2), demonstrating relatively good recoveries (Zhang et al., 2019). Between acetic to isovaleric acid, recoveries generally increased as the concentration of the reference standard increased from 5 to 1000 µM, whilst longer-chain fatty acids (including valeric acid) displayed the opposite trend, generally decreasing. The recovery of larger fatty acids (≥C5 acids) was generally greater than the shorter chain counterparts (particularly C2-C4 acids). The reproducibility of the method was good, as determined by the %RSDs for both retention time (t_R, min) and peak integrals. Across all acids, the intra and inter-day %RSDs for t_R ranged from 0.00-0.35% and 0.12-0.52% respectively (Table S4.1). For the peak integrals, these ranged from 2.57–4.65%. The results of both outcomes demonstrate good analytical stability of our approach, with recovery rates and stability similar to others (García-Villalba et al., 2012; Zhao et al., 2016; Zhang et al., 2019).

4.3.4 Determination of matrix effects

Following the equation shown in section 4.2.5.6, conducted utilising the method depicted in Figure 4.2, we sought to investigate any potential matrix effects of the protonated faecal water obtained from human faecal samples towards the signal obtained from GC-MS analysis. As shown in Table 4.3, no signal suppression was observed across the range of concentrations tested (5, 500, and 1000 μM). Rather, a small but insignificant signal enhancement was detected across all concentrations tested. With all signal enhancement values < 1.40% (except acetic acid at 1000 μM which was 1.97%) the current method was deemed suitable for application to human faecal samples. Our results are in agreement with previous studies, whereby the use of water as a surrogate for a faecal sample matrix has been successfully used to construct calibration curves for subsequent sample quantification (Kim et al., 2022).

Table 4.2 Calculated recovery across human faecal samples tested

Conc (μM)	Acetic	Propionic	Isobuteric	Butyric	Isovaleric	Valeric	4-methylvaleric	Hexanoic	Heptanoic
5	79.14 ± 9.19	77.49 ± 6.48	79.6 ± 4.63	79.45 ± 6.54	82.06 ± 6.62	86.91 ± 6.02	90.51 ± 4.99	90.68 ± 5.03	93.03 ± 2.81
500	78.80 ± 5.57	79.43 ± 3.57	82.16 ± 2.63	82.65 ± 1.41	85.87 ± 1.07	85.72 ± 0.74	87.38 ± 0.60	87.19 ± 0.63	86.79 ± 1.06
1000	79.23 ± 3.29	80.41 ± 3.48	83.77 ± 2.96	85.48 ± 2.07	87.3 ± 1.89	86.63 ± 2.01	86.35 ± 1.80	85.90 ± 1.65	85.88 ± 1.89

Displayed is the Mean **±** SD, across samples extracted, derivatised, and ran in triplicate.

Table 4.3 Calculated matrix effects across human faecal samples tested

Concentration (μM)	Acetic	Propionic	Isobuteric	Butyric	Isovaleric	valeric	4-methylvaleric	Hexanoic	Heptanoic
5	-1.07	-1.16	-0.70	-0.29	-0.61	-0.76	-0.78	-0.67	-0.71
500	-1.12	-0.95	-0.99	-0.82	-0.95	-0.87	-0.75	-0.68	-0.77
1000	-1.97	-1.39	-1.39	-1.11	-1.15	-1.13	-0.92	-0.80	-0.78

Negative values indicate enhancement of target signal. Values depicted are percentages (%).

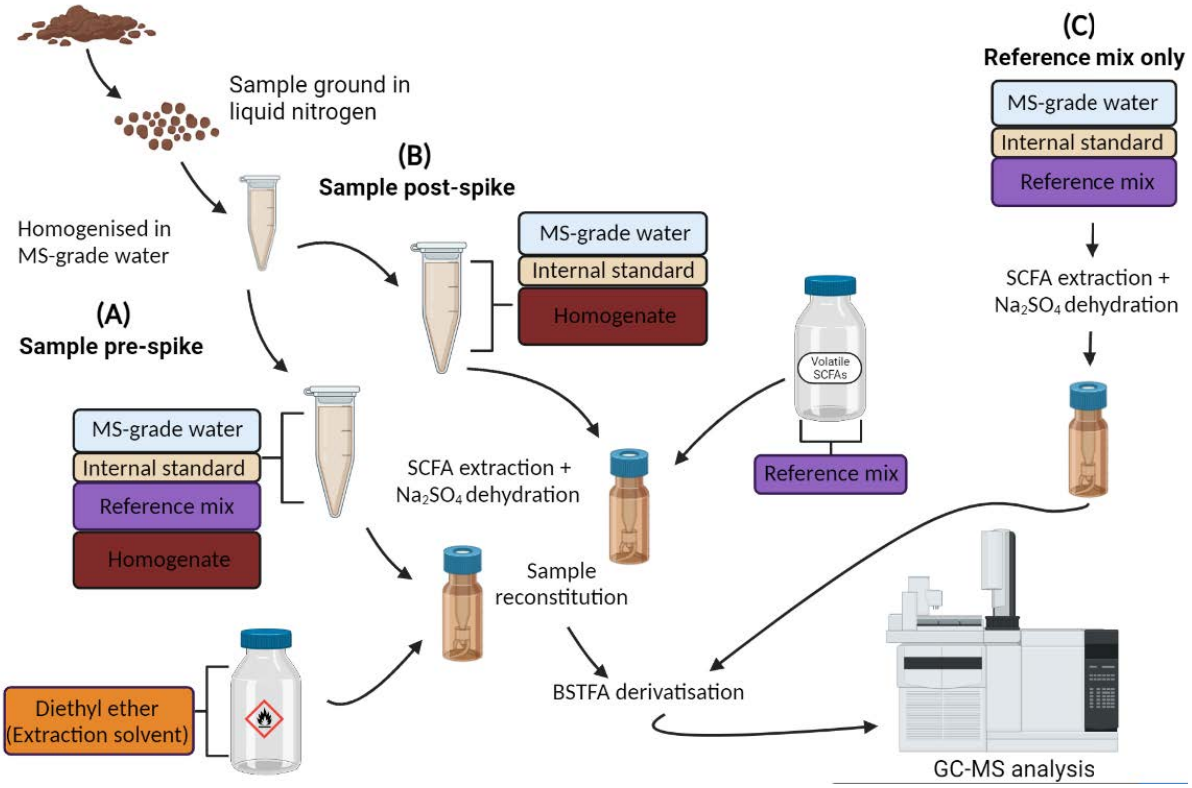

Figure 4.2 Process of sample reconstitution to determine both sample recovery and presence of any matrix effects in faecal samples for targeted fatty acid analysis. (A) Process of sample pre-spike, where the reference mixture is added prior to extraction with diethyl ether (DE). Additional DE is added following extraction and Na_2SO_4 to alter the final concentration prior to derivatisation and GC-MS analysis. (B) Process of sample post-spike, where the reference mixture is added following sample extraction with diethyl ether (DE). The reference mixture concentration and volume added is calculated to match the pre-spike sample, prior to derivatisation and GC-MS analysis. (C) Reference mix sample only, prepared similarly in parallel in only MS-grade water to represent an efficient extraction without any potential sample matrix interference. Figure created with BioRender.

4.3.5 Faecal SCFA identification and quantification

Following the determination that extraction of volatile fatty acids from donor faecal samples yielded negligible matrix effects (Table 4.3), samples were quantified using a calibration curve series of the pure volatile fatty acid reference standard, diluted and extracted from MS-grade water. The quantified volatile fatty acids from are depicted in Figure S4.2, with the respective spectra also shown in Figure 4.1. As expected, the three most abundant acids quantified were (mean ± SD) acetic (42.69 ± 2.17 mmol/kg), propionic (22.99 ± 0.33 mmol/kg), and butyric acid (12.62 ± 0.03 mmol/kg). All other acids were quantifiable, but significantly lower in concentration, except heptanoic acid which fell under the limit of quantification within the donor faecal sample from a patient with CF. Of note, we were also able to detect alternate peaks on the spectra (Table 4.1), which were putatively identified as 2-methylbutanoic acid and lactic acid. Lactic acid is produced by a subset of the microbial community, serves as substrates in complex cross-feeding pathways, in turn impacting host intestinal physiology (Louis et al., 2022) and therefore may be of clinical relevance for quantification moving forwards. The overgrowth of *Enterococcaceae*, which contains potentially pathogen members has been associated with enhanced lactate in faeces isolated from people with CF (Wang et al., 2019).

4.4 Conclusion

The current study has demonstrated the applicability of a modified GC-MS method to accurately profile and quantify a wide range of fatty acids from human faecal samples, in both health and disease. This derivatisation-based approach illustrates high sensitivity, excellent linearities ($R^2 \geq 0.993$), good recovery (78.80-93.03%), and sound repeatability (RSD% < 5), in addition to low LOQs (0.185 to 0.473 μM). Furthermore, other potentially relevant metabolites in microbial dysbiosis have been putatively identified through library searching, of which should help facilitate our understanding of the microbiota and its functionality within intestinal health and disease.

4.5 Author contributions

RM, DR, and CvdG conceived the study. RM and CDS carried out the metabolomic method development. RM carried out faecal sample processing. RM was responsible for the creation of the original draft of the manuscript. RJM, CDS, DR, and CvdG contributed to the development of the final manuscript. CvdG is the guarantor of this work. All authors read and approved the final manuscript.

4.6 Supplementary figures and tables

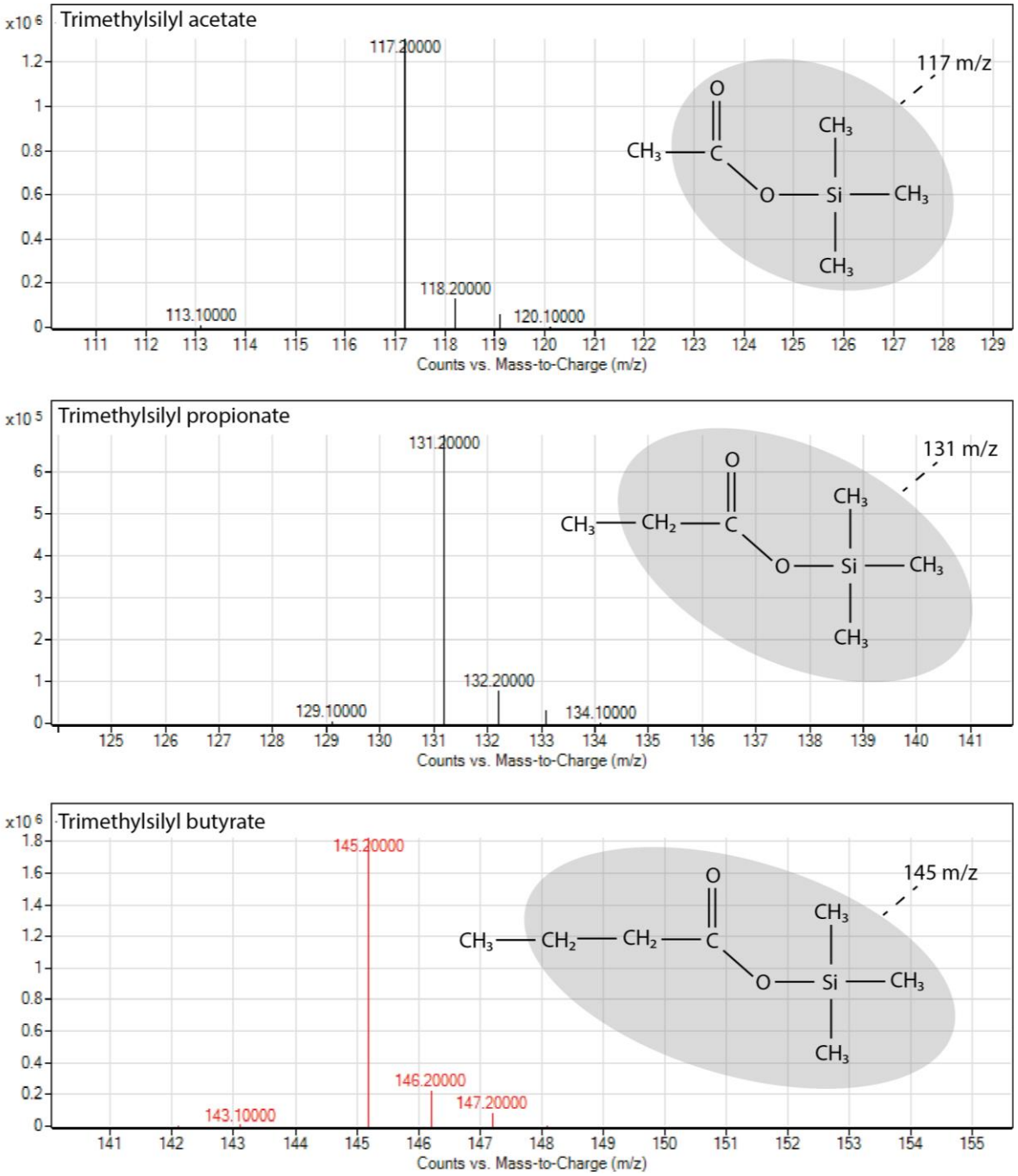

Figure S4.1 Mass spectra of acetic, propionic, and butyric acids from their derivatised forms as trimethylsilyl esters. Shown are the fragmentation patterns obtained from total ion count (TIC) spectra of the volatile fatty acid reference mix (500 µM). The structure of each trimethylsilyl ester is shown to the right of each mass spectrum. Trimethyl acetate and propionate both produce fragments that overlap with the target ions proposed for the ^{13}C internal standard equivalents (119 and 134 m/z respectively). The mass spectrum for trimethyl butyrate (red) does not demonstrate overlap with the target ion for ^{13}C-butyric acid (149 m/z), and thus was deemed suitable for use as an internal standard in the downstream normalisation of GC-MS spectra.

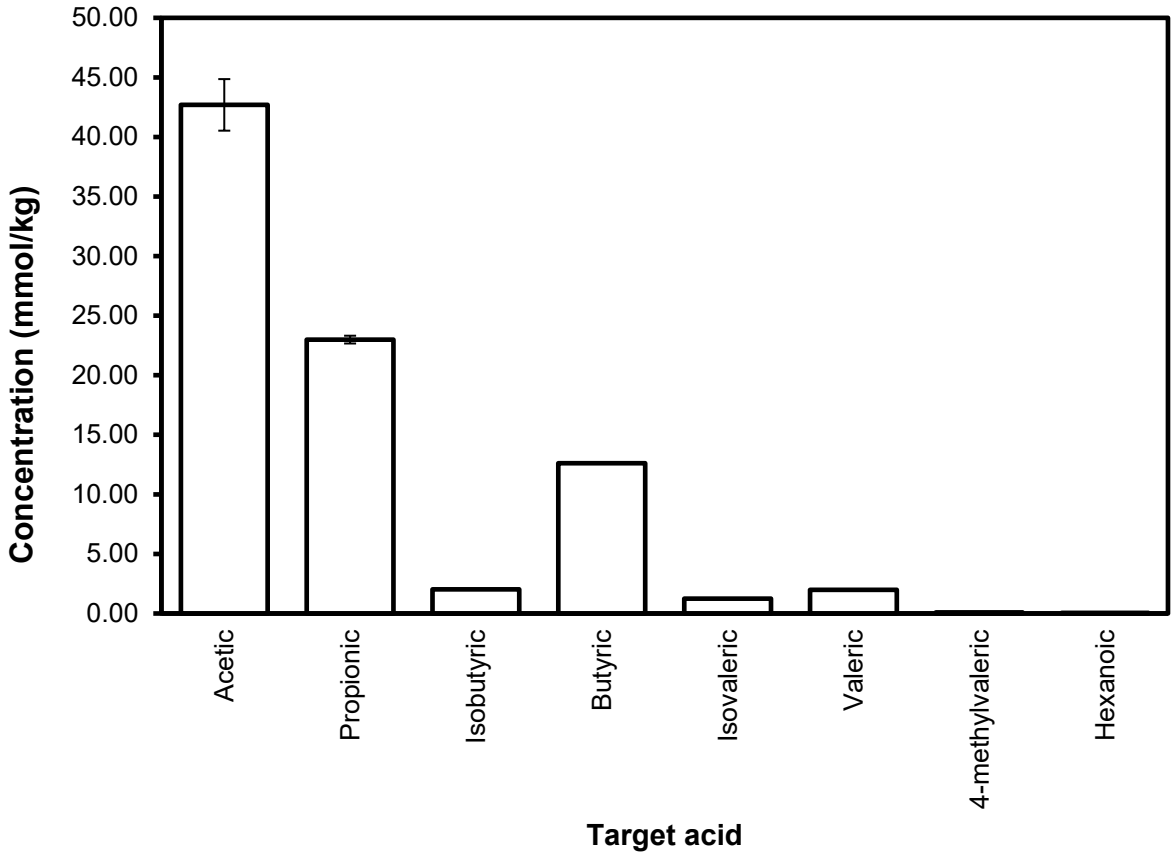

Figure S4.2 Quantification of short to medium-chain fatty acids from a faecal donor sample. Extraction, derivatisation, and GC-MS analysis was carried out in triplicate. Error bars denote standard deviation of the mean. Heptanoic acid quantification did not surpass the calculated limit of quantification from the initial calibration series (< 0.185 μM), therefore was omitted from downstream analysis to calculate the original sample concentration in mmol/kg.

Table S4.1 Intra- and inter-day stability of retention times for the target metabolites.

Fatty acid metabolite	Intra-day stability (%RSD, range)	Inter-day stability (%RSD)
Acetic	**0.16-0.35**	**0.52**
Propionic	**0.24-0.17**	**0.18**
Isobutyric	**0.13-0.16**	**0.19**
Butyric	**0.05-0.11**	**0.14**
Isovaleric	**0.05-0.08**	**0.15**
Valeric	**0.05-0.07**	**0.15**
4-methylvaleric	**0.00-0.06**	**0.12**
Hexanoic	**0.00-0.06**	**0.13**
Heptanoic	**0.00-0.05**	**0.12**

Inter-day stability was determined over the course of four batches.

Chapter 5: Tezacaftor/Ivacaftor therapy has negligible effects on the cystic fibrosis gut microbiome

This Chapter is published in the journal *Microbiology Spectrum* and is presented in submitted manuscript format:

Ryan M, Claudio DS, Liam H, Christabella N, Giles M, R. SA, Damian R, Christopher van der G. 2023. Tezacaftor/Ivacaftor therapy has negligible effects on the cystic fibrosis gut microbiome. Microbiol Spectr 0:e01175-23.

Tezacaftor/Ivacaftor therapy has negligible effects on the cystic fibrosis gut microbiome

Ryan Marsh [a,b], Claudio Dos Santos [c], Liam Hanson [a,c], Christabella Ng [d,e], Giles Major [d,f], Alan R Smyth [d,e], Damian Rivett [c #], Christopher van der Gast [a,b,g #]

[a] Department of Life Sciences, Manchester Metropolitan University, Manchester, UK

[b] Department of Applied Sciences, Northumbria University, Newcastle, UK

[c] Department of Natural Sciences, Manchester Metropolitan University, Manchester, UK

[d] School of Medicine, University of Nottingham, Nottingham, UK

[e] NIHR Nottingham Biomedical Research Centre, Nottingham, UK

[f] Nestlé Institute of Health Sciences, Société des Produits Nestlé, Lausanne, Switzerland

[g] Department of Respiratory Medicine, Salford Royal NHS Foundation Trust, Salford, UK

[#] Correspondence to: Professor Chris van der Gast, Department of Applied Sciences, Faculty of Health and Life Sciences, Ellison Building, Newcastle Upon Tyne, Tyne and Wear, NE1 8ST, UK; Chris.vandergast@northumbria.ac.uk. Dr Damian Rivett, Department of Natural Sciences, Faculty of Science and Engineering, John Dalton Building, Chester Street, Manchester, M1 5GD, UK; d.rivett@mmu.ac.uk

Keywords: gut microbiome, gut microbiota, dysbiosis, CFTR modulator therapy

Abstract word count: 226

Manuscript word count: 3642

Highlights

- Tezacaftor/Ivacaftor had no impact upon microbiota diversity or composition.
- Tezacaftor/Ivacaftor had no impact upon faecal short-chain fatty acid composition.
- Controls remain significantly different to pwCF with respect to microbiota structure and function.
- No significant differences in patient symptoms or gut function succeeded Tezacaftor/Ivacaftor use.

Abstract

People with cystic fibrosis (pwCF) experience a range of persistent gastrointestinal symptoms throughout life. There is evidence indicating interaction between the microbiota and gut pathophysiology in CF. However, there is a paucity of knowledge into potential effects of CF transmembrane conductance regulator (CFTR) modulator therapies on the gut microbiome. In a pilot study, we investigated the impact of Tezacaftor/Ivacaftor dual combination CFTR modulator therapy on the gut-microbiota and metabolomic functioning in pwCF. Faecal samples from 12 pwCF taken at baseline and following placebo or Tezacaftor/Ivacaftor administration were subjected to microbiota sequencing and to targeted metabolomics to assess the short-chain fatty acid (SCFA) composition. Ten healthy matched controls were included as a comparison. Inflammatory calprotectin levels and patient symptoms were also investigated. No significant differences were observed in overall gut microbiota characteristics between any of the study stages, extended also across intestinal inflammation, gut symptoms, and SCFA targeted metabolomics. However, microbiota and SCFA metabolomic compositions, in pwCF, were significantly different from controls in all study treatment stages. CFTR modulator therapy with Tezacaftor/Ivacaftor had negligible effects on both the gut microbiota and SCFA composition across the course of the study and did not alter towards compositions observed in healthy controls. Future longitudinal CFTR modulator studies will investigate more effective CFTR modulators and should use prolonged sampling periods, to determine whether longer-term changes occur in the CF gut microbiome.

Importance

People with cystic fibrosis (pwCF) experience persistent gastrointestinal (GI) symptoms throughout life. The research question “how can we relieve gastro-intestinal symptoms, such as stomach pain, bloating, and nausea?” remains a top priority for clinical research in CF. While CF transmembrane conductance regulator (CFTR) modulator therapies are understood to correct underlying issues of CF disease and increasing numbers of pwCF are now receiving some form of CFTR modulator treatment. It is not known how these therapies affect the gut microbiome or GI system. In this pilot study we investigated, for the first time, effects of the dual combination CFTR modulator medicine, Tezacaftor/Ivacaftor. We found it had negligible effects upon patient GI symptoms, intestinal inflammation, or gut microbiome composition and functioning. Our findings are important as they fill important knowledge gaps on the relative effectiveness of these widely used treatments. We are now investigating triple combination CFTR modulators with prolonged sampling periods.

5.1 Introduction

People with cystic fibrosis (pwCF) experience a range of persistent gastrointestinal (GI) abnormalities that affect quality of life. The research question “how can we relieve gastro-intestinal symptoms, such as stomach pain, bloating, and nausea?” continues to be amongst the top priorities for clinical research in CF (Gillan et al., 2022; Rowbotham et al., 2023). Also present with GI abnormalities is dysbiosis of the gut microbiome; which are changes to the resident microbiota and their functional outputs that are hypothesised to exacerbate abnormalities associated with CFTR dysfunction (Thavamani et al., 2021). Indeed, changes to the gut microbiota have previously been associated with markers of intestinal function, inflammation, and local tissue damage (Flass et al., 2015; De Freitas et al., 2018), indicating a role of the microbiome in the multifactorial aetiology of intestinal disease in the CF gut. We have previously demonstrated such relationships between gut microbiota composition and intestinal function in pwCF, including markers of gut pathophysiology and intestinal function, as measured by magnetic resonance imaging (Marsh et al., 2022).

Over two-thirds of pwCF in the UK are now receiving CF transmembrane conductance regulator (CFTR) modulator therapies (Cystic Fibrosis Trust, 2022), which can correct the underlying problems of mutated CFTR protein functioning, including trafficking, gating, and conductance at the cell epithelial surface (Lopes-Pacheco, 2020). In comparison to the lower airways, our knowledge of the effects of CFTR modulator therapies upon CF GI pathophysiology is limited. Whilst improvements to BMI, patient growth rates, and intestinal pH increases are better defined (Rowe et al., 2014; Wainwright et al., 2015; Gelfond et al., 2017; Stallings et al., 2018), there remain differing results concerning the modulation of intestinal inflammation from the small number of available studies, all of which were focused

on Ivacaftor or Lumacaftor/Ivacaftor CFTR modulator-based treatment (Ooi et al., 2018; Tetard et al., 2020; Ronan et al., 2022). Likewise, studies investigating changes to the microbiota are also scarce and relate mostly to monotherapy approaches (Ooi et al., 2018; Kristensen et al., 2021; Pope et al., 2021; Ronan et al., 2022). The CF gut microbiota is currently divergent from healthy controls throughout life and further compounded by CF-associated lifestyle factors such as antibiotic therapies and dietary changes (Nielsen et al., 2016; Burke et al., 2017; Antosca et al., 2019; Kristensen et al., 2020; Loman et al., 2020). It is, however, reasonable to suggest restoration of CFTR function could remodulate the bacterial composition back to a signature observed in healthy controls, given that the primary consequence of CFTR dysfunction alone is sufficient to induce dysbiosis in the CF population (Meeker et al., 2020). This may arise from the restoration of fluidity at the site of the intestinal epithelia, or through various other pathways and mechanisms in which the CFTR protein plays a key role (Hanssens et al., 2021).

A new clinical research priority for CF is to understand “what are the effects of modulators on systems outside the lungs such as … gastrointestinal?” (*Cystic Fibrosis Refresh Top 10 priorities (priority setting in association with the JLA)*, 2022). As new CFTR modulator therapies become available it is important to understand potential impacts on the GI system, including the gut microbiome. Therefore, in the current pilot study we aimed to investigate the impact of Tezacaftor/Ivacaftor dual combination CFTR modulator therapy on the gut microbiome in pwCF. This was achieved by analysing and comparing the gut microbiota along with short-chain fatty acid (SCFA) targeted metabolomics from faecal samples taken from pwCF at baseline and following placebo or Tezacaftor/Ivacaftor dual combination CFTR modulator therapy. These samples were collected as part of a randomised crossover trial of Tezacaftor/Ivacaftor vs. placebo (NCT04006873). Faecal samples

from healthy matched controls were included as a comparison (Marsh et al., 2022). SCFAs were specifically targeted as these microbially-produced metabolites are known to play important roles in gut health and development of disease (Tan et al., 2014). Patient clinical characteristics at baseline are detailed in Table 5.1.

Table 5.1 Clinical characteristics of pwCF during Tezacaftor/Ivacaftor trial period and healthy controls.

Characteristic	pwCF	healthy controls
Baseline age (Mean ± SD)	20.8 ± 7.8	21.4 ± 7.4
Male (%)	8 (66.6)	5 (50)
Baseline BMI (Mean ± SD)	21.4 ± 2.5	22.9 ± 4.4
F508del/F508del (%)	12 (100)	0 (0)
Pancreatic insufficient (%)	12 (100)	0 (0)
Baseline FEV1% (Mean ± SD)	80.6 ± 19.6	-
Regular antibiotics (%)	11 (91.6)	0 (0)
Additional antibiotics during trial (%)	6 (50)	-

Regular antibiotics during trial includes: oral azithromycin (7/12, 58.3%); inhaled tobramycin (2/12, 16.7%); inhaled aztreonam (1/12, 8.3%); and inhaled colistimethate sodium (4/12, 33.3%). Additional antibiotic treatment includes: oral Ciprofloxacin (4/12, 33.3%); oral clarithromycin (1/12, 8.3%): and intravenous (IV) antibiotics (1/12, 8.3%).

5.2 Results

Bacterial taxa within the whole microbiota were partitioned into common core and rare satellite taxa after plotting distribution-abundance relationships for all for sample groups from baseline, placebo, and Tezacaftor/Ivacaftor treatment periods, and the healthy controls (Figure S5.1). Core taxa within each treatment period along with the healthy control group are given in Table S5.1. Diversity and composition for the whole microbiota, as well as the core and satellite taxa, between treatment period were compared (Figure 5.1A and B).

No significant differences were observed in whole microbiota diversity between any of the treatment periods ($P > 0.05$ in all instances) (Figure 5.1A, Table S5.2). Significant differences in diversity were observed in core taxa between baseline and placebo ($P = 0.007$) and placebo and Tezacaftor/Ivacaftor treatment groups ($P = 0.039$). Core taxa diversity was not significantly different between baseline and Tezacaftor/Ivacaftor groups ($P > 0.05$) (Figure 5.1A, Table S5.2). For the satellite taxa, no significant differences in diversity were observed between treatment periods ($P > 0.05$ in all instances) (Figure 5.1A, Table S5.2). Additionally, composition of the whole microbiota and the core and satellite taxa groups were not significantly different between treatment periods ($P > 0.05$ in all instances) (Figure 5.1B, Table S5.3).

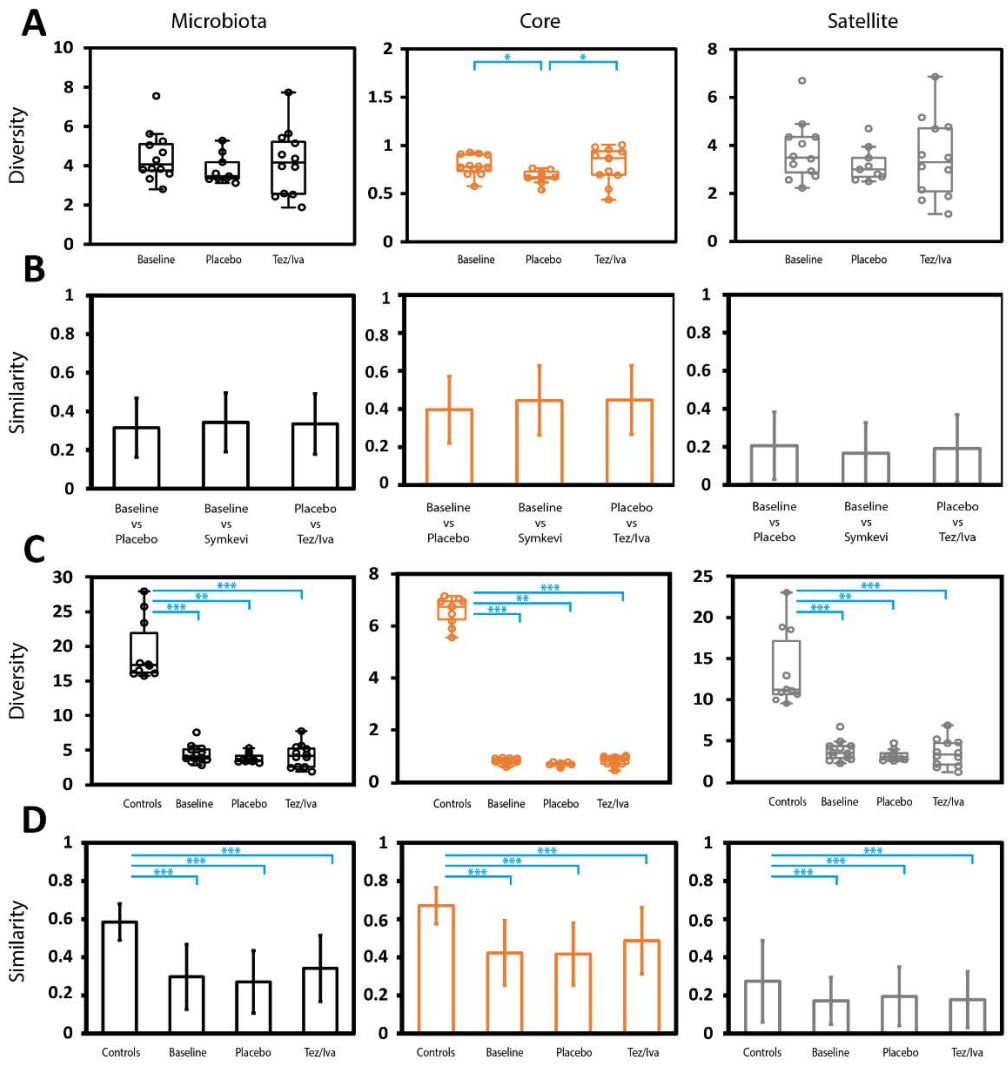

Figure 5.1 Comparisons of microbiota diversity and similarity indices. (**A**) Differences in Fisher's alpha index of diversity across pwCF during the various treatment periods. Circles indicate individual patient data for microbiota (black), partitioned core (orange), and partitioned satellite (grey) taxa. Error bars represent 1.5 times the inter-quartile range (IQR). Asterisks denote significant differences in diversity between treatment periods following Kruskal-Wallis testing. Summary statistics are provided in Table S5.2. (**B**) Microbiota variation measured across various treatment periods, utilising the Bray-Curtis index. Shown is the similarity between different treatment periods. Error bars represent standard deviation of the mean. ANOSIM tests were conducted between sampling phases; Summary statistics are provided in Table S5.3. (**C**) Differences in Fisher's alpha index of diversity across pwCF from this trial compared to previously matched healthy controls. Asterisks denote significant differences in diversity between treatment periods following Kruskal-Wallis testing. Summary statistics are provided in Table S5.4. (**D**) Microbiome variation across the various treatment periods in pwCF and matched healthy controls, utilising the Bray-Curtis index. Shown is the within-group similarity between. Error bars represent standard deviation of the mean. Asterisks denote significant differences following ANOSIM testing; Summary statistics are provided in Table S5.5. ***; $P < 0.0001$, **; $P < 0.001$, *; $P < 0.05$. Tez/Iva; Tezacaftor/Ivacaftor. Group sizes: Baseline, n = 12; placebo, n = 9; Tez/Iva, n = 12.

Next diversity and composition for the microbiota, core taxa, and the satellite taxa between each treatment period and the matched healthy control group were compared (Figure 5.1C and D). In all instances, diversity in the control group was found to be significantly higher when compared to each treatment period ($P < 0.05$ in all instances) (Figure 5.1C, Table S5.4). Similarly, the microbiota, core taxa, and satellite taxa compositions of the healthy control samples were significantly different from pwCF for all treatment periods ($P < 0.05$ in all instances) (Figure 5.1D, Table S5.5). To visualise how Tezacaftor/Ivacaftor treatment might shift the microbiota composition back to that observed in healthy controls, samples were spatially plotted utilising Bray-Curtis distances (Figure 5.2). Healthy control samples clustered more tightly to one another, indicating they were more similar to each other, when compared to samples within any of the treatment periods (Figure 5.1D and 5.2). Also, the healthy control microbiota samples clustered away from the treatment stage microbiota samples, which all overlapped with one another. No shift within the Tezacaftor/Ivacaftor group back towards a healthy microbiota composition was observed (Figure 5.2).

Changes in microbially produced SCFA metabolites were also investigated (Figure 5.3). SCFA metabolites, including their target and confirmation ions, are listed in Table S5.6. SCFA metabolite compositions were not significantly different between treatment stage sample groups ($P > 0.05$ in all instances) (Table S5.7). Conversely, significant differences in SCFA compositions between healthy controls and all treatment stages were observed ($P < 0.05$ in all instances) (Table S5.7). In terms of specific SCFAs, SIMPER analysis (Table S5.8) showed that acetic, propionic, and butyric acid cumulatively contributed >73% of these differences. Furthermore, their combined relative levels were increased in pwCF compared to healthy controls, which constituted mean (± SD) collective levels of 92.5% (±6.6%) and 84.3%

(±6.6%) respectively. This coincided with higher relative levels of longer SCFAs in healthy controls, particularly those containing ≥5 carbons, of which there were significant differences compared to pwCF as seen in Supplementary Table S5.9. Additionally, Isobutryic acid relative levels were significantly decreased in both baseline (*P* = 0.048) and placebo (*P* = 0.009), but not Tezacaftor/Ivacaftor (*P* = 0.429) pwCF samples compared with healthy controls (Table S5.9).

Finally, no significant differences in intestinal inflammation, as measured by faecal calprotectin, were observed between Tezacaftor/Ivacaftor and baseline/placebo phases of the study (median [IQR]: 13.7 [5.2-25.8] vs 12.6 [8.0-21.5] µg/g, *P* = 0.954). However, both phases were significantly different from the healthy controls (3.7 [2.8-4.8] µg/g, *P* = 0.010 and *P* = 0.018 respectively). Also, no differences across participant symptom scores between Tezacaftor/Ivacaftor and off-treatment samples through the PAC-SYM (*P* = 0.393) or CFAbd (*P* = 0.297) questionnaires were observed (Tables S5.10-S5.11).

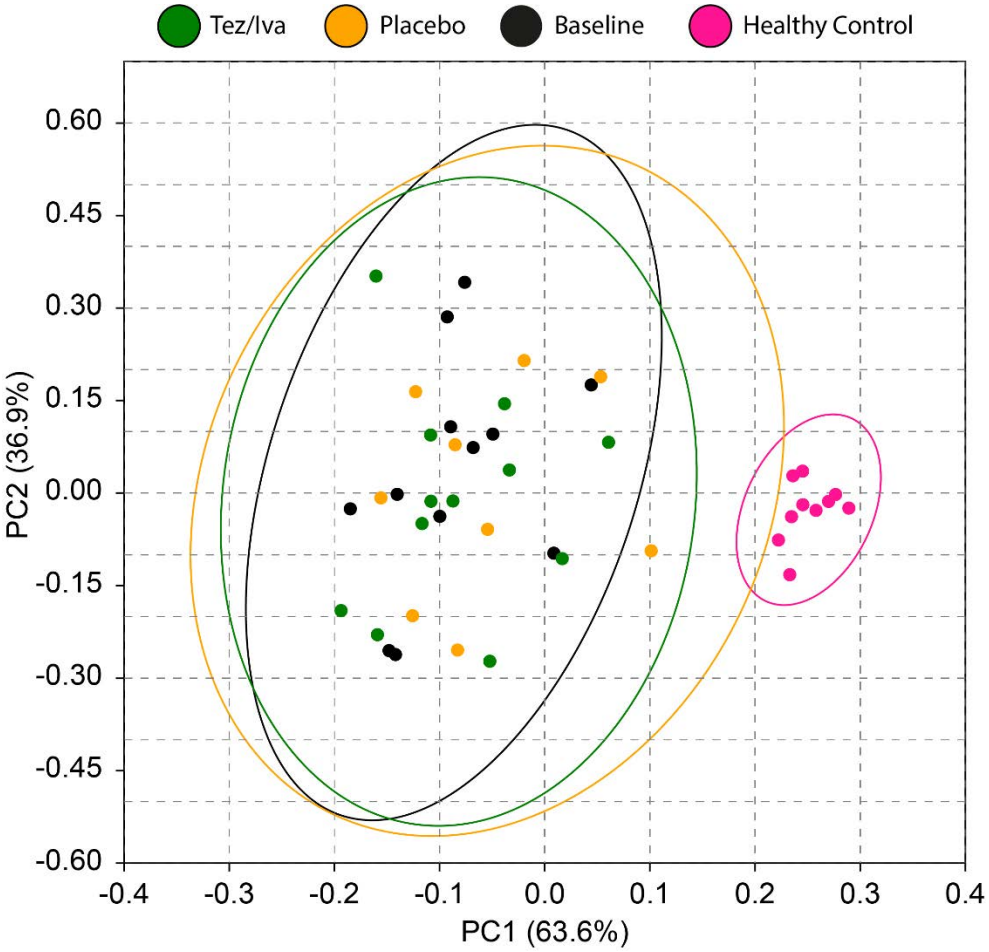

Figure 5.2 Principal coordinates analysis (PCoA) of gut microbiota composition from different treatment periods, and also matched healthy controls, utilising Bray-Curtis distances. Each data point represents an individual sample. Elipses represent a 95% confidence level between groups. Colour of data point is indicative of group as depicted. ANOSIM statistics for bacterial compositions between treatment periods and comparisons with healthy controls are found in Tables S5.3 and S5.5 respectively. Group sizes: Baseline, n = 12; placebo, n = 9; Tez/Iva, n = 12.

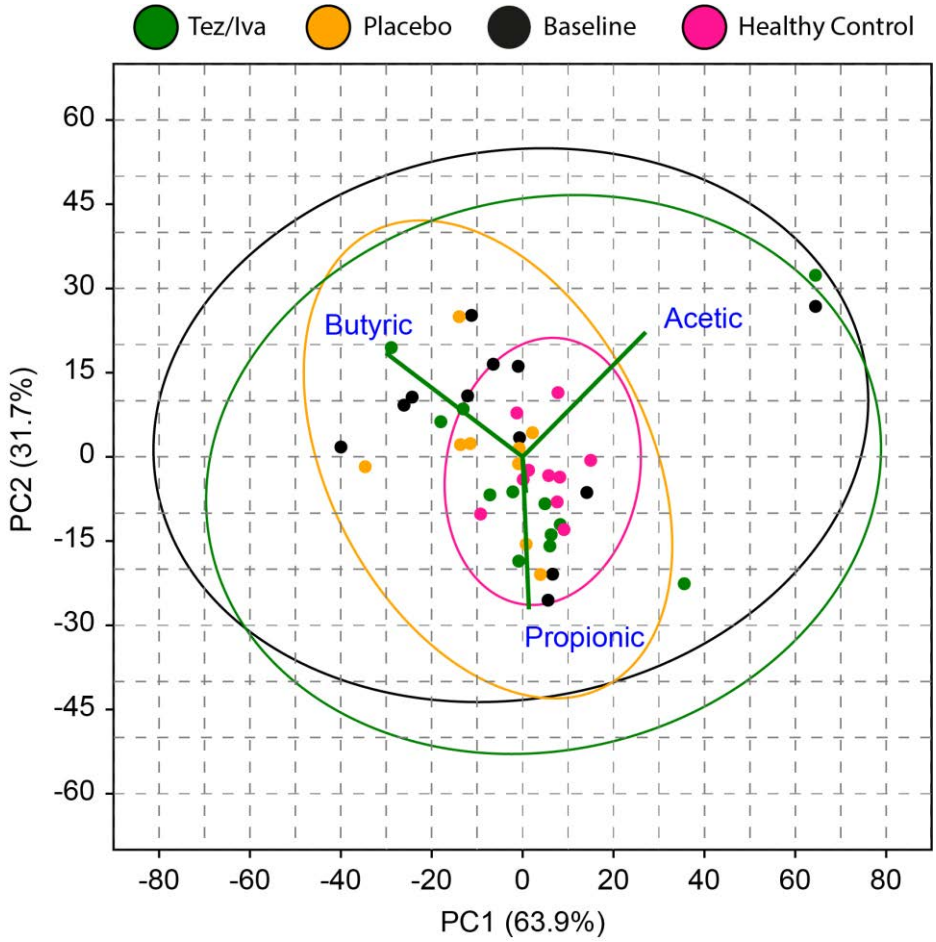

Figure 5.3 Principal component analysis (PCA) plot of the SCFA (C2-C7) profiles of grouped samples at baseline, placebo, and treatment periods. Also included are healthy control subjects for comparison. Elipses represent a 95% confidence level between groups. Colour of data point is indicative of group as depicted. Summary statistics are found in the Supplementary Results, including ANOSIM testing (Table S5.7), SIMPER analysis (Table S5.8) and Kruskal-Wallis testing of individual SCFAs (Table S5.9).

5.3 Discussion

As new CFTR modulator therapies become available to greater numbers of eligible pwCF it is crucial to investigate potential treatment effects on not just the lungs but a wide range of systems in CF, including the GI system (*Cystic Fibrosis Refresh Top 10 priorities (priority setting in association with the JLA)*, 2022; Marsh et al., 2022). To the best of our knowledge, this is the first study investigating the impact of Tezacaftor/Ivacaftor on the gut microbiome in pwCF. Here we examined the impact of Tezacaftor/Ivacaftor administration on the gut microbiota composition and metabolomic functioning by means of 16S rRNA targeted amplicon sequencing and targeted SCFA metabolomics. Our results indicate that Tezacaftor/Ivacaftor treatment had negligible effects on gut microbiota diversity and no significant differences on microbiota composition when compared to baseline or placebo treatment periods. There were differences across the core taxa observed within the placebo treatment period, however the similar magnitude of Fisher's alpha likely indicates these changes render little biological significance and are resultant of alternate temporal variation. Furthermore, pwCF samples across all treatment periods exhibited significantly reduced diversity and intra-group similarity, alongside a significantly different composition of bacterial taxa compared to matched healthy controls, suggestive of a perturbated community that is commonly observed in the CF gut. (Burke et al., 2017; Kristensen et al., 2020; Loman et al., 2020; Marsh et al., 2022).

Previous studies investigating the effects of CFTR modulator therapy on the gut microbiota have mainly been limited to Ivacaftor treatment, where the majority of studies observed no differences across bacterial diversity or overall composition following Ivacaftor usage (Ooi et al., 2018; Pope et al., 2021; Ronan et al., 2022). Whilst Kristensen et al did observe significant changes to the aforementioned

(Kristensen et al., 2021), this was only evident following extended 12 months of treatment in pwCF harbouring the p.Ser1251Asn mutation. Given the increased efficacy of Ivacaftor for pwCF undergoing treatment for class III mutations relative to those administered dual-therapy to treat F508del in the respiratory domain (Gramegna et al., 2020), it may be possible that this reduced efficacy also extends to the site of the intestinal tract and changes to the microbiota are more subtle in such cohorts of pwCF. This will be clarified as further studies on CFTR modulators and the intestinal microbiome encompass greater numbers of participants.

Additionally, Pope et al investigated dual-combination Lumacaftor/Ivacaftor treatment in a F508del cohort (Pope et al., 2021), but did not observe any effects upon bacterial diversity or composition. Heterogeneity across studies published thus far includes clinical and patient characteristics that have previously been shown to impact or associate with microbiota composition, including CFTR genotypes (Schippa et al., 2013; Bazett et al., 2015; Meeker et al., 2020), patient age (Manor et al., 2016; Loman et al., 2020), sex (Marsh et al., 2022), and varying antibiotic regimens (Burke et al., 2017; De Freitas et al., 2018; Kristensen et al., 2020). These factors, alongside variable pancreatic function across patients, should be considered in the wider context of the different outcomes observed.

Our cohort had an overall (mean ± SD) lung function (FEV_1 %) of 80.6 ± 19.6 at baseline the largest value we are aware of for a CFTR modulator-based gut microbiota study. Future studies may elucidate the relevance of baseline respiratory characteristics towards gut microbiota changes following CFTR modulator usage, given the strong evidence for a gut-lung axis in CF (Burke et al., 2017; Price and O'Toole, 2021). Alongside others, we have previously demonstrated the large association of antibiotic therapy with microbiota composition across pwCF (Burke et

al., 2017; Antosca et al., 2019; Marsh et al., 2022), and in the current study all but one patient was receiving regular antibiotic therapy as part of their routine care. Additionally, 50% (6/12) of pwCF were administered additional antibiotic therapy either during, or recently preceding their faecal samples and clinical assessments.

With regards to the functionality of the microbiota, we did not observe any differences in the faecal relative levels of SCFAs between any of the treatment periods in this study. Although only approximately 5% of SCFAs are excreted in faeces (Ruppin et al., 1980; Rechkemmer et al., 1988), faecal levels of SCFAs have been shown to relate to disease severity and patient symptoms across inflammatory bowel diseases (IBDs) (Treem et al., 1994; Huda-Faujan et al., 2010; Müller et al., 2021) and therefore may be of use in the CF gut as a biomarkers of microbiota functional capacity. This is unsurprising, given the relationship of butyrate in particular with anti-inflammatory properties and enhancement of epithelial integrity (Donohoe et al., 2011; Arpaia et al., 2013; Chang et al., 2014). Faecal levels of prominent SCFAs, including acetic, propionic, and butyric acid have previously been shown to be lower in the CF gut compared to healthy controls (Vernocchi et al., 2018). When extending our analyses to matched healthy controls we found significant differences in composition compared to pwCF. Whilst compositional differences were mainly driven by levels of acetic, propionic, and butyric acid, subsequent univariate analyses between pwCF and healthy controls revealed differences in the relative levels longer-chain SCFAs. Isobutyric relative levels were significantly increased in controls compared to baseline and placebo, but not Tezacaftor/Ivacaftor pwCF samples, which could reflect temporal changes such as increased protein availability and subsequent amino acid fermentation resulting from dietary fluctuations (Oliphant and Allen-Vercoe, 2019). We detected that valeric, hexanoic, and heptanoic acid were significantly increased in healthy control

subjects compared pwCF. Whilst these longer-chain fatty acids have also been implicated in IBD (De Preter et al., 2015), future investigation should adopt extensive integrative approaches to better understand relationships between the microbiome, metabolome, and intestinal clinical outcomes further. This may elucidate any potential functional redundancy of the microbiota (Wang et al., 2019) more clearly in the context of CFTR modulator treatment that is likely administered in the presence of antibiotic therapies and other lifestyle alterations that persist within CF.

Persistent intestinal abnormalities and symptoms are a hallmark of CF gastrointestinal disease, including intestinal inflammation for which significant differences were observed between pwCF and healthy controls, but not across the various treatment periods in pwCF. The latter is similar to Ronan et al (Ronan et al., 2022), but contrary to results from others (Ooi et al., 2018; Stallings et al., 2018; Tetard et al., 2020), further suggesting intestinal inflammation in CF is multi-factorial by nature. The lower faecal calprotectin values obtained in our study (compared to other CF studies) during all treatment phases, suggests that the participants in our study had less gut inflammation. A cut-off value of <50 ug/g is generally used to define normal levels (Ellemunter et al., 2017). A more comprehensive approach may therefore be required to determine the severity of intestinal inflammation in future studies. Small intestinal bacterial overgrowth is another common abnormality of the CF gut, that has so far persisted during interventions with Lumacaftor/Ivacaftor therapy (Gabel et al., 2022). As it is often related to increased oro-caecal transit times (Dorsey and Gonska, 2017), it will be interesting to determine if Tezacaftor/Ivacaftor impacts such gut function metrics, given the relationships with the microbiota we have previously described in pwCF (Marsh et al., 2022).

Whilst no differences across intestinal symptoms in our cohort through the CFAbd and PAC-SYM questionnaires were observed, it is anticipated that more recent triple combination therapies such as Elexacaftor/Lumicaftor/Ivacaftor (ETI) may alleviate the GI manifestations and symptoms of CF. Indeed, preliminary data surrounding its usage and patient symptoms is promising, based on the reduction of symptoms across the CFAbd-scores reported by Mainz et al (Mainz et al., 2022). Triple combination therapy (for patients with at least one copy of the common F508del mutation) leads to fewer pulmonary exacerbations and overall improved respiratory health (Keogh et al., 2022). This may in turn allow for a reduction in antibiotic use and a re-shaping of the gut microbiota, so that it resembles more closely signatures observed in healthy controls. It is also logical to postulate that the initiation of CFTR modulator treatment earlier in life will also increase microbiota similarity between pwCF and the wider population, particularly if other GI manifestations are minimised. Should this not arise, despite patient clinical improvement, the further integration of multi-omic approaches will likely clarify if the predisposed microbial community exhibit changes to functionality that promote a favourable intestinal environment for pwCF. Finally, ETI therapy demonstrates increased efficacy across intestinal epithelia as compared to Tezacaftor/Ivacaftor in biopsies from pwCF homozygous for the F508del mutation, which our current cohort all exhibited (Graeber et al., 2022). As we obtain deeper knowledge surrounding triple-therapy modulator usage, the findings of this study should therefore contribute valuable insights to the complex challenge of comprehending the associations between restoring CFTR functionality and alterations to the intestinal microbiota.

A limitation of this pilot study is inevitably the small sample size of our cohort, which limits the power of specific analyses and restricts the ability to investigate confidently the effects of the various antibiotic regimens (antibiotic class, dosage, frequency) across our patients. Whilst the treatment period was also relatively short, longer-

term administration has previously failed to elicit changes to the intestinal microbiota across pwCF with similar genotypes (Pope et al., 2021), however this does not include Tezacaftor/Ivacaftor administration. The double-blind crossover element of our study was limited to 9/12 (75%) of participants due to disruption from the COVID-19 pandemic and patient desires to switch to available open-label treatment, although samples at baseline and during Tezacaftor/Ivacaftor treatment were obtained from all participants. The principal strength of this study is the important first insights gained into the efficacy of Tezacaftor/Ivacaftor treatment in modulating the gut microbiota and its potential metabolomic capacity in a clinically representative cohort of pwCF harbouring the F508del mutation. Our future work will look to encompass both respiratory and intestinal microbiota analyses, alongside extensive gut function metrics, and absolute quantification of microbiota-derived metabolites, following CFTR modulator therapy.

5.4 Conclusions

This cross-over pilot study has revealed no significant impact of Tezacaftor/Ivacaftor administration on gut microbiota composition or relative levels of faecal SCFAs within pwCF. Compositionally, the microbiota of pwCF is still very much distinct compared to that of healthy controls, demonstrating a lack of remodulation of the gut microbiome by modulator therapy. The negligible effects observed in this study may be related to the short administration period of Tezacaftor/Ivacaftor, alongside other characteristics of pwCF, including continuous antibiotic treatment and sustained pancreatic insufficiency. Future studies with more efficacious CFTR modulators may elucidate the impact of modulating CFTR function, and implications of the CF lifestyle, on the microbiota more clearly.

5.5 Materials and Methods

5.5.1 Study participants and design

An overview of the study participants and design can be found in Chapter 2.1.2. The full study design is described in the Supplementary Materials. Patient clinical characteristics at baseline are detailed in Table 5.1. Written informed consent, or parental consent and assent for paediatric participants, was obtained from all participants. Study approval was obtained from the UK National Research Ethics Committee (19/WM/0130). All faecal samples obtained were immediately stored at -80°C prior to processing for microbiota sequencing and metabolomics to reduce changes before downstream community analysis (Gorzelak et al., 2015).

5.5.2 Targeted amplicon sequencing

DNA from dead or damaged cells, as well as extracellular DNA was excluded from analysis via PMA treatment prior to DNA extraction, as described previously (Rogers et al., 2013). DNA extraction was performed with the as described in Chapter 2.2.3, utilising the FastPrep-24™ 5G bead beating grinder and lysis system. DNA was amplified using the paired-end sequencing approach targeting the bacterial 16S rRNA gene region (V4-V5) as previously described (Marsh et al., 2022), with integrated phasing as described in Chapter 2.2.4.2. Pooled barcoded amplicon libraries were sequenced on the Illumina MiSeq platform (V3 Chemistry). Extended methodology, primers and PCR conditions can be found in the Supplementary Materials.

5.5.3 Sequence processing and analysis

Sequence processing was carried out using Cutadapt v3.5 and R (Version 4.0.1) as described in Chapter 2.3.1 The full protocol is detailed in the Supplementary

Materials. Raw sequence data reported in this study has been deposited in the European Nucleotide Archive under the study accession number PRJEB57754.

5.5.4 Gas-chromatography mass-spectrometry (GC-MS) of faecal samples to investigate SCFA levels.

GC-MS analysis was carried out using an Agilent 7890B/5977 Single Quadrupole Mass Selective Detector (MSD) (Agilent Technologies) equipped with a non-polar HP-5ms Ultra Inert capillary column (30 m × 0.25 mm × 0.25 µm) (Agilent Technologies). Faecal sample processing was performed as detailed in Chapter 2.2.8.2. Selected ion monitoring (SIM) mode was used for subsequent analyses; all confirmation and target ions lists are summarised in Table S5.6. GC-MS parameters are listed in Chapter 2.2.8.3. Agilent MassHunter workstation version B.07.00 programs were used to perform post-run analyses. A ^{13}C-short chain fatty acids stool mixture (Merck Life Science, Poole, UK) was used as the internal standard to normalise all spectra obtained prior to analyses. Extended information surrounding sample processing, SCFA extraction, derivatisation, and GC-MS parameters can be found in the Supplementary Materials.

5.5.5 Faecal Calprotectin measurement

Stool was extracted for downstream assays using the ScheBo® Master Quick-Prep (ScheBo Biotech, Giessen, Germany), according to the manufacturer instructions. Faecal calprotectin was analysed using the BÜHLMANN fCAL ELISA (Bühlmann Laboratories Aktiengesellschaft, Schonenbuch, Switzerland), according to the manufacturer's protocol.

5.5.6 Statistical Analysis

Regression analysis, including calculated coefficients of determination (r^2), degrees of freedom (df), *F*-statistic and significance values (*P*) were calculated as described in Chapter 2.3.2. Fisher's alpha index of diversity and the Bray-Curtis index of similarity were calculated using PAST v3.21 (Hammer et al., 2001), as described in Chapters 2.3.3 and 2.3.4 respectively. Significant differences in microbiota diversity were determined using Kruskal-Wallis performed using XLSTAT. Analysis of similarities (ANOSIM) with Bonferroni correction was used to test for significance in microbiota and SCFA composition, and was performed in PAST, including SIMPER analysis to determine which taxa and SCFAs contributed most to compositional differences between groups (Chapter 2.3.5).

5.5.7 Data availability

Raw sequence data reported in this study has been deposited in the European Nucleotide Archive under the study accession number PRJEB57754.

5.6 Acknowledgements

This work was funded by CF Trust grant (VIA 77) awarded to CvdG. The wider 'Gut Imaging for Function & Transit in Cystic Fibrosis Study 2' (GIFT-CF2) was supported with funding from a Cystic Fibrosis Trust grant (VIA 061), a Cystic Fibrosis Foundation award (Clinical Pilot and Feasibility Award SMYTH18A0-I), and a Vertex Pharmaceuticals Investigator-Initiated Study award (IIS-2018-106697). CvdG, DR, ARS, GM, and RM conceived the microbiome study. RM, and LH performed microbiota sample processing and analysis. RM and CDS carried out the metabolomic analysis. RM, DR, and CvdG performed the data and statistical analysis. CN, GM, and AS were responsible for sample collection, clinical care records and documentation. RJM, CN, GM, and CvdG verified the underlying data.

RJM, DR, and CvdG were responsible for the creation of the original draft of the manuscript. RJM, CN, GM, DR, ARS, and CvdG contributed to the development of the final manuscript. CvdG is the guarantor of this work. All authors read and approved the final manuscript.

5.7 Declaration of Competing Interest

RJM, CDS, and LH have nothing to disclose. DR and CvdG report grant funding from Vertex Pharmaceuticals outside of the submitted work. CN, GM, and ARS report grants and speaker honorarium from Vertex Pharmaceuticals outside the submitted work.

5.8 Supplementary Methods

5.8.1 Study participants and design

Fourteen pwCF, homozygous for F508del, were initially recruited from Nottingham University Hospitals NHS Trust. Participants were asked to provide stool samples whilst attending the Sir Peter Mansfield Imaging Centre at the University of Nottingham. Ultimately, 12 pwCF (mean age at baseline, 20.8 ± 7.80 years, median age, 20 years) provided samples available for inclusion in our analyses. Participants were asked to fast overnight and prior to the refraining from the use of laxatives and anti-diarrhoeals during their visit. Regular pancreatic enzyme replacement therapy and physiotherapy procedures were admitted.

Clinical assessments and sample collections were performed at baseline, with further samples collected following either Tezacaftor/Ivacaftor or an identical looking placebo administration, in a randomised double-blind two period-crossover fashion. Randomisation was carried out externally to those involved in analyses or in the management of patients in the study. Tezacaftor/Ivacaftor and placebo formulations were visually matched and coded to ensure blindness to investigators. Both treatments were administered for 28 days with an intermediate 28-day washout period. Tezacaftor/Ivacaftor was taken during the morning and Ivacaftor in the evening with patients advised to administer treatment alongside fat-containing foods. Between day 19-21 of each phase, participants provided faecal samples whilst at clinic, and completed the validated PAC-SYM and CF-Abd questionnaires to assess gut symptoms (Frank et al., 1999; Jaudszus et al., 2019).

Full crossover from baseline to both treatments (placebo and Tezacaftor/Ivacaftor) was achieved for 9/12 pwCF, with the remaining 3 patients receiving open label Tezacaftor/Ivacaftor treatment following baseline and 2 pwCF not completing the study in a capacity enabling subsequent microbiota analysis. Faecal samples from

10 age-matched healthy controls (mean age, 21.4 ± 7.40 years, median age, 20 years) from our previous study were available for microbiota and metabolomic comparison also (Marsh et al., 2022). Further clinical trial details can be found at clinicaltrials.gov, under number NCT04006873 (https://clinicaltrials.gov/ct2/show/NCT04006873).

5.8.2 PMA treatment prior to DNA extraction

1 mg PMA (Biotium, CA, USA) was hydrated in 98 µL 20% dimethyl sulfoxide (DMSO) to give a working stock concentration of 20 mM. 300 mg of stool thawed out from -80°C was homogenised in 3 ml PBS, and centrifuged at 3200 g, for 5 minutes. The pellet was then resuspended in 1 ml PBS prior to splitting into 500 µL fractions for subsequent PMA treatment. 1.25 µL of PMA (20 mM) was added to give a final concentration of 50 µM. Following the addition of PMA to samples in opaque Eppendorf tubes, PMA was mixed by vortexing for 10 seconds, followed by incubation for 15 minutes at room temperature (~20°C). This step was repeated before the transfer of samples to clear 1.5 mL Eppendorf tubes and placement within a LED lightbox. Treatment occurred for 15 minutes to allow PMA intercalation into DNA from compromised bacterial cells. Samples were then centrifuged at 10,000 x *g* for 5 minutes. The supernatant was discarded, and the cellular pellet was resuspended in 200 µL PBS.

5.8.3 Targeted amplicon sequencing – Bacterial 16S rRNA gene

Step 1 amplicon generation with primers based on the universal primer sequences 515F and 926R as described by Walters et al. (Walters et al., 2016), was performed under the following conditions: Initial denaturation of 180 seconds at 98°C, followed

by: 25 cycles of 30 seconds at 95°C, 30 seconds at 55°C and 30 seconds at 72°C. A final extension of 5 minutes at 72°C was also included to complete the reaction. Step 2, the addition of dual barcodes and Illumina adaptor sequences was performed under the following conditions: Initial denaturation of 30 seconds at 98°C, followed by: 10 cycles of 10 seconds at 98°C, 20 seconds at 62°C and 30 seconds at 72°C. A final extension of 2 minutes at 72°C was also included to complete this reaction. This resulted in the generation of an ~550 bp amplicon spanning the V4-V5 hypervariable regions of the 16S rRNA gene.

5.8.4 Sequencing Controls and Library Pooling

PCR and DNA extraction negative controls were implemented, alongside the use of mock community positive controls, which included a Gut Microbiome Standard (ZYMO RESEARCH™). Following Barcode attachment in the second PCR step, clean-up and subsequent amplicon size selection was performed with AMPure XP beads (Beckman Coulter™) and quantified using a Qubit™ dsDNA HS kit. Sample concentrations were then manually normalised, pooled, and diluted to the final library concentrations requited for use on the Illumina MiSeq system.

5.8.5 Sequence processing and analysis

DADA2 was used to demultiplex and remove primer sequences, validate the quality profiles of forward and reverse reads and subsequently trim, infer sequence variants, merge denoised paired-reads, remove chimeras, and finally assign taxonomy via Naive Bayesian Classifier implementation (Callahan et al., 2016). This included the use of the Genome Taxonomy Database (GTDB) reference sequences (Parks et al., 2018). Unidentifiable ASVs were run through a BLAST

(https://blast.ncbi.nlm.nih.gov/Blast.cgi) and matched appropriately based on query coverage where possible. Taxa with 2 ≥ reads for a single sample were removed and excluded from subsequent statistical analysis. ASVs from the same bacterial taxon were collapsed to form a single OTU for a given taxon.

5.8.6 GC-MS: Sample processing and SCFA preparation

Faecal samples stored at -80°C were ground in liquid nitrogen before 50 mg of ground faeces was added to 500 µl MS-grade water. Samples were lysed and homogenised utilising inert ZR BashingBead Lysis Tubes (Cambridge bioscience, UK), using the FastPrep-24 5G instrument (MP Biomedicals, California, USA) with two cycles at a speed of 6.0 m/s for 40 seconds each. Samples were then incubated at 4°C whilst mixing for 30 minutes using an ELMI Intelli-Mixer™ RM-2L at 80 rpm. Samples were centrifuged at 13,000 x *g* for 30 mins. The supernatant containing faecal SCFAs was removed. 150 µL of supernatant was protonated with 5M HCl before the addition of anhydrous diethyl ether (1:1 v/v), samples were vortexed for 10 seconds, and incubated on ice for 5 mins. Following incubation, samples were mixed with the ELMI Intelli-Mixer™ RM-2L as before for 15 minutes, then centrifuged at 10,000 x *g* for 5 mins. The DE layer containing faecal SCFAs was transferred to a new Eppendorf tube pre-loaded with 25 mg Na_2SO_4. The remaining layer was then re-extracted with another 150 µL DE as before. Samples were equally pooled and then 40 µl was then transferred to a GC-MS vial, with the addition of 2 µl N, O-bis(trimethylsilyl) trifluoroacetamide (BSTFA). Samples were vortexed then incubated for 3 hours at 37°C before loading onto the GC-MS. MS grade water processed in parallel was used as a blank sample to correct the background.

5.8.7 GC-MS Analysis

GC-MS analysis was carried out using an Agilent 7890B/5977 Single Quadrupole Mass Selective Detector (MSD) (Agilent Technologies) equipped with a non-polar HP-5ms Ultra Inert capillary column (30 m × 0.25 mm × 0.25 µm) (Agilent Technologies). The Agilent 7693 Autosampler was used to inject 1.0 µL of the derivatised sample in triplicate at a split ratio of 20:1 at 265°C, with a solvent delay of 2 minutes 30 seconds. The initial oven temperature was held at 40°C for 2 minutes, followed by a 10°C/min temperature ramp to 140°C, then increased to 300°C at the rate of 40°C/min and kept at this temperature for 6 minutes. Electron impact (EI) mode ionisation was utilised at 70 eV, with the instrumental parameters set at 230, 150 and 300°C for source, quadrupole and interface temperatures, respectively. Selected ion monitoring (SIM) mode was used for quantification; all confirmation and target ions lists are summarised in Supplementary Table S5.6. Agilent MassHunter workstation version B.07.00 programs were used to perform post-run analyses. A ^{13}C-short chain fatty acids stool mixture (Merck Life Science, Poole, UK) was used as the internal standard to normalise all spectra obtained prior to analyses.

5.9 Supplementary Results

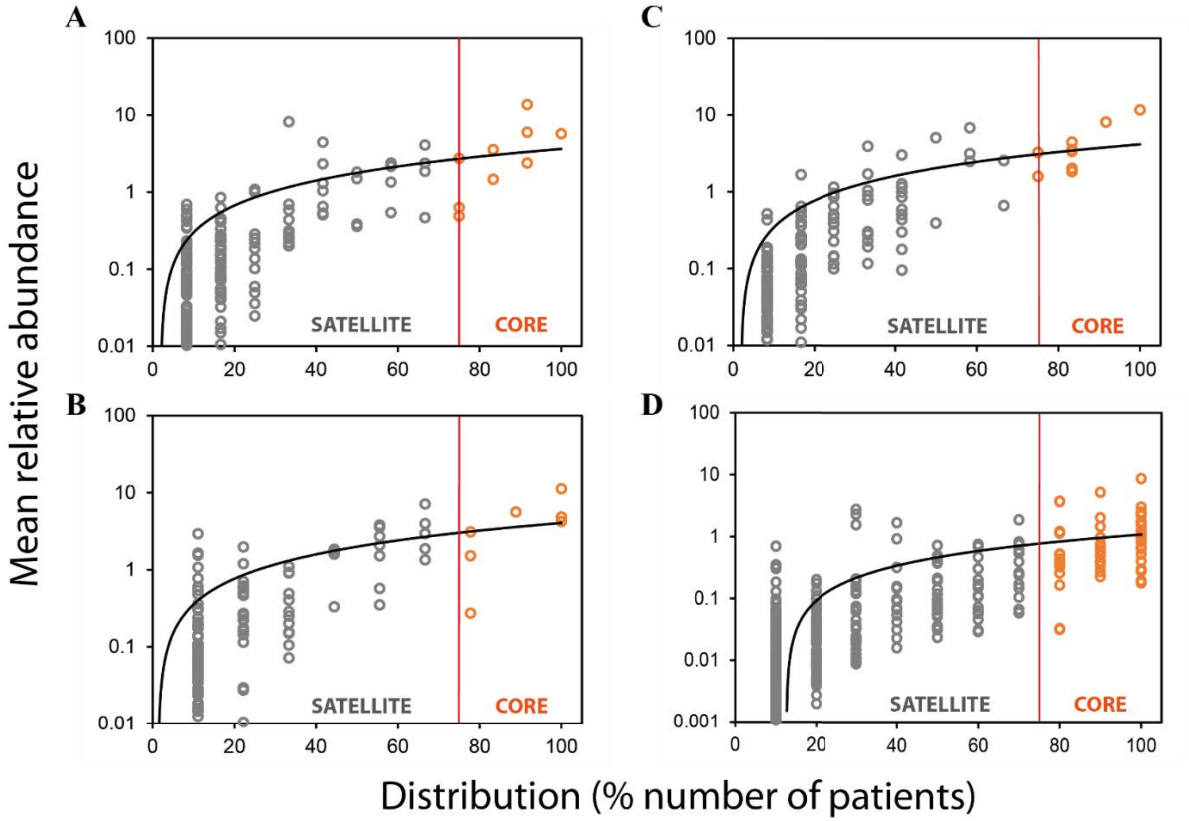

Figure S5.1 Distribution and abundance of bacterial taxa across treatment stages (A-C) and healthy control participants (D). Given is the percentage number of patients harbouring each bacterial taxon, plotted against the mean relative abundance across those samples. Core taxa are depicted by the orange circles and fall in the upper quartile of distribution, separated by the red vertical line at 75% distribution. Satellite taxa (grey) are all samples below this distribution. Distribution-abundance relationship regression statistics: (a) $r^2 = 0.45$, $F_{1,196} = 152.6$, $P < 0.0001$. (b) $r^2 = 0.60$, $F_{1,175} = 245.9$, $P < 0.0001$. (c) $r^2 = 0.57$, $F_{1,175} = 245.9$, $P < 0.0001$. (d) $r^2 = 0.28$, $F_{1,465} = 182.8$, $P < 0.0001$.

Table S5.1 Core taxa between different treatment phases.

	Baseline		Placebo		Tez/Iva		Controls	
Taxa	Prev.	Rel. abundance	Prev.	Rel. abundance	Prev.	Rel. abundance	Prev.	Rel. abundance
Blautia wexlerae	91.67	13.67	100.00	11.23	100.00	11.66	100.00	2.99
Escherichia coli	58.33	2.39	66.67	3.97	75.00	1.59	90.00	2.02
Blautia faecis	66.67	2.37	77.78	3.09	83.33	3.36	100.00	1.53
Dorea longicatena	83.33	3.55	100.00	4.22	83.33	4.44	100.00	0.97
Fusicatenibacter saccharivorans	100.00	5.70	88.89	5.60	83.33	3.54	100.00	2.36
Enterococcus 24	75.00	2.74	66.67	1.34	58.33	2.50	10.00	0.30
Streptococcus 27	91.67	2.38	66.67	1.87	83.33	2.02	100.00	0.19
Anaerobutyricum hallii	91.67	5.97	100.00	4.82	91.67	8.09	100.00	1.77
Anaerostipes hadrus	66.67	4.06	55.56	3.79	75.00	3.26	100.00	1.27
Parabacteroides distasonis	83.33	1.46	77.78	1.52	83.33	1.84	90.00	0.97
Erysipelatoclostridium ramosum	75.00	0.63	77.78	0.27	41.67	0.50	20.00	0.04
Agathobaculum 309	75.00	0.49	44.44	0.33	41.67	0.18	90.00	0.50

Given is prevalence, the percent number of samples a given core taxon was detected in, and average relative abundance across those samples. Taxon names are derived from condensed ASVs of the same species. ASV numbers have been used to differentiate between taxa within the same genus that could not be identified at the species level. Core taxa are highlighted orange, whereas satellite taxa are grey. Given the length of the ribosomal sequences analysed, species identities should be considered putative.

Table S5.2. Kruskall-Wallis tests of bacterial alpha diversity utilising Fishers alpha index.

	Microbiota		Core taxa		Satellite taxa	
Baseline vs Placebo	K (Observed value)	1.823	K (Observed value)	7.293	K (Observed value)	1.136
	K (Critical value)	3.841	K (Critical value)	3.841	K (Critical value)	3.841
	DF	1	DF	1	DF	1
	p-value (one-tailed)	0.177	p-value (one-tailed)	0.007	p-value (one-tailed)	0.286
Baseline vs Tez/Iva	K (Observed value)	0.053	K (Observed value)	0.083	K (Observed value)	0.213
	K (Critical value)	3.841	K (Critical value)	3.841	K (Critical value)	3.841
	DF	1	DF	1	DF	1
	p-value (one-tailed)	0.817	p-value (one-tailed)	0.773	p-value (one-tailed)	0.644
Placebo vs Tez/Iva	K (Observed value)	0.247	K (Observed value)	4.247	K (Observed value)	0.081
	K (Critical value)	3.841	K (Critical value)	3.841	K (Critical value)	3.841
	DF	1	DF	1	DF	1
	p-value (one-tailed)	0.619	p-value (one-tailed)	0.039	p-value (one-tailed)	0.776

Table S5.3 Bacterial ANOSIM summary statistics between treatment phases, utilising the Bray-Curtis index.

	Microbiota		**Core taxa**		**Satellite taxa**	
Baseline	R value:	-0.0652	R value:	0.0768	R value:	-0.0392
vs	*p* same:	0.8216	*p* same:	0.1373	*p* same:	0.6724
Placebo	Bonferroni-corrected p value	0.8366	Bonferroni-corrected p value	0.143	Bonferroni-corrected p value	0.6674
	permutation *N*:	9999	permutation *N*:	9999	permutation *N*:	9999
Baseline	R value:	-0.0720	R value:	0.0359	R value:	0.0484
vs	*p* same:	0.9328	*p* same:	0.1987	*p* same:	0.1946
Tez/Iva	Bonferroni-corrected p value	0.9363	Bonferroni-corrected p value	0.2036	Bonferroni-corrected p value	0.2006
	permutation *N*:	9999	permutation *N*:	9999	permutation *N*:	9999
Placebo	R value:	-0.0323	R value:	0.0686	R value:	0.0047
vs	*p* same:	0.6349	*p* same:	0.1529	*p* same:	0.4308
Tez/Iva	Bonferroni-corrected p value	0.6423	Bonferroni-corrected p value	0.1548	Bonferroni-corrected p value	0.437
	permutation *N*:	9999	permutation *N*:	9999	permutation *N*:	9999

Table S5.4 Kruskal-Wallis tests of bacterial alpha diversity utilising Fishers alpha index

	Control vs Baseline		Control vs Placebo		Control vs Tez/Iva	
Micro	K (Observed value)	15.652	K (Observed value)	13.500	K (Observed value)	15.652
	K (Critical value)	3.841	K (Critical value)	3.841	K (Critical value)	3.841
	DF	1	DF	1	DF	1
	p-value (one-tailed)	<0.0001	p-value (one-tailed)	0.0002	p-value (one-tailed)	<0.0001
Core	K (Observed value)	15.652	K (Observed value)	13.500	K (Observed value)	15.652
	K (Critical value)	3.841	K (Critical value)	3.841	K (Critical value)	3.841
	DF	1	DF	1	DF	1
	p-value (one-tailed)	<0.0001	p-value (one-tailed)	0.0002	p-value (one-tailed)	<0.0001
Sat	K (Observed value)	15.652	K (Observed value)	13.500	K (Observed value)	15.652
	K (Critical value)	3.841	K (Critical value)	3.841	K (Critical value)	3.841
	DF	1	DF	1	DF	1
	p-value (one-tailed)	<0.0001	p-value (one-tailed)	0.0002	p-value (one-tailed)	<0.0001

Table S5.5 Bacterial ANOSIM summary statistics between treatment stages and controls, utilising the Bray-Curtis index.

	Healthy vs Baseline		**Healthy vs Placebo**		**Healthy vs Tez/Iva**	
Micro	R value:	0.5914	R value:	0.5646	R value:	0.6308
	p same:	0.0001	*p* same:	0.0001	*p* same:	0.0001
	Bonferroni-corrected p value	0.0001	Bonferroni-corrected p value	0.0002	Bonferroni-corrected p value	0.0001
	permutation *N*:	9999	permutation *N*:	9999	permutation *N*:	9999
	Healthy vs Baseline		**Healthy vs Placebo**		**Healthy vs Tez/Iva**	
Core	R value:	0.568	R value:	0.4809	R value:	0.7156
	p same:	0.0001	*p* same:	0.0001	*p* same:	0.0001
	Bonferroni-corrected p value	0.0001	Bonferroni-corrected p value	0.0001	Bonferroni-corrected p value	0.0001
	permutation *N*:	9999	permutation *N*:	9999	permutation *N*:	9999
	Healthy vs Baseline		**Healthy vs Placebo**		**Healthy vs Tez/Iva**	
Sat	R value:	0.7736	R value:	0.89	R value:	0.7634
	p same:	0.0001	*p* same:	0.0001	*p* same:	0.0001
	Bonferroni-corrected p value	0.0001	Bonferroni-corrected p value	0.0001	Bonferroni-corrected p value	0.0001
	permutation *N*:	9999	permutation *N*:	9999	permutation *N*:	9999

Table S5.6 Analytical parameters for SCFA analysis with GC-MS

SCFA	t_R (min)	Target ion (m/z)	Confirmation ion (m/z)
Acetic acid	2.52	117	75
Propionic acid	3.81	131	75
Iso-butyric acid	4.39	145	117
Butyric acid	5.22	145	117
Iso-valeric acid	6.07	159	117
Valeric acid	6.85	159	117
4-methylvaleric acid	7.86	173	117
Hexanoic acid	8.41	173	117
Heptanoic acid	9.9	187	117
^{13}C-acetic acid	2.52	119	77
^{13}C-propionic acid	3.81	134	77
^{13}C-butyric acid	5.22	149	119

t_R - Retention time

Table S5.7 Short chain fatty acid compositional ANOSIM summary statistics between treatment stages and controls, utilising the Bray-Curtis index.

Healthy vs Baseline		**Healthy vs Placebo**		**Healthy vs Tez/Iva**	
R value:	0.2518	R value:	0.242	R value:	0.108
p same:	0.0034	*p* same:	0.0047	*p* same:	0.041
Bonferroni-corrected p value	0.0050	Bonferroni-corrected p value	0.0051	Bonferroni-corrected p value	0.0459
permutation *N*:	9999	permutation *N*:	9999	permutation *N*:	9999
Baseline vs Placebo		**Baseline vs Tez/Iva**		**Placebo vs Tez/Iva**	
R value:	-0.0423	R value:	0.0360	R value:	-0.0208
p same:	0.6966	*p* same:	0.1911	*p* same:	0.5437
Bonferroni-corrected p value	0.7043	Bonferroni-corrected p value	0.1933	Bonferroni-corrected p value	0.5464
permutation *N*:	9999	permutation *N*:	9999	permutation *N*:	9999

Table S5.8 SIMPER results between SCFA relative levels between controls and pwCF.

Controls vs Baseline

SCFA	Av. dissim	Contrib. %	Cumulative %	Mean Healthy	Mean baseline
Butyric	9.935	34.6	34.6	30.9	41.6
Acetic	6.991	24.35	58.95	32.7	34.2
Propionic	4.899	17.06	76.01	20.7	17.8
Valeric	2.388	8.317	84.33	5.41	0.634
Isovaleric	1.591	5.54	89.87	3.7	3.07
Isobutyric	1.357	4.727	94.59	3.5	2.13
Hexanoic	1.239	4.314	98.91	2.6	0.426
Heptanoic	0.2202	0.7667	99.67	0.443	0.00833
4-methylvaleric	0.09348	0.3256	100	0.091	0.148
				Dissimilarity	**28.71**

Controls vs Placebo

SCFA	Av. dissim	Contrib. %	Cumulative %	Mean Healthy	Mean placebo
Butyric	7.031	32.66	32.66	30.9	43.1
Propionic	4.41	20.49	53.14	20.7	23
Acetic	4.315	20.04	73.19	32.7	28.1
Valeric	1.993	9.259	82.45	5.41	1.69
Hexanoic	1.25	5.805	88.25	2.6	0.176
Isobutyric	1.132	5.257	93.51	3.5	1.56
Isovaleric	1.115	5.181	98.69	3.7	2.4
Heptanoic	0.2197	1.02	99.71	0.443	0.0111
4-methylvaleric	0.06227	0.2892	100	0.091	0.0944
				Dissimilarity	**21.53**

Controls vs Tez/Iva

SCFA	Av. dissim	Contrib. %	Cumulative %	Mean Healthy	Mean Tez/Iva
Butyric	7.08	28.44	28.44	30.9	31.4
Acetic	6.069	24.38	52.83	32.7	34.6
Propionic	5.101	20.5	73.32	20.7	24.1
Valeric	2.048	8.228	81.55	5.41	1.91
Isovaleric	1.738	6.983	88.53	3.7	4.61
Isobutyric	1.329	5.34	93.87	3.5	3.2
Hexanoic	1.25	5.021	98.89	2.6	0.172
Heptanoic	0.2197	0.8827	99.77	0.443	0.0117
4-methylvaleric	0.05608	0.2253	100	0.091	0.0842
				Dissimilarity	**24.89**

Table S5.9 Differences in relative levels of SCFAs between healthy control subjects and pwCF during different treatment phases.

	P value		
SCFA	**Baseline**	**Placebo**	**Tez/Iva**
Acetic	0.742	0.253	0.210
Propionic	0.166	0.327	0.262
Iso-butyric	0.048	0.009	0.429
Butyric	0.210	0.022	0.843
Iso-valeric	0.210	0.165	0.895
Valeric	0.000	0.003	0.006
4-methylvaleric	0.086	0.253	0.323
Hexanoic	0.099	0.060	0.013
Heptanoic	0.040	0.060	0.086

Given are *p* values obtained following Kruskal-Wallis testing of the relative levels of SCFAs within the healthy control samples and all treatment phases. Dark green - $p < 0.001$, Green - $p < 0.01$, Light Green - $p < 0.05$, Yellow – $p < 0.1$.

Table S5.10 Summary statistics for PAC-SYM scores across Tezacaftor/Ivacaftor and off-treamtent samples.

Variable	Observations	Minimum	Maximum	Mean	Std. deviation
Tezacaftor/Ivacaftor	12	0.000	1.000	0.409	0.385
Off-treatment	14	0.000	2.330	0.636	0.625

Kruskal-Wallis test / Two-tailed test:

K (Observed value)	0.730
K (Critical value)	3.841
DF	1
p-value (one-tailed)	0.393
alpha	0.050

An approximation has been used to compute the *P*-value.

1

Table S5.11 Summary statistics for CFAbd scores across Tezacaftor/Ivacaftor and off-treamtent samples.

Variable	Observations	Minimum	Maximum	Mean	Std. deviation
Off-treatment	14	1.400	43.100	20.829	12.583
Tezacaftor/Ivacaftor	12	1.400	45.100	15.483	12.910

t-test for two independent samples / Two-tailed test:

Difference	5.345
t (Observed value)	1.067
|t| (Critical value)	2.064
DF	24
p-value (Two-tailed)	0.297
alpha	0.050

2

Chapter 6: An observational study investigating the impact of extended Elexacaftor/Tezacaftor/Ivacaftor therapy on the gut microbiota, associated metabolites, and patient outcomes in cystic fibrosis.

This Chapter is written in manuscript format, prior to submission to the *Journal of Cystic Fibrosis.*

Ryan Marsh [a,b], Claudio Dos Santos [c], Liam Hanson [a,c], Alex Yule [d,e], Christabella Ng [d,e], Giles Major [d,f], Alan R Smyth [d,e], Damian Rivett [c *], Christopher van der Gast [a,b,g *]

[a] Department of Life Sciences, Manchester Metropolitan University, UK

[b] Department of Applied Sciences, Northumbria University, Newcastle, UK

[c] Department of Natural Sciences, Manchester Metropolitan University, UK

[d] School of Medicine, University of Nottingham, UK

[e] NIHR Nottingham Biomedical Research Centre, UK

[f] Nestlé Institute of Health Sciences, Société des Produits Nestlé, Lausanne, Switzerland

[g] Department of Respiratory Medicine, Salford Royal NHS Foundation Trust, Salford, UK

* Correspondence to: Professor Chris van der Gast, Department of Life Sciences, Faculty of Science and Engineering, John Dalton Building, Chester Street, Manchester, M1 5GD, UK; C.vanderGast@mmu.ac.uk

Dr Damian Rivett, Department of Natural Sciences, Faculty of Science and Engineering, John Dalton
Building, Chester Street, Manchester, M1 5GD, UK; d.rivett@mmu.ac.uk

Keywords: gut microbiome, gut microbiota, dysbiosis, CFTR modulator therapy, Elexacaftor/Tezacaftor/Ivacaftor, Kaftrio, Trikafta

Highlights

- Elexacaftor/Tezacaftor/Ivacaftor (ETI) therapy had subtle impacts upon microbiota composition in pwCF.
- Distinct differences persist in the CF gut microbiota following extended ETI therapy when pwCF are compared with controls.
- Faecal SCFA concentrations of acetic, propionic and butyric acid were similar between pwCF and controls, irrespective of ETI therapy.

Abstract

Background: People with cystic fibrosis (pwCF) experience persistent gastrointestinal symptoms throughout life. There is evidence indicating interaction between the microbiota and gut pathophysiology in CF. However, there is a paucity of knowledge into potential effects of CF transmembrane conductance regulator (CFTR) modulator therapies on the gut microbiome. In a pilot study, we investigated the impact of Elexacaftor/Tezacaftor/Ivacaftor (ETI) CFTR modulator therapy on the gut-microbiota, metabolomic functioning, and clinical outcomes in pwCF.

Study design: Faecal samples from 20 pwCF were acquired before and following 3, 6, and 17+ months of ETI therapy. Samples were subjected to microbiota sequencing and targeted metabolomics to profile and quantify short-chain fatty acid (SCFA) composition. Ten healthy matched controls were included as a comparison. Clinical data, including markers of intestinal function and patient symptoms, were integrated to investigate relationships.

Results: Whilst ETI therapy did moderately impact core taxa diversity and composition over time, no significant increases in overall microbiota diversity or distinct changes to the whole microbiota composition including faecal SCFAs, were observed in pwCF. Bacterial composition similarity slightly increased with controls as treatment progressed, yet healthy control participants maintained a more diverse microbiota, including a significantly different composition of both bacterial taxa and faecal SCFA levels throughout the study period. Extended ETI therapy also had minimal impact symptom scores obtained from the Patient Assessment of Constipation-Symptoms questionnaire (PAC-SYM), and also markers of intestinal function.

Conclusions: ETI therapy in pwCF leads to very subtle changes in microbiota composition following prolonged administration, with no major differences in faecal SCFAs. Collectively, the composition of the faecal microbiota and these functional metabolites remains significantly different from healthy controls following extended therapy. Future studies should maintain frequent, prolonged sampling periods with larger cohorts to investigate modulator effects, but also CF-associated lifestyle factors in this era of CF treatment and how this may impact gut symptoms and abnormalities.

6.1 Introduction

Alongside the classical respiratory complications of cystic fibrosis (CF) are also the gastrointestinal abnormalities of disease. People with CF (pwCF) suffer from persistent intestinal symptoms and abnormalities that impact both morbidity and mortality (Smith et al., 2020). This has continued despite the transition of treatment for CF entering the phase of highly effective CFTR modulator therapies, which correct the underlying defect of chloride and bicarbonate transport across epithelial surfaces of the body (Lopes-Pacheco, 2020). Although the majority of pwCF are now receiving CFTR modulator based therapy (Cystic Fibrosis Trust, 2023), the need to better understand the relationships between intestinal symptoms and abnormalities persists, as determined by pwCF, carers, and clinicians (*Cystic Fibrosis Refresh Top 10 priorities (priority setting in association with the JLA)*, 2022). It is understood that intestinal dysbiosis, that is the disruption of the microbial communities inhabiting the intestinal tract, is frequent in CF and leads to compositions of bacteria distinctly different from healthy controls from birth and throughout adulthood (Madan et al., 2012; Burke et al., 2017; Coffey et al., 2019). Whilst this could be further compounded by the CF-associated lifestyle, such as dietary habits and frequent antibiotic usage (Debray et al., 2018; Kristensen et al., 2020), disruption of CFTR activity alone is seemingly sufficient to elicit structural changes to the microbiota (Meeker et al., 2020). Furthermore, the altered gut microbiota in pwCF has previously been associated with various manifestations of the GI tract (Flass et al., 2015; De Freitas et al., 2018; Dayama et al., 2020). Given this evidence, it is hopeful that CFTR modulators may alter the gut microbiota composition to resemble that of healthy individuals more closely, alongside improving other common intestinal abnormalities and symptoms in pwCF.

Previous studies investigating CFTR modulators and microbiota within the gastrointestinal tract have been mostly limited to Ivacaftor (Ooi et al., 2018; Kristensen et al., 2021; Pope et al., 2021; Ronan et al., 2022) and a couple of dual-modulator studies (Pope et al., 2021), including previous work within Chapter 5 (Marsh et al., 2023). With respect to the microbiota structure, previous findings vary across studies incorporating different modulators, patient demographics, and treatment lengths (Ooi et al., 2018; Kristensen et al., 2021; Pope et al., 2021; Ronan et al., 2022). Results for the frequently observed inflammation in the gut following modulator treatment are also contrasting. Some studies observed a reduction in faecal calprotectin following modulator usage (Ooi et al., 2018; Stallings et al., 2018; Tetard et al., 2020), whilst others (Ronan et al., 2022) and our own group (Chapter 5, unpublished data), did not measure any notable reduction.

Following the approval of Elexacaftor/Tezacaftor/Ivacaftor (ETI) triple modulator therapy for pwCF from NHS England, almost half of all pwCF in the United Kingdom are now registered users (Cystic Fibrosis Trust, 2022). ETI therapy demonstrates increased clinical efficacy as compared to previous dual or mono-therapy approaches (Dawood et al., 2022), yet little information is available on intestinal outcomes and the impact upon the gut microbiota. Given the scarcity of current evidence, the aim of this pilot study was to therefore assess the impact of ETI therapy in pwCF upon the intestinal microbiota. We characterised the respective gut microbiota of pancreatic insufficient pwCF ≥ 12 years, harbouring the F508del mutation, before and following ETI therapy of up to 20 months thereafter. Furthermore, we combined microbiota data with targeted metabolomics of quantified faecal short-chain fatty acids (SCFAs), patient clinical data, and markers of intestinal function as measured by magnetic resonance imaging (MRI) (Ng et al., 2021). Patient symptoms were also measured before and after initiating ETI therapy.

Samples and clinical data from 10 matched healthy controls were available for analysis. We hypothesised that ETI therapy would increase gut microbiota diversity, reshape community structure, and potentially lead to functional changes to resemble outcomes measured in healthy controls.

6.2 Methods

6.2.1 Study participants and design

An overview of the study participants and design can be found in Chapter 2.1.3. Extended study design, including protocols, methods, and other results are also described in the Supplementary Materials. An overview of participant clinical characteristics is detailed in Table 6.1, with comprehensive participant information and MRI data detailed in Tables S6.1 and S6.2, respectively. Access to the MRI data, which is currently unpublished, was kindly granted by the University of Nottingham MRI research team at the Sir Peter Mansfield Imaging Centre. Written informed consent, or parental consent and assent for paediatric participants, was obtained from all participants. Study approval was obtained from the UK National Research Ethics Committee (20/PR/0508). All faecal samples obtained were immediately stored at -80°C prior to processing for microbiota sequencing and metabolomics to reduce changes before downstream community analysis (Gorzelak et al., 2015).

6.2.2 Targeted amplicon sequencing

DNA from dead or damaged cells, as well as extracellular DNA was excluded from analysis via PMA treatment prior to DNA extraction, as described previously (Rogers et al., 2013). DNA extraction was performed with the as described in Chapter 2.2.3, utilising the FastPrep-24™ 5G bead beating grinder and lysis system. DNA was

amplified using the paired-end sequencing approach targeting the bacterial 16S rRNA gene region (V4-V5) as previously described (Marsh et al., 2022), with integrated phasing as described in Chapter 2.2.4.2. Pooled barcoded amplicon libraries were sequenced on the Illumina MiSeq platform (V3 Chemistry). Extended methodology, primers and PCR conditions can be found in the Supplementary Materials.

6.2.3 Sequence processing and analysis

Sequence processing was carried out using Cutadapt v3.5 and R (Version 4.0.1) as described in Chapter 2.3.1 The full protocol is detailed in the Supplementary Materials. Raw sequence data reported in this study has been deposited in the European Nucleotide Archive under the study accession number PRJEB61286.

6.2.4 Gas-chromatography mass-spectrometry (GC-MS) of faecal samples to investigate SCFA levels

GC-MS analysis was carried out using an Agilent 7890B/5977 Single Quadrupole Mass Selective Detector (MSD) (Agilent Technologies) equipped with a non-polar HP-5ms Ultra Inert capillary column (30 m × 0.25 mm × 0.25 µm) (Agilent Technologies). Faecal sample processing was performed as detailed in Chapter 2.2.8.2. Selected ion monitoring (SIM) mode was used for subsequent analyses; all confirmation and target ions lists are summarised in Table S5.6. GC-MS parameters are listed in Chapter 2.2.8.3. Agilent MassHunter workstation version B.07.00 programs were used to perform post-run analyses. A ^{13}C-short chain fatty acids stool mixture (Merck Life Science, Poole, UK) was used as the internal standard to normalise all spectra obtained prior to analyses and subsequent quantification of target metabolites. Extended information surrounding sample processing, SCFA

extraction, derivatisation, and GC-MS parameters can be found in the Supplementary Materials.

6.2.5 Faecal Calprotectin measurement

Stool was extracted for downstream assays using the ScheBo® Master Quick-Prep (ScheBo Biotech, Giessen, Germany), according to the manufacturer instructions. Faecal calprotectin was analysed using the BÜHLMANN fCAL ELISA (Bühlmann Laboratories Aktiengesellschaft, Schonenbuch, Switzerland), according to the manufacturer's protocol.

6.2.6 Statistical Analysis

Regression analysis, including calculated coefficients of determination (r^2), degrees of freedom (df), *F*-statistic and significance values (*P*) were calculated as described in Chapter 2.3.2. Fisher's alpha index of diversity and the Bray-Curtis index of similarity were calculated using PAST v3.21 (Hammer et al., 2001), as described in Chapters 2.3.3 and 2.3.4 respectively. Significant differences in microbiota diversity were determined using Kruskal-Wallis performed using XLSTAT. Analysis of similarities (ANOSIM) with Bonferroni correction was used to test for significance in microbiota and SCFA composition, and was performed in PAST, including SIMPER analysis to determine which taxa and SCFAs contributed most to compositional differences between groups (Chapter 2.3.5). Student's t-tests used to determine differences in metadata were also performed in XLSTAT.

Table 6.1 Overall clinical characteristics of controls and pwCF at baseline.

Characteristic	pwCF	Controls
Baseline Age (Mean ± SD)	21.0 ± 8.6	21.4 ± 7.4
Male (%)	15 (75)	5 (50)
Baseline BMI (Mean ± SD)	21.1 ± 3.4	22.9 ± 4.4
F508del/F508del (%)	13 (65)	0 (0)
Baseline FEV1% (Mean ± SD)	79.1 ± 20.5	-
Pancreatic insufficient (%)	20 (100)	0 (0)
Cystic fibrosis-related diabetes (%)	4 (20)	-
Antibiotics during study (%)	14 (70)	0 (0)

6.3 Results

Following sequence processing and taxa assignment, the microbiota data across each pwCF treatment period from baseline, and the healthy control participants was partitioned for further sub-analysis. Microbiota data was partitioned into common abundant core taxa, and rarer less frequent satellite taxa following the establishment of significant distribution abundance relationships of the taxa across all treatment duration groups and the healthy control participants (Figure S6.1). The core taxa (Table S6.4) constituted 70.1% of the total abundance for the healthy controls, whilst across pwCF they averaged 30.0% ± 6.1 (Mean ± SD).

Diversity of the whole microbiota, core taxa, and satellite taxa was plotted across the increasing ETI treatment periods in pwCF (Figure 6.1A). When comparing the mean absolute change in diversity between treatment time-points and the net change from baseline (Figure 6.1B), significant decreases in diversity were observed between baseline and 6 months of ETI therapy ($P = 0.0005$), which aligned with a sharp reduction between months 3 to 6 across the whole ($P = 0.035$) and core taxa ($P = 0.002$) analyses (Table S6.5). The core taxa diversity in particular was more volatile to change over the treatment period and increased significantly between 6 months and the extended sampling period ($P = 0.0002$), which then also incurred a significant net change from baseline ($P = 0.0001$) (Table S6.5). Extending our analyses for comparison of diversity with healthy controls, it was evident that the healthy control participants had significantly higher microbiota diversity than that of pwCF across all partitions of the community (Figure 6.1C, Table S6.6). Of note, this difference between pwCF and healthy participants was reduced following extended ETI therapy ($P = 0.001$) across all partitions of the microbiota (Figure 6.1C, Table S6.6).

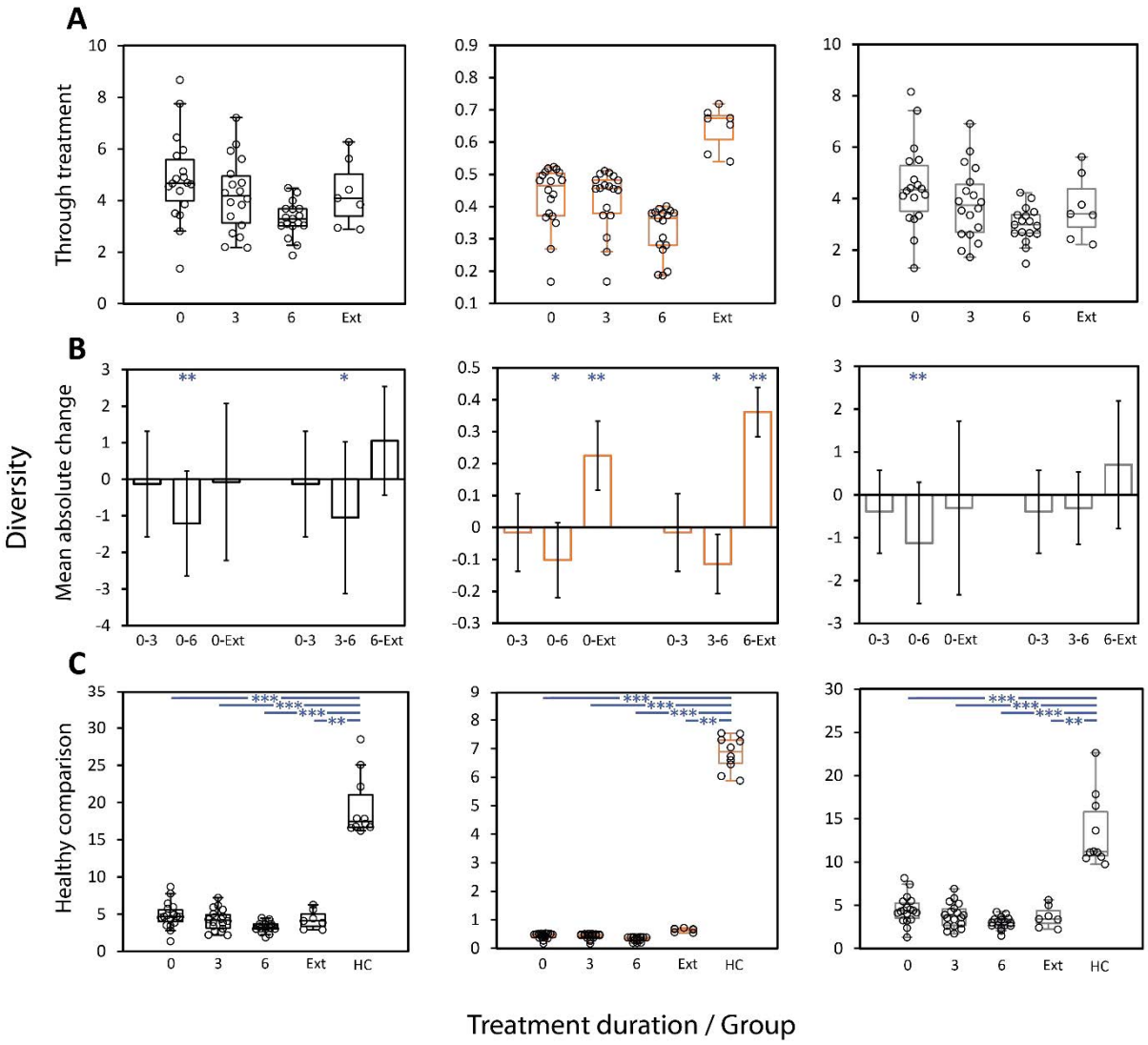

Figure 6.1 Microbiota diversity compared across groups utilising Fisher's alpha index of diversity. Black plots indicate the whole microbiota, whilst orange and grey denote the core and satellite taxa respectively. (A) Diversity across pwCF at baseline or following ETI treatment. Black circles denote individual patient participant data. Error bars represent 1.5 times the inter-quartile range (IQR). (B) Absolute change in diversity over time in pwCF, including sequential and net changes. Error bars represent the standard deviation (SD) of the mean change. Asterisks denote significant differences in diversity between treatment periods following Kruskal-Wallis testing (Table S6.5). (C) Diversity of pwCF and also healthy controls for comparison. Black circles denote individual patient participant data. Error bars represent 1.5 times the inter-quartile range (IQR). Asterisks denote significant differences in diversity between pwCF treatment periods and healthy controls following Kruskal-Wallis testing (Table S6.6). Abbrevaitions; 0,3 and 6 – Samping time point (months), Ext – Extended (17+ months) sampling period, HC – Healthy control participants. *P* values; ***; P < 0.0001, **; P < 0.001, *; P < 0.05.

In terms of whole microbiota composition across the study, within-group similarity was largest for the healthy control participants, with a mean similarity (± SD) of 0.44 ± 0.06 (Figure 6.2A). The composition of the microbiota, however, did become more similar in pwCF as treatment progressed. Within-group similarity at baseline in pwCF increased from 0.22 ± 0.09, to 0.32 ± 0.09 following extended ETI therapy (Figure 6.2A). A similar trend was observed across the core taxa, as within-group similarity of the pwCF group (0.60 ± 0.12) during the extended sampling period eventually exceed that of the healthy control participants (0.57 ± 0.06). For the satellite taxa, within-group microbiota similarity was much lower as expected, with no significant differences throughout the study period in pwCF, with similarity in the extended sampling period (0.19 ± 0.07) comparable to the healthy control participants (0.19 ± 0.04).

Comparing the composition of the microbiota across the ETI treatment periods and the overall net change from baseline, revealed no overall significant differences across the whole microbiota (Figure 6.2B, Table S6.7). Both core (P = 0.0001) and satellite (P = 0.0347) taxa significantly differed between months 3 and 6 (Table S6.7), with the core taxa at month 6 also significantly different from baseline (P = 0.0002). Parallel to the outcomes in diversity, healthy control participants had a significantly different microbiota composition across the whole microbiota as compared to pwCF on ETI therapy across all treatment lengths (Figure 6.2C, Table S6.8). A similar trend was observed for the core and satellite taxa analyses, but there was increased inter-group similarity between following extended ETI samples and healthy controls (Figure 6.2C, Table S6.8).

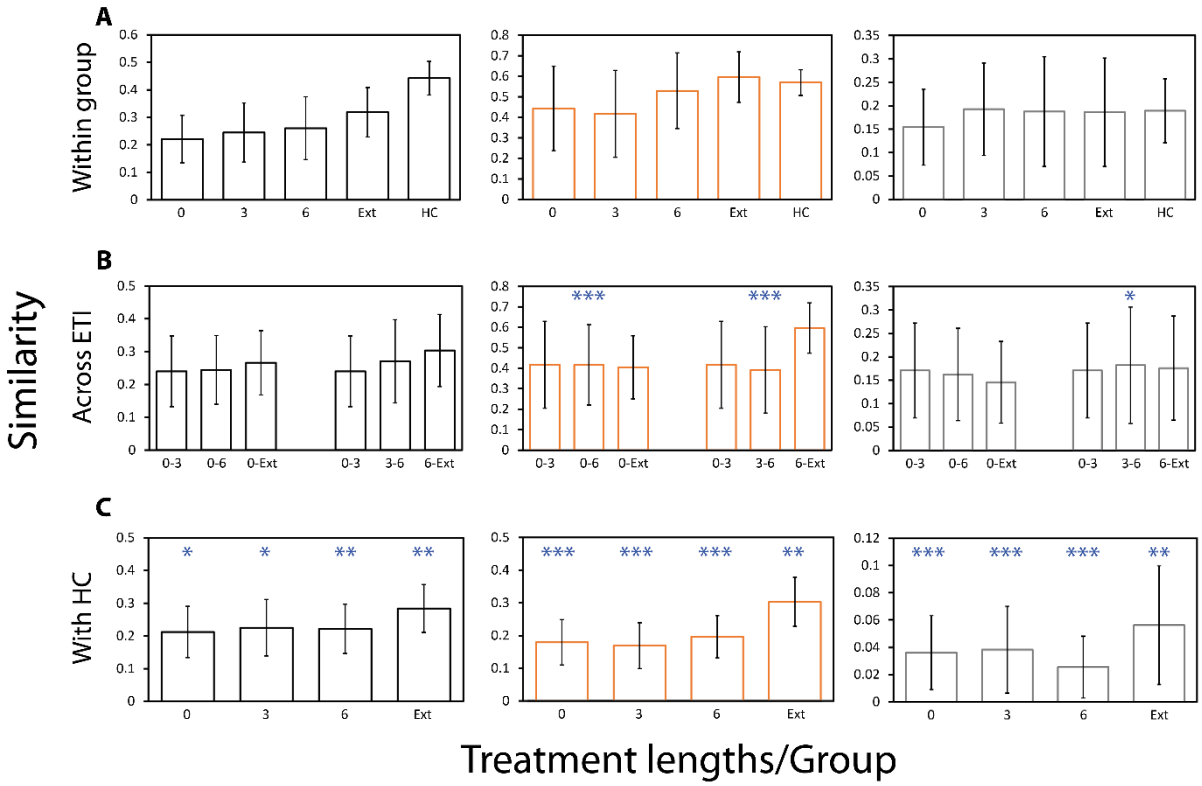

Figure 6.2 Microbiota similarity compared across groups utilising the Bray-Curtis index of similarity. (A) Within-group similarity across pwCF at baseline or following ETI treatment, and healthy controls. (B) Inter-group similarity change over time in pwCF, including sequential and net changes. (C) Inter-group similarity between pwCF on ETI and healthy control participants. Error bars represent standard deviation of the mean. Asterisks inicate significant differences in microbiota composition following the use of one-way ANOSIM testing. Summary statistics are presented in Tables S6.7-6.8.

To understand which taxa were driving the dissimilarity maintained between healthy control participants and pwCF following extended ETI therapy, SIMPER analysis was conducted (Table 6.2). The top drivers of dissimilarity between the groups were *Blautia* sp. (OTU 1), *Bifidobacterium adolescentis*, *Bacteroides dorei*, *Eubacterium rectale*, and *Anaerostipes hadrus*. Overall, 24 taxa comprised over 50% of the dissimilarity between the groups and this consisted of many prominent short-chain fatty acid producing bacteria from other genera, including *Faecalibacterium, Ruminococcus*, and *Collinsella,* Interestingly, some of these taxa were increased in the pwCF group compared to the healthy controls. Additional SIMPER analysis between baseline and following extended ETI therapy revealed that similar taxa were also drivers of the change seen across the treatment period in pwCF (Table S6.9).

To investigate the relationships between participant clinical variables and microbiota composition, redundancy analysis (RDA) was performed. Within comparisons between pwCF following extended ETI and the healthy control participants (Table 6.3), whole microbiota variability was explained by (in ascending order) by the presence of CF disease, antibiotic usage, and age. For the core taxa analysis, CF disease was the primary driver of variation, with sex also contributing. CF disease was also the main contributor of variation in the satellite taxa, followed by antibiotic usage and patient small bowel water content (SBWC). When relating variability of the microbiota solely within pwCF (from baseline to extended ETI) (Table S6.10), multiple variables significantly explained the variation in the whole microbiota, including disease mildness (FEV_1%), BMI, antibiotic usage, sex, and SBWC. Excluding BMI, these variables also significantly explained variation across the core taxa. For the satellite taxa analysis, ETI treatment length also significantly explained a small percentage of the variation. Species RDA biplots were then plotted to

visualise how the taxa driving differences across pwCF and controls related to significant clinical variables identified from the RDA approach. Between the healthy controls and pwCF on extended ETI (Figure 6.3), a group of taxa containing *Faecalibacterium* and *Bacteroides* members collectively clustered strongly away from CF disease and the usage of antibiotics, whilst taxa such as *Blautia* sp. (OTU 1), *Ruminoccocus gnavus, Enterococcus* sp. (OTU 26), and *Eubacterium hallii* demonstrated the opposite trend. Some taxa were explained primarily by both participant age and sex. This included *Blautia luti*, *Dorea longicatena*, *Holdemanella biformis*, *Bacteroides dorei*, *Escherichia coli*, and *Bifidobacterium adolescentis*. In terms of SBWC, this significantly explained the variation across a group of taxa including *Fusicatenibacter saccharivorans* and *Gemmiger formicilis*. Within pwCF exclusively (baseline to extended ETI), different taxa and variables comprised the RDA biplot due to outcomes from the previous SIMPER and RDA analyses (Figure S6.2). Some similar trends were observed however, including the strong association of *Enterococcus* sp. (OTU 24) with antibiotic usage and *Blautia* sp. (OTU 1) away from more mild CF disease.

Table 6.2 Similarity of percentage (SIMPER) analysis of microbiota dissimilarity (Bray-Curtis) between healthy control and pwCF samples following extended treatment with ETI.

Taxa	% Relative abundance		Av. Dissimilarity	% Contribution	Cumulative (%)
	ETI Extended	Healthy Controls			
Blautia_1	11.70	4.91	3.24	4.53	4.53
Bifidobacterium adolescentis	4.90	0.81	2.35	3.28	7.81
Bacteroides dorei	3.79	3.35	2.12	2.95	10.77
Eubacterium rectale	3.68	4.78	2.02	2.82	13.58
Anaerostipes hadrus	4.35	1.99	2.00	2.79	16.37
Fusicatenibacter saccharivorans	5.73	3.69	1.96	2.74	19.11
Ruminococcus bromii	3.34	2.93	1.93	2.70	21.81
Gemmiger formicilis	4.24	1.05	1.90	2.65	24.46
Blautia luti	5.55	3.01	1.63	2.27	26.73
Bacteroides vulgatus	1.66	3.32	1.62	2.26	28.99
Collinsella aerofaciens	3.33	0.19	1.59	2.23	31.21
Dorea longicatena	4.39	1.79	1.47	2.05	33.26
Eubacterium hallii	4.81	2.39	1.26	1.76	35.02
Escherichia coli	2.27	1.99	1.26	1.76	36.78
Blautia obeum	0.98	2.51	1.15	1.61	38.38
Ruminococcus gnavus	2.48	0.04	1.13	1.58	39.96
Bacteroides uniformis	0.14	2.55	1.11	1.55	41.51
Holdemanella biformis	2.01	0.45	1.09	1.52	43.03
Blautia faecis	2.12	2.30	0.98	1.38	44.40
Faecalibacterium duncaniae	2.09	2.15	0.98	1.37	45.78
Enterococcus_26	2.07	0.31	0.98	1.37	47.15
Faecalibacterium longum	0.42	2.19	0.96	1.35	48.49
Ruminococcus faecis	2.27	1.61	0.96	1.34	49.84
Faecalibacterium prausnitzii	0.00	2.04	0.95	1.32	51.16

Taxa identified as core are highlighted in orange, with satellite taxa highlighted in grey. The mean relative abundance (%) across both groups is given, alongside the percentage contribution which is the mean dissimilarity of taxa divided by the mean dissimilarity (71.26%) across samples. Cumulative percent does not equal 100% as the list is not exhaustive, rather the taxa that make up 50% of dissimilarity between groups. Given the length of the 16S gene regions sequenced, taxon identification should be considered putative.

Table 6.3 Redundancy analysis to explain percent variation across whole microbiota, core, and satellite taxa of the significant clinical variables across healthy control participants and pwCF receiving Extended ETI therapy.

	Microbiota			Core taxa			Satellite taxa		
	Var. Exp (%)	pseudo-*F*	*P* (adj)	Var. Exp (%)	pseudo-*F*	*P* (adj)	Var. Exp (%)	pseudo-*F*	*P* (adj)
Age	10.1	2.0	0.008						
Antibiotics	10.6	2.0	0.018				10.8	1.9	0.012
CF Disease	13.3	2.3	0.002	27.5	5.7	0.002	16.0	3.3	0.002
SBWC							10.8	1.8	0.050
Sex				10.0	2.2	0.028			
Total	**23.9**			**37.5**			**37.6**		

Both the composition and absolute quantification of short-chain fatty acids from pwCF and healthy control samples were also investigated (Figure S6.3). Combined, the relative abundance of acetic, propionic, and butyric acid accounted for the vast majority of SCFAs across both the pwCF ETI treatment periods (94.0% ± 4.5, Mean ± SD) and healthy controls (89.6% ± 4.8, Mean ± SD). There were no significant differences from baseline, or subsequent sampling periods, in the absolute concentration or relative abundance of SCFAs across pwCF receiving ETI therapy (Fig S6.3, Tables S6.11-6.12). There were, however, significant differences between ETI samples and healthy controls (Fig S6.3, Table S6.13-6.14). This included significant increases in both absolute concentration and relative abundance of valeric (Fig S6.3 A and C) and heptanoic acid (Fig S6.3 B and D) within healthy control samples compared with all ETI sampling periods ($P < 0.05$ in all instances), with hexanoic acid also significantly increased compared to pwCF, except those on extended ETI ($P = 0.143$) (Fig S6.3 B and D). On the contrary, the only significantly increased SCFA in pwCF was butyric acid, with significantly higher concentrations measured during the extended ETI sampling period as compared to health controls ($P = 0.0147$) (Fig S6.3A).

The overall composition of SCFAs remained similar in pwCF throughout ETI therapy but remained significantly different from healthy controls during both the 6 months and extended ETI therapy periods ($P < 0.05$ in all instances) (Table S6.15). Over 50% of this dissimilarity was driven by acetic and butyric acid in both cases (Table S6.16). Exploratory RDA revealed that only a few SCFA, namely propionic, butyric, and valeric acid could significantly explain any variation across the microbiota composition across all samples, and to a minimal extent (Table S6.17). RDA biplots were constructed to visualise the relationships between SIMPER taxa and these SCFAs within both pwCF and healthy controls (Figure S6.4). Results were mixed,

with high variability across particular genera, including *Bacteroides*, *Blautia*, *Ruminococcus,* whilst others such as *Faecalibacterium* and *Eubacterium* behaved similarly and were more closely clustered. Other taxa were strongly dissociated with the SCFAs from the RDA biplot model, including *Blautia* spp. (OTU 1) and *Fusicatenibacter saccharivorans*.

Finally, when comparing symptoms and gut function across pwCF and healthy controls, it was evident that ETI therapy did not significantly improve PAC-SYM scores irrespective of treatment length ($P > 0.05$ in all instances) (Table S6.18). In terms of functionality, no significant differences in oro-caecal transit time (OCTT) ($P = 0.842$) or SBWC ($P = 0.064$) between pwCF and healthy controls occurred, however the latter was markedly increased (Table S6.19).

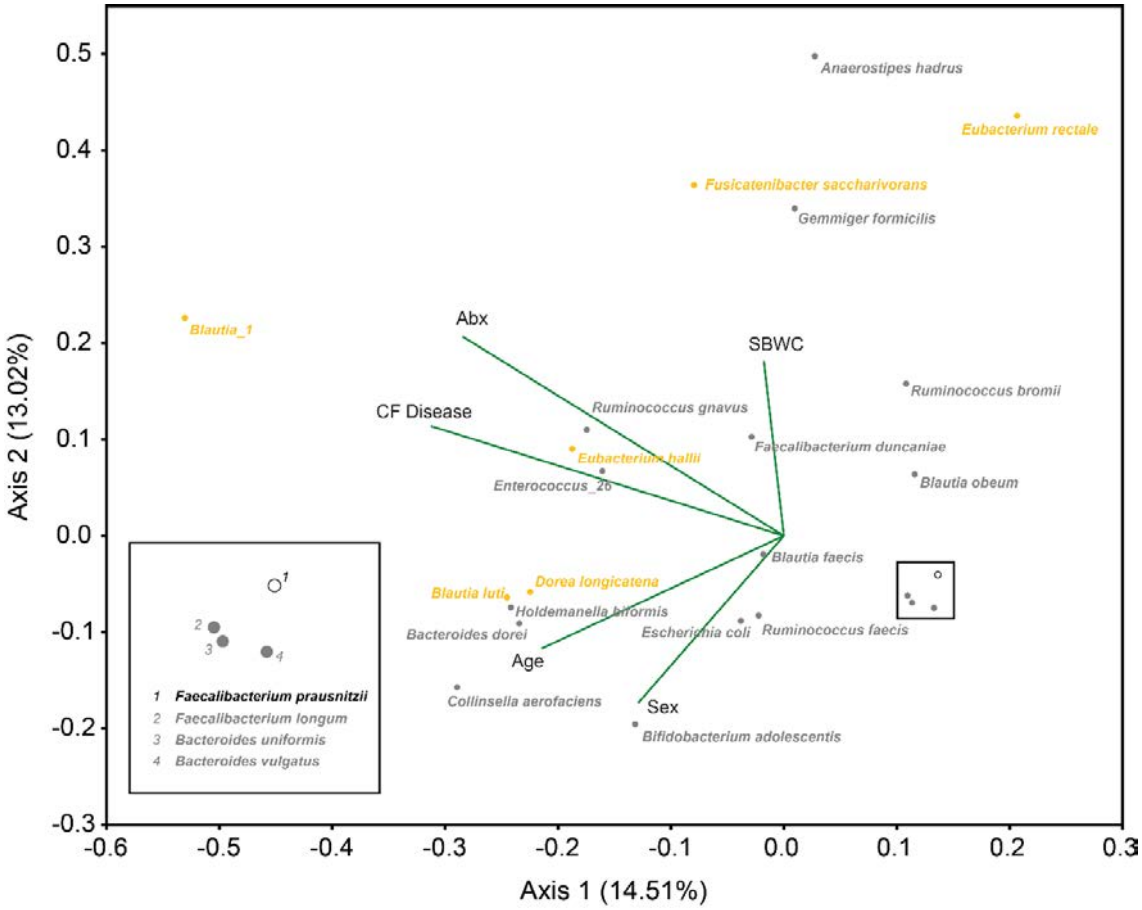

Figure 6.3 Redundancy analysis species biplots for the whole microbiota. The 24 taxa contributing most to the dissimilarity (cumulatively > 50%) between healthy control and pwCF samples following extended ETI therapy from the SIMPER analysis (Table 6.2) are shown independently of the total number of ASVs identified (531). Orange points represent taxa that were identified as core for the pwCF group following extended ETI therapy, grey points are satellite, and the white (black stroke) points represent taxa that were absent. Biplot lines depict clinical variables that significantly account for total variation in taxa relative abundance within whole microbiota analysis at the $p \leq 0.05$ level (Table 6.3). Species plots depict the strength of explanation provided by the given clinical variables, with taxa shown in the same direction of a particular clinical variable considered to have a higher value than those that are not. 'Abx' – Antibiotics during sampling period, 'SBWC' – Small bowel water content corrected for body surface area. The percentage of microbiota variation explained by each axis is given in parentheses.

6.4 Discussion

As the efficacy of CFTR modulators continues to increase in alleviating respiratory complications of CF, there is need to clarify if patient improvements further translate at the site of the intestinal tract. This includes both GI abnormalities and patient symptoms in wake of CFTR modulators treatment, including the effects upon the gut microbiota, for which data remains scarce and to the best of our knowledge has not been characterised in pwCF following ETI therapy. Here the impact of ETI on the gut microbiota and their associated metabolites was examined, utilising 16S rRNA gene sequencing and integrated targeted metabolomics to profile and quantify faecal levels of short-chain fatty acids. Our results indicate that ETI therapy had negligible effects on the diversity of the whole microbiota in pwCF, which remains significantly lower than that of healthy control participants (Manor et al., 2016; Burke et al., 2017; Miragoli et al., 2017).This is in agreement with previous studies incorporating less efficacious CFTR modulators (Ooi et al., 2018; Pope et al., 2021; Ronan et al., 2022). Kristensen et al (Kristensen et al., 2021) did however observe an increase in faecal microbiota diversity, but only following extended (12 month) Ivacaftor therapy in a group of pwCF harbouring the S1251N mutation. In this cohort, core taxa diversity was significantly higher in pwCF following extended ETI therapy compared to both baseline and 6 months, yet collectively still represented a minor constituent of total community abundance as compared to the satellite taxa. Whether or not the expansion and proliferation core taxa across pwCF is due to the altered fluidity of the intestinal tract, or other associated lifestyle changes upon modulator therapy remains to be explored.

In terms of microbiota organisation and structure a similar theme to the diversity ensued, in which no significant differences in microbiota composition succeeded prolonged ETI therapy, again similar to what others have reported (Ooi et al., 2018;

Pope et al., 2021; Ronan et al., 2022). Whole microbiota, and core taxa composition became slightly more similar in pwCF as treatment time with ETI progressed from baseline through to the extended period, suggestive that increased CFTR function in the CF intestinal environment may favour the expansion of commonly shared taxa. No obvious trends were observed across the satellite taxa, which remained low in similarity both within pwCF and compared to healthy controls. This is unsurprising, given satellite taxa distribution classically relates to random environmental perturbations or atypical habitats (Magurran, 2007; van der Gast et al., 2011). There was an increased similarity between all partitions of the microbiota between pwCF and healthy controls as treatment progressed, yet there remains a significant difference in microbiota composition as previously observed throughout life in pwCF (Burke et al., 2017; Coffey et al., 2019; Kristensen et al., 2020; Marsh et al., 2022).

When investigating which taxa drove the differences maintained between healthy control participants and pwCF following extended ETI therapy, many of the top contributors were taxa previously associated with prominent short chain fatty acid production in the gut, including species of the recently expanded *Faecalibacterium* (Sakamoto et al., 2022), *Eubacterium*, and *Blautia* (Venegas et al., 2019). Comparison of pwCF from baseline to extended ETI revealed *F. prausnitzii* did not substantially contribute to the dissimilarity, whilst relative abundances of *Eubacterium* were generally increased, and *Blautia* species fluctuated, over the treatment period in pwCF. Alongside this, no significant differences in SCFA relative or absolute levels across pwCF were identified, further extending between pwCF and healthy controls in acetic, propionic, isobutyric, butyric and isovaleric acid. These findings are in agreement with Baldwin-Hunter et al, who recently analysed colonic aspirates from adult pwCF and controls undergoing surveillance

colonoscopy (Baldwin-Hunter et al., 2023). This collectively may support elements of functional redundancy surrounding major short-chain fatty acid production in the distal colon in pwCF (Wang et al., 2019), and is further supported by the low microbial variation explained by here by faecal SCFA levels when both pwCF and control samples were collated. In contrast, Vernocchi et al did demonstrate significant reductions in major SCFAs across children with CF as compared to controls (Vernocchi et al., 2018), which may raise the possibility of age-dependent functional redundancy. Whether the significant increase in butyric acid concentration measured across extended ETI samples is due to the expansion of beneficial core taxa also remains to be validated, as few core taxa from extended ETI pwCF taxa directly associated with increased faecal butyric acid levels. Rather, an association with *Bifidobacterium adolescentis* was observed, which also clustered relatively closely to *Faecalibacterium* members. This result itself is perhaps unsurprising, given the cross-feeding relationship previously established by the two genera in increasing butyrate levels (Rios-Covian et al., 2015). Similar to Baldwin-Hunter et al again (Baldwin-Hunter et al., 2023), both valeric and hexanoic acid concentration and relative abundances were significantly larger in healthy control participants compared to pwCF. Furthermore, valeric acid did significantly explain variation in the microbiota across all samples collated for analysis, with those associated taxa typically satellite members of the microbiota in pwCF. Any potential implications of this remain to be clarified in CF as valeric and hexanoic acid have previously been shown to significantly decrease within intestinal pro-inflammatory environments as compared to healthy controls (De Preter et al., 2015).

When investigating the relationships between bacterial taxa, participant clinical data, and gut function, the strong impact of CF disease and antibiotic exposure upon microbiota composition was observed, similar to previous work (Marsh et al., 2022).

CF disease was the primary explanator, inclusive of the core taxa also, which is unsurprising given the strong associations between CFTR genotype alone and gut microbiota composition (Meeker et al., 2020). Alongside the whole microbiota, antibiotic usage was a principal explanator of satellite composition within our cohort with antibiotic class, dosage, and frequency highly variable across pwCF in this study. These results further extended to exclusive analysis of pwCF, whereby antibiotic usage was a prominent explanator of the bacterial community across all partitions, alongside disease mildness (determined by FEV1%). Given the speculated impact of antibiotics upon the gut microbiota previously reported (Duytschaever et al., 2013; Burke et al., 2017; Vernocchi et al., 2018; Enaud et al., 2019; Marsh et al., 2022), it remains in question whether this will persist following sustained CFTR modulator therapy that commences earlier in life across pwCF (Keogh et al., 2022). When investigating which taxa from the SIMPER analysis associated with these principal drivers of microbiota variation across all participants, species both typically identified as favourable and adverse to the host were identified. This included *Blautia* spp. and *Eubacterium hallii* which contain functional capacity for anti-inflammatory butyrate synthesis from a range of substrates (Rivière et al., 2016), but also *Enterococcus* spp. and *Ruminococcus gnavus*, which have both been shown to increase in the CF gut and associate with intestinal inflammation (Fouhy et al., 2017; Henke et al., 2019; Kristensen et al., 2020), suggestive of acquired resistance to recurrent antibiotic regimes in CF (Taylor et al., 2021). Upon analysis of pwCF samples solely, some discrepancies did emerge, with *Blautia* spp. (OTU 1) strongly dissociated with more mild CF disease whereas *Eubacterium hallii* displayed the opposite relationship. The relationships between disease severity and microbial composition also warrant further investigation of the putative lung-gut axis in CF (Madan et al., 2012; Hoen et al., 2015; Testa et al., 2022). Regarding antibiotic usage, again inconsistencies surfaced, with *Enterococcus* spp. strongly associated,

but then *Ruminococcus gnavus* instead primarily associated with increased disease mildness. The implications of such taxa changes upon host immunology at the site of the intestinal tract remains to be elucidated, with the refinement of intestinal organoid systems a potential solution for determining such intricate relationships between the microbiota and host (Bozzetti and Senger, 2022).

Across all samples, age and sex were also explanators of the whole microbiota and core taxa respectively, associating with taxa such as *Escherichia coli* and *Bifidobacterium adolescentis*. This may be explained in part by the strong ratio of males to females, alongside the wide age range of our participants, with the relative abundance of the aforementioned impacted by age across both CF and general life (Duytschaever et al., 2013; Hoffman et al., 2014; Arboleya et al., 2016; Matamouros et al., 2018). In terms of gut function, SBWC remained elevated across pwCF as observed previously (Ng et al., 2021) and continues to explain satellite taxa composition as we have previously demonstrated (Marsh et al., 2022). The physiological mechanisms behind this increased SBWC are proposed to result from gastro-ileal abnormalities in CF (Dellschaft et al., 2022), including delayed ileal-emptying which might have consequences for downstream taxa in the large intestine.

Away from the microbiota analyses, it was evident that patient symptoms, as measured by overall PAC-SYM scores, were not improved upon treatment with ETI. This is consistent with our previous cohort undertaking Tezacaftor/Ivacaftor therapy (Chapter 5), yet Mainz et al have recently described improvements within pwCF GI symptoms upon ETI therapy when utilising the tailored CFAbd questionnaire (Mainz et al., 2022). This remains to be validated within this pilot study specifically, but also as future studies encompass this tool for patient-reported outcome measures in CF. Intestinal inflammation is a common occurrence in pwCF (Munck, 2014; Dorsey and

Gonska, 2017; Beaufils et al., 2020). Unfortunately, we were unable to incorporate our limited faecal calprotectin data into this study. Previous modulator studies have reported mixed results in the reduction of faecal calprotectin (Stallings et al., 2018; Tetard et al., 2020; Ronan et al., 2022). However, with ETI therapy specifically, there is evidence of a reduction following 6 months of administration (Schwarzenberg et al., 2022).

Away from the clear caveat of group size in our pwCF cohort receiving extended ETI therapy, the relatively large sampling gap between this period and the preceding sampling point of 6 months should be acknowledged. Nonetheless, our extended sampling period highlights the value of further understanding alternate lifestyle factors in altering the CF microbiota, patient symptoms and intestinal abnormalities, as treatment with CFTR modulators alone may not be optimal to achieve this goal. This will require further research into the ability of specific dietary intake, antibiotic administration, and probiotic usage to shape the microbiota and patient outcomes (Esposito et al., 2022; Caley et al., 2023), especially since resilience of the gut microbiota has been recently suggested following diet and exercise intervention in pwCF (Knoll et al., 2023).

In conclusion, we have demonstrated that ETI therapy in pwCF leads to very subtle changes in microbiota composition following prolonged administration, with no differences in faecal SCFAs. Collectively the composition of the faecal microbiota and these functional metabolites remains significantly different from healthy controls following extended therapy. Future studies should maintain frequent, prolonged sampling periods with larger cohorts to investigate modulator effects, but also CF-associated lifestyle factors in this era of CF treatment.

6.5 Acknowledgements

This work was funded by CF Trust grant (VIA 77) awarded to CvdG and DWR. The wider ‘Gut Imaging for Function & Transit in Cystic Fibrosis Study 3’ (GIFT-CF3) was supported with funding from a Cystic Fibrosis Trust grant (VIA 061), a Cystic Fibrosis Foundation award (Clinical Pilot and Feasibility Award SMYTH18A0-I), and a Vertex Pharmaceuticals Investigator-Initiated Study award (IIS-2018-106697).

6.6 Author contributions

CvdG, DR, ARS, GM, and RM conceived the microbiome study. RM, and LH performed microbiota sample processing and analysis. RM and CDS carried out the metabolomic analysis. RM, DR, and CvdG performed the data and statistical analysis. AY, CN, GM, and AS were responsible for sample collection, clinical care records and documentation. RJM, AY, and CvdG verified the underlying data. RJM, DR, and CvdG were responsible for the creation of the original draft of the manuscript. RJM, GM, DR, ARS, and CvdG contributed to the development of the final manuscript. CvdG is the guarantor of this work. All authors read and approved the final manuscript.

6.7 Declaration of Competing Interest

RJM, CDS, and LH have nothing to disclose. DR and CvdG report grant funding from Vertex Pharmaceuticals outside of the submitted work. AY, CN, GM, and ARS report grants and speaker honorarium from Vertex Pharmaceuticals outside the submitted work.

6.8 Supplementary Methods and Results

6.8.1 Study participants and design

Twenty-four pwCF, possessing either F508del homozygosity or compound heterozygotes with at least one copy of F508del, were initially recruited from Nottingham University Hospitals NHS Trust. Participants were asked to provide stool samples whilst attending the Sir Peter Mansfield Imaging Centre at the University of Nottingham. Ultimately, 20 pwCF (mean age at baseline, 21.0 ± 8.6 years, median age, 18 years provided samples available for inclusion in our analyses. Participants were asked to fast overnight and prior to the refraining from the use of laxatives and anti-diarrhoeals during their visit. Regular pancreatic enzyme replacement therapy and physiotherapy procedures were admitted.

Clinical assessments and sample collections were performed at baseline, with further samples collected following ETI therapy for 3 and 6 months, with some participants further extending analysis over an additional 12 month to form this observational study. Whilst at clinic gut physiology assessment utilising magnetic resonance imaging (MRI) was performed. This included measurement of oro-caecal transit time (OCTT) and small bowel water content (SBWC) following the consumption of a standardised meal. During attendance, participants also provided faecal samples, and completed the validated PAC-SYM to assess their gut symptoms (Frank et al., 1999).

From the recruited cohort, sampling faecal sampling was achieved for 19 pwCF 3 months post-ETI, 18 pwCF 6 months post-ETI, and finally in 7 pwCF for the extended ETI period. Faecal samples from 10 age-matched healthy controls (mean age, 21.4 ± 7.40 years, median age, 20 years) from our previous study were available for microbiota and metabolomic comparison also (Marsh et al., 2022).

Further clinical trial details can be found at clinicaltrials.gov, under the trial number NCT04618185 (https://clinicaltrials.gov/ct2/show/NCT04618185).

6.8.2 PMA treatment prior to DNA extraction

1 mg PMA (Biotium, CA, USA) was hydrated in 98 µl 20% dimethyl sulfoxide (DMSO) to give a working stock concentration of 20 mM. 300 mg of thawed stool was homogenised in 1.5 ml PBS, and then centrifuged at 3200 x *g*, for 5 minutes. The pellet was then resuspended in 0.5 ml PBS prior to subsequent PMA treatment. 1.25 µl of PMA (20 mM) was added to give a final concentration of 50 µM. Following the addition of PMA to samples in opaque Eppendorf tubes, PMA was mixed by vortexing for 10 seconds, followed by incubation for 15 minutes at room temperature (~20°C). This step was repeated before the transfer of samples to clear 1.5 ml Eppendorf tubes and placement within a LED lightbox. Treatment occurred for 15 minutes to allow PMA intercalation into DNA from compromised bacterial cells. Samples were then centrifuged at 10,000 x *g* for 5 minutes. The supernatant was discarded, and the cellular pellet was resuspended in 200 µl PBS.

6.8.3 Targeted amplicon sequencing – Bacterial 16S rRNA gene

Step 1 amplicon generation with primers based on the universal primer sequences 515F and 926R as described by Walters et al. (Walters et al., 2016), was performed under the following conditions: Initial denaturation of 180 seconds at 98°C, followed by: 25 cycles of 30 seconds at 95°C, 30 seconds at 55°C and 30 seconds at 72°C. A final extension of 5 minutes at 72°C was also included to complete the reaction. Step 2, the addition of dual barcodes and Illumina adaptor sequences was performed under the following conditions: Initial denaturation of 30 seconds at 98°C,

followed by: 10 cycles of 10 seconds at 98°C, 20 seconds at 62°C and 30 seconds at 72°C. A final extension of 2 minutes at 72°C was also included to complete this reaction. This resulted in the generation of an ~550 bp amplicon spanning the V4-V5 hypervariable regions of the 16S rRNA gene.

6.8.4 Sequencing Controls and Library Pooling

PCR and DNA extraction negative controls were implemented, alongside the use of mock community positive controls, which included a Gut Microbiome Standard (ZYMO RESEARCH™). Following Barcode attachment in the second PCR step, clean-up and subsequent amplicon size selection was performed with AMPure XP beads (Beckman Coulter™) and quantified using a Qubit™ dsDNA HS kit. Sample concentrations were then manually normalised, pooled, and diluted to the final library concentrations requited for use on the Illumina MiSeq system.

6.8.5 Sequence processing and analysis

Initial sequencing files were processed using cutadapt (Version 3.5.0) to trim and remove upstream adaptor sequences prior to sequence analysis (Martin, 2011). DADA2 was used to demultiplex and remove primer sequences, validate the quality profiles of forward and reverse reads and subsequently trim, infer sequence variants, merge denoised paired-reads, remove chimeras, and finally assign taxonomy via Naive Bayesian Classifier implementation (Callahan et al., 2016). This included the use of a dedicated human intestinal 16S rRNA grnr reference database (Ritari et al., 2015). Unidentifiable ASVs were run through BLAST (Altschul et al., 1997) (https://blast.ncbi.nlm.nih.gov/Blast.cgi) and matched appropriately based on query coverage where possible. Taxa with 2 ≥ reads for a single sample were

removed and excluded from subsequent statistical analysis. ASVs from the same bacterial taxon were collapsed to form a single OTU for a given taxon. The R package decontam was used to remove any potential source of contamination across samples (Davis et al., 2018), utilising the prevalence-based contamination identification approach with a threshold classification of $P = 0.1$.

6.8.6 GC-MS: Sample processing and SCFA preparation

Faecal samples stored at -80°C were ground in liquid nitrogen before 50 mg of ground faeces was added to 500 µl MS-grade water. Samples were lysed and homogenised utilising inert ZR BashingBead Lysis Tubes (Cambridge bioscience, UK), using the FastPrep-24 5G instrument (MP Biomedicals, California, USA) with two cycles at a speed of 6.0 m/s for 40 seconds each. Samples were then incubated at 4°C whilst mixing for 30 minutes using an ELMI Intelli-Mixer™ RM-2L at 80 rpm. Samples were centrifuged at 13,000 x *g* for 30 mins. The supernatant containing faecal SCFAs was removed. 150 µl of supernatant was protonated with 5M HCl before the addition of anhydrous diethyl ether (1:1 v/v), samples were vortexed for 10 seconds, and incubated on ice for 5 mins. Following incubation, samples were mixed with the ELMI Intelli-Mixer™ RM-2L as before for 15 minutes, then centrifuged at 10,000 x *g* for 5 mins. The DE layer containing faecal SCFAs was transferred to a new Eppendorf tube pre-loaded with 25 mg Na2SO4. The remaining layer was then re-extracted with another 150 µl DE as before. Samples were equally pooled and then 40 ul was then transferred to a GC-MS vial, with the addition of 2 ul N, O-bis(trimethylsilyl) trifluoroacetamide (BSTFA). Samples were vortexed then incubated for 3 hours at 37°C before loading onto the GC-MS. MS grade water processed in parallel was used as a blank sample to correct the background.

6.8.7 GC-MS Analysis

GC-MS analysis was carried out using an Agilent 7890B/5977 Single Quadrupole Mass Selective Detector (MSD) (Agilent Technologies) equipped with a non-polar HP-5ms Ultra Inert capillary column (30 m × 0.25 mm × 0.25 µm) (Agilent Technologies). The Agilent 7693 Autosampler was used to inject 1.0 µl of the derivatised sample in triplicate at a split ratio of 20:1 at 265°C, with a solvent delay of 2 minutes 30 seconds. The initial oven temperature was held at 40°C for 2 minutes, followed by a 10°C/min temperature ramp to 140°C, then increased to 300°C at the rate of 40°C/min and kept at this temperature for 6 minutes. Electron impact (EI) mode ionisation was utilised at 70 eV, with the instrumental parameters set at 230, 150 and 300°C for source, quadrupole and interface temperatures, respectively. Selected ion monitoring (SIM) mode was used for quantification; all confirmation and target ions lists are summarised in Supplementary Table S6.2. Agilent MassHunter workstation version B.07.00 programs were used to perform post-run analyses. A ^{13}C-short chain fatty acids stool mixture (Merck Life Science, Poole, UK) was used as the internal standard to normalise all spectra obtained prior to analyses. A ^{13}C-short chain fatty acids stool mixture (Merck Life Science, Poole, UK) was used as the internal standard to normalise all spectra obtained prior to analyses. A volatile fatty acid mixture (Merck Life Science, UK) was used to construct calibration curves for the quantification of target metabolites.

6.9 Supplementary Results

Table S6.1 Clinical metadata for pwCF and healthy control participants.

			Genotype									Antibiotics						
ID	Group	Treatment length (Months)	1	2	Sex	Age (Years)	BMI	PI	CFRD	FCP	FEV1%	Ami	Ant	Mac	Mon	Pol	Sul	Tet
023	pwCF	B	F508del	1154insTC, p.Phe342HishX28	M	12	17.5	Y	N	-	94	-	-	-	-	-	-	-
		3			M	12	18.0			-	89	-	-	-	-	-	-	-
		6			M	12	18.4			-	94	-	-	-	-	-	-	-
		Ext			M	13	19.0			-	89	-	-	-	-	-	-	-
046	pwCF	B	F508del	F508del	F	22	21.9	Y	N	14.1	57	-	-	+	-	-	-	-
		3*			F	23	21.2			7.0	71.4	-	-	+	-	-	-	-
		6			F	23	21.4			7.0	73.5	-	-	+	-	-	-	-
194	pwCF	B	F508del	F508del	M	21	22.8	Y	Y	<5	91	-	-	-	-	-	-	-
		3			M	21	23.3			<5	98.9	-	-	-	-	-	-	-
		6			M	21	24.3			<5	93.1	-	-	-	-	-	-	-
247	pwCF	B	F508del	F508del	M	15	20.8	Y	N	27.6	101	-	-	-	-	-	-	-
		3			M	18	21.7			-	-	-	-	-	-	-	-	-
253	pwCF	B	F508del	F508del	M	13	21.8	Y	N	9.8	81	-	-	+	-	-	-	-
		3			M	15	27.0			-	101.5	-	-	+	-	-	-	-
		6			M	15	28.0			-	98.2	-	-	+	-	-	-	-
257	pwCF	B	F508del	F508del	M	16	17.7	Y	N	0.3	-	-	+	-	-	-	+	-
		3			M	16	19.1			-	95.9	-	+	-	-	-	+	-
		6			M	16	19.5			-	85.7	-	+	-	-	-	+	-
		Ext			M	17	19.6			-	98	-	+	-	-	-	+	+
336	pwCF	B	F508del	1138INSG	M	35	28.2	Y	Y	-	55	-	-	+	-	-	-	-
		3			M	36	29.3			-	63.9	-	-	+	-	-	-	-
		6¥			M	36	29.0			-	64	-	-	+	-	-	-	-

398	pwCF	B	F508del	1507del	F	13	17.8	Y	N	-	101	-	-	+	-	-	-	-
		3			F	13	18.6			-	115	-	-	+	-	-	-	-
		6			F	13	18.4			-	100	-	-	+	-	-	-	-
		Ext			F	14	20.6			-	102	-	-	+	-	-	-	-
437	pwCF	B*	F508del	F508del	M	17	20.5	Y	N	-	-	-	-	+	-	-	-	-
		3			M	17	21.3			-	98	-	-	+	-	-	-	-
		6			M	17	21.2			-	99.4	-	-	+	-	-	-	-
		Ext			M	19	21.3			-	104	-	-	+	-	-	-	-
503	pwCF	B	F508del	F508del	F	29	21.7	Y	N	32.0	57	-	-	-	-	-	-	-
		3			F	30	23.1			-	83.3	-	-	-	-	-	-	-
		6*			F	30	23.6			-	84.3	-	-	-	-	-	-	-
559	pwCF	B	F508del	F508del	M	17	20.4	Y	N	-	-	-	-	+	-	+	-	-
		6			M	18	21.4			<5	106	-	-	+	-	-	-	-
696	pwCF	B	F508del	711+1G->T, c579+1G>T	M	12	16.9	Y	N	-	95	-	-	+	-	-	-	-
		3			M	12	18.1			-	93	-	-	+	-	-	-	-
		6			M	13	17.7			-	93.3	-	-	+	-	-	-	-
741	pwCF	B	F508del	1507del	M	13	14.7	Y	N	<5	58.3	+	-	+	-	-	-	-
		3			M	13	15.7			<5	77.9	+	-	+	-	-	-	-
		6			M	13	15.5			<5	72	+	-	+	-	-	-	-
752	pwCF	B	F508del	F508del	M	19	20.8	Y	N	-	116	-	-	-	-	-	-	-
		3			M	19	21.1			-	-	-	-	-	-	-	-	-
		6			M	20	21.0			-	115.5	-	-	-	-	-	-	-
		Ext			M	21	22.9			-	118	-	-	-	-	-	-	-
756	pwCF	3	F508del	1154insTC, p.Phe342HisfsX28	F	16	22.6	Y	N	-	66	-	-	+	-	-	-	-
		6			F	16	22.2			-	80.4	-	-	+	-	-	-	-
802	pwCF	B	F508del	F508del	M	19	20.6	Y	N	7.4	99	-	-	-	-	+	-	-
		3			M	21	25.3			8.0	-	-	-	-	-	-	-	-
		6			M	22	26.2			8.0	111.7	-	-	-	-	-	-	-
820	pwCF	B	F508del	F508del	M	31	25.2	Y	Y	-	60	+	-	+	-	+	-	-
		3			M	32	27.3			6.0	76.8	+	-	+	-	+	-	-
		6			M	32	28.1			6.0	73.6	+	-	+	-	+	-	-

		Ext			M	33	28.2			-	79.3	+	-	+	-	+	-	-
868	pwCF	B	F508del	F508del	M	25	18.5	Y	N	33.2	-	+	-	-	+	-	-	-
		3			M	26	20.6			-	-	+	-	-	+	-	-	-
		6			M	26	19.6			-	67.3	+	-	-	+	-	-	-
871	pwCF	B	F508del	gLn1291his	F	35	25.9	Y	N	29.0	75	-	-	-	-	-	-	-
		3			F	35	27.2			-	-	-	-	-	-	-	-	-
884	pwCF	B	F508del	F508del	M	40	26.3	Y	Y	-	58.7	-	-	+	+	-	-	-
		3			M	40	27.4			3.4	67.4	-	-	+	+	-	-	-
		6			M	40	28.2			3.4	71.4	-	-	+	+	-	-	-
		Ext			M	41	27.8			-	68	-	-	+	+	-	-	-
152	HC	-	Unknown	Unknown	F	21	21.3	N	-	4.2	-	-	-	-	-	-	-	-
159	HC	-	Unknown	Unknown	M	13	23.5	N	-	2.7	-	-	-	-	-	-	-	-
205	HC	-	Unknown	Unknown	F	19	31.9	N	-	3.8	-	-	-	-	-	-	-	-
431	HC	-	Unknown	Unknown	M	12	18.0	N	-	2.4	-	-	-	-	-	-	-	-
501	HC	-	Unknown	Unknown	F	27	28.7	N	-	7.2	-	-	-	-	-	-	-	-
548	HC	-	Unknown	Unknown	M	24	24.5	N	-	3.6	-	-	-	-	-	-	-	-
673	HC	-	Unknown	Unknown	M	19	20.3	N	-	0.9	-	-	-	-	-	-	-	-
749	HC	-	Unknown	Unknown	F	35	19.6	N	-	3.0	-	-	-	-	-	-	-	-
964	HC	-	Unknown	Unknown	F	15	19.2	N	-	12.7	-	-	-	-	-	-	-	-
986	HC	-	Unknown	Unknown	M	29	22.6	N	-	5.0	-	-	-	-	-	-	-	-

Treatment length points marked indicate samples for which no *metagenomic or ¥metabolomic analysis was available, due incomplete stool sampling or following removal of reads/data from downstream processing. CF participants were either F508del homozygous, or F508del heterozygous. All patients were pancreatic insufficient but contained no CF-related diabetes. For antibiotic usage, '+' indicates routine use of antibiotic class during the period for which the respective sample was obtained. Abbreviations: pwCF - People with CF, HC - Healthy controls, B - Baseline, FEV1 – Percent predicted forced expiratory volume in 1 second, BMI – Body mass index, PI – Pancreatic insufficiency, CFRD – Cystic fibrosis-related diabetes, FCP - Faecal calprotectin, Antibiotics; Ami – Aminoglycosides, Ant – Antimycobacterials, Mac – Macrolides, Mon – Monobactams, Pol – Polymixins, Sul – Sulfonamides, Tet – Tetracyclines.

Table S6.2 Magnetic resonance imaging (MRI) data between pwCF and healthy control participants.

Participant ID	Group	Treatment length (Months)	OCTT	SBWC
023	pwCF	B	390	54.10
		3	390	71.45
		6	390	83.34
		Ext	240	43.08
046	pwCF	B	120	83.35
		3*	390	49.31
		6	390	56.03
194	pwCF	B	390	79.48
		3	390	119.20
		6	390	72.16
247	pwCF	B	180	273.09
		3	300	62.29
253	pwCF	B	390	82.92
		3	390	74.79
		6	390	82.09
257	pwCF	B	240	40.56
		3	390	53.51
		6	120	20.44
		Ext	120	58.45
336	pwCF	B	390	45.65
		3	390	51.95
		6	390	57.06
398	pwCF	B	390	136.36
		3	240	180.52
		6	240	102.51
		Ext	360	169.15
437	pwCF	B*	390	99.35
		3	390	93.81
		6	360	83.35
		Ext	180	86.85
503	pwCF	B	390	31.25
		3	390	49.21
		6*	240	59.00
559	pwCF	B	390	74.30
		6	390	95.80
696	pwCF	B	360	43.59
		3	360	54.28
		6	300	37.07
741	pwCF	B	390	38.34
		3	360	45.91
		6	390	51.92

752	pwCF	B	390	42.38
		3	300	105.59
		6	390	96.71
		Ext	180	138.62
756	pwCF	3	390	105.59
		6	390	96.71
802	pwCF	B	390	133.05
		3	390	38.02
		6	390	25.13
820	pwCF	B	300	41.53
		3	300	59.30
		6	300	49.08
		Ext	300	54.55
868	pwCF	B	390	82.84
		3	300	118.88
		6	240	113.28
871	pwCF	B	-	-
		3	-	-
884	pwCF	B	300	97.00
		3	300	47.33
		6	390	58.21
		Ext	240	59.05
152	HC	-	180	61.51
159	HC	-	150	18.40
205	HC	-	360	40.35
431	HC	-	150	72.69
501	HC	-	360	47.56
548	HC	-	300	57.04
673	HC	-	360	24.16
749	HC	-	240	10.79
964	HC	-	180	26.19
986	HC	-	180	89.90

B; Baseline, 3; 3 Months ETI therapy, 6; 6 Months ETI therapy, Ext; Extended ETI therapy, OCTT; Oro-caecal transit time, SBWC; Small bowel water content (corrected for body surface area).

Table S6.3 Analytical parameters for SCFA analysis with GC-MS

SCFA	t_R (min)	Target ion (m/z)	Confirmation ion (m/z)
Acetic acid	2.52	117	75
Propionic acid	3.81	131	75
Iso-butyric acid	4.39	145	117
Butyric acid	5.22	145	117
Iso-valeric acid	6.07	159	117
Valeric acid	6.85	159	117
4-methylvaleric acid	7.86	173	117
Hexanoic acid	8.41	173	117
Heptanoic acid	9.9	187	117
^{13}C-acetic acid	2.52	119	77
^{13}C-propionic acid	3.81	134	77
^{13}C-butyric acid	5.22	149	119

t_R - Retention time

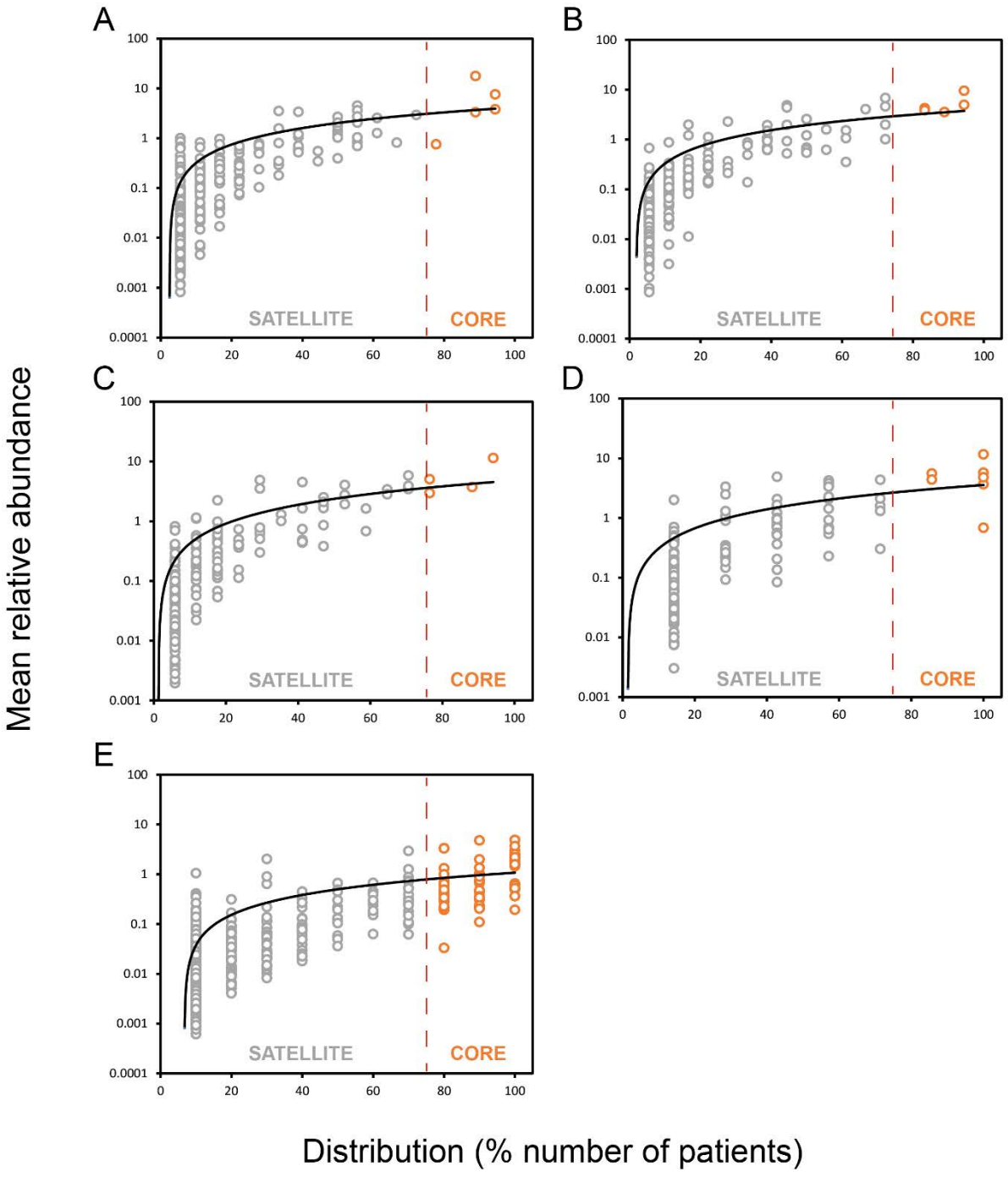

Figure S6.1 Distribution and abundance of bacterial taxa across lengthening ETI treatment (0, 3, 6, Ext months) stages (A, B, C, D respectively) and healthy control participants (E). Given is the percentage number of patients harbouring each bacterial taxon, plotted against the mean relative abundance across those samples. Core taxa are depicted by the orange circles and fall in the upper quartile of distribution, separated by the red vertical line at 75% distribution. Satellite taxa (grey) are all samples below this distribution. Distribution-abundance relationship regression statistics: (a) r^2 = 0.45, $F_{1,320}$ = 249.4, P < 0.0001. (b) r^2 = 0.63, $F_{1,253}$ = 434.1, P < 0.0001. (c) r^2 = 0.65, $F_{1,196}$ = 358.5, P < 0.0001. (d) r^2 = 0.53, $F_{1,146}$ = 167.2, P < 0.0001. (e) r^2 = 0.40, $F_{1,482}$ = 321.4, P < 0.0001.

Table S6.4 Core taxa throughout ETI therapy and control participants.

	Mean relative abundance (%)				
	ETI duration (months)				
Genus	0	3	6	12	HC
Blautia 1	17.69	9.54	11.45	11.66	4.91
Blautia luti	4.49	6.79	5.83	5.55	3.01
Fusicatenibacter saccharivorans	7.61	4.24	2.96	5.73	3.69
Dorea longicatena	3.61	4.61	5.05	4.39	1.79
Eubacterium hallii	3.79	3.56	3.73	4.81	2.39
Bacteroides dorei	2.67	2.56	4.05	3.79	3.35
Anaerostipes hadrus	2.73	4.06	2.83	4.35	1.99
Eubacterium rectale	1.39	2.55	3.43	3.68	4.78
Collinsella aerofaciens	3.37	4.85	3.52	3.33	0.19
Gemmiger formicilis	1.05	4.40	4.51	4.24	1.05
Clostridium disporicum	2.92	4.97	3.90	1.60	0.70
Bifidobacterium adolescentis	0.82	2.29	4.88	4.90	0.81
Streptococcus 6	3.32	3.87	3.40	1.43	0.19
Blautia faecis	2.53	1.98	1.94	2.12	2.30
Bacteroides vulgatus	1.57	0.52	2.23	1.66	3.32
Escherichia coli	2.05	0.70	1.66	2.27	1.99
Romboutsia timonensis	1.16	1.96	2.75	0.76	1.32
Ruminococcus faecis	1.20	0.96	1.64	2.27	1.61
Blautia obeum	1.75	1.07	0.73	0.98	2.51
Faecalibacterium duncaniae	0.49	0.86	0.52	2.09	2.15
Intestinibacter bartlettii	0.34	1.07	1.01	1.22	0.63
Bacteroides uniformis	0.66	0.49	0.41	0.14	2.55
Eubacterium desmolans	0.76	1.01	0.68	0.69	0.67
Faecalibacillus 70	0.18	0.78	0.70	0.54	1.45
Dorea phocaeensis	0.27	0.68	0.86	1.31	0.31
Coprococcus comes	0.52	0.52	0.44	0.92	0.57
Faecalibacterium longum	0.03	0.14	0.15	0.42	2.19
Parabacteroides distasonis	1.04	0.21	0.15	0.11	0.90
Faecalibacterium prausnitzii	0.14	0.00	0.03	0.00	2.04
Roseburia hominis	0.60	0.24	0.22	0.00	1.00
Blautia intestinalis	0.29	0.27	0.58	0.00	0.50
Gemmiger 86	0.03	0.17	0.21	0.47	0.75
Barnesiella intestinihominis	0.01	0.03	0.01	0.00	1.58
Hominisplanchenecus faecis	0.49	0.31	0.03	0.14	0.50
Alistipes putredinis	0.00	0.00	0.00	0.00	1.35
Eubacterium coprostanoligenes	0.04	0.39	0.04	0.27	0.43
Blautia torques	0.21	0.04	0.07	0.30	0.39
Clostridium 146	0.00	0.27	0.03	0.18	0.43
Eubacterium ramulus	0.14	0.17	0.07	0.32	0.21
Ruminococcus champanellensis	0.00	0.02	0.00	0.21	0.65
Lachnoclostridium edouardi	0.09	0.15	0.04	0.00	0.53
Alistipes onderdonkii	0.04	0.00	0.01	0.00	0.64
Eubacterium ventriosum	0.03	0.05	0.04	0.26	0.29
Bacteroides caccae	0.03	0.03	0.15	0.06	0.36

Odoribacter splanchnicus	0.01	0.00	0.00	0.00	0.60
Coprococcus catus	0.08	0.07	0.02	0.14	0.22
Waltera intestinalis	0.02	0.00	0.00	0.00	0.49
Oscillibacter 413	0.00	0.00	0.00	0.00	0.48
Evtepia gabavorous	0.00	0.00	0.00	0.00	0.47
Vescimonas fastidiosa	0.00	0.03	0.00	0.00	0.41
Lentihominibacter faecis	0.06	0.08	0.07	0.08	0.11
Roseburia inulinivorans	0.05	0.00	0.00	0.00	0.34
Marseillibacter massiliensis	0.00	0.03	0.00	0.00	0.34
Alistipes obesi	0.00	0.00	0.00	0.00	0.36
Alistipes marseilloanorexicus	0.02	0.00	0.00	0.00	0.32
Eubacterium eligens	0.00	0.05	0.00	0.00	0.29
Alistipes shahii	0.00	0.00	0.00	0.00	0.24
Vescimonas 720	0.00	0.00	0.00	0.00	0.23
Oscillibacter massiliensis	0.00	0.01	0.01	0.00	0.20
Pseudomonas 1352	0.01	0.00	0.00	0.00	0.03

Table S6.5 Kruskall-Wallis tests of bacterial alpha diversity across treatment time-points (months) utilising Fisher's alpha index.

	Microbiota		**Core**		**Satellite**	
0-3	K (Observed value)	1.851	K (Observed value)	0.169	K (Observed value)	1.894
	K (Critical value)	3.841	K (Critical value)	3.841	K (Critical value)	3.841
	DF	1	DF	1	DF	1
	p-value (one-tailed)	0.174	p-value (one-tailed)	0.681	p-value (one-tailed)	0.169
0-6	K (Observed value)	12.240	K (Observed value)	9.021	K (Observed value)	11.333
	K (Critical value)	3.841	K (Critical value)	3.841	K (Critical value)	3.841
	DF	1	DF	1	DF	1
	p-value (one-tailed)	0.0005	p-value (one-tailed)	0.003	p-value (one-tailed)	0.001
0-Ext	K (Observed value)	0.938	K (Observed value)	14.538	K (Observed value)	1.059
	K (Critical value)	3.841	K (Critical value)	3.841	K (Critical value)	3.841
	DF	1	DF	1	DF	1
	p-value (one-tailed)	0.333	p-value (one-tailed)	0.0001	p-value (one-tailed)	0.304
3-6	K (Observed value)	4.462	K (Observed value)	9.938	K (Observed value)	2.946
	K (Critical value)	3.841	K (Critical value)	3.841	K (Critical value)	3.841
	DF	1	DF	1	DF	1
	p-value (one-tailed)	0.035	p-value (one-tailed)	0.002	p-value (one-tailed)	0.086
6-Ext	K (Observed value)	2.623	K (Observed value)	14.280	K (Observed value)	1.614
	K (Critical value)	3.841	K (Critical value)	3.841	K (Critical value)	3.841
	DF	1	DF	1	DF	1
	p-value (one-tailed)	0.105	p-value (one-tailed)	0.0002	p-value (one-tailed)	0.204

Table S6.6 Kruskal-Wallis tests of bacterial alpha diversity between treatment time-points (months) and healthy controls utilising Fisher's alpha index.

	Microbiota		**Core**		**Satellite**	
0-HC	K (Observed value)	18.621	K (Observed value)	18.621	K (Observed value)	18.626
	K (Critical value)	3.841	K (Critical value)	3.841	K (Critical value)	3.841
	DF	1	DF	1	DF	1
	p-value (one-tailed)	0.000	p-value (one-tailed)	<0.0001	p-value (one-tailed)	<0.0001
3-HC	K (Observed value)	18.621	K (Observed value)	18.626	K (Observed value)	18.626
	K (Critical value)	3.841	K (Critical value)	3.841	K (Critical value)	3.841
	DF	1	DF	1	DF	1
	p-value (one-tailed)	<0.0001	p-value (one-tailed)	<0.0001	p-value (one-tailed)	<0.0001
6-HC	K (Observed value)	18.214	K (Observed value)	18.214	K (Observed value)	18.220
	K (Critical value)	3.841	K (Critical value)	3.841	K (Critical value)	3.841
	DF	1	DF	1	DF	1
	p-value (one-tailed)	<0.0001	p-value (one-tailed)	<0.0001	p-value (one-tailed)	<0.0001
Ext-HC	K (Observed value)	11.667	K (Observed value)	11.667	K (Observed value)	11.681
	K (Critical value)	3.841	K (Critical value)	3.841	K (Critical value)	3.841
	DF	1	DF	1	DF	1
	p-value (one-tailed)	0.001	p-value (one-tailed)	0.001	p-value (one-tailed)	0.001

Table S6.7 Bacterial ANOSIM summary statistics across ETI treatment lengths, utilising the Bray-Curtis index.

	Microbiota		Core		Satellite	
0-3	R	-0.02372	R	0.02923	R	0.0382
	p (same)	0.7567	p (same)	0.1471	p (same)	0.1355
	Bonferroni-corrected p value	0.7598	Bonferroni-corrected p value	0.1481	Bonferroni-corrected p value	0.1421
	Permutations	9999	Permutations	9999	Permutations	9999
0-6	R	-0.03417	R	0.1835	R	0.03914
	p (same)	0.8365	p (same)	0.0001	p (same)	0.1395
	Bonferroni-corrected p value	0.8495	Bonferroni-corrected p value	0.0002	Bonferroni-corrected p value	0.1477
	Permutations	9999	Permutations	9999	Permutations	9999
0-Ext	R	-0.1927	R	0.1942	R	0.09095
	p (same)	0.9837	p (same)	0.0547	p (same)	0.1684
	Bonferroni-corrected p value	0.985	Bonferroni-corrected p value	0.0614	Bonferroni-corrected p value	0.1763
	Permutations	9999	Permutations	9999	Permutations	9999
3-6	R	-0.0664	R	0.2078	R	0.07737
	p (same)	0.9938	p (same)	0.0001	p (same)	0.034
	Bonferroni-corrected p value	0.9947	Bonferroni-corrected p value	0.0001	Bonferroni-corrected p value	0.0347
	Permutations	9999	Permutations	9999	Permutations	9999
6-Ext	R	-0.1876	R	0.1817	R	0.04437
	p (same)	0.9798	p (same)	0.0591	p (same)	0.288
	Bonferroni-corrected p value	0.9806	Bonferroni-corrected p value	0.0639	Bonferroni-corrected p value	0.2944
	Permutations	9999	Permutations	9999	Permutations	9999

Table S6.8 Bacterial ANOSIM summary statistics between ETI treatment lengths and healthy control participants, utilising the Bray-Curtis index.

	Microbiota		Core		Satellite	
0-HC	R	0.2775	R	0.7931	R	0.8795
	p (same)	0.0018	p (same)	0.0001	p (same)	0.0001
	Bonferroni-corrected p value	0.0023	Bonferroni-corrected p value	0.0001	Bonferroni-corrected p value	0.0001
	Permutations	9999	Permutations	9999	Permutations	9999
3-HC	R	0.3104	R	0.7432	R	0.8999
	p (same)	0.0015	p (same)	0.0001	p (same)	0.0001
	Bonferroni-corrected p value	0.0021	Bonferroni-corrected p value	0.0001	Bonferroni-corrected p value	0.0001
	Permutations	9999	Permutations	9999	Permutations	9999
6-HC	R	0.3751	R	0.9177	R	0.9299
	p (same)	0.0002	p (same)	0.0001	p (same)	0.0001
	Bonferroni-corrected p value	0.0002	Bonferroni-corrected p value	0.0001	Bonferroni-corrected p value	0.0001
	Permutations	9999	Permutations	9999	Permutations	9999
Ext-HC	R	0.6697	R	0.9957	R	0.8723
	p (same)	0.0002	p (same)	0.0001	p (same)	0.0001
	Bonferroni-corrected p value	0.0002	Bonferroni-corrected p value	0.0002	Bonferroni-corrected p value	0.0002
	Permutations	9999	Permutations	9999	Permutations	9999

Table S6.9 Similarity of percentage (SIMPER) analysis of microbiota dissimilarity (Bray-Curtis) between baseline and pwCF samples following extended treatment with ETI.

Taxa	% Relative abundance		Av. Dissimilarity	% Contribution	Cumulative (%)
	Baseline	Ext ETI			
Blautia 1	17.70	11.70	5.59	7.62	7.621
Fusicatenibacter saccharivorans	7.61	5.73	3.56	4.85	12.47
Blautia luti	4.49	5.55	2.48	3.38	15.85
Bifidobacterium adolescentis	0.82	4.90	2.31	3.14	18.99
Collinsella aerofaciens	3.37	3.33	2.27	3.10	22.09
Anaerostipes hadrus	2.73	4.35	2.24	3.05	25.14
Bacteroides dorei	2.67	3.79	2.21	3.01	28.15
Dorea longicatena	3.61	4.39	2.01	2.74	30.89
Gemmiger formicilis	1.05	4.24	1.82	2.48	33.36
Bifidobacterium 21	3.50	0.22	1.67	2.27	35.64
Enterococcus 26	2.55	2.07	1.54	2.10	37.74
Eubacterium rectale	1.39	3.68	1.53	2.09	39.82
Ruminococcus bromii	0.16	3.34	1.48	2.02	41.84
Streptococcus 6	3.32	1.43	1.43	1.95	43.79
Eubacterium hallii	3.79	4.81	1.37	1.87	45.66
Clostridium disporicum	2.92	1.60	1.37	1.87	47.53
Ruminococcus gnavus	1.26	2.48	1.33	1.81	49.34
Escherichia coli	2.05	2.27	1.29	1.75	51.09

Taxa identified as core are highlighted in orange, with satellite taxa highlighted in grey. The mean relative abundance (%) across both groups is given, alongside the percentage contribution which is the mean dissimilarity of taxa divided by the mean dissimilarity (73.40%) across samples. Cumulative percent does not equal 100% as the list is not exhaustive, rather the taxa that make up 50% of dissimilarity between groups. Given the length of the 16S gene regions sequenced, taxon identification should be considered putative.

Table S6.10 Redundancy analysis to explain percent variation across whole microbiota, core, and satellite taxa of the significant clinical variables across pwCF receiving ETI therapy.

	Microbiota			Core taxa			Satellite taxa		
	Var. Exp (%)	pseudo-*F*	*P* (adj)	Var. Exp (%)	pseudo-*F*	*P* (adj)	Var. Exp (%)	pseudo-*F*	*P* (adj)
Antibiotics	4.9	2.8	0.010	5.6	3.3	0.050	5.4	2.9	0.002
							6.5	3.4	0.002
BMI	5.2	2.9	0.016						
Disease mild.	7.4	3.9	0.002	9.6	5.2	0.006	3.4	1.9	0.012
SBWC	3.4	2.0	0.046	4.9	3.0	0.038			
Sex	3.7	2.2	0.038	5.5	3.1	0.082	2.6	1.5	0.050
Treatment length							2.9	1.7	0.048
Total	**24.6**			**25.6**			**20.8**		

Var. Exp (%) represents the percentage of the microbiota for which can be explained by a given clinical variable from the redundancy analysis model. *P* (adj) is following false discovery rate correction of significance values. Antibiotics refers to if a given participant was receiving any class of routine antibiotic during the sampling period. Disease mild. – Disease mildness utilising FEV_1% as a proxy, SBWC – Small bowel water content corrected for body surface area.

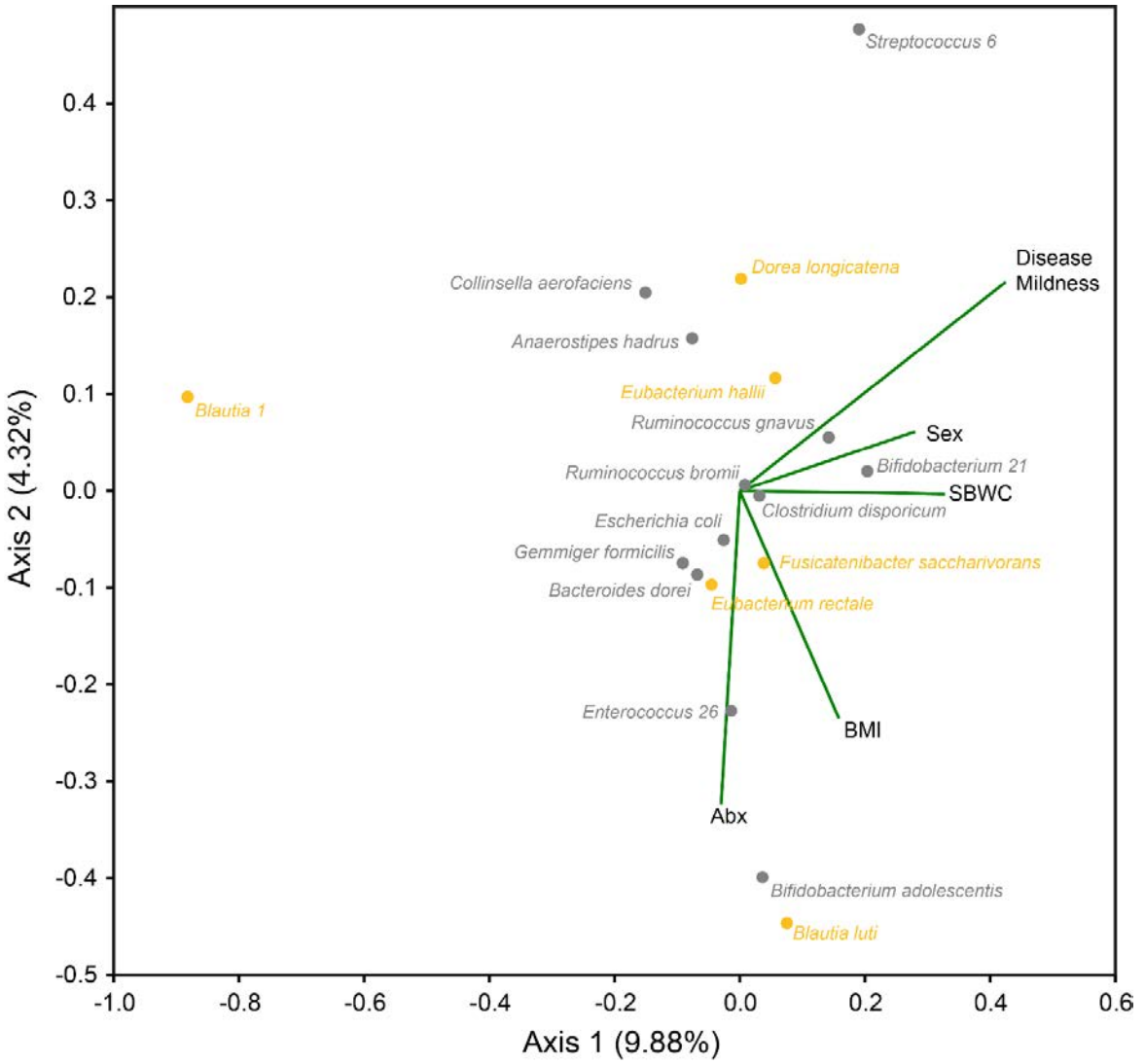

Figure S6.2 Redundancy analysis species biplots for the whole microbiota within pwCF. The 24 taxa contributing most to the dissimilarity (cumulatively > 50%) within pwCF samples at baseline and following extended ETI therapy from the SIMPER analysis (Table S6.9) are shown independently of the total number of ASVs identified (353). Orange points represent taxa that were identified as core for the pwCF group following extended ETI therapy, grey points are satellite, and the white (black stroke) points represent taxa that were absent. Biplot lines depict clinical variables that significantly account for total variation in taxa relative abundance within whole microbiota analysis at the $p \leq 0.05$ level (Table S6.10). Species plots depict the strength of explanation provided by the given clinical variables, with taxa shown in the same direction of a particular clinical variable considered to have a higher value than those that are not. 'Abx' – Antibiotics during sampling period, 'BMI' – Body mass index, 'Disease Mildness' – Disease mildness based on increased FEV1% across patients, 'SBWC' – Small bowel water content corrected for body surface area. The percentage of microbiota variation explained by each axis is given in parentheses.

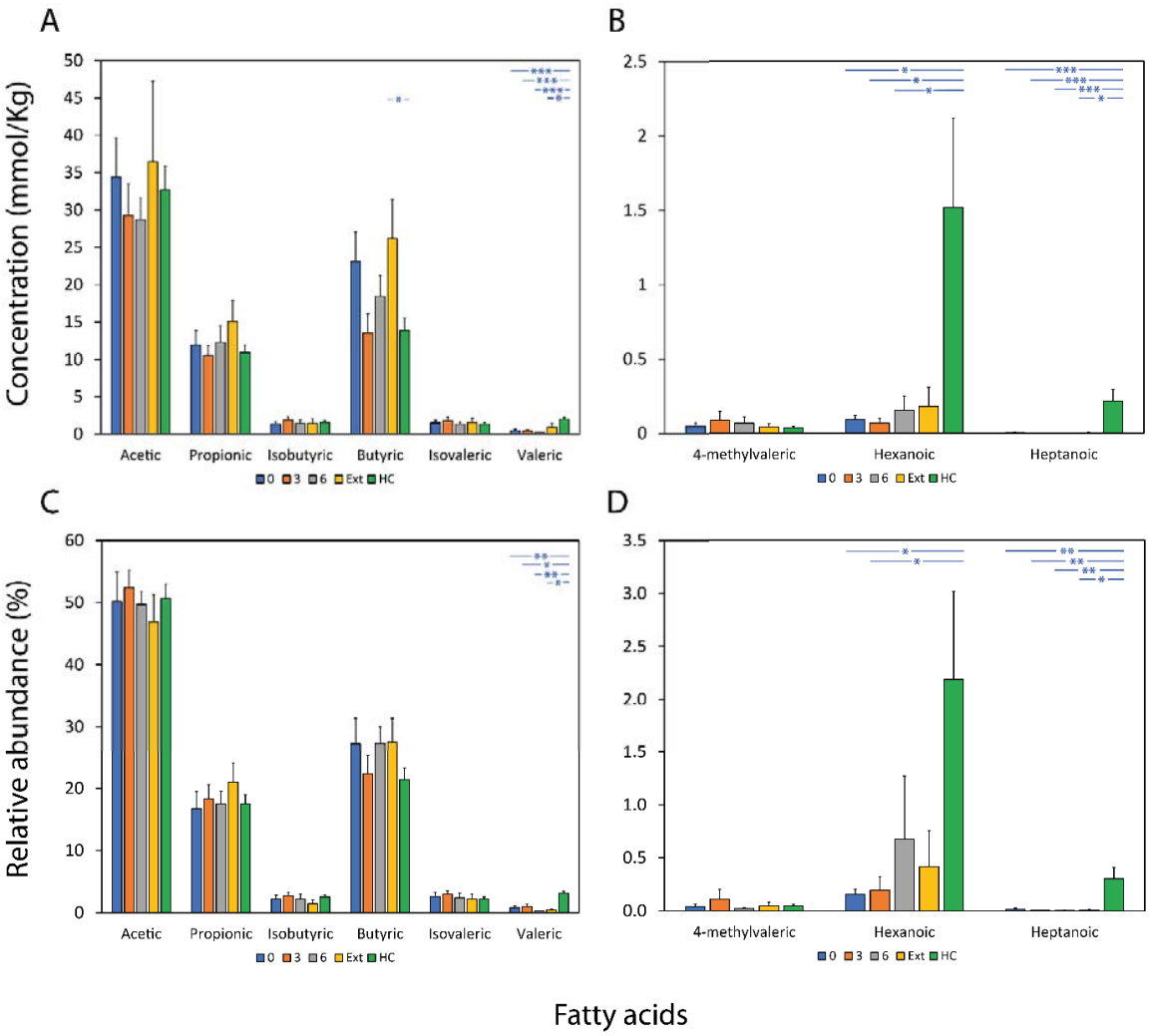

Figure S6.3 Changes in faecal fatty acid concentration (A-B) and relative abundance (C-D) across ETI treatment periods (months) and healthy control samples. Error bars denote standard error of the mean (SEM). Asterisks between bars denote significance differences in absolute quantification (A-B) or relative abundance (C-D) of faecal fatty acids between groups following Kruskal-Wallis testing. ***; $P < 0.0001$, **; $P < 0.001$, *; $P < 0.05$. Summary statistics are found in Tables S6.11-6.14.

Table S6.11 Kruskal-Wallis tests of faecal fatty acid quantification between across ETI treatment time-points.

		Fatty acid								
		Acetic	Propionic	Isobutyric	Butyric	Isovaleric	Valeric	4-methyl	Hexanoic	Heptanoic
0-3	K (Observed value)	0.189	0.179	0.511	1.765	0.003	0.214	0.025	1.470	2.016
	K (Critical value)	3.841	3.841	3.841	3.841	3.841	3.841	3.841	3.841	3.841
	DF	1	1	1	1	1	1	1	1	1
	p-value (one-tailed)	0.6635	0.6721	0.4749	0.1841	0.9534	0.6440	0.8755	0.2254	0.1556
3-6	K (Observed value)	0.107	0.236	0.810	2.793	0.351	0.086	0.095	1.872	0.137
	K (Critical value)	3.841	3.841	3.841	3.841	3.841	3.841	3.841	3.841	3.841
	DF	1	1	1	1	1	1	1	1	1
	p-value (one-tailed)	0.7442	0.6268	0.3682	0.0947	0.5535	0.7697	0.7579	0.1712	0.7116
6-Ext	K (Observed value)	0.044	1.059	0.000	2.289	0.366	2.476	0.007	0.004	0.040
	K (Critical value)	3.841	3.841	3.841	3.841	3.841	3.841	3.841	3.841	3.841
	DF	1	1	1	1	1	1	1	1	1
	p-value (one-tailed)	0.8330	0.3035	1.0000	0.1303	0.5450	0.1156	0.9354	0.9517	0.8416
0-6	K (Observed value)	0.653	0.000	0.029	0.267	0.316	0.651	0.061	0.059	1.428
	K (Critical value)	3.841	3.841	3.841	3.841	3.841	3.841	3.841	3.841	3.841
	DF	1	1	1	1	1	1	1	1	1
	p-value (one-tailed)	0.4189	1.0000	0.8651	0.6055	0.5740	0.4198	0.8054	0.8078	0.2321
0-Ext	K (Observed value)	0.011	1.271	0.007	0.188	0.021	1.322	0.013	0.442	0.268
	K (Critical value)	3.841	3.841	3.841	3.841	3.841	3.841	3.841	3.841	3.841
	DF	1	1	1	1	1	1	1	1	1
	p-value (one-tailed)	0.9161	0.2596	0.9343	0.6646	0.8851	0.2502	0.9076	0.5061	0.6049

Table S6.12 Kruskal-Wallis tests of fatty acid relative abundance between across ETI treatment time-points.

		Fatty acid								
		Acetic	Propionic	Isobutyric	Butyric	Isovaleric	Valeric	4-methyl	Hexanoic	Heptanoic
0-3	K (Observed value)	0.240	0.240	0.296	0.500	0.214	0.145	0.279	0.359	0.465
	K (Critical value)	3.841	3.841	3.841	3.841	3.841	3.841	3.841	3.841	3.841
	DF	1	1	1	1	1	1	1	1	1
	p-value (one-tailed)	0.6245	0.6245	0.5865	0.4795	0.6438	0.7034	0.5976	0.5489	0.4951
3-6	K (Observed value)	0.068	0.303	0.706	1.854	0.568	0.806	0.277	0.190	0.061
	K (Critical value)	3.841	3.841	3.841	3.841	3.841	3.841	3.841	3.841	3.841
	DF	1	1	1	1	1	1	1	1	1
	p-value (one-tailed)	0.7943	0.5820	0.4009	0.1734	0.4512	0.3692	0.5987	0.6632	0.8044
6-12	K (Observed value)	0.722	0.722	0.029	0.260	0.029	3.494	0.097	0.080	0.787
	K (Critical value)	3.841	3.841	3.841	3.841	3.841	3.841	3.841	3.841	3.841
	DF	1	1	1	1	1	1	1	1	1
	p-value (one-tailed)	0.3955	0.3955	0.8651	0.6102	0.8651	0.0616	0.7550	0.7768	0.3751
0-6	K (Observed value)	0.186	0.034	0.046	0.186	0.046	0.691	0.005	0.015	0.000
	K (Critical value)	3.841	3.841	3.841	3.841	3.841	3.841	3.841	3.841	3.841
	DF	1	1	1	1	1	1	1	1	1
	p-value (one-tailed)	0.6666	0.8535	0.8294	0.6666	0.8294	0.4059	0.9458	0.9018	1.0000
0-Ext	K (Observed value)	0.178	0.711	0.100	0.011	0.011	0.178	0.003	0.100	0.290
	K (Critical value)	3.841	3.841	3.841	3.841	3.841	3.841	3.841	3.841	3.841
	DF	1	1	1	1	1	1	1	1	1
	p-value (one-tailed)	0.6733	0.3991	0.7518	0.9161	0.9161	0.6733	0.9529	0.7517	0.5901

Table S6.13 Kruskal-Wallis tests of fatty acid quantification between ETI treatment time-points and healthy controls.

		Fatty acid								
		Acetic	Propionic	Isobutyric	Butyric	Isovaleric	Valeric	4-methyl	Hexanoic	Heptanoic
0-HC	K (Observed value)	0.017	0.034	0.771	0.760	0.076	14.713	1.448	5.477	12.746
	K (Critical value)	3.841	3.841	3.841	3.841	3.841	3.841	3.841	3.841	3.841
	DF	1	1	1	1	1	1	1	1	1
	p-value (one-tailed)	0.8951	0.8544	0.3798	0.3833	0.7831	0.0001	0.2289	0.0193	0.0004
3-HC	K (Observed value)	1.388	0.002	0.003	0.928	0.034	13.805	2.177	9.453	17.631
	K (Critical value)	3.841	3.841	3.841	3.841	3.841	3.841	3.841	3.841	3.841
	DF	1	1	1	1	1	1	1	1	1
	p-value (one-tailed)	0.2387	0.9634	0.9600	0.3353	0.8544	0.0002	0.1400	0.0021	0.0000
6-HC	K (Observed value)	0.852	0.021	0.754	0.517	0.589	18.621	1.019	4.056	17.806
	K (Critical value)	3.841	3.841	3.841	3.841	3.841	3.841	3.841	3.841	3.841
	DF	1	1	1	1	1	1	1	1	1
	p-value (one-tailed)	0.3559	0.8856	0.3853	0.4720	0.4430	0.0000	0.3128	0.0440	0.0000
Ext-HC	K (Observed value)	0.375	0.034	0.576	5.952	0.010	5.952	0.146	2.143	8.109
	K (Critical value)	3.841	3.841	3.841	3.841	3.841	3.841	3.841	3.841	3.841
	DF	1	1	1	1	1	1	1	1	1
	p-value (one-tailed)	0.5403	0.8544	0.4477	0.0147	0.9223	0.0147	0.7021	0.1432	0.0044

Table S6.14 Kruskal-Wallis tests of fatty acid relative abundance ETI treatment time-points and healthy controls.

		Fatty acid								
		Acetic	Propionic	Isobutyric	Butyric	Isovaleric	Valeric	4-methyl	Hexanoic	Heptanoic
0-HC	K (Observed value)	0.157	0.004	0.352	0.526	0.000	11.309	2.968	3.915	11.373
	K (Critical value)	3.841	3.841	3.841	3.841	3.841	3.841	3.841	3.841	3.841
	DF	1	1	1	1	1	1	1	1	1
	p-value (one-tailed)	0.6924	0.9474	0.5529	0.4683	1.0000	0.0008	0.0849	0.0478	0.0007
3-HC	K (Observed value)	0.096	0.096	0.246	0.035	1.112	8.862	1.428	5.268	11.966
	K (Critical value)	3.841	3.841	3.841	3.841	3.841	3.841	3.841	3.841	3.841
	DF	1	1	1	1	1	1	1	1	1
	p-value (one-tailed)	0.7565	0.7565	0.6198	0.8524	0.2917	0.0029	0.2321	0.0217	0.0005
6-HC	K (Observed value)	0.600	0.000	1.116	2.623	0.243	15.000	2.964	3.101	12.062
	K (Critical value)	3.841	3.841	3.841	3.841	3.841	3.841	3.841	3.841	3.841
	DF	1	1	1	1	1	1	1	1	1
	p-value (one-tailed)	0.4386	1.0000	0.2908	0.1053	0.6221	0.0001	0.0851	0.0782	0.0005
Ext-HC	K (Observed value)	0.735	0.735	2.535	1.815	0.015	9.375	0.462	1.815	4.343
	K (Critical value)	3.841	3.841	3.841	3.841	3.841	3.841	3.841	3.841	3.841
	DF	1	1	1	1	1	1	1	1	1
	p-value (one-tailed)	0.3913	0.3913	0.1113	0.1779	0.9025	0.0022	0.4967	0.1779	0.0372

Table S6.15 ANOSIM summary statistics of fatty acid relative abundances across ETI treatment time-points and compared with healthy control participants.

	Across ETI Therapy			Between ETI and Healthy Controls	
0-3	R	-0.0061	0-HC	R	0.0794
	p (same)	0.4428		p (same)	0.105
	Bonferroni-corrected p value	0.4516		Bonferroni-corrected p value	0.1067
	Permutations	9999		Permutations	9999
3-6	R	-0.0188	3-HC	R	-0.0013
	p (same)	0.5393		p (same)	0.4222
	Bonferroni-corrected p value	0.5417		Bonferroni-corrected p value	0.4367
	Permutations	9999		Permutations	9999
6-Ext	R	-0.0624	6-HC	R	0.1502
	p (same)	0.6692		p (same)	0.0393
	Bonferroni-corrected p value	0.6744		Bonferroni-corrected p value	0.0407
	Permutations	9999		Permutations	9999
0-6	R	-0.0475	Ext-HC	R	0.2480
	p (same)	0.8064		p (same)	0.0467
	Bonferroni-corrected p value	0.8122		Bonferroni-corrected p value	0.047
	Permutations	9999		Permutations	9999
0-Ext	R	-0.1939			
	p (same)	0.9724			
	Bonferroni-corrected p value	0.9757			
	Permutations	9999			

Table S6.16 Similarity of percentage (SIMPER) analysis of fatty acid compositional dissimilarity between healthy controls and pwCF following 6 months and extended ETI therapy.

Fatty acid	% Relative abundance		Av. Dissimilarity	% Contribution	Cumulative (%)
	ETI 6 Months	Healthy Controls			
Butyric	27.3	21.4	4.767	28.24	28.24
Acetic	49.7	50.6	3.931	23.28	51.52
Propionic	17.5	17.5	3.236	19.17	70.69
Valeric	0.276	3.15	1.438	8.517	79.2
Hexanoic	0.678	2.19	1.177	6.974	86.18
Isobutyric	2.2	2.54	1.112	6.586	92.76
Isovaleric	2.4	2.21	1.048	6.209	98.97
Heptanoic	0.0045	0.305	0.1502	0.8899	99.86
4-methyl	0.0209	0.049	0.02314	0.137	100
Total dissimilarity			**16.88**		

Fatty acid	% Relative abundance		Av. Dissimilarity	% Contribution	Cumulative (%)
	ETI Ext	Healthy Controls			
Acetic	46.9	50.6	4.823	28.73	28.73
Butyric	27.5	21.4	4.329	25.79	54.52
Propionic	21	17.5	3.427	20.41	74.93
Valeric	0.458	3.15	1.347	8.023	82.95
Hexanoic	0.416	2.19	1.065	6.341	89.29
Isobutyric	1.45	2.54	0.8098	4.824	94.12
Isovaleric	2.17	2.21	0.8068	4.806	98.92
Heptanoic	0.01	0.305	0.1491	0.8881	99.81
4-methyl	0.05	0.049	0.0321	0.1912	100
Total dissimilarity			**16.79**		

Table S6.17 RDA to explain percent variation in microbiota from faecal relative SCFA abundance.

SCFA	Var. Exp (%)	pseudo-*F*	*P* (adj)
Valeric	4	2	0.002
Propionic	4	2	0.002
Butyric	2.7	1.4	0.018
Total	**10.7**		

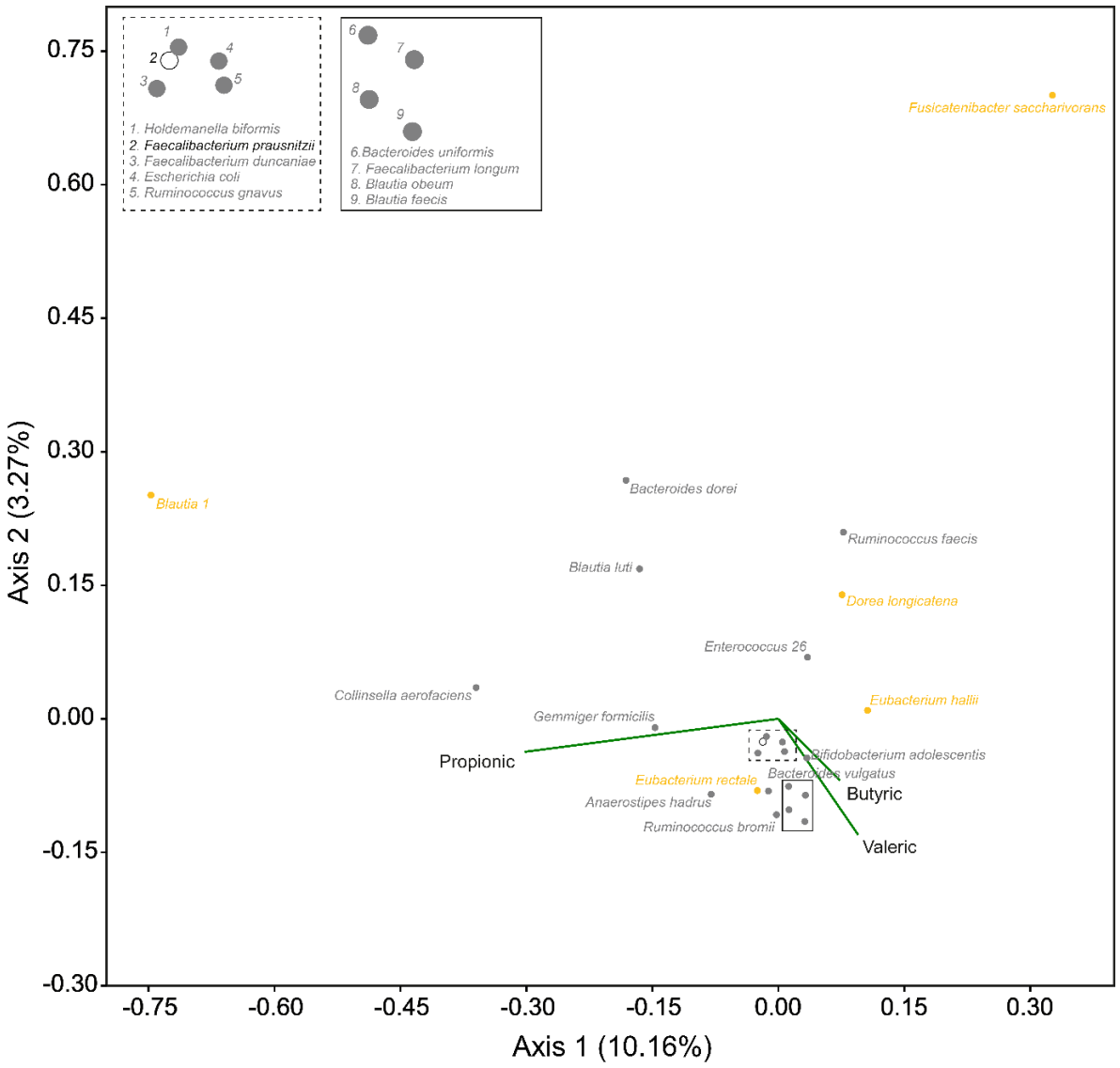

Figure S6.4 Faecal SCFA redundancy analysis species biplots for the whole microbiota. The 24 taxa contributing most to the dissimilarity (cumulatively > 50%) between healthy control and pwCF samples following extended ETI therapy from the SIMPER analysis (Table 6.2) are shown independently of the total number of ASVs identified (531). Orange points represent taxa that were identified as core for the pwCF group following extended ETI therapy, grey points are satellite, and the white (black stroke) points represent taxa that were absent. Biplot lines depict SCFA that significantly explained total variation in taxa relative abundance within whole microbiota analysis at the $p \leq 0.05$ level (Table S6.17). Species plots depict the strength of explanation provided by the given clinical variables, with taxa shown in the same direction of a SCFA considered to have a higher value than those that are not. The percentage of microbiota variation explained by each axis is given in parentheses.

Table S6.18 Summary statistics for paired t-test PAC-SYM results between baseline and ETI treatment

3	Difference	-0.339
	t (Observed value)	-0.398
	|t| (Critical value)	2.160
	DF	13
	p-value (Two-tailed)	0.697
6	Difference	-1.750
	t (Observed value)	-1.923
	|t| (Critical value)	2.179
	DF	12
	p-value (Two-tailed)	0.079
Ext	Difference	-1.429
	t (Observed value)	-1.000
	|t| (Critical value)	2.447
	DF	6
	p-value (Two-tailed)	0.356

Table S6.19 Kruskal-Wallis summary statistics for gut function MRI metrics between baseline and extended ETI samples.

OCTT	K (Observed value)	0.040
	K (Critical value)	3.841
	DF	1
	p-value (one-tailed)	0.842
SBWC	K (Observed value)	3.438
	K (Critical value)	3.841
	DF	1
	p-value (one-tailed)	0.064

Chapter 7: General Discussion

7.1 Introduction

Following the original observations by Dutyschaever and colleagues (Duytschaever et al., 2011), the presence of intestinal dysbiosis in pwCF is now well defined, with dysbiosis evident from birth and maintaining across later life (Hoffman et al., 2014; Burke et al., 2017). The presence of intestinal dysbiosis in CF overlaps with various manifestations of the GI tract and a high burden of intestinal symptoms, which remains a top research priority for the CF community to understand and alleviate (Rowbotham et al., 2023). Understanding the disruption to the complex microbial communities inhabiting the intestinal tract has no doubt been facilitated by the expansion of 16S rRNA gene sequencing processes, with many studies taking advantage of the Illumina MiSeq platform for short read amplicon sequencing across this region (Flass et al., 2015; Antosca et al., 2019; Coffey et al., 2019; Enaud et al., 2019; Loman et al., 2020), for subsequent comparison against various reference databases (Quast et al., 2013; Cole et al., 2014) to assign taxonomy from a given sample. Research strategies have further evolved, to include the use of metagenomics and integration of clinical data to identify potential relationships between microbial community functions and host clinical outcomes (Manor et al., 2016; Vernocchi et al., 2017; Coffey et al., 2019). However, the variability in factors associated with CF disease among diverse patient demographics has added complexity to comprehending the origins of prolonged dysbiosis in CF and its associations with other abnormalities within the intestinal tract.

7.2 Relationships between dysbiosis and clinical factors in pwCF

Throughout this thesis and similar to the results reported by others, the reduced microbial diversity and altered community composition across pwCF is evident (Burke et al., 2017; Coffey et al., 2019; Enaud et al., 2019; Marsh et al., 2022). The presence of CF disease, which primarily explained the core taxa composition was secondary to the administration of antibiotic therapy in pwCF in explaining the overall microbial composition, which was driven by its large impact upon the satellite taxa (Chapters 3 and 6). Antibiotic administration is generally understood to influence microbial composition in CF, with studies demonstrating a high burden of antibiotic therapy upon microbiota diversity and subsequent unfavourable taxonomic changes (Kristensen et al., 2020), whilst others show that only more intense administration (IV antibiotics) can elicit such changes (Burke et al., 2017). The spectrum of antibiotic involvement also widens to demonstrate limited effects of antibiotics as compared to other patient demographic and clinical factors (Vernocchi et al., 2018; Loman et al., 2020; Knoll et al., 2023). The differences across antibiotic frequency, class, and method of administration in these studies of pwCF across childhood and adulthood underscores the need for additional research to gain a clearer understanding of their specific impacts throughout life in CF.

Similar to antibiotic therapy, associations between microbiota dysbiosis and the presence of intestinal inflammation are generally recognised and supported. Similarly to antibiotic usage, this thesis identified an association between intestinal inflammation and the satellite taxa composition across pwCF, albeit to a reduced magnitude (Chapter 3). Of note, satellite taxa included *E. coli*, *B. fragilis*, and in later Chapters *Enterococcus* spp, and *R. gnavus*, of which have been associated with intestinal inflammation in other

studies of the CF intestinal microbiota (Lynch et al., 2013; Hoffman et al., 2014; Enaud et al., 2019). Until proposed functional redundancy is clarified in the CF intestine (Wang et al., 2019), considering microbial involvement within intestinal inflammation should also be extended to the reduction of key short-chain fatty acid producers also. Again, this has been demonstrated throughout the thesis, with a reduction in key drivers of butyrate production including (but not limited to) *F. prausnitzii* and *Eubacterium spp*, as commonly observed across pwCF (Burke et al., 2017; De Freitas et al., 2018; Vernocchi et al., 2018).

This thesis was unable to investigate the impact of pancreatic insufficiency upon the microbiota, as this was a co-correlate in the multivariate models used as all pwCF were PI. There is some evidence for the involvement of pancreatic status (Nielsen et al., 2016), but the bulk of evidence supports little involvement in impacting intestinal microbial composition in CF (Burke et al., 2017; Miragoli et al., 2017; Vernocchi et al., 2018). Given that the vast majority of pwCF are pancreatic insufficient, PERT dosage may constitute a useful variable moving forward in microbiota studies (Freswick et al., 2022). Similarly, dietary habits were not thoroughly investigated throughout this thesis. Dietary intake was not significantly different between pwCF and controls in this thesis and did not contribute to any microbiota differences (Chapter 3), but the collection of metadata was not sustained into later Chapters concerning the use of CFTR modulators. Recent work by Knoll et al. demonstrated relationships between dietary fibre and increased *Solobacterium* abundance (Knoll et al., 2023), but extensive knowledge of diet and intestinal microbiota relationships in pwCF remains severely limited at this stage.

Finally, this work has briefly touched on the gut-lung axis in CF, through the identification of disease mildness (determined by lung function) as a minor explanator of microbial composition in pwCF undertaking ETI therapy. Indeed relationships between lung function and microbial composition and structure have been reported (Burke et al., 2017; Coffey et al., 2019), yet knowledge of these relationships in the era of CFTR modulator treatment remains limited.

7.3 Characterising the function of the CF intestinal microbiota through SCFA analysis

With the targeted metabolomics of faecal SCFAs developed in Chapter 4 and utilised in Chapters 5 and 6, this thesis has demonstrated that differences persist upon composition and quantification of these metabolites occurs between the pwCF and healthy controls. Across the wider literature, there are discrepancies surrounding the differences in the most abundant SCFAs, namely acetic, propionic and butyric acid. Vernocchi et al. reported elevation across all three SCFAs in healthy controls as compared to pwCF (Vernocchi et al., 2018), with Coffey et al. also demonstrating a reduction in butyrate, albeit with a small cohort of 4 healthy controls for comparison (Coffey et al., 2019). On the other hand, it has recently been shown in colonic aspirates between pwCF and controls that no significant differences exist (Baldwin-Hunter et al., 2023), with significant differences rather between the longer fatty acids, including increased valeric and hexanoic acids in controls as also reported in this thesis (Chapter 6). The decreased abundance of valerate (valeric acid) may reflect a reduction in protein fermentation for which this metabolite can be synthesised (Jha and Berrocoso, 2016). This may be plausible given presence of pancreatic insufficiency across all

pwCF enrolled in studies across this thesis. In the GC-MS method developed in Chapter 4, lactic acid was prospectively identified at 8.35 mins RT. Further work to clarify this would be useful, as to investigate relationships between faecal lactic acid abundance and the relative abundance of specific taxa, demonstrated previously by Wang et al. in terms of *Enterococcal* overgrowth (Wang et al., 2019).

Irrespective of the outcomes of the aforementioned studies, which vary across methodologies used to profile and quantify SCFAs (NMR, GC-MS, LC-MS), the ubiquitous limitations of faecal SCFA profiling should be acknowledged, due to the dynamics between and production, absorption, and secretion of SCFAs across the intestinal tract (Sakata, 2019). Nonetheless, faecal quantification may still offer useful insights when paired with dietary data when investigating relationships with microbiota composition and function (Ríos-Covián et al., 2016). Simultaneous analysis of both circulating and faecal SCFAs is likely a more optimal approach to uncover relationships between microbial composition and host outcomes with SCFA levels.

7.4 Impact of CFTR modulators upon intestinal microbiota structure and function

The information surrounding more recent CFTR modulator therapies and effects upon the microbiota and patient intestinal outcomes remain scarce. This thesis reports, for the first time, the effects of Tezacaftor/Ivacaftor upon gut microbiota composition, patient symptoms, and intestinal outcomes in pwCF. Understanding why Tezacaftor/Ivacaftor fails to elicit any significant changes to microbiota structure may relate to the overall efficacy of treatment. Studies in which some meaningful changes were reported to microbiota structure and intestinal outcomes are those utilising

Ivacaftor to treat pwCF harbouring residual function, class III mutations (Ooi et al., 2018; Kristensen et al., 2021). As compared to Tezacaftor/Ivacaftor in the class II F508del population, Ivacaftor in pwCF with class III mutations demonstrates pronounced improvements to the respiratory domain, sweat chloride levels, and patient reported outcomes via the CFQ-R questionnaire (Rowe et al., 2017; Taylor-Cousar et al., 2017; Gramegna et al., 2020). Given all pwCF in this thesis taking Tezacaftor/Ivacaftor were F508del homozygotes, this may be a plausible reason as to why no changes were exerted, in tandem with the recent evidence of high microbiota resilience in pwCF (Knoll et al., 2023). Translation of ETI efficacy from the respiratory domain to include the site of the intestinal tract has been previously demonstrated (Graeber et al., 2022), and it's standardisation would be beneficial moving forward in other studies of CFTR modulators to establish links between localised efficacy and intestinal outcomes in CF. It must also be acknowledged that current literature surrounding CFTR modulator usage encompasses high study heterogeneity, including differences across genotypes, pancreatic status, age, lung function, and antibiotic usage in participants (Ooi et al., 2018; Kristensen et al., 2021; Pope et al., 2021; Ronan et al., 2022).

With regards to triple combination CFTR modulator therapy, recent interim results from a large prospective observational study indicate that restoration of CFTR in participants fails to elicit significant changes to the microbiota (Duong et al., 2023) as demonstrated in Chapter 6 of this thesis, whereby treatment length accounted for ~3% of the satellite taxa variation only across pwCF undertaking ETI therapy. Duong et al. also report that ETI therapy significantly reduced abnormal faecal calprotectin levels observed across pwCF, thereby introducing complexity into the comprehension of microbial involvement in CF intestinal inflammation. The limited cohort information currently available makes

wider interpretations difficult at this stage. Furthermore, whether individual bacterial species change or wider taxonomic trends surface upon treatment, as seen within other CFTR modulator studies (Ooi et al., 2018; Pope et al., 2021; Ronan et al., 2022), remains to be elucidated in larger ETI studies. Multiple studies are set to explore or report the relationships between ETI therapy and patient outcomes further, including but not limited to Igloo-CF, KAF-BIOTA (NCT05937815), PROMISE (NCT04613128, NCT04038047), and GRAMPUS-CF (NCT05934656). With the increased sampling numbers across these cohorts, better understanding of sampling duration impact and predefined host-physiology and abnormalities in the face of modulator treatment, will ensue. The GRAMPUS-CF SRC in particular will look to thoroughly elucidate any relationships between patient symptoms, intestinal abnormalities, and the gut microbiota, which unfortunately fell beyond the scope of what this thesis could uncover.

7.5 Study limitations and caveats

7.5.1 Study group characteristics and population

An obvious caveat to the various studies within this thesis is the small sample sizes across both healthy controls and pwCF, in both cross-sectional and longitudinal aspects. This is perhaps to be expected with the nature of such pilot studies, yet healthy control groups were age and gender-matched, and the CF participants harboured the highly prevalent F508del mutation as to reflect its prevalence across the majority of the wider CF population. Participants also aged from adolescence to adulthood (12-36 years), with age identified as a contributing factor to microbiota composition across Chapter 6. Larger cohorts moving forward will undoubtedly enable clearer elucidation of microbial dynamics across children, adolescents, and adults with CF in the wake of CFTR modulator therapy. As for associated clinical data, the acquirement of extensive dietary information was not attainable throughout this thesis, with patient symptom data (CFAbd scores) also not able to be processed in time for inclusion in the analysis presented in Chapter 6. The consistent inclusion of the CFAbd-Score for the assessment of intestinal symptoms moving forward in studies of pwCF offers a standardised, CF-specific measurement tool that may uncover patient symptoms previously missed with other reporting methods (Jaudszus et al., 2019, 2022).

7.5.2 16S rRNA gene analyses pipeline

Whilst amplicon sequencing of the 16S rRNA gene has no doubt revolutionised the ease to which microbial communities can be characterised to a respectable resolution, there are indeed some pitfalls and limitations of this workflow. This is evident throughout the process, with the original choice of DNA extraction method shown to introduce bias early within this process (Brooks et al., 2015), which can be further influenced by number of PCR cycles and the choice of DNA polymerase used for reactions (Sze and Schloss, 2019). Furthermore, the primer target itself, the specific region of the 16S rRNA gene, can have profound effects upon outcome of microbial community analysis including the ability of characterise bacterial taxa down to the species level (López-Aladid et al., 2023). The V4-V5 locus chosen for the studies within this thesis has been successfully used across various mock communities (Fouhy et al., 2016), including across other studies investigating the faecal microbiota in CF (Antosca et al., 2019; Loman et al., 2020). Nonetheless, some biases may still have arisen, such as the underrepresentation of *Bifidobacteria* which has been observed previously across faecal samples (Alcon-Giner et al., 2017). Towards the back end of the workflow, the choice of reference database within analysis pipelines for taxanomic alignment can also yield differences in outcomes (Abellan-Schneyder et al., 2021).

7.6 Future work

7.6.1 Further study of CFTR modulators and CF associated factors impacting dysbiosis.

It is readily apparent that further research is required across pwCF administered CFTR modulator treatment, particularly to understand the impact of the more efficacious treatments such as ETI therapy upon the intestinal microbiota and general physiology and health. If subsequent research confirms the limited impact as detailed with Chapters 5 and 6 of this thesis within adolescents and adults with CF, there will undoubtedly be increased attention to the administration of CFTR modulators in the younger CF population, given the predominantly favourable safety profile and high efficacy of ETI in younger pwCF (Kapouni et al., 2023), and recent licensing across ages 6-11 years in the united kingdom. The next step for recent modulator therapies will entail administration across infants, similar to the route of Ivacaftor (Rosenfeld et al., 2018). The reduced resilience and stability of the microbiota across this age (Lozupone et al., 2012) offers perhaps the most promising age for intervention. Should therapy fail to elicit changes to microbiota and host outcomes at this time in development, it will further highlight the need to understand the role of other CF-associated lifestyle factors and host physiology. This is already particularly relevant individuals who cannot currently access CFTR modulator therapy due to their CFTR genotype, who wait upon the development of alternate therapies to increase functional CFTR production (Allen et al., 2023).

As for host physiology and microbiota relationships, this thesis has introduced such relations in the context of intestinal function and microbiota composition in CF. More specifically, the relationships between oro-caecal transit time, small bowel water

content, and colonic volumes have been demonstrated with microbiota composition and variability across pwCF and healthy controls in Chapter 3. Whilst CFTR modulators had seemingly little impact upon these metrics (Chapters 5 and 6), there is a need to further understand their implications and relationships with the microbiota, of which remains an under-appreciated area of research (Procházková et al., 2023). The progression from pilot to large multi-centre studies would undoubtedly allow for more intricate analysis of such gut function metrics in tandem with the microbiota, not to mention also other pwCF demographics including pancreatic insufficiency, lung function, dietary history, and antibiotic usage. The latter could be expanded, such that the impact of antibiotic class, dosage, and duration upon the gut microbiota could be better understood. This is particularly favourable given the large association of antibiotic usage with microbiota composition as shown in Chapter 3.

7.6.2 Integration of multi-omic approaches with outcomes in pwCF

The bulk of analysis carried out within this thesis was surrounding the utilisation of 16S rRNA gene sequencing on the Illumina MiSeq platform, to characterise the microbial communities across healthy controls and pwCF. Third-generation sequencing platforms, such as the Nanopore approach offered by Oxford Nanopore and Pacbio's Single-Molecule Real-Time Sequencing allow for the integration of long-read DNA sequencing at high-throughput. This will allow for clearer taxonomic resolution and therefore increased accuracy of bacterial identification and subsequent community characterisation as the entirety of the 16S rRNA gene can be sequenced. This further extends to their use in wider functional genomics, from the facilitation of contiguous DNA sequences to infer the functional characteristics of the community, including

metabolic capabilities and virulence factors such as genes encoding antibiotic resistance. This may be of interest given the high burden of antibiotics within CF. Indeed these approaches are also available by Illumina's shotgun sequencing methods, with multiple CF studies previously utilising this approach to understand microbial community composition and functional capabilities (Hoffman et al., 2014; Manor et al., 2016; Hayden et al., 2020).

The continued integration of multi-omic approaches will be crucial in comprehensively understanding the function of the intestinal microbiota in CF. The work in this thesis encompassed the use of GC-MS targeted metabolomics to investigate and characterise SCFA composition and quantification across pwCF and healthy controls. Whilst a sensible target due to their myriad of functional impacts upon host physiology and immune homeostasis (Wong et al., 2006; Puertollano et al., 2014), and uncharacterised in the era of CFTR modulator treatment, further work investigating the metabolome in CF is likely to benefit from untargeted approaches. Indeed, some other -omic approaches have been carried out previously within the CF intestinal environment, including proteomics (Debyser et al., 2016) and integrated metagenomic/metabolomic approaches (Fouhy et al., 2017; Vernocchi et al., 2018). There is, however, a paucity of knowledge remaining in the era of CFTR modulator therapy that further integrates clinical outcomes including patient symptoms in CF, further extending to the identification of any novel biomarkers and therapeutic targets in the CF intestine relating to host outcomes (Qiu et al., 2023). The goal moving forward should be to therefore use these sophisticated approaches to elucidate any potential relationships.

7.6.3 Understanding inter-kingdom relationships: roles of fungi and viruses in the CF intestine

Aside from the presence of bacteria, the colonisation of the intestine with fungi, viruses, and archaea is poorly understood in CF. Despite having a lower diversity than bacteria, fungal members of the microbial community demonstrate higher intra and inter-variability between healthy subjects in a longitudinal fashion (Nash et al., 2017). Often termed the 'mycobiome', the resident fungi of the intestinal have been shown to interact and impact disease outcomes, with bacterial-fungal relationships evident across inflammatory bowel diseases (Sokol et al., 2017; Underhill and Braun, 2022). In CF infants, a recent study awaiting peer-review has highlighted the increased abundance of fungi, particularly *Candida* and *Saccharomyces*, in pwCF accompanying low bacterial diversity observed across participants (Salerno et al., 2023). Further work is required to elucidate any implications of this fungal expansion, and for the clarification of any bacterial-fungal interactions in the CF gut.

Likewise, the viral community, or the 'virome' is poorly understood in CF. Overall, the gut virome is primarily composed of prokaryotic viruses, often referred to as bacteriophages. Such bacteriophages have the ability to modulate the bacterial community, through lysing and killing of particular targets (Brüssow et al., 2004; Rohwer and Thurber, 2009), whilst others may induce beneficial traits to improve bacterial host fitness (Ogilvie and Jones, 2015). Limited work characterising the intestinal virome in CF has been carried out, with some evidence of changes between pwCF and healthy controls documented. This includes a significant different viral composition between groups, with functional changes reported also, including relationships between particular viral abundance and intestinal inflammation (Coffey et

al., 2020). Should similar results be consistently reported moving forward, this may propel targeted phage therapy as a viable intervention within CF intestinal disease if any drawbacks to therapy can be eliminated (Loc-Carrillo and Abedon, 2011).

7.6.4 Alternate therapies and investigative approaches

Aside from trying to modulate the gut microbiota through CFTR therapy, probiotics, and diet for example, a plausible approach moving forward may well be the use of faecal microbiota transplantation (FMT) in pwCF. This describes the transfer of faecal matter (following processing and preparation) from healthy donors directly into upper GI tract, or directly into the large intestine through colonoscopy (Gupta et al., 2016). Classically, FMT has been employed with success to treat *Clostridium difficile* infection, which is often associated with abdominal pain and diarrhoea in the wider population (Tixier et al., 2022). Coincidently, *C. difficile* carriage in the CF population is high, albeit with lower rates of symptomatic infection (Wu et al., 1983; Peach et al., 1986; Bauer et al., 2014), and indeed FMTs have been successfully used to alleviate infection and associated symptoms in pwCF (Dunwoody et al., 2018).

Aside from the use of FMTs to alleviate apparent ‘one microbe, one disease’ paradigms, there is hope for their use to positively modulate complex microbial environments, such as the states of dysbiosis exhibited within CF and other diseases harbouring intestinal abnormalities. Examples include inflammatory bowel disease, whereby more pronounced microbial community changes are generally observed in ‘responders’ to treatment compared to ‘non-responders’ (Imdad et al., 2023). Changes in particular taxa, including reductions in potentially pathogenic *Enterobacteriaceae* are documented in FMT recipients, although community structural changes (diversity and

composition) have been revert over time (Hsu et al., 2023). In CF specifically, the use of ‘healthy donor’ FMT inoculation in germ-free CF mice fails to prevent microbial dysbiosis and significant differences compared to wild-type controls similarly inoculated (Meeker et al., 2020). An approach for FMT to render more success in CF community is therefore probably one that succeeds modulation of the underlying mechanism causative to disease, with a tighter control of confounding factors upon dysbiosis. This may be plausible given the anticipated reduction in antibiotic usage across pwCF during the current era of triple CFTR modulator therapy (Keogh et al., 2022).

In terms of molecular approaches to investigate microbiota organisation in CF intestinal disease, high-throughput sequencing approaches have greatly benefited from the properties of the 16S rRNA gene. Alongside this however, the 16S rRNA gene could also be used in a qPCR setting. Whilst overlooked in this body of work, qPCR of the 16S rRNA gene has successfully been applied in parallel to amplicon sequencing for absolute quantification of bacterial load (Ahmed et al., 2019; Knoll et al., 2023), whereby the latter approach is more suited to changes in structure and relative abundances, due to the normalisation of DNA throughout pre-sequencing PCR purposes, including barcode attachment and library pooling. Furthermore, should specific taxa be defined as markers for intestinal health and function in CF, targeted qPCR will allow for rapid quantification of such bacterial groups. This may serve as a cheaper, faster, intermediate tool in clinical settings, moving away from classical culture-based approaches (Smyth et al., 2014).

In vitro approaches have also developed tremendously over the last decade and will undoubtedly serve as a key tool in further understanding homeostatic and mechanistic issues across human disease across various tissues. Traditionally the Caco-2 cell line

has been utilised with high success to model the intestinal epithelium (Sambuy et al., 2005), however more recently the interest in organoids has exploded. This describes the production of three-dimensional biological structures that resemble normal physiology as seen *in vivo*. A prime example is the development of intestinal epithelial organoid systems, which were originally pioneered in the murine model (Sato et al., 2009). The ability to study is possible host-microbe interactions is possible (Puschhof et al., 2021), with faecal microbiota injections successfully delivered to organoid luminal systems, of which the hypoxic environment can sustain the growth of commensals typically found in distal segments of the intestinal tract where environmental conditions are similar (Williamson et al., 2018). The challenges that remain to be overcome include producing standardised, sophisticated organoid models that encompass dynamic environmental variables and changes in local physiology to recapitulate that which is naturally observed across the intestinal tract (Chapman and Stewart, 2023).

7.7 Conclusion

The advancement of 16S rRNA gene sequencing alongside wider multi-omic approaches has revealed a diverse range of associations between the gut microbiota and gastrointestinal outcomes in CF. This thesis has demonstrated similar relationships, including identifying associations between the gut microbiota and intestinal function CF. Additionally, preliminary insights surrounding the impact of more recent CFTR modulator treatments upon the gut microbiota and associated functions have been highlighted. This entailed the combined use of 16S rRNA gene sequencing and a developed method for the sensitive analysis of faecal short-chain fatty acids. Highlighting the sustained differences between pwCF and healthy controls in this era

of treatment for CF, it warrants the further investigation of microbiota function through more sophisticated metagenomic and untargeted metabolomic techniques, to unravel the complex relationships between the microbiota, manifestations of the intestinal tract, and patient symptoms in CF.

References

Abellan-Schneyder, I., Matchado, M. S., Reitmeier, S., Sommer, A., Sewald, Z., Baumbach, J., List, M. and Neuhaus, K. (2021) 'Primer, Pipelines, Parameters: Issues in 16S rRNA Gene Sequencing.' *mSphere*, 6(1) pp. e01202-20.

Achour, L., Nancey, S., Moussata, D., Graber, I., Messing, B. and Flourié, B. (2007) 'Faecal Bacterial Mass and Energetic Losses in Healthy Humans and Patients with a Short Bowel Syndrome.' *European Journal of Clinical Nutrition*, 61(2) pp. 233–238.

Adriaanse, M. P. M., van der Sande, L. J. T. M., van den Neucker, A. M., Menheere, P. P. C. A., Dompeling, E., Buurman, W. A. and Vreugdenhil, A. C. E. (2015) 'Evidence for a Cystic Fibrosis Enteropathy.' *PLoS One*, 10(10) p. e0138062.

Ahmed, B., Cox, M. J., Cuthbertson, L., James, P., Cookson, W. O. C., Davies, J. C., Moffatt, M. F. and Bush, A. (2019) 'Longitudinal Development of the Airway Microbiota in Infants with Cystic Fibrosis.' *Scientific Reports*, 9(1) p. 5143.

Ahmed, I., Greenwood, R., de Costello, B. L., Ratcliffe, N. M. and Probert, C. S. (2013) 'An Investigation of Fecal Volatile Organic Metabolites in Irritable Bowel Syndrome.' *PLoS One*, 8(3) p. e58204.

Akshintala, V. S., Talukdar, R., Singh, V. K. and Goggins, M. (2019) 'The Gut Microbiome in Pancreatic Disease.' *Clinical Gastroenterology and Hepatology*, 17(2) pp. 290–295.

Al-Momani, H., Perry, A., Stewart, C. J., Jones, R., Krishnan, A., Robertson, A. G., Bourke, S., Doe, S., Cummings, S. P., Anderson, A., Forrest, T., Griffin, S. M., Brodlie, M., Pearson, J. and Ward, C. (2016) 'Microbiological Profiles of Sputum and Gastric Juice Aspirates in Cystic Fibrosis Patients.' *Scientific Reports*, 6 p. 26985.

Alcon-Giner, C., Caim, S., Mitra, S., Ketskemety, J., Wegmann, U., Wain, J., Belteki, G., Clarke, P. and Hall, L. J. (2017) 'Optimisation of 16S rRNA Gut Microbiota Profiling of Extremely Low Birth Weight Infants.' *BMC Genomics*, 18, November, p. 841.

Allen, Lucy, Allen, Lorna, Carr, S. B., Davies, G., Downey, D., Egan, M., Forton, J. T., Gray, R., Haworth, C., Horsley, A., Smyth, A. R., Southern, K. W. and Davies, J. C. (2023) 'Future Therapies for Cystic Fibrosis.' *Nature Communications*, 14(1) p. 693.

Altschul, S. F., Madden, T. L., Schäffer, A. A., Zhang, J., Zhang, Z., Miller, W. and Lipman, D. J. (1997) 'Gapped BLAST and PSI-BLAST: A New Generation of Protein Database Search Programs.' *Nucleic Acids Research*, 25(17) pp. 3389–3402.

Anderson, J. L., Miles, C. and Tierney, A. C. (2017) 'Effect of Probiotics on Respiratory, Gastrointestinal and Nutritional Outcomes in Patients with Cystic Fibrosis: A Systematic Review.' *Journal of Cystic Fibrosis*, 16(2) pp. 186–197.

Anderson, J. L., Tierney, A. C., Miles, C., Kotsimbos, T. and King, S. J. (2022) 'Probiotic Use in Adults with Cystic Fibrosis is Common and Influenced by Gastrointestinal Health Needs: A Cross-Sectional Survey Study.' *Journal of Human Nutrition and Dietetics*, 35(3) pp. 444–454.

Antosca, K. M., Chernikova, D. A., Price, C. E., Ruoff, K. L., Li, K., Guill, M. F., Sontag, N. R., Morrison, H. G., Hao, S., Drumm, M. L., MacKenzie, T. A., Dorman, D.

B., Feenan, L. M., Williams, M. A., Dessaint, J., Yuan, I. H., Aldrich, B. J., Moulton, L. A., Ting, L., Martinez-del Campo, A., Stewart, E. J., Karagas, M. R., O'Toole, G. A. and Madan, J. C. (2019) 'Altered Stool Microbiota of Infants with Cystic Fibrosis Shows a Reduction in Genera Associated with Immune Programming from Birth.' *Journal of Bacteriology*, 201(16) pp. e00274-19.

Arboleya, S., Watkins, C., Stanton, C. and Ross, R. P. (2016) 'Gut Bifidobacteria Populations in Human Health and Aging.' *Frontiers in Microbiology*, 7 p. 1204.

Arpaia, N., Campbell, C., Fan, X., Dikiy, S., Veeken, J. van der, DeRoos, P., Liu, H., Cross, J. R., Pfeffer, K., Coffer, P. J. and Rudensky, A. Y. (2013) 'Metabolites Produced by Commensal Bacteria pr Promote Peripheral Regulatory T Cell Generation.' *Nature*, 504(7480) pp. 451–455.

Arumugam, M., Raes, J., Pelletier, E., Le Paslier, D., Yamada, T., Mende, D. R., Fernandes, G. R., Tap, J., Bruls, T., Batto, J. M., Bertalan, M., Borruel, N., Casellas, F., Fernandez, L., Gautier, L., Hansen, T., Hattori, M., Hayashi, T., Kleerebezem, M., Kurokawa, K., Leclerc, M., Levenez, F., Manichanh, C., Nielsen, H. B., Nielsen, T., Pons, N., Poulain, J., Qin, J., Sicheritz-Ponten, T., Tims, S., Torrents, D., Ugarte, E., Zoetendal, E. G., Wang, J., Guarner, F., Pedersen, O., De Vos, W. M., Brunak, S., Doré, J., Weissenbach, J., Ehrlich, S. D. and Bork, P. (2011) 'Enterotypes of The Human Gut Microbiome.' *Nature*, 473(7346) pp. 174–180.

De Baere, S., Eeckhaut, V., Steppe, M., De Maesschalck, C., De Backer, P., Van Immerseel, F. and Croubels, S. (2013) 'Development of a HPLC-UV Method for the Quantitative Determination of Four Short-Chain Fatty Acids and Lactic Acid Produced by Intestinal Bacteria During in vitro Fermentation.' *Journal of Pharmaceutical and Biomedical Analysis*, 80 pp. 107–115.

Baker, S. S., Borowitz, D., Duffy, L., Fitzpatrick, L., Gyamfi, J. and Baker, R. D. (2005) 'Pancreatic Enzyme Therapy and Clinical Outcomes in Patients with Cystic Fibrosis.' *The Journal of Pediatrics*, 146(2) pp. 189–193.

Baldwin-Hunter, B. L., Rozenberg, F. D., Annavajhala, M. K., Park, H., DiMango, E. A., Keating, C. L., Uhlemann, A.-C. and Abrams, J. A. (2023) 'The Gut Microbiome, Short Chain Fatty Acids, and Related Metabolites in Cystic Fibrosis Patients with and without Colonic Adenomas.' *Journal of Cystic Fibrosis*, 22(4) pp. 738–744.

Bareil, C. and Bergougnoux, A. (2020) 'CFTR gene variants, epidemiology and molecular pathology.' *Archives de Pédiatrie*, 27 Suppl 1 pp. eS8–eS12.

Bauer, M. P., Farid, A., Bakker, M., Hoek, R. A. S., Kuijper, E. J. and van Dissel, J. T. (2014) 'Patients with Cystic Fibrosis have a High Carriage Rate of Non-Toxigenic *Clostridium difficile*.' *Clinical Microbiology and Infection*, 20(7) pp. O446-9.

Baxter, N. T., Schmidt, A. W., Venkataraman, A., Kim, K. S., Waldron, C. and Schmidt, T. M. (2019) 'Dynamics of Human Gut Microbiota and Short-Chain Fatty Acids in Response to Dietary Interventions with Three Fermentable Fibers.' *mBio*, 10(1) pp. e02566-18.

Bazett, M., Honeyman, L., Stefanov, A. N., Pope, C. E., Hoffman, L. R. and Haston, C. K. (2015) 'Cystic Fibrosis Mouse Model-Dependent Intestinal Structure and Gut Microbiome.' *Mammalian Genome*, 26(5–6) pp. 222–234.

Beaufils, F., Mas, E., Mittaine, M., Addra, M., Fayon, M., Delhaes, L., Clouzeau, H., Galode, F. and Lamireau, T. (2020) 'Increased Fecal Calprotectin Is Associated with Worse Gastrointestinal Symptoms and Quality of Life Scores in Children with Cystic Fibrosis.' *Journal of Clinical Medicine*, 9(12) p. 4080.

Beck, J. and Schwanghart, W. (2010) 'Comparing Measures of Species Diversity From Incomplete Inventories: An Update.' *Methods in Ecology and Evolution*, 1(1) pp. 38–44.

Belzer, C. and de Vos, W. M. (2012) 'Microbes Inside--From Diversity to Function: The Case of *Akkermansia*.' *The ISME journal*, 6(8) pp. 1449–1458.

Di Benedetto, L., Raia, V., Pastore, A., Albano, F., Spagnuolo, M. I., De Vizia, B. and Guarino, A. (1998) '*Lactobacillus casei* Strain GG as Adjunctive Treatment to Children with Cystic Fibrosis.' *Journal of Pediatric Gastroenterology and Nutrition*, 26(5) p. 542.

Den Besten, G., Havinga, R., Bleeker, A., Rao, S., Gerding, A., Van Eunen, K., Groen, A. K., Reijngoud, D. J. and Bakker, B. M. (2014) 'The Short-Chain Fatty Acid Uptake Fluxes by Mice on a Guar Gum Supplemented Diet Associate with Amelioration of Major Biomarkers of the Metabolic Syndrome.' *PLoS One*, 9(9) p. e107392.

Bhatt, J. M. (2013) 'Treatment of Pulmonary Exacerbations in Cystic Fibrosis.' *European Respiratory Review*, 22(129) pp. 205–216.

Bianchi, F., Dall'Asta, M., Del Rio, D., Mangia, A., Musci, M. and Scazzina, F. (2011) 'Development of a Headspace Solid-Phase Microextraction Gas Chromatography–Mass Spectrometric Method for the Determination of Short-Chain Fatty Acids from Intestinal Fermentation.' *Food Chemistry*, 129(1) pp. 200–205.

Van Biervliet, S., Hauser, B., Verhulst, S., Stepman, H., Delanghe, J., Warzee, J.-P., Pot, B., Vandewiele, T. and Wilschanski, M. (2018) 'Probiotics in Cystic Fibrosis Patients: A Double Blind Crossover Placebo Controlled Study: Pilot Study from the ESPGHAN Working Group on Pancreas/CF.' *Clinical Nutrition ESPEN*, 27 pp. 59–65.

Bihan, D. G., Rydzak, T., Wyss, M., Pittman, K., McCoy, K. D. and Lewis, I. A. (2022) 'Method for Absolute Quantification of Short Chain Fatty Acids via Reverse Phase Chromatography Mass Spectrometry.' *PLoS One*, 17(4) p. e0267093.

Borowitz, D., Goss, C. H., Stevens, C., Hayes, D., Newman, L., O'Rourke, A., Konstan, M. W., Wagener, J., Moss, R., Hendeles, L., Orenstein, D., Ahrens, R., Oermann, C. M., Aitken, M. L., Mahl, T. C., Young, K. R. J., Dunitz, J. and Murray, F. T. (2006) 'Safety and Preliminary Clinical Activity of a Novel Pancreatic Enzyme Preparation in Pancreatic Insufficient Cystic Fibrosis Patients.' *Pancreas*, 32(3) pp. 258–263.

Boyle, M. P. and De Boeck, K. (2013) 'A New Era in the Treatment of Cystic Fibrosis: Correction of the Underlying CFTR Defect.' *The Lancet Respiratory Medicine*, 1(2) pp. 158–163.

Bozzetti, V. and Senger, S. (2022) 'Organoid Technologies for the Study of Intestinal Microbiota–Host Interactions.' *Trends in Molecular Medicine*, 28(4) pp. 290–303.

ter Braak, C. and Smilauer, P. (2012) *CANOCO Reference Manual and User's Guide: Software for Ordination.* Ithaca: Microcomputer Power.

Bray, J. R. and Curtis, J. T. (1957) 'An Ordination of the Upland Forest Communities of Southern Wisconsin.' *Ecological Monographs*, 27(4) pp. 325–349.

Brooks, J. P., Edwards, D. J., Harwich, M. D., Rivera, M. C., Fettweis, J. M., Serrano, M. G., Reris, R. A., Sheth, N. U., Huang, B., Girerd, P., Strauss, J. F., Jefferson, K. K., Buck, G. A. and Members), V. M. C. (additional (2015) 'The Truth about Metagenomics: Quantifying and Counteracting Bias in 16S rRNA Studies.' *BMC Microbiology*, 15 p. 66.

Brüssow, H., Canchaya, C. and Hardt, W.-D. (2004) 'Phages and the Evolution of Bacterial Pathogens: From Genomic Rearrangements to Lysogenic Conversion.' *Microbiology and Molecular Biology Reviews*, 68(3) pp. 560–602.

Bruzzese, E., Callegari, M. L., Raia, V., Viscovo, S., Scotto, R., Ferrari, S., Morelli, L., Buccigrossi, V., Lo Vecchio, A., Ruberto, E. and Guarino, A. (2014) 'Disrupted Intestinal Microbiota and Intestinal Inflammation in Children with Cystic Fibrosis and its Restoration with Lactobacillus gg: A Randomised Clinical Trial.' *PLoS One*, 9(2) p. e87796.

Bruzzese, E., Raia, V., Gaudiello, G., Polito, G., Buccigrossi, V., Formicola, V. and Guarino, A. (2004) 'Intestinal Inflammation is a Frequent Feature of Cystic Fibrosis and is Reduced by Probiotic Administration.' *Alimentary Pharmacology and Therapeutics*, 20(7) pp. 813–819.

Bruzzese, E., Raia, V., Spagnuolo, M. I., Volpicelli, M., De Marco, G., Maiuri, L. and Guarino, A. (2007) 'Effect of *Lactobacillus* GG Supplementation on Pulmonary Exacerbations in Patients with Cystic Fibrosis: A Pilot Study.' *Clinical Nutrition*, 26(3) pp. 322–328.

Bukin, Y. S., Galachyants, Y. P., Morozov, I. V, Bukin, S. V, Zakharenko, A. S. and Zemskaya, T. I. (2019) 'The Effect of 16S rRNA Region Choice on Bacterial Community Metabarcoding Results.' *Scientific Data*, 6 p. 190007.

Burke, D. G., Fouhy, F., Harrison, M. J., Rea, M. C., Cotter, P. D., Sullivan, O. O., Stanton, C., Hill, C., Shanahan, F., Plant, B. J. and Ross, R. P. (2017) 'The Altered Gut Microbiota in Adults with Cystic Fibrosis.' *BMC Microbiology*, 17(1) p. 58.

Di Cagno, R., De Angelis, M., De Pasquale, I., Ndagijimana, M., Vernocchi, P., Ricciuti, P., Gagliardi, F., Laghi, L., Crecchio, C., Guerzoni, M., Gobbetti, M. and Francavilla, R. (2011) 'Duodenal and Faecal Microbiota of Celiac Children: Molecular, Phenotype and Metabolome Characterization.' *BMC Microbiology*, 11 p. 219.

Caley, L. R., White, H., de Goffau, M. C., Floto, R. A., Parkhill, J., Marsland, B. and Peckham, D. G. (2023) 'Cystic Fibrosis-Related Gut Dysbiosis: A Systematic Review.' *Digestive Diseases and Sciences*, 68(5) pp. 1797–1814.

Callahan, B. J., McMurdie, P. J., Rosen, M. J., Han, A. W., Johnson, A. J. A. and Holmes, S. P. (2016) 'DADA2: High Resolution Sample Inference from Illumina Amplicon Data.' *Nature Methods*, 13(7) pp. 4–5.

del Campo, R., Garriga, M., Agrimbau, J., Lamas, A., Maiz, L., Canton, R. and

Suarez, L. (2009) ‘Improvement of Intestinal Comfort in Cystic Fibrosis Patients After Probiotics Consumption.’ *Journal of Cystic Fibrosis*, 8 pp. S89–S89.

del Campo, R., Garriga, M., Pérez-Aragón, A., Guallarte, P., Lamas, A., Máiz, L., Bayón, C., Roy, G., Cantón, R., Zamora, J., Baquero, F. and Suárez, L. (2014) ‘Improvement of Digestive Health and Reduction in Proteobacterial Populations in the Gut Microbiota of Cystic Fibrosis Patients using a *Lactobacillus reuteri* Probiotic Preparation: A Double Blind Prospective Study.’ *Journal of Cystic Fibrosis*, 13(6) pp. 716–722.

Capurso, L. (2019) ‘Thirty Years of *Lactobacillus rhamnosus* GG: A Review.’ *Journal of Clinical Gastroenterology*, 53 Suppl 1 pp. S1–S41.

Cerf-Bensussan, N. and Gaboriau-Routhiau, V. (2010) ‘The Immune System and the Gut Microbiota: Friends or Foes?’ *Nature Reviews Immunology*, 10(10) pp. 735–744.

Chai, L.-N., Wu, H., Wang, X.-J., He, L.-J. and Guo, C.-F. (2023) ‘The Mechanism of Antimicrobial Activity of Conjugated Bile Acids against Lactic Acid Bacilli.’ *Microorganisms*, 11(7) p. 1823.

Chan, H. C., Ruan, Y. C., He, Q., Chen, M. H., Chen, H., Xu, W. M., Chen, W. Y., Xie, C., Zhang, X. H. and Zhou, Z. (2009) ‘The Cystic Fibrosis Transmembrane Conductance Regulator in Reproductive Health and Disease.’ *Journal of Physiology*, 587(10) pp. 2187–2195.

Chan, J. C. Y., Kioh, D. Y. Q., Yap, G. C., Lee, B. W. and Chan, E. C. Y. (2017) ‘A Novel LCMSMS Method for Quantitative Measurement of Short-Chain Fatty Acids in Human Stool Derivatized with 12C- and 13C-Labelled Aniline.’ *Journal of Pharmaceutical and Biomedical Analysis*, 138 pp. 43–53.

Chang, P. V, Hao, L., Offermanns, S. and Medzhitov, R. (2014) ‘The Microbial Metabolite Butyrate Regulates Intestinal Macrophage Function via Histone Deacetylase Inhibition.’ *Proceedings of the National Academy of Sciences of the United States of America*, 111(6) pp. 2247–2252.

Chapman, J. A. and Stewart, C. J. (2023) ‘Methodological Challenges in Neonatal Microbiome Research.’ *Gut Microbes*, 15(1) p. 2183687.

Claesson, M. J., Jeffery, I. B., Conde, S., Power, S. E., O’Connor, E. M., Cusack, S., Harris, H. M. B., Coakley, M., Lakshminarayanan, B., O’Sullivan, O., Fitzgerald, G. F., Deane, J., O’Connor, M., Harnedy, N., O’Connor, K., O’Mahony, D., van Sinderen, D., Wallace, M., Brennan, L., Stanton, C., Marchesi, J. R., Fitzgerald, A. P., Shanahan, F., Hill, C., Ross, R. P. and O’Toole, P. W. (2012) ‘Gut Microbiota Composition Correlates with Diet and Health in the Elderly.’ *Nature*, 488(7410) pp. 178–184.

Clarke, K. R. (1993) ‘Non-Parametric Multivariate Analyses of Changes in Community Structure.’ *Australian Journal of Ecology*, 18(1) pp. 117–143.

Coelho, G. D. P., Ayres, L. F. A., Barreto, D. S., Henriques, B. D., Prado, M. R. M. C. and Passos, C. M. Dos (2021) ‘Acquisition of Microbiota According to the Type of Birth: An Integrative Review.’ *Revista Latino-Americana de Enfermagem*, 29 p. e3446.

Coffey, M. J., Low, I., Stelzer-Braid, S., Wemheuer, B., Garg, M., Thomas, T., Jaffe,

A., Rawlinson, W. D. and Ooi, C. Y. (2020) 'The Intestinal Virome in Children with Cystic Fibrosis Differs from Healthy Controls.' *PLoS One*, 15(5) p. e0233557.

Coffey, M. J., Nielsen, S., Wemheuer, B., Kaakoush, N. O., Garg, M., Needham, B., Pickford, R., Jaffe, A., Thomas, T. and Ooi, C. Y. (2019) 'Gut Microbiota in Children With Cystic Fibrosis: A Taxonomic and Functional Dysbiosis.' *Scientific Reports*, 9(1) p. 18593.

Cole, J. R., Wang, Q., Fish, J. A., Chai, B., McGarrell, D. M., Sun, Y., Brown, C. T., Porras-Alfaro, A., Kuske, C. R. and Tiedje, J. M. (2014) 'Ribosomal Database Project: Data and Tools for High Throughput rRNA Analysis.' *Nucleic Acids Research*, 42(Database issue) pp. D633–D642.

Collins, S. (2018) 'Nutritional Management of Cystic Fibrosis – An Update for the 21st Century.' *Paediatric Respiratory Reviews*, 26 pp. 4–6.

Colombo, C., Ellemunter, H., Houwen, R., Munck, A., Taylor, C. and Wilschanski, M. (2011) 'Guidelines for the Diagnosis and Management of Distal Intestinal Obstruction Syndrome in Cystic Fibrosis Patients.' *Journal of Cystic Fibrosis*, 10(SUPPL. 2) pp. S24–S28.

Corey, M., McLaughlin, F. J., Williams, M. and Levison, H. (1988) 'A Comparison of Survival, Growth, and Pulmonary Function in Patients with Cystic Fibrosis in Boston and Toronto.' *Journal of Clinical Epidemiology*, 41(6) pp. 583–591.

Cui, X., Wu, X., Li, Q. and Jing, X. (2020) 'Mutations of the Cystic Fibrosis Transmembrane Conductance Regulator Gene in Males with Congenital Bilateral Absence of the Vas Deferens: Reproductive Implications and Genetic Counseling (Review).' *Molecular Medicine Reports*, 22(5) pp. 3587–3596.

Cuthbertson, L., Walker, A. W., Oliver, A. E., Rogers, G. B., Rivett, D. W., Hampton, T. H., Ashare, A., Elborn, J. S., De Soyza, A., Carroll, M. P., Hoffman, L. R., Lanyon, C., Moskowitz, S. M., O'Toole, G. A., Parkhill, J., Planet, P. J., Teneback, C. C., Tunney, M. M., Zuckerman, J. B., Bruce, K. D. and Van Der Gast, C. J. (2020) 'Lung Function and Microbiota Diversity in Cystic Fibrosis.' *Microbiome*, 8(1) p. 45.

Cystic Fibrosis Refresh Top 10 priorities (priority setting in association with the JLA) (2022). [Online] https://www.jla.nihr.ac.uk/priority-setting-partnerships/cystic-fibrosis-refresh/top-10-priorities.htm.

Cystic Fibrosis Trust (2020) *UK Cystic Fibrosis Trust, UK Cystic Fibrosis Registry. 2019 Annual Data Report*. London.

Cystic Fibrosis Trust (2022) *UK Cystic Fibrosis Trust. UK Cystic Fibrosis Registry. 2021 Annual Data Report*. London.

Cystic Fibrosis Trust (2023) *UK Cystic Fibrosis Trust, UK Cystic Fibrosis Registry. 2022 Annual Data Report*. London.

Dalzell, A. M., Freestone, N. S., Billington, D. and Heaf, D. P. (1990) 'Small Intestinal Permeability and Orocaecal Transit Time in Cystic Fibrosis.' *Archives of Disease in Childhood*, 65(6) pp. 585–588.

Davis, N. M., Proctor, D. M., Holmes, S. P., Relman, D. A. and Callahan, B. J. (2018) 'Simple Statistical Identification and Removal of Contaminant Sequences in Marker-

Gene and Metagenomics Data.' *Microbiome*, 6(1) p. 226.

Dawood, S. N., Rabih, A. M., Niaj, A., Raman, A., Uprety, M., Calero, M. J., Villanueva, M. R. B., Joshaghani, N., Villa, N., Badla, O., Goit, R., Saddik, S. E. and Mohammed, L. (2022) 'Newly Discovered Cutting-Edge Triple Combination Cystic Fibrosis Therapy: A Systematic Review.' *Cureus*, 14(9) p. e29359.

Dayama, G., Priya, S., Niccum, D. E., Khoruts, A. and Blekhman, R. (2020) 'Interactions Between the Gut Microbiome and Host Gene Regulation in Cystic Fibrosis.' *Genome Medicine*, 12(1) p. 12.

Debray, D., El Mourabit, H., Merabtene, F., Brot, L., Ulveling, D., Chrétien, Y., Rainteau, D., Moszer, I., Wendum, D., Sokol, H. and Housset, C. (2018) 'Diet-Induced Dysbiosis and Genetic Background Synergize With Cystic Fibrosis Transmembrane Conductance Regulator Deficiency to Promote Cholangiopathy in Mice.' *Hepatology Communications*, 2(12) pp. 1533–1549.

Debyser, G., Mesuere, B., Clement, L., Van de Weygaert, J., Van Hecke, P., Duytschaever, G., Aerts, M., Dawyndt, P., De Boeck, K., Vandamme, P. and Devreese, B. (2016) 'Faecal Proteomics: A Tool to Investigate Dysbiosis and Inflammation in Patients with Cystic Fibrosis.' *Journal of Cystic Fibrosis*, 15(2) pp. 242–250.

Deletang, K. and Taulan-Cadars, M. (2022) 'Splicing Mutations in the CFTR Gene as Therapeutic Targets.' *Gene Therapy*, 29(7–8) pp. 399–406.

Dellschaft, N., Hoad, C., Marciani, L., Gowland, P. and Spiller, R. (2022) 'Small Bowel Water Content Assessed by MRI in Health and Disease: A Collation of Single-Centre Studies.' *Alimentary Pharmacology & Therapeutics*, 55(3) pp. 327–338.

Derrien, M., Alvarez, A.-S. and de Vos, W. M. (2019) 'The Gut Microbiota in the First Decade of Life.' *Trends in Microbiology*, 27(12) pp. 997–1010.

Despotes, K. A. and Donaldson, S. H. (2022) 'Current State of CFTR Modulators for Treatment of Cystic Fibrosis.' *Current Opinion in Pharmacology*, 65 p. 102239.

Dice, L. R. (1945) 'Measures of the Amount of Ecologic Association Between Species.' *Ecology*, 26(3) pp. 297–302.

Donaldson, G. P., Lee, S. M. and Mazmanian, S. K. (2015) 'Gut Biogeography of the Bacterial Microbiota.' *Nature Reviews Microbiology*, 14(1) pp. 20–32.

Donaldson, S. H., Pilewski, J. M., Griese, M., Cooke, J., Viswanathan, L., Tullis, E., Davies, J. C., Lekstrom-Himes, J. A. and Wang, L. T. (2018) 'Tezacaftor/ivacaftor in Subjects with Cystic Fibrosis and F508del/F508del-CFTR or F508del/G551D-CFTR.' *American Journal of Respiratory and Critical Care Medicine*, 197(2) pp. 214–224.

Donohoe, D. R., Garge, N., Zhang, X., Sun, W., O'Connell, T. M., Bunger, M. K. and Bultman, S. J. (2011) 'The Microbiome and Butyrate Regulate Energy Metabolism and Autophagy in the Mammalian Colon.' *Cell Metabolism*, 13(5) pp. 517–526.

Dorsey, J. and Gonska, T. (2017) 'Bacterial Overgrowth, Dysbiosis, Inflammation, and Dysmotility in the Cystic Fibrosis Intestine.' *Journal of Cystic Fibrosis*, 16 pp. S14–S23.

Dunwoody, R., Steel, A., Landy, J. and Simmonds, N. (2018) ‘Clostridium difficile and Cystic Fibrosis: Management Strategies and the Role of Faecal Transplantation.’ *Paediatric Respiratory Reviews*, 26 pp. 16–18.

Duong, J. T., Pope, C. E., Hayden, H. S., Miller, C., Raftery, D., Salipante, S. J., Pittman, J., Ratjen, F., Rosenfeld, M., Rowe, S. M., Solomon, G. M., Nichols, D. and Hoffman, L. R. (2023) ‘EPS5.02 Faecal Microbiota Changes in Patients with Cystic Fibrosis with 6 Months of Elexacaftor/Tezacaftor/Ivacaftor: Preliminary Findings from the PROMISE Study.’ *Journal of Cystic Fibrosis*, 22 p. S49.

Duytschaever, G., Huys, G., Bekaert, M., Boulanger, L., De Boeck, K. and Vandamme, P. (2011) ‘Cross-Sectional and Longitudinal Comparisons of the Predominant Fecal Microbiota Compositions of a Group of Pediatric Patients with Cystic Fibrosis and Their Healthy Siblings.’ *Applied and Environmental Microbiology*, 77(22) pp. 8015–8024.

Duytschaever, G., Huys, G., Bekaert, M., Boulanger, L., Boeck, K. De and Vandamme, P. (2013) ‘Dysbiosis of *Bifidobacteria* and *Clostridium Cluster XIVa* in the Cystic Fibrosis Fecal Microbiota.’ *Journal of Cystic Fibrosis*, 12(3) pp. 206–215.

Ehsan, Z. and Clancy, J. P. (2015) ‘Management of *Pseudomonas aeruginosa* Infection in Cystic Fibrosis Patients using Inhaled Antibiotics with a Focus on Nebulized Liposomal Amikacin.’ *Future Microbiology*, 10(12) pp. 1901–1912.

van Eijk, H. M. H., Bloemen, J. G. and Dejong, C. H. C. (2009) ‘Application of Liquid Chromatography-Mass Spectrometry to Measure Short Chain Fatty Acids in Blood.’ *Journal of Chromatography B: Analytical Technologies in the Biomedical and Life Sciences*, 877(8–9) pp. 719–724.

Elborn, J. S. (2016) ‘Cystic Fibrosis.’ *The Lancet*, 388(10059) pp. 2519–2531.

Ellemunter, H., Engelhardt, A., Schüller, K. and Steinkamp, G. (2017) ‘Fecal Calprotectin in Cystic Fibrosis and Its Relation to Disease Parameters: A Longitudinal Analysis for 12 Years.’ *Journal of Pediatric Gastroenterology and Nutrition*, 65(4) pp. 438–442.

Emwas, A.-H. M. (2015) ‘The Strengths and Weaknesses of NMR Spectroscopy and Mass Spectrometry with Particular Focus on Metabolomics Research.’ *Methods in Molecular Biology*, 1277 pp. 161–193.

Emwas, A.-H., Roy, R., McKay, R. T., Tenori, L., Saccenti, E., Gowda, G. A. N., Raftery, D., Alahmari, F., Jaremko, L., Jaremko, M. and Wishart, D. S. (2019) ‘NMR Spectroscopy for Metabolomics Research.’ *Metabolites*, 9(7) p. 123.

Enaud, R., Hooks, K. B., Barre, A., Barnetche, T., Hubert, C., Massot, M., Bazin, T., Clouzeau, H., Bui, S., Fayon, M., Berger, P., Lehours, P., Bébéar, C., Nikolski, M., Lamireau, T., Delhaes, L. and Schaeverbeke, T. (2019) ‘Intestinal Inflammation in Children with Cystic Fibrosis Is Associated with Crohn’s-Like Microbiota Disturbances.’ *Journal of Clinical Medicine*, 8(5) p. 645.

Esposito, S., Testa, I., Mariotti Zani, E., Cunico, D., Torelli, L., Grandinetti, R., Fainardi, V., Pisi, G. and Principi, N. (2022) ‘Probiotics Administration in Cystic Fibrosis: What Is the Evidence?’ *Nutrients*, 14(15) p. 3160.

Fallahi, G., Motamed, F., Yousefi, A., Shafieyoun, A., Najafi, M., Khodadad, A., Farhmand, F., Ahmadvand, A. and Rezaei, N. (2013) 'The Effect of Probiotics on Fecal Calprotectin in Patients with Cystic Fibrosis.' *The Turkish Journal of Pediatrics*, 55(5) pp. 475–478.

Farjadian, S., Moghtaderi, M., Kashef, S., Alyasin, S., Najib, K. and Saki, F. (2013) 'Clinical and Genetic Features in Patients with Cystic Fibrosis in Southwestern Iran.' *Iranian Journal of Pediatrics*, 23(2) pp. 212–215.

De Filippo, C., Cavalieri, D., Di Paola, M., Ramazzotti, M., Poullet, J. B., Massart, S., Collini, S., Pieraccini, G. and Lionetti, P. (2010) 'Impact of Diet in Shaping Gut Microbiota Revealed by a Comparative Study in Children from Europe and Rural Africa.' *Proceedings of the National Academy of Sciences of the United States of America*, 107(33) pp. 14691–14696.

Fiorotto, R., Scirpo, R., Trauner, M., Fabris, L., Hoque, R., Spirli, C. and Strazzabosco, M. (2011) 'Loss of CFTR Affects Biliary Epithelium Innate Immunity and causes TLR4-NF-κB-Mediated Inflammatory Response in Mice.' *Gastroenterology*, 141(4) pp. 1498–508, 1508.e1–5.

Fisher, R. A., Corbet, A. S. and Williams, C. B. (1943) 'The Relation Between the Number of Species and the Number of Individuals in a Random Sample of an Animal Population.' *The Journal of Animal Ecology*, 12(1) pp. 42–58.

Flass, T., Tong, S., Frank, D. N., Wagner, B. D., Robertson, C. E., Kotter, C. V., Sokol, R. J., Zemanick, E., Accurso, F., Hoffenberg, E. J. and Narkewicz, M. R. (2015) 'Intestinal Lesions are Associated with Altered Intestinal Microbiome and are More Frequent in Children and Young Adults with Cystic Fibrosis and Cirrhosis.' *PLoS One*, 10(2) p. e0116967.

Fouhy, F., Clooney, A. G., Stanton, C., Claesson, M. J. and Cotter, P. D. (2016) '16S rRNA Gene Sequencing of Mock Microbial Populations- Impact of DNA Extraction Method, Primer Choice and Sequencing Platform.' *BMC Microbiology*, 16(1) p. 123.

Fouhy, F., Ronan, N. J., O'Sullivan, O., McCarthy, Y., Walsh, A. M., Murphy, D. M., Daly, M., Flanagan, E. T., Fleming, C., McCarthy, M., Shortt, C., Eustace, J. A., Shanahan, F., Rea, M. C., Ross, R. P., Stanton, C. and Plant, B. J. (2017) 'A Pilot Study Demonstrating the Altered Gut Microbiota Functionality in Stable Adults with Cystic Fibrosis.' *Scientific Reports*, 7(1) p. 6685.

Franco, D. L., Disbrow, M. B., Kahn, A., Koepke, L. M., Harris, L. A., Harrison, M. E., Crowell, M. D. and Ramirez, F. C. (2015) 'Duodenal Aspirates for Small Intestine Bacterial Overgrowth: Yield, PPIs, and Outcomes after Treatment at a Tertiary Academic Medical Center.' *Gastroenterology Research and Practice*, 2015 p. 971582.

Frank, L., Kleinman, L., Farup, C., Taylor, L. and Miner, P. J. (1999) 'Psychometric Validation of a Constipation Symptom Assessment Questionnaire.' *Scandinavian Journal of Gastroenterology*, 34(9) pp. 870–877.

Fraquelli, M., Baccarin, A., Corti, F., Conti, C. B., Russo, M. C., Valle, S. Della, Pozzi, R., Cressoni, M., Conte, D. and Colombo, C. (2016) 'Bowel Ultrasound Imaging in Patients with Cystic Fibrosis: Relationship with Clinical Symptoms and CFTR

Genotype.' *Digestive and Liver Disease*, 48(3) pp. 271–276.

De Freitas, M. B., Moreira, E. A. M., Tomio, C., Moreno, Y. M. F., Daltoe, F. P., Barbosa, E., Neto, N. L., Buccigrossi, V. and Guarino, A. (2018) 'Altered Intestinal Microbiota Composition, Antibiotic Therapy and Intestinal Inflammation in Children and Adolescents with Cystic Fibrosis.' *PLoS One*, 13(6) p. e0198457.

Freswick, P. N., Reid, E. K. and Mascarenhas, M. R. (2022) 'Pancreatic Enzyme Replacement Therapy in Cystic Fibrosis.' *Nutrients*, 14(7) p. 1341.

Frost, F., Weiss, F. U., Sendler, M., Kacprowski, T., Rühlemann, M., Bang, C., Franke, A., Völker, U., Völzke, H., Lamprecht, G., Mayerle, J., Aghdassi, A. A., Homuth, G. and Lerch, M. M. (2020) 'The Gut Microbiome in Patients With Chronic Pancreatitis Is Characterized by Significant Dysbiosis and Overgrowth by Opportunistic Pathogens.' *Clinical and Translational gastroenterology*, 11(9) p. e00232.

Furnari, M., De Alessandri, A., Cresta, F., Haupt, M., Bassi, M., Calvi, A., Haupt, R., Bodini, G., Ahmed, I., Bagnasco, F., Giannini, E. G. and Casciaro, R. (2019) 'The Role of Small Intestinal Bacterial Overgrowth in Cystic Fibrosis: A Randomized Case-Controlled Clinical Trial with Rifaximin.' *Journal of Gastroenterology*, 54(3) pp. 261–270.

Gabel, M. E., Wang, H., Gelfond, D., Roach, C., Rowe, S. M., Clancy, J. P., Sagel, S. D. and Borowitz, D. (2022) 'Changes in Glucose Breath Test in Cystic Fibrosis Patients Treated With 1 Month of Lumacaftor/Ivacaftor.' *Journal of Pediatric Gastroenterology and Nutrition*, 75(1) pp. 42–47.

Gao, X., Pujos-Guillot, E., Martin, J. F., Galan, P., Juste, C., Jia, W. and Sebedio, J. L. (2009) 'Metabolite Analysis of Human Fecal Water by Gas Chromatography/Mass Spectrometry with Ethyl Chloroformate Derivatization.' *Analytical Biochemistry*, 393(2) pp. 163–175.

Gao, Z., Yin, J., Zhang, J., Ward, R. E., Martin, R. J., Lefevre, M., Cefalu, W. T. and Ye, J. (2009) 'Butyrate Improves Insulin Sensitivity and Increases Energy Expenditure in Mice.' *Diabetes*, 58(7) pp. 1509–1517.

García-Villalba, R., Giménez-Bastida, J. A., García-Conesa, M. T., Tomás-Barberán, F. A., Carlos Espín, J. and Larrosa, M. (2012) 'Alternative Method for Gas Chromatography-Mass Spectrometry Analysis of Short-Chain Fatty Acids in Faecal Samples.' *Journal of Separation Science*, 35(15) pp. 1906–1913.

Garg, M., Leach, S. T., Coffey, M. J., Katz, T., Strachan, R., Pang, T., Needham, B., Lui, K., Ali, F., Day, A. S., Appleton, L., Moeeni, V., Jaffe, A. and Ooi, C. Y. (2017) 'Age-Dependent Variation of Fecal Calprotectin in Cystic Fibrosis and Healthy children.' *Journal of Cystic Fibrosis*, 16(5) pp. 631–636.

Garriga, M., Pérez-aragón, A., Guallarte, P., Lamas, A., Baquero, F. and Suárez, L. (2014) 'Improvement of Digestive Health and Reduction in Proteobacterial Populations in the Gut Microbiota of Cystic Fibrosis Patients using a *Lactobacillus reuteri* Probiotic Preparation: A Double Blind Prospective Study.' *Journal of Cystic Fibrosis*, 13(6) pp. 716–722.

van der Gast, C. J., Walker, A. W., Stressmann, F. A., Rogers, G. B., Scott, P.,

Daniels, T. W., Carroll, M. P., Parkhill, J. and Bruce, K. D. (2011) 'Partitioning Core and Satellite Taxa From within Cystic Fibrosis Lung Bacterial Communities.' *The ISME Journal*, 5(5) pp. 780–791.

Gelfond, D., Heltshe, S., Ma, C., Rowe, S. M., Frederick, C., Uluer, A., Sicilian, L., Konstan, M., Tullis, E., Roach, R. N. C., Griffin, K., Joseloff, E. and Borowitz, D. (2017) 'Impact of CFTR Modulation on Intestinal pH, Motility, and Clinical Outcomes in Patients with Cystic Fibrosis and the G551D Mutation.' *Clinical and Translational Gastroenterology*, 8(3) pp. e81-6.

Gentzsch, M. and Mall, M. A. (2018) 'Ion Channel Modulators in Cystic Fibrosis.' *Chest*, 154(2) pp. 383–393.

Ghoshal, U. C. (2011) 'How to Interpret Hydrogen Breath Tests.' *Journal of Neurogastroenterology and Motility*, 17(3) pp. 312–317.

Gillan, J. L., Hardisty, G. R., Davidson, D. J. and Gray, R. D. (2022) 'Macrophages from Gut-Corrected CF Mice express Human CFTR and lack a Pro-Inflammatory Phenotype.' *Journal of Cystic Fibrosis*, 21(2) pp. 370–374.

Van Goor, F., Hadida, S., Grootenhuis, P. D. J., Burton, B., Cao, D., Neuberger, T., Turnbull, A., Singh, A., Joubran, J., Hazlewood, A., Zhou, J., McCartney, J., Arumugam, V., Decker, C., Yang, J., Young, C., Olson, E. R., Wine, J. J., Frizzell, R. A., Ashlock, M. and Negulescu, P. (2009) 'Rescue of CF Airway Epithelial Cell Function in vitro by a CFTR Potentiator, VX-770.' *Proceedings of the National Academy of Sciences of the United States of America*, 106(44) pp. 18825–18830.

Van Goor, F., Hadida, S., Grootenhuis, P. D. J., Burton, B., Stack, J. H., Straley, K. S., Decker, C. J., Miller, M., McCartney, J., Olson, E. R., Wine, J. J., Frizzell, R. A., Ashlock, M. and Negulescu, P. A. (2011) 'Correction of the F508del-CFTR Protein Processing Defect in vitro by the Investigational Drug VX-809.' *Proceedings of the National Academy of Sciences of the United States of America*, 108(46) pp. 18843–18848.

Gorzelak, M. A., Gill, S. K., Tasnim, N., Ahmadi-Vand, Z., Jay, M. and Gibson, D. L. (2015) 'Methods for Improving Human Gut Microbiome Data by Reducing Variability through Sample Processing and Storage of Stool.' *PLoS One*, 10(8) p. e0134802.

Graeber, S. Y., Vitzthum, C., Pallenberg, S. T., Naehrlich, L., Stahl, M., Rohrbach, A., Drescher, M., Minso, R., Ringshausen, F. C., Rueckes-Nilges, C., Klajda, J., Berges, J., Yu, Y., Scheuermann, H., Hirtz, S., Sommerburg, O., Dittrich, A.-M., Tümmler, B. and Mall, M. A. (2022) 'Effects of Elexacaftor/Tezacaftor/Ivacaftor Therapy on CFTR Function in Patients with Cystic Fibrosis and One or Two F508del Alleles.' *American Journal of Respiratory & Critical Care Medicine*, 205(5) pp. 540–549.

Gramegna, A., Contarini, M., Aliberti, S., Casciaro, R., Blasi, F. and Castellani, C. (2020) 'From Ivacaftor to Triple Combination: A Systematic Review of Efficacy and Safety of CFTR Modulators in People with Cystic Fibrosis.' *International Journal of Molecular Sciences*, 21(16) p. 5882.

Granados, A., Chan, C. L., Ode, K. L., Moheet, A., Moran, A. and Holl, R. (2019) 'Cystic Fibrosis Related Diabetes: Pathophysiology, Screening and Diagnosis.' *Journal of Cystic Fibrosis*, 18 pp. S3–S9.

Green, J., Carroll, W. and Gilchrist, F. J. (2018) ‘Interventions for Treating Distal Intestinal Obstruction Syndrome (DIOS) in Cystic Fibrosis.’ *Cochrane Database of Systematic Reviews*, 8(8) p. CD012798.

Gupta, S., Allen-Vercoe, E. and Petrof, E. O. (2016) ‘Fecal Microbiota Transplantation: In Perspective.’ *Therapeutic Advances in Gastroenterology*, 9(2) pp. 229–239.

Hallberg, K., Grzegorczyk, A., Larson, G. and Strandvik, B. (1997) ‘Intestinal Permeability in Cystic Fibrosis in Relation to Genotype.’ *Journal of Pediatric Gastroenterology and Nutrition*, 25(3) pp. 290–295.

Hammer, Ø., A.T. Harper, D. and Ryan, P. D. (2001) ‘PAST: Paleontological Statistics Software Package for Education and Data Analysis.’ *Palaeontologia Electronica*, 4(1) p. 9.

Hankel, J., Mößeler, A., Hartung, C. B., Rath, S., Schulten, L., Visscher, C., Kamphues, J. and Vital, M. (2022) ‘Responses of Ileal and Fecal Microbiota to Withdrawal of Pancreatic Enzyme Replacement Therapy in a Porcine Model of Exocrine Pancreatic Insufficiency.’ *International Journal of Molecular Sciences*, 23(19) p. 11700.

Hanssens, L. S., Duchateau, J. and Casimir, G. J. (2021) ‘CFTR Protein: Not Just a Chloride Channel?’ *Cells*, 10(11) p. 2844.

Hayashi, H., Takahashi, R., Nishi, T., Sakamoto, M. and Benno, Y. (2005) ‘Molecular Analysis of Jejunal, Ileal, Caecal and Rectosigmoidal Human Colonic Microbiota using 16S rRNA Gene Libraries and Terminal Restriction Fragment Length Polymorphism.’ *Journal of Medical Microbiology*, 54(11) pp. 1093–1101.

Hayden, H. S., Eng, A., Pope, C. E., Brittnacher, M. J., Vo, A. T., Weiss, E. J., Hager, K. R., Martin, B. D., Leung, D. H., Heltshe, S. L., Borenstein, E., Miller, S. I. and Hoffman, L. R. (2020) ‘Fecal Dysbiosis in Infants with Cystic Fibrosis is Associated with Early Linear Growth Failure.’ *Nature Medicine*, 26(2) pp. 215–221.

Hayee, B., Watson, K. L., Campbell, S., Simpson, A., Farrell, E., Hutchings, P., Macedo, P., Perrin, F., Whelan, K. and Elston, C. (2019) ‘A High Prevalence of Chronic Gastrointestinal Symptoms in Adults with Cystic Fibrosis is Detected using Tools Already Validated in other GI Disorders.’ *United European Gastroenterology Journal*, 7(7) pp. 881–888.

He, Z., Wang, M., Li, H. and Wen, C. (2019) ‘GC-MS-based Fecal Metabolomics Reveals Gender-Attributed Fecal Signatures in Ankylosing Spondylitis.’ *Scientific Reports*, 9(1) p. 3872.

Hedin, C., Van Der Gast, C. J., Rogers, G. B., Cuthbertson, L., McCartney, S., Stagg, A. J., Lindsay, J. O. and Whelan, K. (2016) ‘Siblings of Patients with Crohn’s Disease Exhibit a Biologically Relevant Dysbiosis in Mucosal Microbial Metacommunities.’ *Gut*, 65(6) pp. 944–953.

Hedsund, C., Gregersen, T., Joensson, I. M., Olesen, H. V. and Krogh, K. (2012) ‘Gastrointestinal Transit Times and Motility in Patients with Cystic Fibrosis.’ *Scandinavian Journal of Gastroenterology*, 47(8–9) pp. 920–926.

Hendriks, H. J., van Kreel, B. and Forget, P. P. (2001) 'Effects of Therapy with Lansoprazole on Intestinal Permeability and Inflammation in Young Cystic Fibrosis Patients.' *Journal of Pediatric Gastroenterology & Nutrition*, 33(3) pp. 260–265.

Henen, S., Denton, C., Teckman, J., Borowitz, D. and Patel, D. (2021) 'Review of Gastrointestinal Motility in Cystic Fibrosis.' *Journal of Cystic Fibrosis*, 20(4) pp. 578–585.

Henke, M. T., Kenny, D. J., Cassilly, C. D., Vlamakis, H., Xavier, R. J. and Clardy, J. (2019) '*Ruminococcus gnavus*, a Member of the Human Gut Microbiome Associated with Crohn's Disease, Produces an Inflammatory Polysaccharide.' *Proceedings of the National Academy of Sciences of the United States of America*, 116(26) pp. 12672–12677.

Hoen, A. G., Lia, J., Moulton, L. A., O'Toole, G. A., Housman, M. L., Koestler, D. C., Guill, M. F., Moore, J. H., Hibberd, P. L., Morrison, H. G., Sogin, M. L., Karagas, M. R. and Madan, J. C. (2015) 'Associations Between Gut Microbial Colonization in Early Life and Respiratory Outcomes in Cystic Fibrosis.' *The Journal of Pediatrics*, 167(1) pp. 138-147.e1–3.

Hoffman, L. R., Pope, C. E., Hayden, H. S., Heltshe, S., Levy, R., McNamara, S., Jacobs, M. A., Rohmer, L., Radey, M., Ramsey, B. W., Brittnacher, M. J., Borenstein, E. and Miller, S. I. (2014) '*Escherichia coli* Dysbiosis Correlates with Gastrointestinal Dysfunction in Children with Cystic Fibrosis.' *Clinical Infectious Diseases*, 58(3) pp. 396–399.

Hooper, L. V., Wong, M. H., Thelin, A., Hansson, L., Falk, P. G. and Gordon, J. I. (2001) 'Molecular Analysis of Commensal Host-Microbial Relationships in the Intestine.' *Science*, 291(5505) pp. 881–884.

Hough, N. E., Chapman, S. J. and Flight, W. G. (2020) 'Gastrointestinal Malignancy in Cystic Fibrosis.' *Paediatric Respiratory Reviews*, 35 pp. 90–92.

Houwen, R. H., Van Der Doef, H. P., Sermet, I., Munck, A., Hauser, B., Walkowiak, J., Robberecht, E., Colombo, C., Sinaasappel, M. and Wilschanski, M. (2010) 'Defining DIOS and Constipation in Cystic Fibrosis with a Multicentre Study on the Incidence, Characteristics, and Treatment of DIOS.' *Journal of Pediatric Gastroenterology and Nutrition*, 50(1) pp. 38–42.

Hoving, L. R., Heijink, M., van Harmelen, V., van Dijk, K. W. and Giera, M. (2018) 'GC-MS Analysis of Short-Chain Fatty Acids in Feces, Cecum Content, and Blood Samples.' *Methods in Molecular Biology*, 1730 pp. 247–256.

Hsu, M., Tun, K. M., Batra, K., Haque, L., Vongsavath, T. and Hong, A. S. (2023) 'Safety and Efficacy of Fecal Microbiota Transplantation in Treatment of Inflammatory Bowel Disease in the Pediatric Population: A Systematic Review and Meta-Analysis.' *Microorganisms*, 11(5) p. 1272.

Huda-Faujan, H., Abdulamir, A., Fatimah, A., Muhammad Anas, O., Shuhaimi, M., Yazid, A. and Loong, Y. (2010) 'The Impact of the Level of the Intestinal Short Chain Fatty Acids in Inflammatory Bowel Disease Patients Versus Healthy Subjects.' *The Open Biochemistry Journal*, 4 pp. 53–58.

Huse, S. M., Young, V. B., Morrison, H. G., Antonopoulos, D. A., Kwon, J., Dalal, S.,

Arrieta, R., Hubert, N. A., Shen, L., Vineis, J. H., Koval, J. C., Sogin, M. L., Chang, E. B. and Raffals, L. E. (2014) 'Comparison of Brush and Biopsy Sampling Methods of the Ileal Pouch for Assessment of Mucosa-Associated Microbiota of Human Subjects.' *Microbiome*, 2(1) p. 5.

Husebye, E., Hellström, P. M. and Midtvedt, T. (1994) 'Intestinal Microflora Stimulates Myoelectric Activity of Rat Small Intestine by Promoting Cyclic Initiation and Aboral Propagation of Migrating Myoelectric Complex.' *Digestive Diseases and Sciences*, 39(5) pp. 946–956.

Husebye, E., Hellström, P. M., Sundler, F., Chen, J. and Midtvedt, T. (2001) 'Influence of Microbial Species on Small Intestinal Myoelectric Activity and Transit in Germ-Free Rats.' *American Journal of Physiology - Gastrointestinal and Liver Physiology*, 280 pp. G368–G380.

Iizumi, T., Battaglia, T., Ruiz, V. and Perez Perez, G. I. (2017) 'Gut Microbiome and Antibiotics.' *Archives of Medical Research*, 48(8) pp. 727–734.

Imdad, A., Pandit, N. G., Zaman, M., Minkoff, N. Z., Tanner-Smith, E. E., Gomez-Duarte, O. G., Acra, S. and Nicholson, M. R. (2023) 'Fecal Transplantation for Treatment of Inflammatory Bowel Disease.' *The Cochrane Database of Systematic Reviews*, 4(4) p. CD012774.

Jafari, S.-A., Mehdizadeh-Hakkak, A., Kianifar, H.-R., Hebrani, P., Ahanchian, H. and Abbasnejad, E. (2013) 'Effects of Probiotics on Quality of Life in Children with Cystic Fibrosis; A Randomized Controlled Trial.' *Iranian Journal of Pediatrics*, 23(6) pp. 669–674.

Jaudszus, A., Pfeifer, E., Lorenz, M., Beiersdorf, N., Hipler, U. C., Zagoya, C. and Mainz, J. G. (2022) 'Abdominal Symptoms Assessed With the CFAbd-Score are Associated With Intestinal Inflammation in Patients With Cystic Fibrosis.' *Journal of Pediatric Gastroenterology and Nutrition*, 74(3) pp. 355–360.

Jaudszus, A., Zeman, E., Jans, T., Pfeifer, E., Tabori, H., Arnold, C., Michl, R. K., Lorenz, M., Beiersdorf, N. and Mainz, J. G. (2019) 'Validity and Reliability of a Novel Multimodal Questionnaire for the Assessment of Abdominal Symptoms in People with Cystic Fibrosis (CFAbd-Score).' *Patient*, 12(4) pp. 419–428.

Jeffery, I. B., Lynch, D. B. and O'Toole, P. W. (2016) 'Composition and Temporal Stability of the Gut Microbiota in Older Persons.' *The ISME Journal*, 10(1) pp. 170–182.

Jensen, E. A., Berryman, D. E., Murphy, E. R., Carroll, R. K., Busken, J., List, E. O. and Broach, W. H. (2019) 'Heterogeneity Spacers in 16S rDNA Primers Improve Analysis of Mouse Gut Microbiomes via Greater Nucleotide Diversity.' *BioTechniques*, 67(2) pp. 55–62.

Jha, R. and Berrocoso, J. F. D. (2016) 'Dietary Fiber and Protein Fermentation in the Intestine of Swine and their Interactive Effects on Gut Health and on the Environment: A review.' *Animal Feed Science and Technology*, 212 pp. 18–26.

Jiménez, E., Marín, M. L., Martín, R., Odriozola, J. M., Olivares, M., Xaus, J., Fernández, L. and Rodríguez, J. M. (2008) 'Is Meconium from Healthy Newborns Actually Sterile?' *Research in Microbiology*, 159(3) pp. 187–193.

Joossens, M., Huys, G., Cnockaert, M., De Preter, V., Verbeke, K., Rutgeerts, P., Vandamme, P. and Vermeire, S. (2011) 'Dysbiosis of the Faecal Microbiota in Patients with Crohn's Disease and their Unaffected Relatives.' *Gut*, 60(5) pp. 631–637.

Judkins, T. C., Archer, D. L., Kramer, D. C. and Solch, R. J. (2020) 'Probiotics, Nutrition, and the Small Intestine.' *Current Gastroenterology Reports*. Current Gastroenterology Reports, 22(1) p. 2.

Kaoutari, A. El, Armougom, F., Gordon, J. I., Raoult, D. and Henrissat, B. (2013) 'The Abundance and Variety of Carbohydrate-active Enzymes in the Human Gut Microbiota.' *Nature Reviews Microbiology*, 11(7) pp. 497–504.

Kapouni, N., Moustaki, M., Douros, K. and Loukou, I. (2023) 'Efficacy and Safety of Elexacaftor-Tezacaftor-Ivacaftor in the Treatment of Cystic Fibrosis: A Systematic Review.' *Children (Basel)*, 10(3) p. 554.

Kastl, A. J., Terry, N. A., Wu, G. D. and Albenberg, L. G. (2020) 'The Structure and Function of the Human Small Intestinal Microbiota: Current Understanding and Future Directions.' *Cellular and Molecular Gastroenterology and Hepatology*, 9(1) pp. 33–45.

Kelly, T. and Buxbaum, J. (2015) 'Gastrointestinal Manifestations of Cystic Fibrosis.' *Digestive Diseases and Sciences*, 60(7) pp. 1903–1913.

Keogh, R. H., Cosgriff, R., Andrinopoulou, E. R., Brownlee, K. G., Carr, S. B., Diaz-Ordaz, K., Granger, E., Jewell, N. P., Lewin, A., Leyrat, C., Schlüter, D. K., van Smeden, M., Szczesniak, R. D. and Connett, G. J. (2022) 'Projecting the Impact of Triple CFTR Modulator Therapy on Intravenous Antibiotic Requirements in Cystic Fibrosis using Patient Registry Data Combined with Treatment Effects from Randomised Trials.' *Thorax*, 77(9) pp. 873–881.

Khan, I., Bai, Y., Zha, L., Ullah, N., Ullah, H., Shah, S. R. H., Sun, H. and Zhang, C. (2021) 'Mechanism of the Gut Microbiota Colonization Resistance and Enteric Pathogen Infection.' *Frontiers in Cellular and Infection Microbiology*, 11 p. 716299.

Kim, K.-S., Lee, Y., Chae, W. and Cho, J.-Y. (2022) 'An Improved Method to Quantify Short-Chain Fatty Acids in Biological Samples Using Gas Chromatography-Mass Spectrometry.' *Metabolites*, 12(6) p. 525.

Kircher, M., Stenzel, U. and Kelso, J. (2009) 'Improved Base Calling for the Illumina Genome Analyzer using Machine Learning Strategies.' *Genome Biology*, 10(8) p. R83.

Knoll, R. L., Jarquín-Díaz, V. H., Klopp, J., Kemper, A., Hilbert, K., Hillen, B., Pfirrmann, D., Simon, P., Bähner, V., Nitsche, O., Gehring, S., Markó, L., Forslund, S. K. and Poplawska, K. (2023) 'Resilience and Stability of the CF- Intestinal and Respiratory Microbiome during Nutritional and Exercise Intervention.' *BMC Microbiology*, 23(1) p. 44.

Koenig, J. E., Spor, A., Scalfone, N., Fricker, A. D., Stombaugh, J., Knight, R., Angenent, L. T. and Ley, R. E. (2011) 'Succession of Microbial Consortia in the Developing Infant Gut Microbiome.' *Proceedings of the National Academy of Sciences of the United States of America*, 108(Supplement 1) pp. 4578–4585.

König, J., Schreiber, R., Voelcker, T., Mall, M. and Kunzelmann, K. (2001) 'The Cystic Fibrosis Transmembrane Conductance Regulator (CFTR) Inhibits ENaC through an Increase in the Intracellular Cl- Concentration.' *EMBO Reports*, 2(11) pp. 1047–1051.

Krista, D. and G., P. E. (2017) '*Enterococci* and Their Interactions with the Intestinal Microbiome.' *Microbiology Spectrum*, 5(6) pp. 10.1128/microbiolspec.bad-0014–2016.

Kristensen, M. I., de Winter-De Groot, K. M., Berkers, G., Chu, M. L. J. N., Arp, K., Ghijsen, S., Heijerman, H. G. M., Arets, H. G. M., Majoor, C. J., Janssens, H. M., van der Meer, R., Bogaert, D. and van der Ent, C. K. (2021) 'Individual and Group Response of Treatment with Ivacaftor on Airway and Gut Microbiota in People with CF and a s1251n Mutation.' *Journal of Personalized Medicine*, 11(5) p. 350.

Kristensen, M., Prevaes, S. M. P. J., Kalkman, G., Tramper-Stranders, G. A., Hasrat, R., de Winter- de Groot, K. M., Janssens, H. M., Tiddens, H. A., van Westreenen, M., Sanders, E. A. M., Arets, B., Keijser, B., van der Ent, C. K. and Bogaert, D. (2020) 'Development of the Gut Microbiota in Early Life: The Impact of Cystic Fibrosis and Antibiotic Treatment.' *Journal of Cystic Fibrosis*, 19(4) pp. 553–561.

de la Cuesta-Zuluaga, J., Mueller, N. T., Álvarez-Quintero, R., Velásquez-Mejía, E. P., Sierra, J. A., Corrales-Agudelo, V., Carmona, J. A., Abad, J. M. and Escobar, J. S. (2019) 'Higher Fecal Short-Chain Fatty Acid Levels are Associated with Gut Microbiome Dysbiosis, Obesity, Hypertension and Cardiometabolic Disease Risk Factors.' *Nutrients*, 11(1) p. 51.

Lederberg, J. and McCray, A. T. (2001) 'Ome SweetOmics - A Genealogical Treasury of Words.' *The Scientist*, 15(7) p. 8.

Lewindon, P. J., Robb, T. A., Moore, D. J., Davidson, G. P. and Martin, A. J. (1998) 'Bowel Dysfunction in Cystic Fibrosis: Importance of Breath Testing.' *Journal of Paediatrics and Child Health*, 34(1) pp. 79–82.

Li, K. Y., Wang, J. L., Wei, J. P., Gao, S. Y., Zhang, Y. Y., Wang, L. T. and Liu, G. (2016) 'Fecal Microbiota in Pouchitis and Ulcerative Colitis.' *World Journal of Gastroenterology*, 22(40) pp. 8929–8939.

Li, L., Krause, L. and Somerset, S. (2017) 'Associations between Micronutrient Intakes and Gut Microbiota in a Group of Adults with Cystic Fibrosis.' *Clinical Nutrition*, 36(4) pp. 1097–1104.

Li, L. and Somerset, S. (2014) 'Digestive System Dysfunction in Cystic Fibrosis: Challenges for Nutrition Therapy.' *Digestive and Liver Disease*, 46(10) pp. 865–874.

Li, W., Soave, D., Miller, M. R., Keenan, K., Lin, F., Gong, J., Chiang, T., Stephenson, A. L., Durie, P., Rommens, J., Sun, L. and Strug, L. J. (2014) 'Unraveling the Complex Genetic Model for Cystic Fibrosis: Pleiotropic Effects of Modifier Genes on Early Cystic Fibrosis-Related Morbidities.' *Human Genetics*, 133(2) pp. 151–161.

Liebisch, G., Ecker, J., Roth, S., Schweizer, S., Öttl, V., Schött, H. F., Yoon, H., Haller, D., Holler, E., Burkhardt, R. and Matysik, S. (2019) 'Quantification of Fecal Short Chain Fatty Acids by Liquid Chromatography Tandem Mass Spectrometry—Investigation of Pre-Analytic Stability.' *Biomolecules*, 9(4) p. 121.

De Lisle, R. C. (2007) 'Altered Transit and Bacterial Overgrowth in the Cystic Fibrosis

Mouse Small Intestine.' *American Journal of Physiology - Gastrointestinal and Liver Physiology*, 293(1) pp. 104–111.

De Lisle, R. C. and Borowitz, D. (2013) 'The Cystic Fibrosis Intestine.' *Cold Spring Harbor Perspectives in Medicine*, 3(9) p. a009753.

De Lisle, R. C., Meldi, L. and Mueller, R. (2012) 'Intestinal Smooth Muscle Dysfunction Develops Postnatally in Cystic Fibrosis Mice.' *Journal of Pediatric Gastroenterology and Nutrition*, 55(6) pp. 689–694.

De Lisle, R. C., Mueller, R. and Boyd, M. (2011) 'Impaired Mucosal Barrier Function in the Small Intestine of the Cystic Fibrosis Mouse.' *Journal of Pediatric Gastroenterology and Nutrition*, 53(4) pp. 371–379.

De Lisle, R. C., Sewell, R. and Meldi, L. (2010) 'Enteric Circular Muscle Dysfunction in the Cystic Fibrosis Mouse Small Intestine.' *Neurogastroenterology and Motility*, 22(3) pp. 341-e87.

Lisowska, A., Wójtowicz, J. and Walkowiak, J. (2009) 'Small Intestine Bacterial Overgrowth is Frequent in Cystic Fibrosis: Combined Hydrogen and Methane Measurements are Required for its Detection.' *Acta Biochimica Polonica*, 56(4) pp. 631–634.

Liu, X., Li, T., Riederer, B., Lenzen, H., Ludolph, L., Yeruva, S., Tuo, B., Soleimani, M. and Seidler, U. (2015) 'Loss of Slc26a9 Anion Transporter Alters Intestinal Electrolyte and HCO3(-) Transport and Reduces Survival in CFTR-Deficient Mice.' *European Journal of Physiology*, 467(6) pp. 1261–1275.

Loc-Carrillo, C. and Abedon, S. T. (2011) 'Pros and Cons of Phage Therapy.' *Bacteriophage*, 1(2) pp. 111–114.

Loman, B. R., Shrestha, C. L., Thompson, R., Groner, J. A., Mejias, A., Ruoff, K. L., O'Toole, G. A., Bailey, M. T. and Kopp, B. T. (2020) 'Age and Environmental Exposures Influence the Fecal Bacteriome of Young Children with Cystic Fibrosis.' *Pediatric Pulmonology*, 55 pp. 1661–1670.

Lopes-Pacheco, M. (2020) 'CFTR Modulators: The Changing Face of Cystic Fibrosis in the Era of Precision Medicine.' *Frontiers in Pharmacology*, 10 p. 1662.

López-Aladid, R., Fernández-Barat, L., Alcaraz-Serrano, V., Bueno-Freire, L., Vázquez, N., Pastor-Ibáñez, R., Palomeque, A., Oscanoa, P. and Torres, A. (2023) 'Determining the Most Accurate 16S rRNA Hypervariable Region for Taxonomic Identification from Respiratory Samples.' *Scientific Reports*, 13(1) p. 3974.

Louis, P., Duncan, S. H., Sheridan, P. O., Walker, A. W. and Flint, H. J. (2022) 'Microbial Lactate Utilisation and the Stability of the Gut Microbiome.' *Gut Microbiome*, 3 p. e3.

Lovat, L. B. (1996) 'Age Related Changes in Gut Physiology and Nutritional Status.' *Gut*, 38(3) pp. 306–309.

Lozupone, C. A., Stombaugh, J. I., Gordon, J. I., Jansson, J. K. and Knight, R. (2012) 'Diversity, Stability and Resilience of the Human Gut Microbiota.' *Nature*, 489(7415) pp. 220–230.

Lynch, S. V., Goldfarb, K. C., Wild, Y. K., Kong, W., De Lisle, R. C. and Brodie, E. L. (2013) 'Cystic Fibrosis Transmembrane Conductance Regulator Knockout Mice Exhibit Aberrant Gastrointestinal Microbiota.' *Gut Microbes*, 4(1) pp. 41–47.

Ma, J., Li, Z., Zhang, W., Zhang, C., Zhang, Y., Mei, H., Zhuo, N., Wang, H., Wang, L. and Wu, D. (2020) 'Comparison of Gut Microbiota in Exclusively Breast-Fed and Formula-Fed Babies: A Study of 91 Term Infants.' *Scientific Reports*, 10(1) p. 15792.

Madan, J. C., Koestle, D. C., Stanton, B. A., Davidson, L., Moulton, L. A., Housman, M. L., Moore, J. H., Guill, M. F., Morrison, H. G., Sogin, M. L., Hampton, T. H., Karagas, M. R., Palumbo, P. E., Foster, J. A., Hibberd, P. L. and O'Toole, G. A. (2012) 'Serial Analysis of the Gut and Respiratory Microbiome.' *mBio*, 3(4) pp. e00251-12.

Magurran, A. E. (2007) 'Species Abundance Distributions Over Time.' *Ecology Letters*, 10(5) pp. 347–354.

Magurran, A. E. and Henderson, P. A. (2003) 'Explaining the Excess of Rare Species in Natural Species Abundance Distributions.' *Nature*, 422(6933) pp. 714–716.

Mainz, J. G., Zagoya, C., Polte, L., Naehrlich, L., Sasse, L., Eickmeier, O., Smaczny, C., Barucha, A., Bechinger, L., Duckstein, F., Kurzidim, L., Eschenhagen, P., Caley, L., Peckham, D. and Schwarz, C. (2022) 'Elexacaftor-Tezacaftor-Ivacaftor Treatment Reduces Abdominal Symptoms in Cystic Fibrosis-Early results Obtained With the CF-Specific CFAbd-Score.' *Frontiers in Pharmacology*, 14 p. 1207356.

Majid, H. A., Emery, P. W. and Whelan, K. (2011) 'Faecal Microbiota and Short-Chain Fatty Acids in Patients Receiving Enteral Nutrition with Standard or Fructo-Oligosaccharides and Fibre-Enriched Formulas.' *Journal of Human Nutrition and Dietetics*, 24(3) pp. 260–268.

Malagelada, C., Bendezú, R. A., Seguí, S., Vitrià, J., Merino, X., Nieto, A., Sihuay, D., Accarino, A., Molero, X. and Azpiroz, F. (2020) 'Motor Dysfunction of the Gut in Cystic Fibrosis.' *Neurogastroenterology and Motility*, 32(9) p. e13883.

Maneerattanaporn, M. and Chey, W. D. (2007) 'Small Intestinal Bacterial Overgrowth.' *Practical Gastroenterology and Hepatology: Small and Large Intestine and Pancreas*, 3(2) pp. 112–122.

Manor, O., Levy, R., Pope, C. E., Hayden, H. S., Brittnacher, M. J., Carr, R., Radey, M. C., Hager, K. R., Heltshe, S. L., Ramsey, B. W., Miller, S. I., Hoffman, L. R. and Borenstein, E. (2016) 'Metagenomic Evidence for Taxonomic Dysbiosis and Functional Imbalance in the Gastrointestinal Tracts of Children with Cystic Fibrosis.' *Scientific Reports*, 6 p. 22493.

Marks, P. A., Rifkind, R. A., Richon, V. M., Breslow, R., Miller, T. and Kelly, W. K. (2001) 'Histone Deacetylases and Cancer: Causes and Therapies.' *Nature Reviews Cancer*, 1(3) pp. 194–202.

Marsh, R., Gavillet, H., Hanson, L., Ng, C., Mitchell-Whyte, M., Major, G., Smyth, A. R., Rivett, D. and van der Gast, C. (2022) 'Intestinal Function and Transit Associate with Gut Microbiota Dysbiosis in Cystic Fibrosis.' *Journal of Cystic Fibrosis*, 21(3) pp. 506–513.

Marsh, R., Dos Santos, C., Hanson, L., Ng, C., Major, G., Smyth, A. R., Rivett, D. and van der Gast, C. (2023) 'Tezacaftor/Ivacaftor Therapy has Negligible Effects on the Cystic Fibrosis Gut Microbiome.' *Microbiology Spectrum*, 11(5) p. e0117523.

Martin, C. R., Zaman, M. M., Ketwaroo, G. A., Bhutta, A. Q., Coronel, E., Popov, Y., Schuppan, D. and Freedman, S. D. (2012) 'CFTR Dysfunction Predisposes to Fibrotic Liver Disease in a Murine Model.' *American Journal of Physiology-Gastrointestinal and Liver Physiology*, 303(4) pp. G474–G481.

Martin, M. (2011) 'Cutadapt Removes Adapter Sequences from High-Throughput Sequencing Reads.' *EMBnet Journal*, 17(1) pp. 10–12.

Matamouros, S., Hayden, H. S., Hager, K. R., Brittnacher, M. J., Lachance, K., Weiss, E. J., Pope, C. E., Imhaus, A. F., McNally, C. P., Borenstein, E., Hoffman, L. R. and Miller, S. I. (2018) 'Adaptation of Commensal Proliferating *Escherichia coli* to the Intestinal Tract of Young Children with Cystic Fibrosis.' *Proceedings of the National Academy of Sciences of the United States of America*, 115(7) pp. 1605–1610.

McBennett, K. A., Davis, P. B. and Konstan, M. W. (2022) 'Increasing Life Expectancy in Cystic Fibrosis: Advances and Challenges.' *Pediatric pulmonology*, 57(Suppl 1) pp. S5–S12.

McCormack, J., Bell, S., Senini, S., Walmsley, K., Patel, K., Wainwright, C., Serisier, D., Harris, M. and Bowler, S. (2007) 'Daily Versus Weekly Azithromycin in Cystic Fibrosis Patients.' *European Respiratory Journal*, 30(3) pp. 487–495.

Meeker, S. M., Mears, K. S., Sangwan, N., Brittnacher, M. J., Weiss, E. J., Treuting, P. M., Tolley, N., Pope, C. E., Hager, K. R., Vo, A. T., Paik, J., Frevert, C. W., Hayden, H. S., Hoffman, L. R., Miller, S. I. and Hajjar, A. M. (2020) 'CFTR Dysregulation Drives Active Selection of the Gut Microbiome.' *PLoS Pathogens*, 16(1) p. e1008251.

Middleton, P. G., Mall, M. A., Dřevínek, P., Lands, L. C., McKone, E. F., Polineni, D., Ramsey, B. W., Taylor-Cousar, J. L., Tullis, E., Vermeulen, F., Marigowda, G., McKee, C. M., Moskowitz, S. M., Nair, N., Savage, J., Simard, C., Tian, S., Waltz, D., Xuan, F., Rowe, S. M. and Jain, R. (2019) 'Elexacaftor-Tezacaftor-Ivacaftor for Cystic Fibrosis with a Single Phe508del Allele.' *The New England Journal of Medicine*, 381(19) pp. 1809–1819.

Million, M., Tidjani Alou, M., Khelaifia, S., Bachar, D., Lagier, J.-C., Dione, N., Brah, S., Hugon, P., Lombard, V., Armougom, F., Fromonot, J., Robert, C., Michelle, C., Diallo, A., Fabre, A., Guieu, R., Sokhna, C., Henrissat, B., Parola, P. and Raoult, D. (2016) 'Increased Gut Redox and Depletion of Anaerobic and Methanogenic Prokaryotes in Severe Acute Malnutrition.' *Scientific Reports*, 6(1) p. 26051.

Miragoli, F., Federici, S., Ferrari, S., Minuti, A., Rebecchi, A., Bruzzese, E., Buccigrossi, V., Guarino, A. and Callegari, M. L. (2017) 'Impact of Cystic Fibrosis Disease on Archaea and Bacteria Composition of Gut Microbiota.' *FEMS Microbiology Ecology*, 93(2) p. fiw230.

Mirzaei, R., Afaghi, A., Babakhani, S., Sohrabi, M. R., Hosseini-Fard, S. R., Babolhavaeji, K., Khani Ali Akbari, S., Yousefimashouf, R. and Karampoor, S. (2021) 'Role of Microbiota-Derived Short-Chain Fatty Acids in Cancer Development and

Prevention.' *Biomedicine and Pharmacotherapy*, 139 p. 111619.

Müller, B., Rasmusson, A. J., Just, D., Jayarathna, S., Moazzami, A., Novicic, Z. K. and Cunningham, J. L. (2021) 'Fecal Short-Chain Fatty Acid Ratios as Related to Gastrointestinal and Depressive Symptoms in Young Adults.' *Psychosomatic Medicine*, 83(7) pp. 693–699.

Munck, A. (2014) 'Cystic Fibrosis: Evidence for Gut Inflammation.' *The International Journal of Biochemistry & Cell Biology*, 52 pp. 180–183.

Muniz, L. R., Knosp, C. and Yeretssian, G. (2012) 'Intestinal Antimicrobial Peptides during Homeostasis, Infection, and Disease.' *Frontiers in Immunology*, 3 p. 310.

Muyzer, G., de Waal, E. C. and Uitterlinden, A. G. (1993) 'Profiling of Complex Microbial Populations by Denaturing Gradient Gel Electrophoresis Analysis of Polymerase Chain Reaction-Amplified Genes Coding for 16S rRNA.' *Applied and Environmental Microbiology*, 59(3) pp. 695–700.

Nagana Gowda, G. A. and Raftery, D. (2021) 'NMR-Based Metabolomics.' *Advances in Experimental Medicine and Biology*, 1280 pp. 19–37.

Nagpal, R., Mainali, R., Ahmadi, S., Wang, S., Singh, R., Kavanagh, K., Kitzman, D. W., Kushugulova, A., Marotta, F. and Yadav, H. (2018) 'Gut Microbiome and Aging: Physiological and Mechanistic Insights.' *Nutrition and Healthy Aging*, 4(4) pp. 267–285.

Nagy, E., Urbán, E. and Nord, C. E. (2011) 'Antimicrobial Susceptibility of *Bacteroides Fragilis* Group Isolates in Europe: 20 years of Experience.' *Clinical Microbiology and Infection*, 17(3) pp. 371–379.

Naik, T., Sharda, M. and Pandit, A. (2020) 'High-Quality Single Amplicon Sequencing Method for Illumina MiSeq Platform using Pool of "N" (0-10) Spacer-Linked Target Specific Primers without PhiX Spike-in.' *BMC Genomics*, 24 p. 141.

Di Nardo, G., Oliva, S., Menichella, A., Pistelli, R., De Biase, R. V., Patriarchi, F., Cucchiara, S. and Stronati, L. (2014) 'Lactobacillus reuteri ATCC55730 in Cystic Fibrosis.' *Journal of Pediatric Gastroenterology and Nutrition*, 58(1) pp. 81–86.

Nash, A. K., Auchtung, T. A., Wong, M. C., Smith, D. P., Gesell, J. R., Ross, M. C., Stewart, C. J., Metcalf, G. A., Muzny, D. M., Gibbs, R. A., Ajami, N. J. and Petrosino, J. F. (2017) 'The Gut Mycobiome of the Human Microbiome Project healthy Cohort.' *Microbiome*, 5(1) p. 153.

Nelson, M. C., Morrison, H. G., Benjamino, J., Grim, S. L. and Graf, J. (2014) 'Analysis, Optimization and Verification of Illumina-Generated 16S rRNA Gene Amplicon Surveys.' *PLoS One*, 9(4) p. e94249.

Ng, C., Dellschaft, N. S., Hoad, C. L., Marciani, L., Ban, L., Prayle, A. P., Barr, H. L., Jaudszus, A., Mainz, J. G., Spiller, R. C., Gowland, P., Major, G. and Smyth, A. R. (2021) 'Postprandial Changes in Gastrointestinal Function and Transit in Cystic Fibrosis Assessed by Magnetic Resonance Imaging.' *Journal of Cystic Fibrosis*, 20(4) pp. 591–597.

Ng, S. M. and Moore, H. S. (2021) 'Drug Therapies for Reducing Gastric Acidity in people with Cystic Fibrosis.' *The Cochrane Database of Systematic Reviews*, 4(4) p.

CD003424.

Nielsen, S., Needham, B., Leach, S. T., Day, A. S., Jaffe, A., Thomas, T. and Ooi, C. Y. (2016) 'Disrupted Progression of the Intestinal Microbiota with Age in children with Cystic Fibrosis.' *Scientific Reports*, 6 p. 24857.

Niu, J., Xu, L., Qian, Y., Sun, Z., Yu, D., Huang, J., Zhou, X., Wang, Y., Zhang, T., Ren, R., Li, Z., Yu, J. and Gao, X. (2020) 'Evolution of the Gut Microbiome in Early Childhood: A Cross-Sectional Study of Chinese Children.' *Frontiers in Microbiology*, 11 p. 439.

Norkina, O., Burnett, T. G. and De Lisle, R. C. (2004) 'Bacterial Overgrowth in the Cystic Fibrosis Transmembrane Conductance Regulator Null Mouse Small Intestine.' *Infection and Immunity*, 72(10) pp. 6040–6049.

O'Sullivan, B. P. and Freedman, S. D. (2009) 'Cystic Fibrosis.' *Lancet*, 373(9678) pp. 1891–1904.

Ogilvie, L. A. and Jones, B. V (2015) 'The Human Gut Virome: A Multifaceted Majority.' *Frontiers in Microbiology*, 11(6) p. 918.

Oliphant, K. and Allen-Vercoe, E. (2019) 'Macronutrient Metabolism by the Human Gut Microbiome: Major Fermentation By-Products and their Impact on Host Health.' *Microbiome*, 7(1) p. 91.

Ooi, C. Y., Dorfman, R., Cipolli, M., Gonska, T., Castellani, C., Keenan, K., Freedman, S. D., Zielenski, J., Berthiaume, Y., Corey, M., Schibli, S., Tullis, E. and Durie, P. R. (2011) 'Type of CFTR Mutation Determines Risk of Pancreatitis in Patients with Cystic Fibrosis.' *Gastroenterology*, 140(1) pp. 153–161.

Ooi, C. Y. and Durie, P. R. (2016) 'Cystic Fibrosis from the Gastroenterologist's Perspective.' *Nature Reviews Gastroenterology and Hepatology*, 13(3) pp. 175–185.

Ooi, C. Y., Syed, S. A., Rossi, L., Garg, M., Needham, B., Avolio, J., Young, K., Surette, M. G. and Gonska, T. (2018) 'Impact of CFTR Modulation with Ivacaftor on Gut Microbiota and Intestinal Inflammation.' *Scientific Reports*, 8(17834).

Pang, T., Leach, S. T., Katz, T., Jaffe, A., Day, A. S. and Ooi, C. Y. (2015) 'Elevated Fecal M2-Pyruvate Kinase in children with Cystic Fibrosis: A Clue to the Increased Risk of Intestinal Malignancy in Adulthood?' *Journal of Gastroenterology and Hepatology*, 30(5) pp. 866–871.

De Paola, E. L., Montevecchi, G., Masino, F., Antonelli, A. and Lo Fiego, D. Pietro (2017) 'Single Step Extraction and Derivatization of Intramuscular Lipids for Fatty Acid Ultra Fast GC Analysis: Application on Pig Thigh.' *Journal of Food Science and Technology*, 54(3) pp. 601–610.

Paranjape, S. M. and Mogayzel, P. J. J. (2018) 'Cystic fibrosis in the Era of Precision Medicine.' *Paediatric Respiratory Reviews*, 25 pp. 64–72.

Parks, D. H., Chuvochina, M., Waite, D. W., Rinke, C., Skarshewski, A., Chaumeil, P. A. and Hugenholtz, P. (2018) 'A Standardized Bacterial Taxonomy based on Genome Phylogeny Substantially Revises the Tree of Life.' *Nature Biotechnology*, 36(10) p. 996.

Peach, S. L., Borriello, S. P., Gaya, H., Barclay, F. E. and Welch, A. R. (1986) 'Asymptomatic Carriage of *Clostridium difficile* in patients with Cystic Fibrosis.' *Journal of Clinical Pathology*, 39(9) pp. 1013–1018.

Peng, L., Li, Z.-R., Green, R. S., Holzman, I. R. and Lin, J. (2009) 'Butyrate Enhances the Intestinal Barrier by Facilitating Tight Junction Assembly via Activation of AMP-Activated Protein Kinase in Caco-2 cell Monolayers.' *The Journal of Nutrition*, 139(9) pp. 1619–1625.

Png, C. W., Lindén, S. K., Gilshenan, K. S., Zoetendal, E. G., McSweeney, C. S., Sly, L. I., McGuckin, M. A. and Florin, T. H. J. (2010) 'Mucolytic Bacteria with Increased Prevalence in IBD Mucosa Augment in vitro Utilization of Mucin by other Bacteria.' *The American Journal of Gastroenterology*, 105(11) pp. 2420–2428.

Pokusaeva, K., Fitzgerald, G. F. and Van Sinderen, D. (2011) 'Carbohydrate Metabolism in Bifidobacteria.' *Genes and Nutrition*, 6(3) pp. 285–306.

Polyakova, O. V, Mazur, D. M., Artaev, V. B. and Lebedev, A. T. (2013) 'Determination of Polycyclic Aromatic Hydrocarbons in Water by Gas Chromatography/Mass Spectrometry with Accelerated Sample Preparation.' *Journal of Analytical Chemistry*, 68(13) pp. 1099–1103.

Pope, C. E., Vo, A. T., Hayden, H. S., Weiss, E. J., Durfey, S., McNamara, S., Ratjen, A., Grogan, B., Carter, S., Nay, L., Parsek, M. R., Singh, P. K., McKone, E. F., Aitken, M. L., Rosenfeld, M. R. and Hoffman, L. R. (2021) 'Changes in Fecal Microbiota with CFTR Modulator Therapy: A Pilot Study.' *Journal of Cystic Fibrosis*, 20(5) pp. 742–746.

De Preter, V., Machiels, K., Joossens, M., Arijs, I., Matthys, C., Vermeire, S., Rutgeerts, P. and Verbeke, K. (2015) 'Faecal Metabolite Profiling Identifies Medium-Chain Fatty Acids as Discriminating Compounds in IBD.' *Gut*, 64, March, pp. 447–458.

Price, C. E. and O'Toole, G. A. (2021) 'The Gut-Lung Axis in Cystic Fibrosis.' *Journal of Bacteriology*, 203(20) p. e0031121.

Primec, M., Mičetić-Turk, D. and Langerholc, T. (2017) 'Analysis of Short-Chain Fatty Acids in Human Feces: A Scoping Review.' *Analytical Biochemistry*, 526 pp. 9–21.

Procházková, N., Falony, G., Dragsted, L. O., Licht, T. R., Raes, J. and Roager, H. M. (2023) 'Advancing Human Gut Microbiota Research by Considering Gut Transit Time.' *Gut*, 72(1) pp. 180–191.

Puertollano, E., Kolida, S. and Yaqoob, P. (2014) 'Biological Significance of Short-Chain Fatty Acid Metabolism by the Intestinal Microbiome.' *Current Opinion in Clinical Nutrition & Metabolic Care*, 17(2) pp. 139–144.

Puschhof, J., Pleguezuelos-Manzano, C., Martinez-Silgado, A., Akkerman, N., Saftien, A., Boot, C., de Waal, A., Beumer, J., Dutta, D., Heo, I. and Clevers, H. (2021) 'Intestinal Organoid Cocultures with Microbes.' *Nature Protocols*, 16(10) pp. 4633–4649.

Qiu, S., Cai, Y., Yao, H., Lin, C., Xie, Y., Tang, S. and Zhang, A. (2023) 'Small Molecule Metabolites: Discovery of Biomarkers and Therapeutic Targets.' *Signal*

Transduction and Targeted Therapy, 8 p. 132.

Quast, C., Pruesse, E., Yilmaz, P., Gerken, J., Schweer, T., Yarza, P., Peplies, J. and Glöckner, F. O. (2013) 'The SILVA Ribosomal RNA Gene Database Project: Improved Data Processing and Web-Based Tools.' *Nucleic Acids Research*, 41(Database issue) pp. D590–D596.

Rainey, F. A., Hollen, B. J. and Small, A. (2009) *Genus I. Clostridium Prazmowski 1880, 23AL*. De Vos, P., Garrity, G. M., Jones, D., Krieg, N. R., Ludwig, W., Rainey, F. A., Schleifer, K.-H., and Whitman, W. B. (eds) *Bergey's Manual of Systematic Bacteriology Volume 3: The Firmicutes*. 2nd ed.

Ramos, A. F. P., de Fuccio, M. B., Moretzsohn, L. D., Barbosa, A. J. A., Passos, M. do C. F., Carvalho, R. S. and Coelho, L. G. V. (2013) 'Cystic Fibrosis, Gastroduodenal Inflammation, Duodenal Ulcer, and *H. pylori* infection: The "Cystic Fibrosis Paradox" Revisited.' *Journal of Cystic Fibrosis*, 12(4) pp. 377–383.

Rechkemmer, G., Rönnau, K. and Engelhardt, W. V. (1988) 'Fermentation of Polysaccharides and Absorption of Short Chain Fatty Acids in the Mammalian Hindgut.' *Comparative Biochemistry and Physiology Part A: Physiology*, 90(4) pp. 563–568.

Renz, H., Brandtzaeg, P. and Hornef, M. (2012) 'The Impact of Perinatal Immune Development on Mucosal Homeostasis and Chronic Inflammation.' *Nature Reviews Immunology*, 12(1) pp. 9–23.

Reyman, M., van Houten, M. A., van Baarle, D., Bosch, A. A. T. M., Man, W. H., Chu, M. L. J. N., Arp, K., Watson, R. L., Sanders, E. A. M., Fuentes, S. and Bogaert, D. (2019) 'Impact of Delivery Mode-Associated Gut Microbiota Dynamics on Health in the First Year of Life.' *Nature Communications*, 10(1) p. 4997.

Ridley, K. and Condren, M. (2020) 'Elexacaftor-Tezacaftor-Ivacaftor: The First Triple-Combination Cystic Fibrosis Transmembrane Conductance Regulator Modulating Therapy.' *The Journal of Pediatric Pharmacology and Therapeutics*, 25(3) pp. 192–197.

Rinninella, E., Raoul, P., Cintoni, M., Franceschi, F., Miggiano, G., Gasbarrini, A. and Mele, M. (2019) 'What is the Healthy Gut Microbiota Composition? A Changing Ecosystem across Age, Environment, Diet, and Diseases.' *Microorganisms*, 7(1) p. 14.

Rios-Covian, D., Gueimonde, M., Duncan, S. H., Flint, H. J. and De Los Reyes-Gavilan, C. G. (2015) 'Enhanced Butyrate Formation by Cross-Feeding between *Faecalibacterium prausnitzii* and *Bifidobacterium adolescentis*.' *FEMS Microbiology Letters*, 362(21) p. fnv176.

Ríos-Covián, D., Ruas-Madiedo, P., Margolles, A., Gueimonde, M., de Los Reyes-Gavilán, C. G. and Salazar, N. (2016) 'Intestinal Short Chain Fatty Acids and their Link with Diet and Human Health.' *Frontiers in Microbiology*, 7 p. 185.

Ritari, J., Salojärvi, J., Lahti, L. and de Vos, W. M. (2015) 'Improved Taxonomic Assignment of Human Intestinal 16S rRNA Sequences by a Dedicated Reference Database.' *BMC Genomics*, 16(1) p. 1056.

Rivière, A., Selak, M., Lantin, D., Leroy, F. and De Vuyst, L. (2016) '*Bifidobacteria* and Butyrate-Producing Colon Bacteria: Importance and Strategies for their Stimulation in the Human Gut.' *Frontiers in Microbiology*, 7 p. 979.

Roager, H. M., Hansen, L. B. S., Bahl, M. I., Frandsen, H. L., Carvalho, V., Gøbel, R. J., Dalgaard, M. D., Plichta, D. R., Sparholt, M. H., Vestergaard, H., Hansen, T., Sicheritz-Pontén, T., Nielsen, H. B., Pedersen, O., Lauritzen, L., Kristensen, M., Gupta, R. and Licht, T. R. (2016) 'Colonic Transit Time is related to Bacterial Metabolism and Mucosal Turnover in the Gut.' *Nature Microbiology*, 1 p. 16093.

Rogers, G. B., Cuthbertson, L., Hoffman, L. R., Wing, P. A. C., Pope, C., Hooftman, D. A. P., Lilley, A. K., Oliver, A., Carroll, M. P., Bruce, K. D. and Van Der Gast, C. J. (2013) 'Reducing Bias in Bacterial Community Analysis of Lower Respiratory Infections.' *ISME Journal*, 7(4) pp. 697–706.

Rohwer, F. and Thurber, R. V. (2009) 'Viruses Manipulate the Marine Environment.' *Nature*, 459(7244) pp. 207–212.

Ronan, N. J., Einarsson, G. G., Deane, J., Fouhy, F., Rea, M., Hill, C., Shanahan, F., Elborn, J. S., Ross, R. P., McCarthy, M., Murphy, D. M., Eustace, J. A., MM, T., Stanton, C. and Plant, B. J. (2022) 'Modulation, Microbiota and Inflammation in the adult CF Gut: A Prospective Study.' *Journal of Cystic Fibrosis*, 21(5) pp. 837–843.

Rosenfeld, M., Wainwright, C. E., Higgins, M., Wang, L. T., McKee, C., Campbell, D., Tian, S., Schneider, J., Cunningham, S. and Davies, J. C. (2018) 'Ivacaftor Treatment of Cystic Fibrosis in Children Aged 12 to <24 months and with a CFTR Gating Mutation (ARRIVAL): A Phase 3 Single-Arm Study.' *The Lancet. Respiratory Medicine*, 6(7) pp. 545–553.

Rothberg, J. M. and Leamon, J. H. (2008) 'The Development and Impact of 454 Sequencing.' *Nature Biotechnology*, 26(10) pp. 1117–1124.

Rowbotham, N. J., Smith, S., Elliott, Z. C., Cupid, B., Allen, L. J., Cowan, K., Allen, L. and Smyth, A. R. (2023) 'A Refresh of the Top 10 Research Priorities in Cystic Fibrosis.' *Thorax*, 78(8) pp. 840–843.

Rowe, S. M., Daines, C., Ringshausen, F. C., Kerem, E., Wilson, J., Tullis, E., Nair, N., Simard, C., Han, L., Ingenito, E. P., McKee, C., Lekstrom-Himes, J. and Davies, J. C. (2017) 'Tezacaftor-Ivacaftor in Residual-Function Heterozygotes with Cystic Fibrosis.' *The New England Journal of Medicine*, 377(21) pp. 2024–2035.

Rowe, S. M., Heltshe, S. L., Gonska, T., Donaldson, S. H., Borowitz, D., Gelfond, D., Sagel, S. D., Khan, U., Mayer-Hamblett, N., Van Dalfsen, J. M., Joseloff, E. and Ramsey, B. W. (2014) 'Clinical Mechanism of the Cystic Fibrosis Transmembrane Conductance Regulator Potentiator Ivacaftor in G551D-Mediated Cystic Fibrosis.' *American Journal of Respiratory and Critical Care Medicine*, 190(2) pp. 175–184.

Rumman, N., Sultan, M., El-Chammas, K., Goh, V., Salzman, N., Quintero, D. and Werlin, S. (2014) 'Calprotectin in Cystic Fibrosis.' *BMC Pediatrics*, 14 p. 133.

Ruppin, H., Bar-Meir, S., Soergel, K. H., Wood, C. M. and Schmitt, M. G. (1980) 'Absorption of Short-Chain Fatty Acids by the Colon.' *Gastroenterology*, 78(6) pp. 1500–1507.

Rutayisire, E., Huang, K., Liu, Y. and Tao, F. (2016) ‘The Mode of Delivery Affects the Diversity and Colonization Pattern of the Gut Microbiota during the First Year of Infants’ Life: A Systematic Review.’ *BMC Gastroenterology*, 16(1) p. 86.

Saha, S., Day-Walsh, P., Shehata, E. and Kroon, P. A. (2021) ‘Development and Validation of a LC-MS/MS Technique for the Analysis of Short Chain Fatty Acids in Tissues and Biological Fluids without Derivatisation using Isotope Labelled Internal Standards.’ *Molecules*, 26 p. 6444.

Sakamoto, M., Sakurai, N., Tanno, H., Iino, T., Ohkuma, M. and Endo, A. (2022) ‘Genome-Based, Phenotypic and Chemotaxonomic Classification of *Faecalibacterium* Strains: Proposal of Three Novel Species *Faecalibacterium duncaniae* sp. nov., *Faecalibacterium hattorii* sp. nov. and *Faecalibacterium gallinarum* sp.’ *International Journal of Systematic and Evolutionary Microbiology*, 72(4) p. 005379.

Sakata, T. (2019) ‘Pitfalls in Short-Chain Fatty Acid Research: A Methodological Review.’ *Animal Science Journal*, 90(1) pp. 3–13.

Salazar, N., Valdés-Varela, L., González, S., Gueimonde, M. and de Los Reyes-Gavilán, C. G. (2017) ‘Nutrition and the Gut Microbiome in the Elderly.’ *Gut Microbes*, 8(2) pp. 82–97.

Salerno, P., Verster, A., Valls, R., Barrack, K., Price, C., Madan, J., O’Toole, G. A. and Ross, B. D. (2023) ‘Persistent Delay in Maturation of the Developing Gut Microbiota in Infants with Cystic Fibrosis.’ *bioRxiv*.

Sambuy, Y., De Angelis, I., Ranaldi, G., Scarino, M. L., Stammati, A. and Zucco, F. (2005) ‘The Caco-2 Cell Line as a Model of the Intestinal Barrier: Influence of Cell and Culture-related Factors on Caco-2 Cell Functional Characteristics.’ *Cell Biology and Toxicology*, 21(1) pp. 1–26.

Sathe, M. and Houwen, R. (2017) ‘Meconium ileus in Cystic Fibrosis.’ *Journal of Cystic Fibrosis*, 16 Suppl 2 pp. S32–S39.

Sato, T., Vries, R. G., Snippert, H. J., van de Wetering, M., Barker, N., Stange, D. E., van Es, J. H., Abo, A., Kujala, P., Peters, P. J. and Clevers, H. (2009) ‘Single Lgr5 Stem Cells Build Crypt-Villus Structures in vitro without a Mesenchymal Niche.’ *Nature*, 459(7244) pp. 262–265.

Schippa, S., Iebba, V., Santangelo, F., Gagliardi, A., De, R. V., Stamato, A., Bertasi, S., Lucarelli, M., Conte, M. P. and Quattrucci, S. (2013) ‘Cystic Fibrosis Transmembrane Conductance Regulator (CFTR) Allelic Variants Relate to Shifts in Faecal Microbiota of Cystic Fibrosis Patients.’ *PLoS One*, 8(4) p. e61176.

Schirmer, M., Ijaz, U. Z., D’Amore, R., Hall, N., Sloan, W. T. and Quince, C. (2015) ‘Insight into Biases and Sequencing Errors for Amplicon Sequencing with the Illumina MiSeq Platform.’ *Nucleic Acids Research*, 43(6).

Schnapp, Z., Hartman, C., Livnat, G., Shteinberg, M. and Elenberg, Y. (2019) ‘Decreased Fecal Calprotectin Levels in Cystic Fibrosis Patients After Antibiotic Treatment for Respiratory Exacerbation.’ *Journal of Pediatric Gastroenterology and Nutrition*, 68(2) pp. 282–284.

Schwarzenberg, S. J., Vu, P. T., Skalland, M., Hoffman, L. R., Pope, C., Gelfond, D.,

Narkewicz, M. R., Nichols, D. P., Heltshe, S. L., Donaldson, S. H., Frederick, C. A., Kelly, A., Pittman, J. E., Ratjen, F., Rosenfeld, M., Sagel, S. D., Solomon, G. M., Stalvey, M. S., Clancy, J. P., Rowe, S. M. and Freedman, S. D. (2022) 'Elexacaftor/Tezacaftor/Ivacaftor and Gastrointestinal Outcomes in Cystic Fibrosis: Report of Promise-GI.' *Journal of Cystic Fibrosis*, 22(2) pp. 282–289.

Scortichini, S., Boarelli, M. C., Silvi, S. and Fiorini, D. (2020) 'Development and Validation of a GC-FID Method for the Analysis of Short Chain Fatty Acids in Rat and Human Faeces and in Fermentation Fluids.' *Journal of Chromatography B: Analytical Technologies in the Biomedical and Life Sciences*, 1143 p. 121972.

Seekatz, A. M., Schnizlein, M. K., Koenigsknecht, M. J., Baker, J. R., Hasler, W. L., Bleske, B. E., Young, V. B. and Sun, D. (2019) 'Spatial and Temporal Analysis of the Stomach and Small-Intestinal Microbiota in Fasted Healthy Humans.' *mSphere*, 4(2) pp. e00126-19.

Segers, M. E. and Lebeer, S. (2014) 'Towards a Better Understanding of Lactobacillus rhamnosus GG--Host Interactions.' *Microbial Cell Factories*, 13(Suppl 1) p. S7.

Sender, R., Fuchs, S. and Milo, R. (2016) 'Revised Estimates for the Number of Human and Bacteria Cells in the Body.' *PLoS Biology*, 14(8) p. e1002533.

Sherwood, J. S., Ullal, J., Kutney, K. and Hughan, K. S. (2022) 'Cystic Fibrosis Related Liver Disease and Endocrine Considerations.' *Journal of Clinical & Translational Endocrinology*, 27 p. 100283.

Shin, A., Preidis, G. A., Shulman, R. and Kashyap, P. C. (2019) 'The Gut Microbiome in Adult and Pediatric Functional Gastrointestinal Disorders.' *Clinical Gastroenterology and Hepatology*, 17(2) pp. 256–274.

Silva, Y. P., Bernardi, A. and Frozza, R. L. (2020) 'The Role of Short-Chain Fatty Acids From Gut Microbiota in Gut-Brain Communication.' *Frontiers in Endocrinology*, 11 p. 25.

Singh, V. K. and Schwarzenberg, S. J. (2017) 'Pancreatic insufficiency in Cystic Fibrosis.' *Journal of Cystic Fibrosis*, 16 Suppl 2 pp. S70–S78.

Smith, S. and Edwards, C. T. (2017) 'Long-Acting Inhaled Bronchodilators for Cystic Fibrosis.' *The Cochrane Database of Systematic Reviews*, 12(12) p. CD012102.

Smith, S., Rowbotham, N., Davies, G., Gathercole, K., Collins, S. J., Elliott, Z., Herbert, S., Allen, L., Ng, C. and Smyth, A. (2020) 'How can we Relieve Gastrointestinal Symptoms in people with Cystic Fibrosis? An International Qualitative Survey.' *BMJ Open Respiratory Research*, 7 p. e000614.

Smyth, A. R., Bell, S. C., Bojcin, S., Bryon, M., Duff, A., Flume, P., Kashirskaya, N., Munck, A., Ratjen, F., Schwarzenberg, S. J., Sermet-Gaudelus, I., Southern, K. W., Taccetti, G., Ullrich, G. and Wolfe, S. (2014) 'European Cystic Fibrosis Society Standards of Care: Best Practice guidelines.' *Journal of Cystic Fibrosis*, 13(Suppl 1) pp. S23-42.

Smyth, R. L., Croft, N. M., O'Hea, U., Marshall, T. G. and Ferguson, A. (2000) 'Intestinal Inflammation in Cystic Fibrosis.' *Archives of Disease in Childhood*, 82(5)

pp. 394–399.

Sokol, H., Leducq, V., Aschard, H., Pham, H.-P., Jegou, S., Landman, C., Cohen, D., Liguori, G., Bourrier, A., Nion-Larmurier, I., Cosnes, J., Seksik, P., Langella, P., Skurnik, D., Richard, M. L. and Beaugerie, L. (2017) 'Fungal Microbiota Dysbiosis in IBD.' *Gut*, 66(6) pp. 1039–1048.

Song, H. E., Lee, H. Y., Kim, S. J., Back, S. H. and Yoo, H. J. (2019) 'A Facile Profiling Method of Short Chain Fatty Acids using Liquid Chromatography-Mass Spectrometry.' *Metabolites*, 9(9) p. 173.

Southern, K. W., Barker, P. M., Solis-Moya, A. and Patel, L. (2012) 'Macrolide Antibiotics for Cystic Fibrosis.' *Paediatric Respiratory Reviews*, 13(4) pp. 228–229.

Stallings, V. A., Sainath, N., Oberle, M., Bertolaso, C. and Schall, J. I. (2018) 'Energy Balance and Mechanisms of Weight Gain with Ivacaftor Treatment of Cystic Fibrosis Gating Mutations.' *Journal of Pediatrics*, 201 pp. 229-237.e4.

Standard Reference Data Program, National Institute of Standards and Technology, Gaithersburg, MD. Standard Reference Database IA. (n.d.). [Online] [Accessed on 28th August 2023] http://www.nist.gov/srd/nist1a.htm.

Steinkamp, G. and Wiedemann, B. (2002) 'Relationship between Nutritional Status and Lung Function in Cystic Fibrosis: Cross Sectional and Longitudinal Analyses from the German CF Quality Assurance (CFQA) Project.' *Thorax*, 57(7) pp. 596–601.

Strong, T. V., Boehm, K. and Collins, F. S. (1994) 'Localization of Cystic Fibrosis Transmembrane Conductance Regulator mRNA in the Human Gastrointestinal Tract by in situ Hybridization.' *Journal of Clinical Investigation*, 93(1) pp. 347–354.

Subhi, R., Ooi, R., Finlayson, F., Kotsimbos, T., Wilson, J., Lee, W. R., Wale, R. and Warrier, S. (2014) 'Distal Intestinal Obstruction Syndrome in Cystic Fibrosis: Presentation, Outcome and Management in a Tertiary Hospital (2007–2012).' *ANZ Journal of Surgery*, 84(10) pp. 740–744.

Sueblinvong, V. and Whittaker, L. A. (2007) 'Fertility and Pregnancy: Common Concerns of the Aging Cystic Fibrosis Population.' *Clinics in Chest Medicine*, 28(2) pp. 433–443.

Sun, L., Rommens, J. M., Corvol, H., Li, W., Li, X., Chiang, T. A., Lin, F., Dorfman, R., Busson, P.-F., Parekh, R. V, Zelenika, D., Blackman, S. M., Corey, M., Doshi, V. K., Henderson, L., Naughton, K. M., O'Neal, W. K., Pace, R. G., Stonebraker, J. R., Wood, S. D., Wright, F. A., Zielenski, J., Clement, A., Drumm, M. L., Boëlle, P.-Y., Cutting, G. R., Knowles, M. R., Durie, P. R. and Strug, L. J. (2012) 'Multiple Apical Plasma Membrane Constituents are Associated with Susceptibility to Meconium Ileus in Individuals with Cystic Fibrosis.' *Nature Genetics*, 44(5) pp. 562–569.

Sze, M. A. and Schloss, P. D. (2019) 'The Impact of DNA Polymerase and Number of Rounds of Amplification in PCR on 16S rRNA Gene Sequence Data.' *mSphere*, 4(3).

Tabori, H., Arnold, C., Jaudszus, A., Mentzel, H. J., Renz, D. M., Reinsch, S., Lorenz, M., Michl, R., Gerber, A., Lehmann, T. and Mainz, J. G. (2017) 'Abdominal Symptoms in Cystic Fibrosis and their relation to Genotype, History, Clinical and Laboratory Findings.' *PLoS One*, 12(5) p. e0174463.

Takeshita, K., Mizuno, S., Mikami, Y., Sujino, T., Saigusa, K., Matsuoka, K., Naganuma, M., Sato, T., Takada, T., Tsuji, H., Kushiro, A., Nomoto, K. and Kanai, T. (2016) 'A Single Species of *Clostridium Subcluster XIVa* Decreased in Ulcerative Colitis Patients.' *Inflammatory Bowel Diseases*, 22(12) pp. 2802–2810.

Tam, R. Y., van Dorst, J. M., McKay, I., Coffey, M. and Ooi, C. Y. (2022) 'Intestinal Inflammation and Alterations in the Gut Microbiota in Cystic Fibrosis: A Review of the Current Evidence, Pathophysiology and Future Directions.' *Journal of Clinical Medicine*, 11(3) p. 649.

Tan, J., McKenzie, C., Potamitis, M., Thorburn, A. N., Mackay, C. R. and Macia, L. (2014) 'The Role of Short-Chain Fatty Acids in Health and Disease.' *Advances in Immunology*, 121 pp. 91–119.

Tang, Q., Jin, G., Wang, G., Liu, T., Liu, X., Wang, B. and Cao, H. (2020) 'Current Sampling Methods for Gut Microbiota: A Call for More Precise Devices.' *Frontiers in Cellular and Infection Microbiology*, 10 p. 151.

Taylor-Cousar, J. L., Mall, M. A., Ramsey, B. W., McKone, E. F., Tullis, E., Marigowda, G., McKee, C. M., Waltz, D., Moskowitz, S. M., Savage, J., Xuan, F. and Rowe, S. M. (2019) 'Clinical Development of Triple-Combination CFTR Modulators for Cystic Fibrosis Patients with one or two F508del Alleles.' *ERJ Open Research*, 5(2) pp. 00082–02019.

Taylor-Cousar, J. L., Munck, A., McKone, E. F., van der Ent, C. K., Moeller, A., Simard, C., Wang, L. T., Ingenito, E. P., McKee, C., Lu, Y., Lekstrom-Himes, J. and Elborn, J. S. (2017) 'Tezacaftor-Ivacaftor in Patients with Cystic Fibrosis Homozygous for Phe508del.' *The New England Journal of Medicine*, 377(21) pp. 2013–2023.

Taylor, S. L., Leong, L. E. X., Sims, S. K., Keating, R. L., Papanicolas, L. E., Richard, A., Mobegi, F. M., Wesselingh, S., Burr, L. D. and Rogers, G. B. (2021) 'The Cystic Fibrosis Gut as a Potential Source of Multidrug Resistant Pathogens.' *Journal of Cystic Fibrosis*, 20(3) pp. 413–420.

Testa, I., Crescenzi, O. and Esposito, S. (2022) 'Gut Dysbiosis in Children with Cystic Fibrosis: Development, Features and the Role of Gut-Lung Axis on Disease Progression.' *Microorganisms*, 11(1) p. 9.

Tetard, C., Mittaine, M., Bui, S., Beaufils, F., Maumus, P., Fayon, M., Burgel, P.-R., Lamireau, T., Delhaes, L., Mas, E. and Enaud, R. (2020) 'Reduced Intestinal Inflammation With Lumacaftor/Ivacaftor in Adolescents With Cystic Fibrosis.' *Journal of Pediatric Gastroenterology & Nutrition*, 71(6) pp. 778–781.

Tezuka, H. and Ohteki, T. (2019) 'Regulation of IgA Production by Intestinal Dendritic Cells and Related Cells.' *Frontiers in Immunology*, 10 p. 1891.

Than, B. L. N., Linnekamp, J. F., Starr, T. K., Largaespada, D. A., Rod, A., Zhang, Y., Bruner, V., Abrahante, J., Schumann, A., Luczak, T., Niemczyk, A., O'Sullivan, M. G., Medema, J. P., Fijneman, R. J. A., Meijer, G. A., Van den Broek, E., Hodges, C. A., Scott, P. M., Vermeulen, L. and Cormier, R. T. (2016) 'CFTR is a Tumor Suppressor Gene in Murine and Human Intestinal Cancer.' *Oncogene*, 35(32) pp. 4191–4199.

Thavamani, A., Salem, I., Sferra, T. J. and Sankararaman, S. (2021) 'Impact of Altered Gut Microbiota and its Metabolites in Cystic Fibrosis.' *Metabolites*, 11(2) p.

123.

Tixier, E. N., Verheyen, E., Luo, Y., Grinspan, L. T., Du, C. H., Ungaro, R. C., Walsh, S. and Grinspan, A. M. (2022) 'Systematic Review with Meta-Analysis: Fecal Microbiota Transplantation for Severe or Fulminant *Clostridioides difficile*.' *Digestive Diseases and Sciences*, 67(3) pp. 978–988.

Trapnell, B. C., Chu, C. S., Paakko, P. K., Banks, T. C., Yoshimura, K., Ferrans, V. J., Chernick, M. S. and Crystal, R. G. (1991) 'Expression of the Cystic Fibrosis Transmembrane Conductance Regulator Gene in the Respiratory Tract of Normal Individuals and Individuals with Cystic Fibrosis.' *Proceedings of the National Academy of Sciences of the United States of America*, 88(15) pp. 6565–6569.

Treem, W. R., Ahsan, N., Shoup, M. and Hyams, J. S. (1994) 'Fecal Short-Chain Fatty Acids in Children with Inflammatory Bowel Disease.' *Journal of Pediatric Gastroenterology & Nutrition*, 18(2) pp. 159–164.

Underhill, D. M. and Braun, J. (2022) 'Fungal Microbiome in Inflammatory Bowel Disease: A Critical Assessment.' *The Journal of Clinical Investigation*, 132(5) p. e155786.

De Vadder, F., Kovatcheva-Datchary, P., Zitoun, C., Duchampt, A., Bäckhed, F. and Mithieux, G. (2016) 'Microbiota-Produced Succinate Improves Glucose Homeostasis via Intestinal Gluconeogenesis.' *Cell Metabolism*, 24(1) pp. 151–157.

Veit, G., Avramescu, R. G., Chiang, A. N., Houck, S. A., Cai, Z., Peters, K. W., Hong, J. S., Pollard, H. B., Guggino, W. B., Balch, W. E., Skach, W. R., Cutting, G. R., Frizzell, R. A., Sheppard, D. N., Cyr, D. M., Sorscher, E. J., Brodsky, J. L. and Lukacs, G. L. (2016) 'From CFTR Biology toward Combinatorial Pharmacotherapy: Expanded Classification of Cystic Fibrosis Mutations.' *Molecular Biology of the Cell*, 27(3) pp. 424–433.

Venegas, D., De La Fuente, M., Landskron, G., González, M., Quera, R., Dijkstra, G., Harmsen, H., Faber, K. and Hermoso, M. (2019) 'Short Chain Fatty Acids (SCFAs) Mediated Gut Epithelial and Immune Regulation and its Relevance for Inflammatory Bowel Diseases.' *Frontiers in Immunology*, 10 p. 277.

Vermeire, S., Joossens, M., Verbeke, K., Wang, J., Machiels, K., Sabino, J., Ferrante, M., Assche, G. Van, Rutgeerts, P. and Raes, J. (2016) 'Donor Species Richness Determines Faecal Microbiota Transplantation Success in Inflammatory Bowel Disease.' *Journal of Crohn's and Colitis*, 10(4) pp. 387–394.

Vernocchi, P., Del Chierico, F., Quagliariello, A., Ercolini, D., Lucidi, V. and Putignani, L. (2017) 'A Metagenomic and in silico Functional Prediction of Gut Microbiota Profiles may concur in Discovering New Cystic Fibrosis Patient-Targeted Probiotics.' *Nutrients*, 9(12) p. 1342.

Vernocchi, P., Chierico, F. Del, Russo, A., Majo, F., Rossitto, M., Valerio, M., Casadei, L., Storia, A. La, De Filippis, F., Rizzo, C., Manetti, C., Paci, P., Ercolini, D., Marini, F., Fiscarelli, E. V., Dallapiccola, B., Lucidi, V., Miccheli, A. and Putignani, L. (2018) 'Gut Microbiota Signatures in Cystic Fibrosis: Loss of Host CFTR Function Drives the Microbiota Enterophenotype.' *PLoS One*, 13(12) p. e0208171.

Vinolo, M. A. R., Rodrigues, H. G., Nachbar, R. T. and Curi, R. (2011) 'Regulation of

Inflammation by Short Chain Fatty Acids.' *Nutrients*, 3(10) pp. 858–876.

Vogt, T. W. and J. (2003) 'Human Nutrition and Metabolism to Acetate Absorption from the Human Rectum and Distal Colon.' *American Society for Nutritional Sciences*, 133(10) pp. 3145–3148.

Wainwright, C. E., Elborn, J. S., Ramsey, B. W., Marigowda, G., Huang, X., Cipolli, M., Colombo, C., Davies, J. C., De Boeck, K., Flume, P. A., Konstan, M. W., McColley, S. A., McCoy, K., McKone, E. F., Munck, A., Ratjen, F., Rowe, S. M., Waltz, D. and Boyle, M. P. (2015) 'Lumacaftor–Ivacaftor in Patients with Cystic Fibrosis Homozygous for Phe508del CFTR.' *New England Journal of Medicine*, 373(3) pp. 220–231.

Waldhausen, J. H. T. and Richards, M. (2018) 'Meconium Ileus.' *Clinics in Colon and Rectal Surgery*, 31(2) pp. 121–126.

Walker, R. W., Clemente, J. C., Peter, I. and Loos, R. J. F. (2017) 'The Prenatal Gut Microbiome: Are we Colonized with Bacteria in utero?' *Pediatric Obesity*, 12(Suppl 1) pp. 3–17.

Walter, J. and Ley, R. (2011) 'The Human Gut Microbiome: Ecology and Recent Evolutionary Changes.' *Annual Review of Microbiology*, 65(1) pp. 411–429.

Walters, W., Hyde, E. R., Berg-Lyons, D., Ackermann, G., Humphrey, G., Parada, A., Gilbert, J. A., Jansson, J. K., Caporaso, J. G., Fuhrman, J. A., Apprill, A. and Knight, R. (2016) 'Improved Bacterial 16S rRNA Gene (V4 and V4-5) and Fungal Internal Transcribed Spacer Marker Gene Primers for Microbial Community Surveys.' *mSystems*, 1(1) pp. e00009-15.

Wang, H., Liu, Y., Shao, J., Luo, Y., Cai, W. and Chen, L. (2020) 'Rapid and Accurate Simultaneous Determination of Seven Short-Chain Fatty Acids in Feces by Gas Chromatography–Mass Spectrometry (GC-MS): Application in Type 2 Diabetic Rats and Drug Therapy.' *Analytical Letters*, 53(14) pp. 2320–2336.

Wang, Y., Leong, L. E. X., Keating, R. L., Kanno, T., Abell, G. C. J., Mobegi, F. M., Choo, J. M., Wesselingh, S. L., Mason, A. J., Burr, L. D. and Rogers, G. B. (2019) 'Opportunistic Bacteria Confer the Ability to Ferment Prebiotic Starch in the Adult Cystic Fibrosis Gut.' *Gut Microbes*, 10(3) pp. 367–381.

Wang, Z. K. and Yang, Y. S. (2013) 'Upper Gastrointestinal Microbiota and Digestive Diseases.' *World Journal of Gastroenterology*, 19(10) pp. 1541–1550.

Want, E. J. (2018) 'LC-MS Untargeted Analysis.' *Methods in Molecular Biology*, 1738 pp. 99–116.

West, C. E., Jenmalm, M. C. and Prescott, S. L. (2015) 'The Gut Microbiota and its Role in the Development of Allergic Disease: A Wider Perspective.' *Clinical and Experimental Allergy*, 45(1) pp. 43–53.

Williamson, I. A., Arnold, J. W., Samsa, L. A., Gaynor, L., DiSalvo, M., Cocchiaro, J. L., Carroll, I., Azcarate-Peril, M. A., Rawls, J. F., Allbritton, N. L. and Magness, S. T. (2018) 'A High-Throughput Organoid Microinjection Platform to Study Gastrointestinal Microbiota and Luminal Physiology.' *Cellular and Molecular Gastroenterology and Hepatology*, 6(3) pp. 301–319.

Wilschanski, M. and Durie, P. R. (1998) ‘Pathology of Pancreatic and Intestinal Disorders in Cystic Fibrosis.’ *Journal of the Royal Society of Medicine*, 91(Suppl 34) pp. 40–49.

Woese, C. R. (1987) ‘Bacterial Evolution.’ *Microbiological reviews*, 51(2) pp. 221–271.

Woese, C. R. and Fox, G. E. (1977) ‘Phylogenetic Structure of the Prokaryotic Domain: The Primary Kingdoms.’ *Proceedings of the National Academy of Sciences of the United States of America*, 74(11) pp. 5088–5090.

Wong, J. M. W., De Souza, R., Kendall, C. W. C., Emam, A. and Jenkins, D. J. A. (2006) ‘Colonic Health: Fermentation and Short Chain Fatty Acids.’ *Journal of Clinical Gastroenterology*, 40(3) pp. 235–243.

Wu, G. D., Chen, J., Hoffmann, C., Bittinger, K., Chen, Y.-Y., Keilbaugh, S. A., Bewtra, M., Knights, D., Walters, W. A., Knight, R., Sinha, R., Gilroy, E., Gupta, K., Baldassano, R., Nessel, L., Li, H., Bushman, F. D. and Lewis, J. D. (2011) ‘Linking Long-Term Dietary Patterns with Gut Microbial Enterotypes.’ *Science*, 334 pp. 105–109.

Wu, J., Hu, R., Yue, J., Yang, Z. and Zhang, L. (2009) ‘Determination of Fecal Sterols by Gas Chromatography-Mass Spectrometry with Solid-Phase Extraction and Injection-Port Derivatization.’ *Journal of Chromatography A*, 1216(7) pp. 1053–1058.

Wu, L., Wen, C., Qin, Y., Yin, H., Tu, Q., Van Nostrand, J. D., Yuan, T., Yuan, M., Deng, Y. and Zhou, J. (2015) ‘Phasing Amplicon Sequencing on Illumina Miseq for Robust Environmental Microbial Community Analysis.’ *BMC Microbiology*, 15 p. 125.

Wu, T. C., McCarthy, V. P. and Gill, V. J. (1983) ‘Isolation Rate and Toxigenic Potential of *Clostridium difficile* Isolates from Patients with Cystic Fibrosis.’ *The Journal of Infectious diseases*, 148(1) p. 176.

Yamada, A., Komaki, Y., Komaki, F., Micic, D., Zullow, S. and Sakuraba, A. (2018) ‘Risk of Gastrointestinal Cancers in patients with Cystic Fibrosis: A Systematic Review and Meta-Analysis.’ *The Lancet Oncology*, 19(6) pp. 758–767.

Yao, Y., Cai, X., Ye, Y., Wang, F., Chen, F. and Zheng, C. (2021) ‘The Role of Microbiota in Infant Health: From Early Life to Adulthood.’ *Frontiers in Immunology*, 12 p. 708472.

Yatsunenko, T., Rey, F. E., Manary, M. J., Trehan, I., Dominguez-Bello, M. G., Contreras, M., Magris, M., Hidalgo, G., Baldassano, R. N., Anokhin, A. P., Heath, A. C., Warner, B., Reeder, J., Kuczynski, J., Caporaso, J. G., Lozupone, C. A., Lauber, C., Clemente, J. C., Knights, D., Knight, R. and Gordon, J. I. (2012) ‘Human Gut Microbiome Viewed Across Age and Geography.’ *Nature*, 486(7402) pp. 222–227.

Zaneveld, J. R., McMinds, R. and Thurber, R. V. (2017) ‘Stress and Stability: Applying the Anna Karenina Principle to Animal Microbiomes.’ *Nature Microbiology*, 2 p. 17121.

Zhang, H., Sun, J., Liu, X., Hong, C., Zhu, Y., Liu, A., Li, S., Guo, H. and Ren, F. (2013) ‘*Lactobacillus paracasei subsp. paracasei* LC01 Positively Modulates Intestinal Microflora in Healthy Young Adults.’ *Journal of Microbiology*, 51(6) pp. 777–782.

Zhang, S., Wang, H. and Zhu, M. J. (2019) ‘A Sensitive GC/MS Detection Method for

Analyzing Microbial Metabolites Short Chain Fatty Acids in Fecal and Serum Samples.' *Talanta*, 196 pp. 249–254.

Zhao, G., Nyman, M. and Jönsson, J. Å. (2006) 'Rapid Determination of Short-Chain Fatty Acids in Colonic Contents and Faeces of Humans and Rats by Acidified Water-Extraction and Direct-Injection Gas Chromatography.' *Biomedical Chromatography*, 20 pp. 674–682.

Zhao, X., Jiang, Z., Yang, F., Wang, Yan, Gao, X., Wang, Yuefei, Chai, X., Pan, G. and Zhu, Y. (2016) 'Sensitive and Simplified Detection of Antibiotic Influence on the Dynamic and Versatile Changes of Fecal Short-Chain Fatty Acids.' *PLoS One*, 11(12) p. e0167032.

Zheng, X., Qiu, Y., Zhong, W., Baxter, S., Su, M., Li, Q., Xie, G., Ore, B. M., Qiao, S., Spencer, M. D., Zeisel, S. H., Zhou, Z., Zhao, A. and Jia, W. (2013) 'A Targeted Metabolomic Protocol for Short-Chain Fatty Acids and Branched-Chain Amino Acids.' *Metabolomics*, 9(4) pp. 818–827.

Zhou, H., Sun, L., Zhang, S., Zhao, X., Gang, X. and Wang, G. (2020) 'Evaluating the Causal Role of Gut Microbiota in Type 1 Diabetes and Its Possible Pathogenic Mechanisms.' *Frontiers in Endocrinology*, 11 p. 125.